Eliciting VRC01-class antibodies against HIV-1 through immunization

Katherine Rachael Parks

A dissertation

submitted in partial fulfillment of the

requirements for the degree of

Doctor of Philosophy

University of Washington

2020

Reading Committee:

Leonidas Stamatatos, Chair

Rhea Coler

Justin Taylor

Program Authorized to Offer Degree:

Pathobiology

University of Washington

Abstract

Eliciting VRC01-class antibodies against HIV-1 through immunization

Katherine Rachael Parks

Chair of the Supervisory Committee:

Leonidas Stamatatos

Department of Global Health

With more that 37 million people currently infected with HIV-1, there is a need for a vaccine to prevent HIV-1 infection. One goal of an effective HIV-1 vaccine is to elicit broadly neutralizing antibodies (bnAbs). These antibodies (Abs) neutralize the majority of HIV-1 viruses in circulation. bnAbs have been isolated from chronically infected individuals and were shown, in studies of passive administration in non-human primates and humanized mice, to be protective against SHIV and HIV respectively. Thus, it is thought that if bnAbs can be elicited through vaccination, they will be protective.

VRC01-class Abs are amongst the most broad and potent neutralizing and therefore desirable to elicit during vaccination. VRC01-class Abs target the CD4-binding site (CD4-BS) on the HIV-1 Env. All members of this class have high levels of somatic hypermutation (SHM); share similar gene ontogenies, all utilizing the VH1-2*02 allele in the heavy chain paired with one of the following light chains: k3-20, k1-33, λ2-14, k3-15, k1-5; and use the same mode of recognition to engage the CD4-BS. A major roadblock to eliciting such Abs is the fact that the

unmutated or germline precursors which gives rise to these bnAbs fail to bind known recombinant Env. This has led to the development of immunogens that engage the germline (gl)VRC01 precursor, thus named germline-targeting immunogens.

This thesis examines germline-targeting immunogens *in vivo*. The germline-targeting immunogens evaluated are Env-based and also anti-idiotypic antibodies (aiAbs). In Chapter II we evaluated Env-based germline-targeting immunogens. In these studies, we utilized a mouse model expressing B cells with the glVRC01 heavy chain (glH-VRC01 mouse, Table 1.3). Mice were immunized with one of the following germline-targeting immunogens: 426c Core, eOD-GT8, or 426cOD. These immunogens differ in their affinity for glVRC01, the structural presentation of the glVRC01 epitope, and genetically. We found that while all of the glVRC01-targeting immunogens effectively activated VRC01-like B cells *in vivo*, the immunogens selected for B cells with distinct genetic characteristics that influence their ability to recognize diverse Env proteins. These results will inform HIV-1 vaccine design, as both 426c Core and eOD-GT8 are being evaluated in human clinical trials. These results are also more broadly applicable to vaccine design, by highlighting the importance of structure and biophysical and biochemical properties of the immunogen on B cell activation.

While, these germline-targeting immunogens are able to activate VRC01-like B cells *in vivo*, the Abs they produce are non-neutralizing. Therefore in the work reported in Chapter III, we employed a boosting immunogen in an effort to guide the maturation of these B cells to their neutralizing form. We found that priming glH-VRC01 mice with the germline-targeting immunogen 426c Core and boosting with the HxB2 wild type (WT) Core protein increased SHM in the VRC01-like B cell receptors, improved Ab binding to diverse Env proteins and increased

the Abs ability to neutralize the autologous WT virus. This work is the first to identify a prime-boost immunization scheme that can elicit VRC01-class Abs capable of neutralizing a WT virus.

We also evaluated the aiAb, iv8, as a glVRC01-class germline-targeting immunogen in Chapter IV. In an adoptive transfer experiment, we found that iv8 is able to activate and expand B cells expressing the mature 3BNC60 heavy chain and gl3BNC60 light chain (SI-3BNC60, Table 1.3), as well as decrease the non-VRC01-epitope targeted plasma Ab response in comparison to an Env-based immunogen. Iv8 was also able to expand B cells expressing VRC01-class characteristics in the glH-3BNC60 mouse model. Therefore, we have demonstrated that iv8 can activate glVRC01-class B cells *in vivo* and should be considered for use in combination or as an alternative to Env-based immunogens in vaccination studies designed to elicit VRC01-class bnAbs.

Table of Contents

Figures

Tables

Abbreviations

AA = amino acid

Ab = antibody

ADCC = antibody dependent cellular cytotoxicity

ADCP = antibody dependent cellular phagocytosis

aiAb = anti-idiotypic antibody

ART = anti-retroviral therapy

BCR = B cell receptor

BLI = biolayer interferometry

bnAb = broadly-neutralizing antibody

BSA = binding surface area

CD4-BS = CD4-binding site

CDR = complementary determining region

CDRH = complementary determining region heavy chain

CDRL = complementary determining region light chain

CTV = CellTrace Violet

CTL = cytotoxic T lymphocyte

ELISA = enzyme linked immunosorbent assays

EM = electron microscopy

Fab = fragment antigen-binding

Fc = fragment crystallizable

Fer = ferritin

FW = frame work

glVRC01 = germline VRC01

HIV = Human immunodeficiency virus

HC = heavy chain

KI = knock in

KO = knock out

LC = light chain

LC-MS/MS = liquid-chromatography-tandem mass spectrometry

Luc = luciferase

mLC = mouse light chain

MPER = membrane proximal external region

na = not tested

N.B. = no binding

NLGS = N-linked glycosylation site

NR = not reported

ns = negative stain

nt = nucleotide

PBMC = peripheral blood mononuclear cell

RLU = relative luminescence units

SEM = standard error of the mean

SHIV = simian-human immunodeficiency virus

SI = synthetic intermediate

V1 = variable loop 1

V2 = variable loop 2

V3 = variable loop 3

V4 = variable loop 4

V3 = variable loop 5

VH = variable heavy

VL = variable light

WT = wild type

Chapter I. Introduction

Introduction

HIV-1 was discovered as the causative agent of the disease AIDS in 1983 (Barré-Sinoussi et al., 1983; Gallo et al., 1983). At the end of 2018, there were 37.9 million people living with HIV-1 (CDC, 2017). There is no cure for HIV-1 and only life-long anti-retroviral treatment (ART) can prevent progression to AIDS, which only a fraction of HIV-1 infected people receive (Deeks et al., 2015). Therefore, there is a need for the development of preventative measures against HIV-1.

HIV-1 origins and virology

There are two types of HIV: 1 and 2. HIV-2 was transmitted from the sooty mangabey to humans with 8 groups of HIV-2 emerging from the different transmission events. HIV-2 is confined geographically to Western Africa and less pathogenic than HIV-1, with those infected with HIV-2 having lower viral loads, decreased transmission rates, and lower likelihood of progression to AIDS. As a result of lower pathogenicity, the majority of people living with HIV are infected with HIV-1. The origin of HIV-1 stems from a transmission from chimpanzees to humans. There are multiple groups of HIV-1 stemming from the multiple transitions events from chimpanzees to humans, but Group M is largely responsible for the global pandemic (Sharp and Hahn, 2011). The groups can be further divided into clades, with the Group M having 10 clades. In addition to the distinct clades there are circulating recombinant forms (CRFs), which originate when two viruses of different clades recombine. Among the different clades, there can be up to 25-35% genetic diversity (Lau and Wong, 2013).

HIV-1 is a member of the lentivirus genus and the family retroviridae. It is an enveloped virus with two single strands of positive sense RNA. The genome consists ~9,400 base pairs and

encodes 9 genes: Gag, Pol, Env, Nef, Vpr, Tat, Rev, Vif, Vpu. Three of these encode structural proteins: Gag, Pol, Env. Two encode regulatory proteins and modulate the replication of HIV-1: Tat, Rev. The remaining four encode accessary proteins, that are said to be non-essential, but aid in viral replication by helping the virus to evade or manipulate the host immune system: Nef, Vpr, Vif, Vpu.

Envelope (Env) is the major viral surface protein and is encoded by the Env gene. Env mediates viral entry into the host cell by first engaging with the CD4 receptor (Klatzmann et al., 1984). Following CD4 binding, Env undergoes a conformational change that allows it to bind to a co-receptor: CXCR4 (Feng et al., 1996) or CCR5 (Deng et al., 1996; Dragic et al., 1996). While HIV-1 mainly infects CD4 cells, it can also infect other cells expressing these receptors including macrophages, monocytes and microglia (Crowe et al., 1987; He et al., 1997; Klatzmann et al., 1984). After co-receptor binding, membrane fusion occurs between the host cell and the virus. At this point the HIV-1 enzymes and RNA enter into the host cell. The RNA is reverse transcribed into proviral DNA by a virally encoded reverse transcriptase. This is the step in which the majority of genetic diversity among HIV-1 viruses originates, as the reverse transcriptase is error-prone and lacks a proof reading mechanism resulting in amino acid (AA) deletions, insertions, and substitutions (Hübner et al., 1992). Following reverse transcription, the proviral DNA is integrated into the host genome, where it remains stably integrated. The proviral DNA is replicated by the host cell with every cell division and serves as a latent reservoir when the cell is not dividing. Upon reactivation of that host cell, transcription of viral genes can be reinitiated to produce viable virus. During viral replication, the proviral DNA is transcribed. These viral mRNAs associate with the host membrane along with viral proteins. The viral particles bud from the host cell to form new virions that can infect new cells (Deeks et al., 2015).

Treatment and vaccines against HIV-1

While there is no cure for HIV-1, there is treatment. ART consists of drugs that target various stages of viral replication. ART can decrease a patient's viral load to undetectable levels in the plasma and extend their life expectancy. However, if ART is interrupted, viral rebound will occur. Therefore, it requires lifelong adherence. Additionally, ART is accompanied by unpleasant side effects (Pau and George, 2014). In 2018, it was estimated that only 62% of HIV-1 infected individuals had access to ART (WHO). If left untreated, HIV-1 infection leads to a progressive loss of CD4 T cells and increased immunodeficiency (Moir et al., 2011). These individuals become susceptible to AIDS-related illnesses including: pneumonia, candidiasis, multiple viral infections and certain cancers (Goodman et al., 1987; Gottlieb et al., 1981; Ji and Lu, 2017). Therefore, it is important to develop a vaccine to prevent HIV-1 infection.

Initially, vaccines against HIV-1 were designed to elicit antibodies (Abs). These vaccines were composed of recombinant Env protein (Flynn et al., 2005; Pitisuttithum et al., 2006). However, when evaluated in human clinical trials, these vaccines did not prevent HIV-1 infection. Dismayed by the failure of recombinant protein vaccines, the field shifted to the development of vaccines that tried to elicit a protective T cell response given the fact that a strong cytotoxic T lymphocyte (CTL) response was associated with viremic control in HIV-1 infected individuals (Borrow et al., 1994; Koup et al., 1994). This indicated that a vaccine eliciting a strong CTL response could be effective in controlling HIV-1 infection if not protective. However, this strategy also proved unsuccessful with the failure of human clinical trials evaluating DNA vaccines encoding viral proteins (Graham et al., 2006; McElrath et al., 2008). Decades after the discovery of HIV-1, there was the first clinical trial to show efficacy

against HIV-1 infection. The RV144 examined the ability of a canarypox vector encoding Gag, Pol, Env followed by a gp120 protein boost to protect against HIV-1 infection. This trial showed 31% efficacy with protection correlating with V1/V2-specific IgG1 and IgG3 Ab responses, antibody dependent cellular cytotoxicity (ADCC) activity, and a lowered IgA Ab response (Haynes et al., 2012; Rerks-Ngarm et al., 2009). The RV144 trial encouraged the field to again focus on a vaccine against HIV-1 that will elicit protective Abs.

B cells and Abs

Most effective vaccines work through the production of protective Abs (Plotkin and Plotkin, 2011). When not secreted by plasma cells or plasmablasts, Abs are found in a membrane bound form, which is the B cell receptor (BCR). Abs are made up of two identical polypeptides, which consist of a light chain (LC) and a heavy chain (HC). The HCs are linked together by disulfide bonds to form a Y-shaped structure. On the Ab there are two functional regions: the variable and constant region.

The variable region is responsible for antigen recognition. Abs are able to neutralize pathogens by binding to antigen through the variable region and blocking entry into the host cell. The variable region is found on the fragment antigen binding – or Fab region of the Ab. Every Ab has two identical Fab regions, which adds to the strength of the Abs interaction with the cognate antigen – an interaction known as avidity (Figure 1.1C). The antigen specificity of a variable region is determined in part by the genes used to encode the variable region at the amino terminus of the HC and LC of the Fab region. The genes used to encode Abs are found on three distinct genetic loci – one for the HC and two for the LC – kappa and lambda. There are multiple copies of each gene. During B cell development, B cells undergo a process known as somatic or

V(D)J recombination to form the BCR. This is a process where the V, D and J genes for the HC, or V and J genes for the LC, are excised from the chromosome and recombined together to form the variable region (Figure 1.1A). On the HC there are 39 V genes, 27 D genes, and 6 J genes. On the LC, kappa and lambda respectively, there are 40 and 32 V genes and 5 and 4 J genes. The large number of available genes to participate in V(D)J recombination makes the Ab repertoire highly diverse and capable of recognizing diverse antigens.

The variable region can be divided into framework (FW) regions and complementary determining regions (CDR). The CDRs typically make the majority of the contacts with the antigen. The junctions that form between the V, D and J gene segments are the CDR3s (Figure 1.1B). The CDR3 regions are highly diverse as during V(D)J recombination process, nucleotides are added to the ends of the joining genes. The variable region can be further diversified through somatic hypermutation (SHM) – a process of ending the BCR to increase its affinity for foreign antigen through nucleotide changes. Therefore, there are many steps in the process of B cell development, which create BCRs/Abs capable of recognizing diverse pathogens.

The constant region of the HC encodes the Fc domain (Figure 1.1C). The Fc domain is responsible for effector functions. The function of Fc domain is determined by the Ab isotype. There are 5 different isotypes: M, D, G, E and A. The Fc domain of the Ab can bind to Fc receptors on host cells. The cells subsequently eliminate the pathogen through processes such as Ab dependent cellular phagocytosis (ADCP) and ADCC. The Fc domain can also bind to complement proteins and subsequently activate the complement system (Schroeder and Cavacini, 2010; Stanfield and Wilson, 2014).

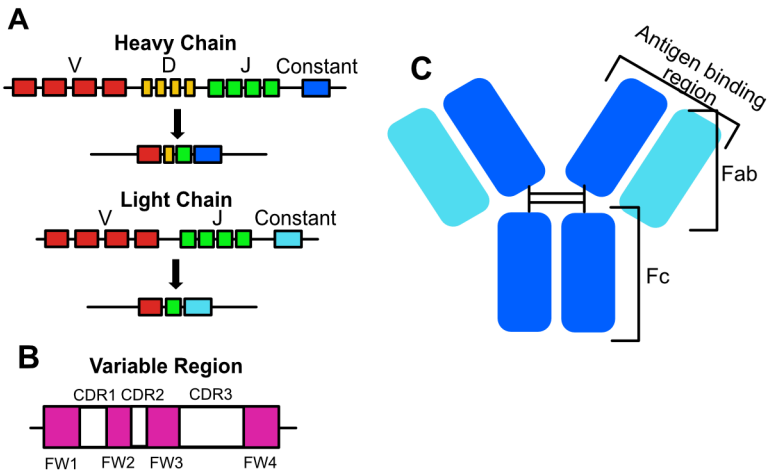

Figure 1.1. Ab structure. (A) VDJ recombination of the HC and LC. The HC and LC recombine chromosomally encoded genes to form the variable region. **(B)** The variable region is composed of four framework regions (pink) and three CDRs (white). **(C)** An Ab with the Fab and Fc domain noted. The HCs are in dark blue and the LCs are in light blue. Disulfide bonds connect the HCs.

HIV-1 Env

The HIV-1 Env is the only surface-expressed viral protein. The Env protein is expressed as a gp160 and is subsequently cleaved by host cell proteases in gp120 and gp41 subunits (Decroly et al., 1994). The gp120 and gp41 subunits remain non-covalently linked and form trimers on the surface of the virus. The gp41 subunit is membrane proximal and it spans the viral membrane. The gp41 subunit contains the fusion machinery necessary to fuse the virus to the host cell and anchors the Env protein to the viral surface. The gp120 subunit is distal to the viral membrane. The gp120 is organized into 5 conserved regions (C1-C5) and 5 variable regions (loops) (V1-V5). The gp120 subunits expresses the receptor and co-receptor binding sites. (Arrildt et al., 2012; Burton and Hangartner, 2016) (Figure 1.2).

The HIV-1 Env has many immune evasion tactics which make it a difficult target for neutralizing Abs. The Env protein is highly genetically diverse. The variable regions are hypervariable in sequence and length (Palmer et al., 1996). Furthermore, the variable regions

also restrict access of Abs to more immuno-dominant epitopes on the HIV-1 Env. Additionally, the HIV-1 Env protein is a densely glycosylated protein. These glycans are added to the Env protein during translation of the protein by the host cell using host machinery, and are therefore less immunogenic. Each gp120 subunit has a median of 25 N-linked glycans added which serve to shield the Env against the Ab response (Burton and Hangartner, 2016). The HIV-1 Env structure itself is very unstable and the gp120 subunits can dissociate leaving behind only the gp41 "stump" (Moore et al., 2006). This loss of the gp120 subunit results in a removal of many potential Ab epitopes. Lastly, the spacing of the Env trimers on the virus is unfavorable for the engagement of BCRs, as there are only an average of 8-10 trimers per virus (Zhu et al., 2003).

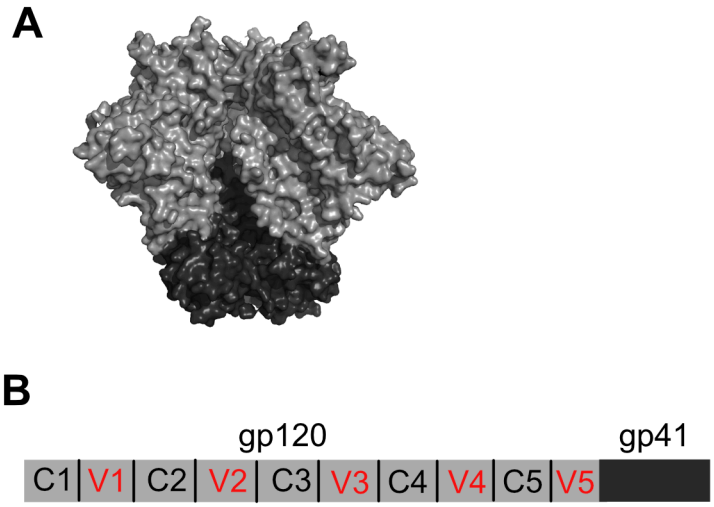

Figure 1.2 . HIV-1 Env structure. (A) The HIV-1 Env trimer is composed of gp120 and gp41 subunits (PDB: 4TVP). The gp120 subunits are colored in light gray and the gp41 subunits are colored in dark gray. **(B)** The linear organization of the gp160 subunit of the HIV-1 Env. Constant regions (C1-C5) are interspersed by variable regions (V1-V5).

The Ab response to HIV-1

The earliest Ab response to HIV-1 Env appears within one week of detectable viremia. These Abs are detected as Ab complexes. A few weeks later, Abs targeting the gp41 arise followed by those targeting the gp120 subunit – primarily the V3 loop. These Abs are non-neutralizing and do not apply pressure on the virus to escape (Tomaras et al., 2008). In the first few months after infection, Abs capable of neutralizing this autologous virus arise. The virus is able to escape these Abs through the acquisition of escape mutations (Frost et al., 2005; Rong et al., 2009). In the years following infection, broadly neutralizing Abs (bnAbs) develop. These Abs can neutralize the majority of circulating viral strains, despite the tremendous amount of genetic diversity, and steric restrictions present on the Env. Approximately, 25% of HIV-1 infected individuals develop cross-neutralizing Abs within a year of infection (Doria-Rose et al., 2010; Sather et al., 2009), and up to 50% will develop cross-neutralizing Abs 2-4 years following infection with the Abs breadth and potency increasing over time (Hraber et al., 2014) . Of these

individuals who develop bnAbs, approximately 1% are considered to be “elite neutralizers” and have plasma with 3 times the potency of a individual producing neutralizing Abs (Simek et al., 2009). It is not fully understood why only a fraction of individuals develop bnAbs, but some factors associated with their development are frequency of T follicular helper cells (Cohen et al., 2014; Locci et al., 2013), duration of infection, low CD4 counts, and high viral load (Gray et al., 2011; Landais et al., 2016; Rusert et al., 2016; Sather et al., 2009).

BnAb epitopes and characteristics

The development of techniques to isolate and sequence B cells from HIV-1 infected individuals displaying broad plasma Ab neutralization has allowed for the genetic and structural characterization of bnAbs. Now, bnAbs targeting many different epitopes of the HIV-1 Env protein have been discovered. These include the V1 and V2 loops on gp120 (commonly referred to as ‘apex’ Abs); membrane proximal external region (MPER) of gp41 (Buchacher et al., 1992, 1994; Huang et al., 2012; Morris et al., 2011; Williams et al., 2017; Zhu et al., 2011; Zwick et al., 2001); V3 glycans positioned at N332 and influenced to varying degrees by N156, N301 and N137 ; gp120-gp41 interface (Falkowska et al., 2014; Huang et al., 2014; Klein et al., 2012a; Scheid et al., 2011); fusion peptide (Kong et al., 2016b); silent face center (Zhou et al., 2018); and the CD4-binding site (CD4-BS) (Barbas et al., 1993; Bonsignori et al., 2014; Corti et al., 2010a; Freund et al., 2015; Georgiev et al., 2013; Gristick et al., 2016; Huang et al., 2016; Kong et al., 2016a; Liao et al., 2013; Wibmer et al., 2016; Wu et al., 2010, 2011; Zhou et al., 2013, 2015) (Figure 1.3). These Abs are summarized in Table 1.1.

bnAbs have many atypical characteristics. These include unusually long CDRH3 regions. The CDRH3 can be >35 AAs long in a bnAb as compared to typical Abs which have a 14-17 AA

long CDRH3s on average (DeKosky et al., 2015; Jardine et al., 2015). The long CDRH3 allows Abs to penetrate past glycans and occluding epitopes on the HIV-1 Env. There are also bnAbs that are poly or auto reactive. This results in a problem in the development of such Abs as B cells producing them can be eliminated during B cell tolerance. BnAbs may also have high levels of SHM. Furthermore, unlike in most Abs, where mutations are concentrated in the CDRs, mutations found in bnAbs occur in both the CDR and FW regions. High levels of SHM are also frequently associated with rare insertion or deletion events. While these unique characteristics enable Abs to overcome the steric restrictions present on the HIV-1 Env protein, they may make bnAbs difficult to elicit during vaccination (Verkoczy, 2017).

Despite these characteristics, there is great interest in eliciting bnAbs through immunization. Studies of passive administration have shown that bnAbs cans protect against SHIV/HIV in non-human primates and humanized mice respectively (Baba et al., 2000; Gautam et al., 2016; Hessell et al., 2009, 2010; Julg et al., 2017; Klein et al., 2012b; Mascola et al., 1999, 2000; Nishimura et al., 2002; Parren et al., 2001; Parsons et al., 2019; Pegu et al., 2014; Shibata et al., 1999; Wu et al., 2018). Therefore it is thought, if these Abs can be elicited by vaccination they may be protective. There is additional support for a vaccine aiming to elicit bnAbs as a result of studies that demonstrate that viral rebound can be controlled in HIV-1 infected individuals who are given bnAb infusions during ART interruption (Bar-On et al., 2018; Caskey et al., 2015; Mendoza et al., 2018).

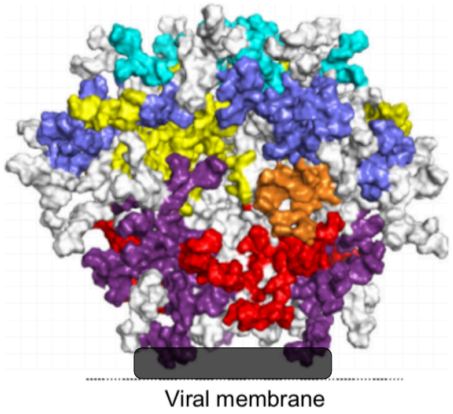

Figure 1.3. Epitopes targeted by bnAbs. The epitopes of bnAbs are highlighted on the HIV-1 Env trimer (PDB: 4TVP): The V1-V2 epitope is in cyan, V3 glycans in periwinkle, CD4-BS in yellow, silent face center in orange, gp120-41 interface in purple, fusion peptide in red, MPER in black. Figure is adapted from (Kwong and Mascola, 2018)**.**

Table 1.1. Summary of bnAbs by epitope targeted (adapted from (Verkoczy, 2017)).

Epitope targeted	bnAb lineage/ class	CDRH3 length	Poly/autoreactive[a]	VH % SHM[b]	Reference
CD4-BS	VRC01	12-15	Y	23 (nt)-48	(Georgiev et al., 2013; Huang et al., 2016; Kong et al., 2016a; Scheid et al., 2011; Wu et al., 2010, 2011; Zhou et al., 2013, 2015)
	IOMA	19	NR	22	(Gristick et al., 2016)
	CH103-106	13	Y	20	(Liao et al., 2013)
	b12	18	Y	21	(Barbas et al., 1993)
	HJ16	19	NR	37	(Corti et al., 2010a)
	CH98	21	Y	25 (nt)	(Bonsignori et al., 2014)
	VRC13	21	NR	52	(Zhou et al., 2015)
	VRC16	20	NR	29	(Zhou et al., 2015)
	8ANC131	13-16	Y	13(nt)-41	(Zhou et al., 2015)
	179NC75	24	NR	36	(Freund et al., 2015)
	CAP257-RH1	11	NR	9 (nt)	(Wibmer et al., 2016)
MPER	4E10	18	Y	19	(Buchacher et al., 1994)
	2F5	22	Y	14	(Buchacher et al., 1992)
	M66.6	21	Y	9	(Zhu et al., 2011)
	CAP206-CH12	15	Y	19	(Morris et al., 2011)
	10E8	20	Y	27	(Huang et al., 2012)
	DH511	24	Y	18	(Williams et al., 2017)

	Z13	19	Y	19	(Zwick et al., 2001)
Fusion Peptide	N123-VRC34	15	NR	15-23 (nt)	(Kong et al., 2016b)
	ACS202	24	Y	16 (nt)	(van Gils et al., 2016)
Silent face center	VRC-PG05	17	NR	13	(Zhou et al., 2018)
V3 glycans	PGT121-123	24	N	21-27	(Walker et al., 2011)
	PGT125-131	19	Y	23-33	(Walker et al., 2011)
	PGT135-137	18	NR	25-29	(Walker et al., 2011)
	DH270	20	NR	6	(Bonsignori et al., 2017)
	VRC24	24	NR	30	(Georgiev et al., 2013)
	3B176	19	Y	34	(Klein et al., 2012a)
	10-1074	24	NR	21	(Mouquet et al., 2012)
Gp120-gp41 interface	2G12	14	N	32	(Buchacher et al., 1994)
	PGT151-158	26	N (PGT151-152), NR (PGT152-158)	26-31	(Falkowska et al., 2014)
	35O22	14	N	44	(Huang et al., 2014)
	8ANC195	20	Y	43	(Scheid et al., 2011)
	CH01-04	24	Y	19-32	(Bonsignori et al., 2011)
V1-V2	PG9	28	Y	17	(Walker et al., 2009)
	PG16	28	N	20	(Walker et al., 2009)
	CAP256-VRC26	35-37	N	13-23	(Doria-Rose et al., 2015)
	PGDM1400	34	N	27 (nt)	(Sok et al., 2014)
	PGT141-145	31-32	N	28-30	(Walker et al., 2011)

[a]Y indicates there was poly/autoreactivity reported. N indicates there was no poly/autoreactivity reported. NR indicates that poly/autoreactivity was not reported.

[b]Percent mutation is shown as percent AA mutations. Nt indicates nucleotide mutation percent was used.

BnAbs directed to the CD4-BS

CD4-BS bnAbs target the conserved region of the CD4-BS on the HIV-1 Env, a region which remains genetically unaltered over time and across viral clades (Zhou et al., 2010). The CD4-BS bnAbs can be classified based on ontogeny and epitope recognition into two groups: VH gene restricted and CDRH3 dominated. The CDRH3 dominated Abs make their contacts with the CD4-BS through their CDRH3 region. VH gene restricted Abs that make their primary Env contacts through their VH gene (Zhou et al., 2015). The VH gene restricted Abs include: VRC01-class Abs, IOMA-class Abs, and 8ANC131-class Abs. Both VRC01-class and IOMA-class Abs utilize the VH1-2 gene (Georgiev et al., 2013; Gristick et al., 2016; Kong et al., 2016a, 2016a, 2016b; Scheid et al., 2011; Wu et al., 2010; Zhou et al., 2013, 2015). 8ANC131-class Abs use the VH1-46 gene (Zhou et al., 2015).

VRC01-class bnAbs

VRC01-class Abs are desirable to elicit through vaccination as they are amongst the most broad and potently neutralizing Abs (Table 1.2). The HC of VRC01-class Abs all derive from the VH1-2*02 allele (Georgiev et al., 2013; Kong et al., 2016a, 2016a, 2016b; Scheid et al., 2011; Wu et al., 2010; Zhou et al., 2013, 2015). Thus, despite being isolated from different donors, members of this class all originate from similar genetic origins. VH1-2 genes are used in 2% of the human Ab repertoire, and of the VH1-2 alleles the *02 allele is expressed in 75-100% of VH1-2 Abs (Arnaout et al., 2011), however not all humans may express this allele (Yacoob et al., 2016). VRC01-class Abs have conserved residues in the HC, which are arginine at position 71 (FW3), tryptophan at position 50 (CDRH2) and an asparagine at position 58 (CDRH2). These residues play a key role in VRC01-class Abs interaction with the CD4-BS: $Trp50_{HC}$ contacts $Asn280_{gp120}$,

Asn58$_{HC}$ contacts Arg456$_{gp120}$, and Arg71$_{HC}$ contacts Asp368$_{gp120}$. These AAs are gene-encoded, meaning they are found in the germline encoded VH1-2*02 gene. In addition, most VRC01-class Abs have a tryptophan at position 100, which makes contacts with Asn/Asp279$_{gp120}$ and provides a stabilizing interaction with the LC (West et al., 2012). Unlike the other conserved residues, which are found in the V gene, the tryptophan at position 100 is located at position 100b in the CDRH3, which is composed of elements of the V, D and J genes. Therefore, it is uncertain if in all cases, the tryptophan at position 100b is due to SHM or germline VDJ recombination. The fact that it has been found in the naïve human repertoire indicates that it can be the result of V(D)J recombination in some cases (Yacoob et al., 2016).

In the LC, VRC01-class Abs use a 5 AA long CDRL3. The key residues within the LC are a glutamic acid at position 96 (CDRL3) and a tryptophan or phenylalanine at position 67 (FW3). The Glu96$_{HC}$ makes contacts with Gly459$_{gp120}$ and/or Asn280$_{gp120}$. The Try/Phe67$_{HC}$ forms a potential interaction with a part of the glycan present at position Asn276$_{gp120}$. Unlike the HC, these AAs are not present in the germline LC and arise from a VJ recombination event or SHM (West et al., 2012). There is also a two-residue deletion in the CDRL1 or, alternatively, AA substitutions to glycine that occur during maturation, both of which avoid a clash between the CDRL1 and glycan at position 276 on the HIV-1 Env (Zhou et al., 2013). Unlike the HC, which employs the same VH gene in the HC, the LC can use a number of different Vk and Vl genes: k3-20, k1-33, λ2-14, k3-15, k1-5 (Georgiev et al., 2013; Kong et al., 2016a, 2016b; Scheid et al., 2011; Wu et al., 2010, 2011; Zhou et al., 2013, 2015).

Furthermore, VRC01-class bnAbs have now been isolated from 10 different individuals infected with different clades of virus. Structural analysis shows that all these Abs recognize the CD4-BS in the same manner: utilizing the CDRH2 region to make the majority of contacts with

the CD4-BS, mimicking the mode of recognition used by the CD4 receptor to contact the HIV-1 Env. The structural convergence among VRC01-class Abs occurs despite the Abs in the VRC01-class having up to 50% sequence diversity (Zhou et al., 2013). This sequence divergence is a result in part of the high amounts of SHM that VRC01-class Abs go through. This shows that there is not a singular evolutionary pathway that B cells expressing the unmutated VRC01-class BCRs must take to produce VRC01-class bNAbs. Thus, a successful immunization can potentially guide these B cells along different pathways to achieve breadth and neutralization.

Table 1.2. Summary of VRC01-class Abs.

bnAb	Year isolated	Donor	VL gene	VH % SHM[a]	VL % SHM[ab]	Reference
VRC01-03	2011	Donor 45	K3-20	40-48	30-33	(Wu et al., 2010)
NIH45-46	2011	Donor 45	K3-20	41	30	(Scheid et al., 2011)
VRC01-PG04, PG04b	2011	Donor 74	K3-20	34-39	35	(Wu et al., 2011)
VRC-CH30-34	2011	Donor 0219	K1-33	44	24-28	(Wu et al., 2011)
3BNC60	2011	Patient 3	K1-33	40	33	(Scheid et al., 2011)
3BNC117	2011	Patient 3	K1-33	37	30	(Scheid et al., 2011)
12A12, 12A21	2011	Patient 12	K1-33	38,40	29,30	(Scheid et al., 2011)
VRC-PG19, PG20	2013	IAVI 23	λ2-14	23,24 (nt)	13, 15 (nt)	(Zhou et al., 2013)
VRC23	2013	Donor 127/C	K3-15	36	26	(Georgiev et al., 2013)
VRC18	2015	Donor C38	K3-20	37	NR	(Zhou et al., 2015)
N6	2016	Donor Z258	K1-33	42	25 (nt)	(Huang et al., 2016)
VRC27	2015	Donor Z258	K1-33	40	NR	(Zhou et al., 2015)
DRVIA7	2016	DRVI01	K1-5	19(nt)	17(nt)	(Kong et al., 2016a)

[a]Percent mutation is shown as percent AA mutations. Nt indicates nucleotide mutation percent was used.
[b]NR indicates not reported.

Germline-targeting immunogens

However, a major challenge in eliciting VRC01-class bnAbs through immunization is the fact that the unmutated precursors, or germline-encoded Abs, do not bind to recombinant Env. Therefore, Env proteins have been specifically designed to have high affinity for the germline form of these Abs. Multiple groups have now been designed VRC01-class germline-targeting immunogens using different approaches, but shared among them is the elimination of steric hindrances and glycans surrounding the VRC01 epitope, which pose the major steric barrier to glVRC01 binding, most notably the glycan at position 276 in loop D of the HIV-1 Env (Jardine et al., 2013, 2015; McGuire et al., 2013, 2014a, 2016; Medina-Ramírez et al., 2017).

<u>426c Core and 426c TM SOSIP</u>

One such VRC01-class germline-targeting immunogen is the 426c Core. The 426c Core is derived from the clade C 426c virus. The 426c Env sequence is a consensus sequence built from the numerous viral variants of the same virus isolated from an acutely infected individual (Gray et al., 2011). Elimination of N-linked glycosylation sites (NLGS) surrounding the CD4-BS in loop D (N276) and V5 loop (N460 and N463) on the 426c Env allowed binding of 4 glVRC01-class Abs: glNIH45-46, glVRC01, glVRC-PG19, and glVRC-PG20 (McGuire et al., 2013). Further modification to the 426c Env eliminated V1-3 and the gp41 subunit. This modification lead to the binding of two additional glVRC01 class Abs, gl3BNC60 and gl12A21, and limit the activation of narrowly, neutralizing Abs (McGuire et al., 2014a, 2016). All of these modifications combined result in the 426c Core immunogen.

In addition to the 426c Core, we have developed and characterized antigenically in collaboration with the Mascola and Kwong groups (NIH/VRC) a 426c Env-derived stabilized

trimer, or SOSIP, that binds glVRC01-class Abs (426c SOSIP TM). In contrast to the 426c Core, which consists of the inner and outer domain of the gp120 subunit, the 426c SOSIP TM is a full-length gp140 (gp120 and gp41 subunits), trimeric Env, but mutated to lack the NLGS in loop D and the V5 loop (McGuire et al., 2016).

eOD-GT8

eOD-GT8 is derived from the HxB2 clade B Env protein. eOD-GT8 consists of only the outer domain of the gp120 monomer. eOD-GT8 has been evolved to generate a high affinity glVRC01-class germline-targeting immunogen. Starting with the eOD, "evolved outer domain", homology modeling and computational methods were used to identify potential Env clashes with glVRC01-class Abs within and surrounding the CD4-BS. Libraries of eOD proteins were generated sampling every AA at these positions. These libraries were displayed on the surface of yeast and selected for high affinity binding to glVRC01-class Abs. The result was eOD-GT8, which can engage 8 glVRC01-class Abs (Jardine et al., 2013, 2015). A similar approach has now been taken with the 426c Env to generate a 426cOD (426c "outer domain") (Chapter II).

426cOD

Briefly, the 426cOD is similar in structure to eOD-GT8 in that it is the outer domain of the gp120 subunit, but is derived from the 426c Env sequence. Mutations were identified in the 426cOD through computational modeling and yeast display that enables 426cOD to bind the glVRC01 Ab. The details of the development of 426cOD are discussed in Chapter II.

BG505 SOSIP.v4.1-GT1

Another glVRC01-class germline-targeting immunogen is the BG505 SOSIP.v4.1-GT1. This immunogen is a soluble stabilized Env trimer derived from the BG505 Env, which is from a clade A virus. It has similar mutations to those present on the 426c Core to eliminate glycan clashes around the CD4-BS, but also has mutations in the V2 region to allow for germline V1-V2 Ab binding (Medina-Ramírez et al., 2017).

Strategies to modify recombinant Env to engage the germline form of bnAbs have now been applied to a number of other classes of bnAbs including those targeting the V3 loop and surrounding glycans – PGT121, and BG18 (Steichen et al., 2016, 2019); and other CD4-BS directed Abs including IOMA (unpublished).

Anti-idiotypic Abs (aiAbs)

An alternative approach to the use of an Env based immunogen to activate the germline form of bnAbs is the use of an aiAb. aiAbs are Abs that bind to the variable region of an Ab or BCR. aiAbs could function as germline-targeting immunogens for classes of bnAbs for which recombinant Env capable of binding the germline form have not yet been discovered, or as a substitute for Env immunogens in an effort to limit the activation of B cells targeting non-neutralizing epitopes on Env. Chapter IV will discuss the use of an aiAb, iv8, to elicit glVRC01-class Abs. Iv8 was produced by immunizing wild type (WT) mice with glVRC01. From these mice, B cells were isolated, immortalized using hybridoma technology and screened for the

production of Abs capable of binding glVRC01-class Abs. Iv8 binds to the germline forms of VRC01, NIH45- 46, 3BNC60, 12A21, and VRC-CH31.

Animal models

Due to the fact that no animal model expresses a homologous allele to the VH1-2*02 allele, transgenic mouse models have been made to study VRC01-class germline-targeting immunogens *in vivo*. These mice express elements of the glVRC01-class Abs (summarized in Table 1.3).

A mouse developed by David Nemazee expresses the glVRC01 HC V gene with the mature CDRH3 (glH-VRC01 mouse) (in one of two alleles; i.e. it is heterozygous for the glVRC01 HC). The glH-VRC01 mouse uses the endogenous mouse LC – therefore, a humanized HC will pair with different mouse LCs. The VRC01 B cell precursor (VH1-2*02 HC, paired with a 5 AA LC) frequency is ~.085% in the glH-VRC01 mouse (Jardine et al., 2015). A similar mouse model exists with the glH-3BNC60 HC V gene (mature CDRH3) knocked in, resulting in a mouse model expressing the gl3BNC60 HC in 100% of the B cells (Dosenovic et al., 2015). A "synthetic intermediate" (SI) form of the glH-3BNC60 mouse model also exists. The SI-3BNC60 mouse expresses the gl3BNC60 LC (mature CDRL3), but the mature 3BNC60 HC (Dosenovic et al., 2018).

The previously mentioned mice have the mature VRC01 or 3BNC60 HC with the mature VRC01 CDRH3 region knocked in. Mice have also been designed to have only the V gene knocked-in. These mice have HCs which express the VH1-2*02 allele but mouse D and J genes, resulting in diverse CDRH3s. This mouse model exists in two forms: one using either the endogenous mLC or the glVRC01 LC, 3-20*01 allele (mature CDRL3). The mouse is

heterozygous for both the transgenes, resulting in the expression of VRC01 precursors at 0.0675% or 37.6% respectively in the naïve B cell repertoire (Tian et al., 2016).

A draw back to using such these knock-in (KI) mouse models is that they express the elements of a VRC01-class precursor above the physiological frequency in humans, which is approximately ~.002% (Arnaout et al., 2011; DeKosky et al., 2015; Jardine et al., 2015).

There are also mouse models with the entire human V, D and J genes knocked in. These include the Kymouse (created by Kymab) (Lee et al., 2014), the Trianni mouse and the VelocImmune mouse (created by Regeneron) (Murphy et al., 2014). The advantage of these mice being that the Ab response will be produce Abs all derived from human V, D and J genes. Therefore the response will be more physiologically relevant to humans. However, in some cases, the glVRC01-class BCR is expressed at a frequency lower than in humans (mouse models are summarized in Table 1.3).

Table 1.3. Transgenic mice expressing elements of a glVRC01-class BCR

Mouse model	Transgene/s	Estimated glVRC01 frequency[a]	Reference
glH-VRC01	glVRC01 HC (mature CDRH3)	.085%	(Jardine et al., 2015)
glH/L-VRC01	glVRC01 HC (mature CDRH3), glVRC01 LC (mature CDRL3)	NR	(Abbott et al., 2018)
glH-3BNC60	gl3BNC60 HC (mature CDRH3)	.1%	(Dosenovic et al., 2015)
SI-3BNC60	Mature 3BNC60 HC, gl3BNC60 LC (mature CDRL3)	90%	(Dosenovic et al., 2018)
glVH1-2 mouse	glVH1-2 V gene	.0675%	(Tian et al., 2016)
glVH1-2/glLC	glVH1-2 V gene, glVRC01 LC (mature CDRH3)	37.6%	(Tian et al., 2016)
Kymouse	human HC VDJ genes and kappa VJ genes (HK) or lambda VJ genes (HL) or kappa and lambda VJ genes (HKL)	HK: .00002% HL and HKL: NR	(Lee et al., 2014),(Sok et al., 2016)
Trianni	Human HC VDJ genes, kappa VJ genes and lambda VJ genes	NR	none
VelocImmune	Human HC VDJ genes, kappa VJ genes	NR	(Murphy et al., 2014)

[a]NR indicates not reported

Guiding the evolution of glVRC01-class B cells

In such transgenic models, it has been shown that while the eOD-GT8 and 426c based germline-targeting immunogens are effective at expanding the germline precursors of the broadly neutralizing B cells, the B cells will not produce neutralizing Abs. This was first reported by Dosenovic et al., following immunization with eOD-GT8 or a 426c based germline-targeting immunogen in the glH-3BNC60 mouse model. This has now been shown by others in multiple glVRC01 transgenic mouse models (Briney et al., 2016; Dosenovic et al., 2015; Jardine et al., 2015; McGuire et al., 2016; Parks et al., 2019; Sok et al., 2016; Tian et al., 2016). Therefore, it is hypothesized that a priming immunization with a germline-targeting immunogen will need to be followed by additional immunizations ('boosts'). These boosting immunizations will guide the maturation of germline Abs to their mature, neutralizing form. In the case of glVRC01-class Abs, boosting immunizations must drive the acquisition of mutations to accommodate the steric hindrances surrounding the CD4-BS – particularly the glycan at position 276, which is conserved on most viruses.

This prime-boost strategy has been shown to be successful in the case of glPGT121 Abs which target a conserved GDIR AA motif at the base of the V3 loop and surrounding glycans on the HIV-1 Env protein. In this study, a transgenic mouse model expressing the glPGT121 BCR was employed. The first immunization is glPGT121 targeting immunogen: 10 MUT. 10 MUT is a germline-targeting immunogen derived from the BG505 SOSIP, which has been specifically designed to bind germline reverted PGT121 Abs (Steichen et al., 2016). This immunization is followed by two vaccinations with 'intermediate' immunogens, and finishes with 3 immunizations of WT, trimeric Env. The result was the production of heterologous tier-2

neutralizing Abs (Escolano et al., 2016). Other groups have now attempted to apply this strategy for other classes of bnAbs.

Prime-boost immunization schemes to elicit VRC01-like Abs have been evaluated, with limited success so far. The first study was conducted by the Schief and Nemazee groups and used the glH-VRC01 mouse model (Briney et al., 2016). This study first immunizes with the eOD-GT8 multimerized on 60-valent particle, followed by a single immunization with the GT3 (a gp120 subunit derived from the heterologous Env, BG505) and lacks the 276 NLGS and the NLGS in V5. This immunization scheme finishes with 2 immunizations with a soluble, trimeric Env (BG505) that also lacks the N276 glycosylation site. Thus, none of these immunogens have a glycan at position 276. This study shows success in generating a VRC01-like response in that it enriches for B cells with VRC01-like sequence characteristics, including 5 AA CDRL3s, some with a glutamic acid at position 96, and VRC01-like mutations in the HC. This immunization scheme elicited Abs displaying limited cross-neutralizing activity that was limited to viruses that lacked the 276 NLGS. Interestingly, two monoclonal Abs were identified that could weakly neutralize a single WT virus (Briney et al., 2016). However, it remains unknown if the 276 NLGS was utilized on these viruses.

The second study was conducted by the Fred Alt and Mascola groups and utilized the glVH1-2/glLC mouse model (Tian et al., 2016). This study tests a prime-boost immunization scheme, which begins with an eOD-GT6 (an early form of eOD-GT8) 60mer immunization, followed by immunizations with 426c Core proteins, which sequentially have glycans added back to the protein (first in V5 and then in Loop D (N276)), and finishes with a soluble stabilized 426c WT trimer. This immunization scheme uses a total of 6 different protein immunogens. This study shows their immunization scheme to successfully expand VRC01-like B cells, which

appear to incur mutations in both the VH and VL genes that are found in the mature VRC01 Ab. However, like the first study there is little evidence that these Abs elicited in this study are capable of neutralizing virus expressing WT Envs, with only one monoclonal Ab exhibiting neutralization of the autologous WT 426c virus. The focus of chapter III is on the identification of a boosting immunogen to the 426c Core that will elicit Abs capable of neutralizing a WT virus, in particular one which expresses the glycan at position 276.

Thesis goals

The major goal of this thesis is to elicit VRC01-class Abs through immunization. Specifically, this work sought utilize VRC01-class germline-targeting immunogens to first expand the VRC01-class precursors *in vivo* and use boosting immunogens to guide their maturation. The work presented here is immediately relevant to HIV-1 vaccine development and human health as the immunogens eOD-GT8 and 426c Core are being evaluated in human clinical trials. Chapter II will focus on the characterization of the primary immune response to VRC01-class germline-targeting immunogens: 426c Core, eOD-GT8, and 426cOD. Chapter III will discuss the identification of a boosting immunogen to the 426c Core in an effort to guide the maturation of VRC01-class B cells *in vivo*. Chapter IV will discuss the possible implementation aiAbs to elicit VRC01-class Abs. Finally, Chapter V will discuss the limitations of this work, potential avenues for further research, and the broader implications of this work on vaccine development.

Chapter II. HIV-1 VRC01 germline-targeting immunogens select distinct epitope-specific B cell receptors

The following text is from a manuscript in submission with minor edits. Yu-Ru Lin is a co-first author on this manuscript.

Abstract

Activation of B cells expressing the precursor BCRs of HIV-1 bnAbs requires specifically-designed immunogens. Here, we compared the abilities of three such germline-targeting immunogens against the VRC01-class receptors to activate the targeted B cells *in vivo*. We show that while a range of affinities can lead to the activation of VRC01 epitope-specific naïve B cells, the biophysical and biochemical context of germline-targeting immunogens dictates which epitope-specific VRC01 BCR variants are initially selected and influence the cross-reactivity and evolutionary fate of the activated VRC01 B cells. Our study indicates that the design of effective immunogens to activate BCRs leading to protective HIV-1 Abs will require a better understanding of how the biophysical properties of the epitope and its surrounding surface on the germline-targeting immunogen influence its interaction with the available receptor variants *in vivo*.

Introduction

The development of high-throughput assays to sequence VH/VL paired genes from individual B cells allowed the interrogation of large numbers of antigen-specific BCRs, prior to and following vaccination or infection (Scheid et al., 2009). Such studies, combined with structural analysis of the Ab-epitope complexes, revealed that bnAbs recognize distinct Env regions, including the CD4-BS, the apex region, the N332 glycan patch and the interface between the gp120 and gp41 subunits (Burton and Hangartner, 2016; Kwong and Mascola, 2012; McCoy and Burton, 2017). Those that bind to the same viral Env epitope can be derived from the same, or very similar, VH/VL pair combinations and have common paratope structures (Chen et al., 2019; Zhou et al., 2013). For instance, the anti-CD4-BS VRC01-class bnAbs are derived from the pairing of VH1-2*02 HCs and Vλ/Vκs (κ3-20, κ3-15, κ1-33, κ1-5, and λ2-14) LCs expressing 5 AA long CDRL3s (Huang et al., 2016; Kwong and Mascola, 2012; Sajadi et al., 2018; Scheid et al., 2011; Umotoy et al., 2019; Zhou et al., 2010, 2013). They recognize their epitope on Env with similar angles of approach and their paratopes share similar structures, despite being up to 30% divergent in AA sequence. Several elements of their VH and VL domains contribute to the strength of their interaction with Env and their breadth of neutralization, but their gene-encoded CDRH2 domains contribute the majority of the Ab buried surface area with Env (Jardine et al., 2016; Zhou et al., 2010), similar to observations made with neutralizing Abs against other viruses.

Natural virion-derived Env proteins capable of engaging the unmutated (commonly referred to as 'germline', gl) VRC01 BCRs expressed on naïve B cells are presently unknown, but specifically designed Env-derived recombinant proteins that bind glVRC01-class Abs have been engineered (Jardine et al., 2015; McGuire et al., 2016; Medina-Ramirez et al., 2017). These

proteins are employed as 'germline-targeting' immunogens to activate glVRC01-like BCRs *in vivo* (Dosenovic et al., 2015; Jardine et al., 2015; Parks et al., 2019). It is, however, expected that subsequent booster immunizations with heterologous, and more native-like, recombinant Env immunogens will be required to guide the maturation of glVRC01 BCRs towards their broadly neutralizing forms (Briney et al., 2016; Dosenovic et al., 2015; Tian et al., 2016).

Here, we examined whether the VRC01 epitope is equally effective in activating glVRC01-expressing B cells *in vivo* when expressed on three different germline-targeting immunogens, eOD-GT8 (Jardine et al., 2015), 426c Core (TM4ΔV1-3) (McGuire et al., 2016) and a newly designed 426c Outer domain (426cOD). eOD-GT8 has entered phase I clinical evaluation (NCT03547245), while the 426c Core is scheduled for clinical evaluation in 2021. We observed that despite the difference in binding affinities to glVRC01-class Abs, all three immunogens were efficient in eliciting VRC01-like Abs. However, while the epitope-specific Abs elicited by the three immunogens utilized the same VH/VL pairings, they differed at key positions by only a few AAs and as a result they displayed distinct Env cross-reactive properties. Our results reveal that the initial BCR selection by an immunogenic epitope is critically dependent on the biophysical properties of the epitope and of its surrounding surface area on the germline-targeting immunogen. Following that initial selection, the relative affinities of the selected BCRs dictate the fate of the corresponding activated B cells. Thus, germline-targeting immunogen-design efforts that are solely based on increasing the epitope-exposure on the immunogen or improving the affinity of an antigen are insufficient to accurately predict which target BCRs will be selected during immunization. As such our study provides relevant information to the design of more effective immunogens that target the precursor BCRs of protective Abs.

Results

Design and characterization of the 426c Env outer domain immunogen

The design of eOD-GT8 is based on the outer domain of the clade B HxB2 Env gp120 subunit (Jardine et al., 2015), while that of 426c Core is based on both the outer and inner domains of the clade C 426c gp120 subunit (McGuire et al., 2016). Here, we engineered a new germline-targeting protein that is derived from the 426c Core but lacks the inner domain (like eOD-GT8), termed 426c outer domain (426cOD). The design of 426cOD was based on that of eOD (which was the universal background of derived variants, such as eOD-GT8) (Jardine et al., 2015; Pejchal et al., 2011) (Supplemental Figure 2.1A). An initial design (426c base) engineered to bind glVRC01-class mAbs was found to bind one of six germline Abs (Supplemental Figure 2.1B). Random library mutagenesis and yeast-display yielded 426cOD, which binds four of eight glVRC01-class mAbs tested (Supplemental Figure 2.1C). We obtained a 3.4 Å X-ray structure of 426cOD bound to mature VRC01 (Figure 2.1A, Supplemental Table 2.1) which confirmed the proper folding of the designed 426cOD (Supplemental Figure 2.1D). Comparison with previously published structures of eOD-GT8 and 426c Core (Scharf et al., 2016) indicated that VRC01 and glVRC01's epitopes overlapped on each immunogen, and this comparison highlights differences in certain surface exposed residues between 426cOD and eOD-GT8 as follows: $S278R_{gp120}$, $Q361K_{gp120}$, $I370F_{gp120}$, $L455T_{gp120}$, $D457Q_{gp120}$, $D460Y_{gp120}$ (Figure 2.1C and Supplemental Figure 2.1A). These differences translate into different electrostatic surface potentials for the 426c-sequence-based immunogens (negatively charged) compared to eOD-GT8 (positively charged), particularly in the gp120 V5 region which interacts with the CDRH2 and the N-terminus of glVRC01 LC (Figure 2.1C).

To compare the interactions of the 3 antigens (426c Core, eOD-GT8 and 426cOD) with glVRC01, we modeled their interactions by superimposing glVRC01-bound structure with WT 426c Core (PDB ID 6MFT) (Borst et al., 2018) and with eOD-GT6 (PDB ID 4JPK) (Jardine et al., 2013) onto our newly solved structure of 426cOD bound to VRC01. We also modeled glVRC01 binding to eOD-GT8 by superimposing glVRC01 onto VRC01c-HuGL2 bound to eOD-GT8 (PDB ID 5IES) (Jardine et al., 2016). 426cOD buries ~971 $Å^2$ and ~1007 $Å^2$ upon binding glVRC01 (modeled interactions onto 6MFT and 4JPK, respectively) while eOD-GT8 buries ~1142 $Å^2$ (modeled interactions onto 5IES) and 426c Core buries ~947 $Å^2$ when binding gl3BNC60 (PDB ID 5FEC) (Scharf et al., 2016). 6-15 estimated H-bonds are formed between modeled glVRC01 and 426cOD (modeled onto 6MFT and 4JPK, respectively). These differences reflect the different conformations adopted by glVRC01 when binding the WT 426 Core (with glycans present) versus the 426c Core (Scharf et al., 2016). 21 estimated H-bonds are formed between glVRC01 modeled with eOD-GT8 while 20 estimated H-bonds are formed between 426c Core and gl3BNC60 (PDB ID 5FEC) (Scharf et al., 2016) (Supplemental Table 2.2-2.6).

The analysis also revealed differences in AA exposures between 426c Core and 426cOD when they interact with glVRC01: Val430, in the β20-21 region of gp120, present only in 426c Core showed some interactions with glVRC01 while Asp48 and Glu49, only present in 426cOD showed some interactions with VRC01. These differences could explain the lack of cross-reactivity between the elicited Abs by the various immunogens.

The glVRC01 HC buries a larger surface area with 426cOD than eOD-GT8 (Supplemental Table 2.6), while the LC buries a larger surface area with eOD-GT8: this is likely because of the LC interactions with bulkier residues present in eOD-GT8 compared to 426cOD:

Arg278$_{gp120}$ and Tyr460$_{gp120}$ in eOD-GT8 in place of Ser278$_{gp120}$ and Asp460$_{gp120}$ in 426cOD. The affinity of glVRC01 mAb for 426cOD is in the same range as for 426c Core (289 nM and 217 nM, respectively), while it is <0.1 nM for eOD-GT8 (Supplemental Figure 2.1E-2.1G).

We examined whether differences in affinity influence the efficiency by which the two immunogens select for naïve B cells that express VRC01 BCRs *in vivo*, and whether and how the presence of the gp120 inner domain of the 426c Core antigen influences this selection at the molecular BCR level.

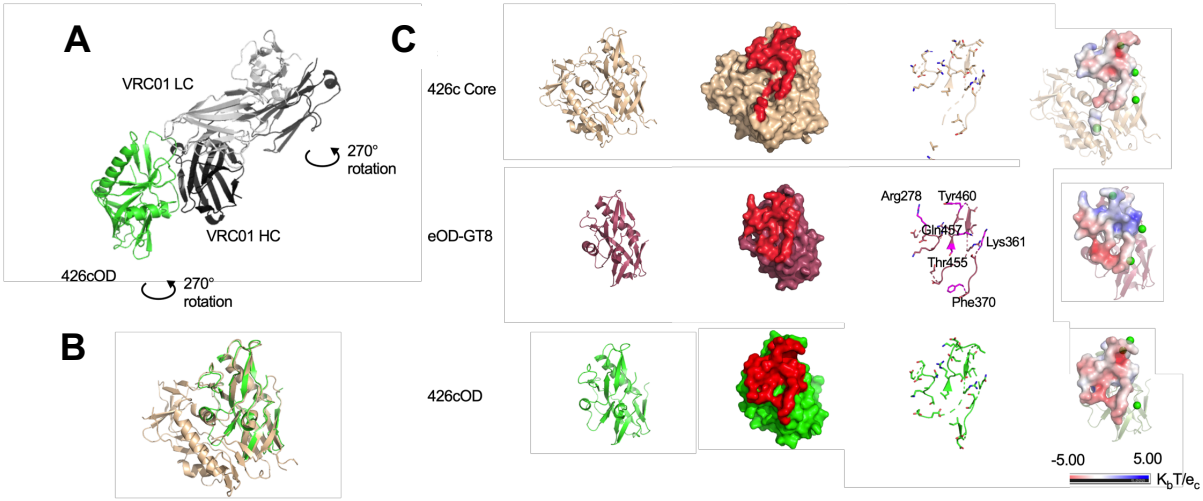

Figure 2.1. Structures of three VRC01 germline-targeting immunogens. (A) Crystal structure of 426cOD (green) bound to human mature VRC01 Fab (LC in gray, HC in black) shown in cartoon representation. **(B)** Overlay of 426c Core (tan, PDB ID 5FA2) and 426cOD (green). **(C)** Structural comparison of the three germline-targeting immunogens. From left to right: Cartoon representation. Surface representation of immunogens with glVRC01 epitope highlighted in red. glVRC01 epitopes shown in stick representation: eOD-GT8 residues that differ from those on 426c Core and 426cOD are highlighted in magenta. Electrostatic potential of glVRC01 epitopes. The location of potential NLGS around the VRC01 epitope on the three antigens are indicated by green dots (electrostatic potentials do not consider the glycans as exact glycosylation at these positions is unknown).

<u>Epitope affinity and the inner domain influences the efficiency by which epitope-specific naïve B cells can be isolated</u>

As orthologs of the human VH1-2*02 gene are not expressed in animal species such as mice, rats, rabbits and non-human primates (West et al., 2012), the abilities of the three antigens to engage glVRC01 BCRs *in vivo* were compared in a well-defined, KI mouse model that is heterozygous for the human inferred germline HC of the VRC01 mAb (glH-VRC01) (Jardine et al., 2015). Approximately 80% of B cells express the human transgene and all express mLCs; only 0.01% of which contain 5 AA long CDRL3s. As a result, approximately 0.08% of naïve B cells are expected to express VRC01-like BCRs, compared to 0.0002% -0.001% of naïve human B cells (Abbott et al., 2018; Jardine et al., 2015).

Individual eOD-GT8+/eOD-GT8 CD4-BS knock out (KO)-, 426c Core+/426c Core CD4-BS KO-, or 426cOD+/426cOD CD4-BS KO- B cells were isolated from the spleens of naïve mice. VH/VL genes were then amplified and sequenced. Approximately 50%, 85% and 60% of HCs isolated with 426c Core, eOD-GT8 and 426cOD, respectively, were the glH-VRC01 HC (indicated as VRC01^{glHC} (Figure 2.2A). The vast majority of mLCs that were selected by either antigen expressed 9 AA-long CDRL3s (Figure 2.2B). eOD-GT8 also selected for 6-8 AA long CDRL3s and 426cOD selected for 10 AA long CDRL3s. Only the two 'outer domain' antigens selected for mLCs expressing 5 AA long CDRL3s. We also sorted naïve B cells with the C4b-based form of 426c Core from three animals. Out of 282 VL genes that were sequenced only three LCs with 5 AA CDRL3s were identified (one from one animal (0.9%), two from another (1.9%) and none from the third animal (0%) (data not shown). The isolation of B cells expressing glVRC01-like BCRs by the two 'outer domain-based' antigens (eOD-GT8 and 426cOD), but not by 426c Core, despite the fact that 426cOD and 426c Core have similar affinities for glVRC01, suggests that the presence of the inner domain limits the accessibility of the VRC01 epitope by BCRs expressed on naïve B cells, but not by soluble Abs. We next

examined whether the differences observed in binding to naïve VRC01 B cells by the three immunogens had any effect on the ability of the immunogens to expand naïve B cells *in vivo*.

Epitope affinity does not influence the efficiency by which epitope-specific B cells expand during immunization

C4b-based nanoparticle forms (heptameric) of the three antigens were used as immunogens (Hofmeyer et al., 2013). Negative stain (ns) electron microscopy (EM) analysis confirmed that all three preparations had similar oligomeric features (Supplemental Figure 2.6). Two weeks post-immunization, CD4-BS-specific class-switched B cells were single cell-sorted from the lymph nodes and spleens and their VH/VL genes sequenced. Approximately 92%, 83% and 67% of the VHs sequenced from the 426c Core-, eOD-GT8- and 426cOD-immunized animals, respectively, were VRC01^{glHC} (Figure 2.2C). Approximately 24%, 34% and 20% of mLCs from the 426c Core-, eOD-GT8-, 426cOD-immunized animals, respectively, expressed 5 AA long CDRL3s (Figure 2.2D). The majority of the mLCs with 5 AA long CDRL3s were derived from κ8-30*1, but κ4-72*01, κV6-15*01, κ12-46*01, κ4–61∗01 and κV4-86*01 derived mLCs were also identified (Figure 2.2E). Thus, the three immunogens are effective in activating B cells expressing VRC01-like BCRs, despite differences in affinities, as others have reported in the case of model antigens (Kouskoff et al., 1998; Yang Shih et al., 2002). Dosenovic et al., also reported that while tetrameric baits of eOD-GT8 do not identify glVRC01-class B cells in the glH-3BNC60 mouse, immunization with the multimeric form of eOD-GT8 results in the activation of such cells (Dosenovic et al., 2015).

Different Env cross-reactivity properties of plasma Abs

Robust autologous plasma Ab responses were elicited by all three immunogens in all animals (Figure 2.2F-2.2H, Supplemental Figure 2.2). A large proportion of plasma Ab responses targeted the autologous CD4-BS in all three cases (Figure 2.2I), although 426c Core was more consistent in eliciting such Abs than the two outer domain immunogens. Thirteen of fourteen animals immunized with 426c Core elicited anti-eOD-GT8 plasma Ab responses (Figure 2.2F), which recognized the VRC01 epitope on eOD-GT8 (Supplemental Figure 2.2A), while only one of fourteen animals immunized with eOD-GT8 elicited (very weak) anti-426c Core plasma Ab responses (Figure 2.2G). All animals immunized with 426cOD elicited plasma Abs against the VRC01 epitope expressed on eOD-GT8, and 4 of 12 animals elicited anti-426c Core plasma Abs (Figure 2.2H and Supplemental Figure 2.2C). In contrast, only 4 of 14 animals immunized with eOD-GT8 generated anti-426cOD plasma Abs and with only partial specificity to the CD4-BS of 426cOD (Figure 2.2G and Supplemental Figure 2.2B).

The absence of anti-426c Core Abs in the plasma of the eOD-GT8-immunized animals was unexpected, as VRC01-like B cells utilizing the same VH/VL pairings (VRC01^{glHC} and κ8-30*1 mLCs) were isolated in both the 426c Core and eOD-GT8-immunized animals. Abs derived from this HC/LC pairing from the eOD-GT8- and 426c Core-immunized animals also displayed different cross-reactive properties. Those derived from the eOD-GT8-immunized animals did not bind 426c Core (but bound eOD-GT8 in a VRC01-epitope-dependent manner) (Supplemental Figure 2.3A), while those derived from the 426c Core-immunized animals recognized both 426c Core and eOD-GT8 (Supplemental Figure 2.3B). In sum, the cross-reactivities of VRC01-like Abs elicited by 426c Core and by eOD-GT8 differ.

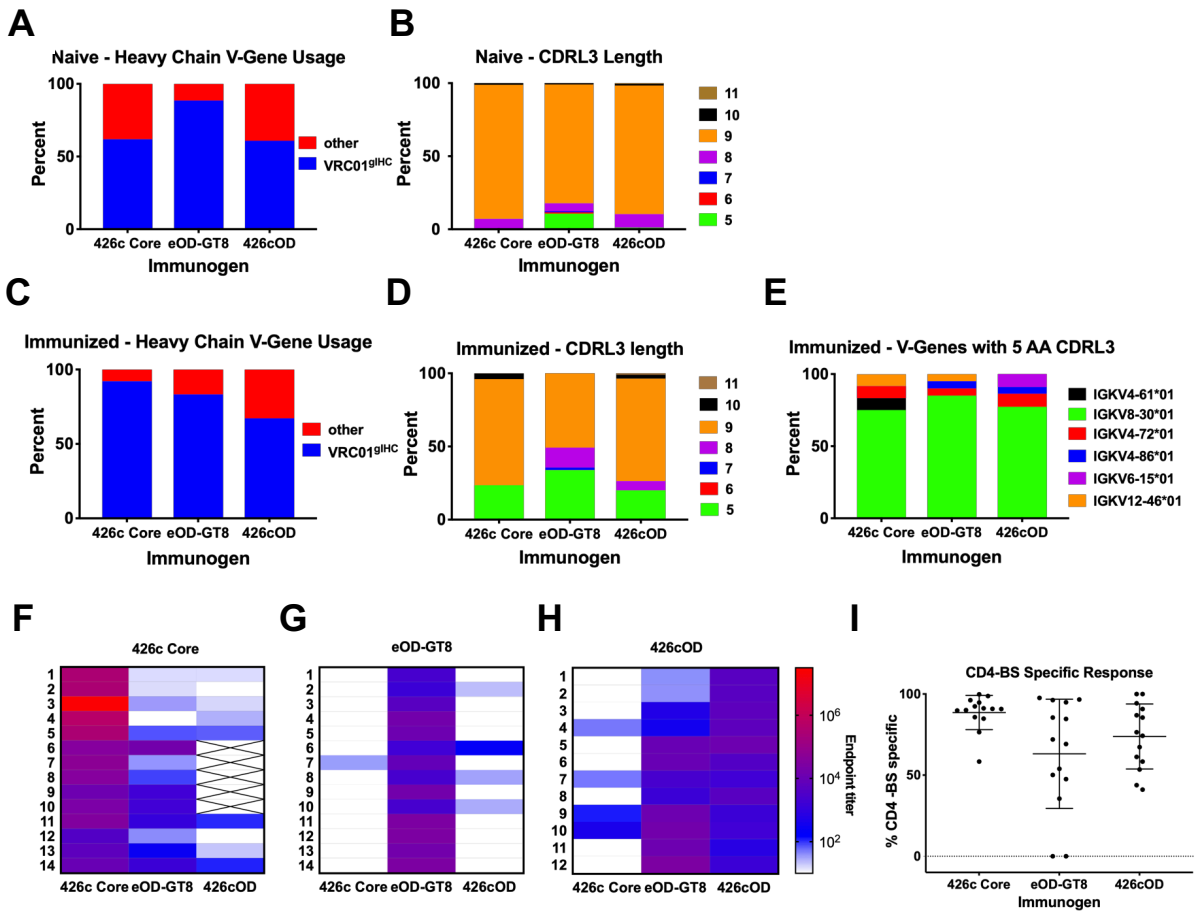

Figure 2.2. Vaccine elicited Ab and B cell responses. VH gene usage (number of sequences: 426c Core n = 21, eOD-GT8 n = 191, 426cOD n = 23 **(A)** and CDRL3 length (number of sequences: 426c Core n = 98, eOD-GT8 n = 225, 426cOD n = 125 **(B)** of naïve B cells sorted with 426c Core, eOD-GT8 or 426cOD. VH gene usage (number of sequences: 426c Core n = 89, eOD-GT8 n = 48, 426cOD n = 67) **(C)** and CDRL3 length (number of sequences: 426c Core n = 51, eOD-GT8 n = 59, 426cOD n = 110) **(D)** of antigen-specific B cells isolated 2 weeks post-immunization. **(E)** VL gene usage of 5 AA long CDRL3 B cells isolated from immunized animals (number of sequences: 426c Core n = 12, eOD-GT8 n = 20, 426cOD n = 22). Percentages indicate the frequency of VH or VL genes with the indicated characteristics out of the total number of VH and VL genes sequenced. **(F-H)** Plasma Ab endpoint titers 2 weeks post immunization with 426c Core **(F)**, eOD-GT8 **(G)** or 426cOD **(H)** against 426c Core, eOD-GT8, and 426cOD. Data is shown as a heatmap, with the strongest response (greater endpoint titer) in red. No color indicates undetectable reactivity. X indicates not tested. 12-14 mice immunized with each immunogen were tested. The animal number is indicated to the left of the heat map. **(I)** Percent of plasma Abs targeting the autologous CD4-BS, elicited by the indicated VRC01 germline-targeting immunogens. Each dot represents an animal.

eOD-GT8 and 426c Core select for different variants of VRC01 BCRs

A key difference between the eOD-GT8- and 426c Core-selected κ8-30*01 mLCs with 5 AA long CDRL3s is the selection of different AAs at the C-terminus of the CDRL3 (at the junction of the V and J genes) (Figure 2.3A). The eOD-GT8-selected CDRL3s with aromatic residues at position 96_{LC} followed by a threonine at position 97_{LC} ($W^{96}T^{97}$or $Y^{96}T^{97}$). As a result, 30% of the 5 AA long CDRL3s had the QQY**WT** motif and 60% had the QQY**YT** motif (Supplemental Table 2.7). This preferential selection was reported by Jardine et al (Jardine et al., 2015). In contrast, the 426c Core-selected κ8-30*01 mLCs with 5 AA long CDRL3s primarily expressed either a negatively charged AA at position 96_{LC} (E^{96}) or a positively charged AA at position 97_{LC} (K^{97}). As a result, 50% of the 5 AA long CDRL3s had the QQY**ET** motif and 50% had the QQY**YK** motif (Supplemental Table 2.8). In addition to these differences in the mLCs, most $VRC01^{glHC}$ sequences from the 426c Core-immunized animals contained a H35N mutation in the CDRH1 (as it exists in mature VRC01), which was not present in the $VRC01^{glHC}$ sequences from the eOD-GT8-immunized animals. 426cOD displayed a B cell selection phenotype with some similarities to those of eOD-GT8 and 426c Core, as it selected for κ8-30*01 mLCs with 5 AA long CDRL3s with ($W^{96}T^{97}$) (QQY**WT;** 20% of sequences), like eOD-GT8, but also with K^{97} (QQY**YK;** 20% of sequences), like 426c Core (Supplemental Table 2.9). The QQY**YS** sequence was the most prevalent (60% of the sequences). We propose that the positive electrostatic surface around the VRC01 epitope on eOD-GT8 disfavors the selection of CDRL3s with a positively charged AA at position 97_{LC} (K^{97}) and that the presence of Y^{30} on eOD-GT8 (D460 on 426c Core) selects for CDRL3s with aromatic residues at position 96 to gain enthalpically favorable aromatic ring interaction (Sangesland et al., 2019). We note that all known human VRC01-class bnAbs do not express such bulky AAs in their CDRL3s (Umotoy et al., 2019; Zhou et al., 2013).

To examine whether the disparate cross-reactivities of the VRC01-like Abs elicited by the germline-targeting immunogens are due to the selection of different AAs in their CDRL3 and CDRH1 domains, we performed targeted mutagenesis on the VRC01^{glHC} and κ8-30*01 genes of two Abs, p2b4 and p2b9, derived from eOD-GT8-immunized animals and examined how the mutations affected the Ab-binding properties. To this end, we introduced H35N or W96E on p2b4 and T97K on p2b9. While neither p2b4 and p2b9 bound to 426c Core, the individual CDRH1 or CDRL3 substitutions resulted in weak but detectable binding (Figure 2.3C). Of note, both type of mutations decreased the binding off-rates to eOD-GT8 and p2b4 with the W96E mutation displayed negligible off-rate to eOD-GT8. When the CDRH1 and CDRL3 substitutions were simultaneously introduced, the binding of both Abs to 426c Core became similar to that of VRC01-like Abs isolated from 426 Core-immunized animals (Figure 2.3B). Conversely, when the reversed mutations K97T or E96W were introduced to two VRC01^{glHC} and κ8-30*01 Abs (p1d3 and p1e5) isolated from the 426c Core-immunized animals, their binding to 426c Core was drastically diminished, while their binding to eOD-GT8 was unaffected (Figure 2.3B).

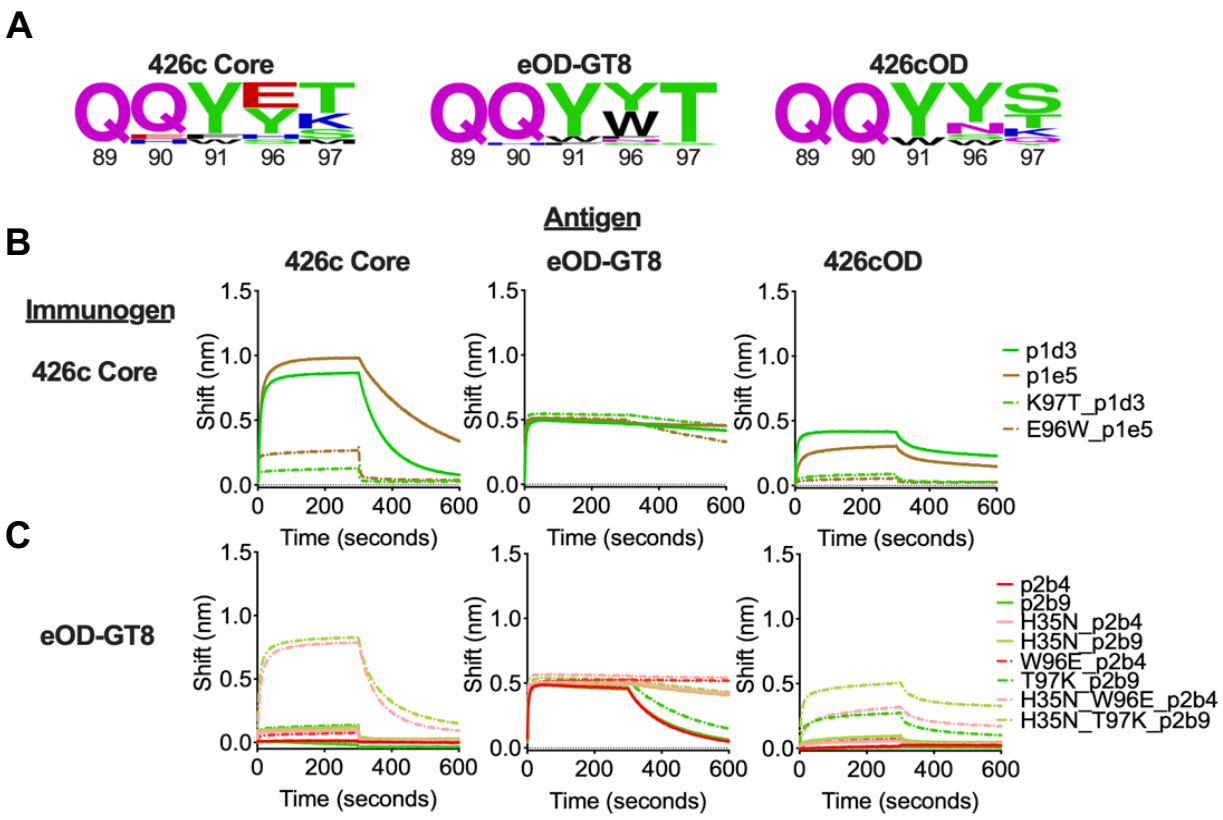

Figure 2.3. VRC01 germline-targeting immunogens select for different AAs within VRC01 BCRs. (A) Logo plots represent 5 AA CDRL3 sequences from antigen-specific B cells isolated 2 weeks post-immunization with the indicated VRC01 germline-targeting immunogens. The numbering of the CDRL3 region is based on the Kabat numbering system. Size of AA reflects frequency of use (number of sequences: 426c Core n = 12, eOD-GT8 n = 20, 426cOD n = 22). **(B-C)** Binding curves of mAbs isolated from 426c Core **(B)** and eOD-GT8 **(C),** and their indicated mutated forms to the indicated antigens.

We recently reported that VRC01-like Abs elicited by 426c Core in this KI mouse model can bind to certain heterologous WT gp120 Core proteins, even in the presence of N276-associated glycans, which normally prevent the binding of germline VRC01-class mAbs to Env (Parks et al., 2019). These heterologous Cores are derived from different clades (93TH057 is clade A/E, Q168a is clade A, and HxB2, 45_01 and QH0692 are clade B), they express a functional N276 glycan site and are not recognized by glVRC01 (Parks et al., 2019). In agreement, two of eight 426c Core-elicited VRC01-like Abs (p1a6 and p1a7) recognized two

(45_01dH1 WT Core and HxB2 WT Core) of the five heterologous WT Cores proteins tested (Figure 2.4A). In contrast, the eOD-GT8-elicited VRC01-like Abs did not display such cross-reactive reactivities (Figure 2.4B). We tested the p2b4 and p2b9 mutants for binding to the heterologous WT Core proteins and observed that the double substitution on the background of p2b4 (H35N, W96E) conferred cross-reactivity to the two heterologous Core proteins recognized by the 426c Core-elicited VRC01-like Abs (Figure 2.4C).

Thus, even though eOD-GT8 and 426c Core effectively stimulate naïve B cells expressing BCRs composed of VRC01^{glHC} paired with κ8-30*01 mLCs with 5 AA long CDRL3s, they select for different AAs at positions 96 and 97 (Kabat numbering) in the CDRL3 (junction of V and J genes). Additionally, the VRC01^{glHC} from the 426c Core-immunized animals almost universally acquired the H35N mutation. Those few AA differences are responsible for differences in the cross-Env recognition potentials of the VRC01-like Abs elicited by eOD-GT8 and by 426c Core. Our results suggest therefore that VRC01-like Abs expressing bulky AAs at position 96 will not bind effectively the VRC01 epitope on heterologous proteins in the presence of the inner gp120 domain. In agreement with this, VRC01-like Abs elicited by 426cOD, expressing tyrosine at position 96, have no binding to any heterologous WT gp120 Core Env proteins (Figure 2.4D). As the first wave of VRC01-like Abs elicited by these germline-targeting immunogens are minimally mutated the Abs did not display neutralizing activities, in agreement with previous reports (Briney et al., 2016; Parks et al., 2019).

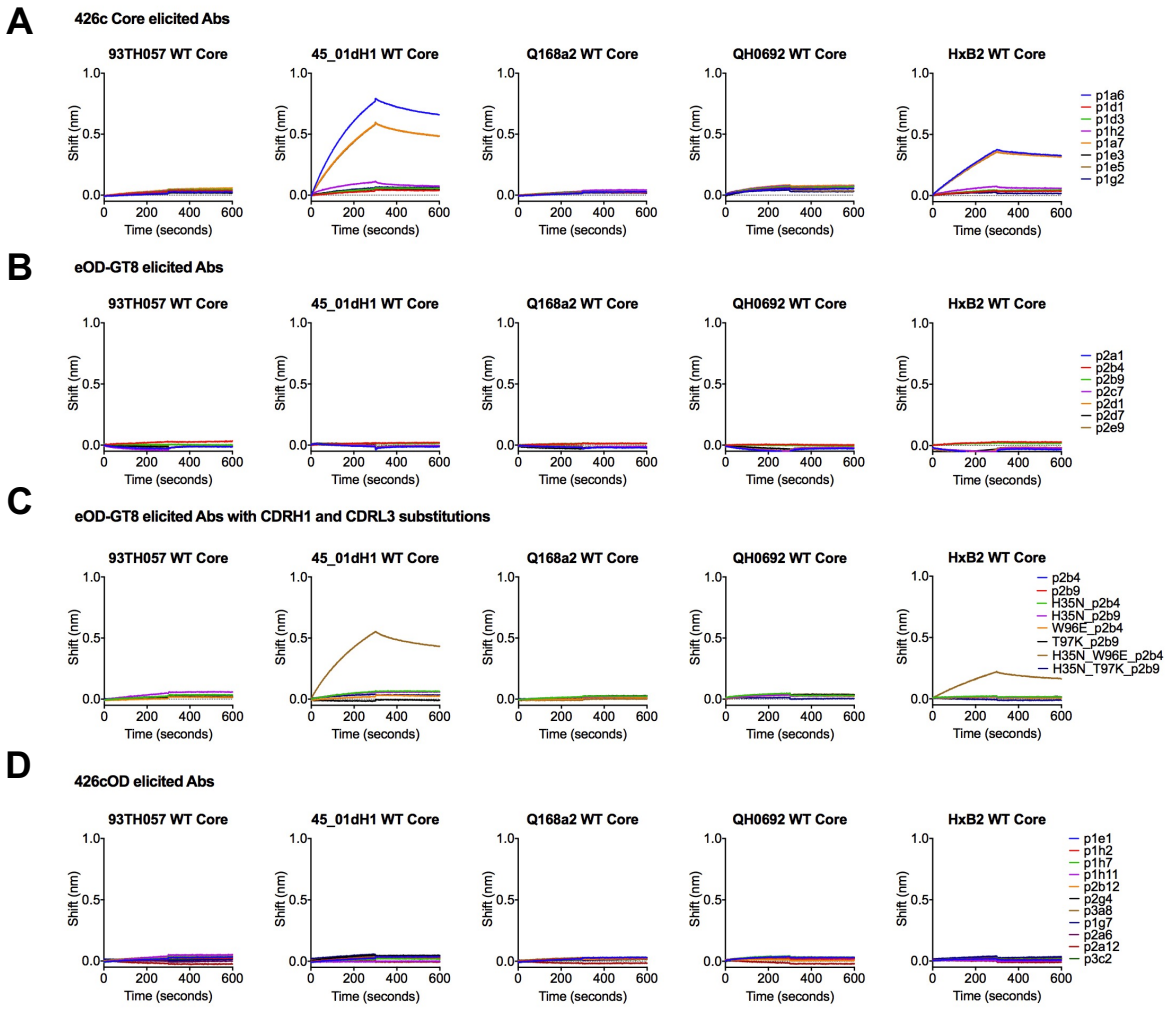

Figure 2.4. Vaccine elicited mAbs binding to multimeric (C4b) heterologous Core Env. BLI was used to evaluate mAb binding to Env. Binding curves of mAbs elicited by 426c Core **(A),** eOD-GT8 **(B)** and 426cOD **(D)** to the indicated heterologous WT Core proteins. **(C)** Binding curves of mAbs elicited by eOD-GT8 with CDRL3 and CDRH1 substitutions to multimeric heterologous Core Env.

Temporal evolution of epitope-specific VRC01-like B cell variants

The germinal center reaction is a dynamic process during which B cell clones compete for antigen and T-cell help (Dal Porto et al., 2002; Kouskoff et al., 1998; Silva et al., 2017). To examine whether and how the VRC01-like B cell responses elicited by the three immunogens evolve over time, animals were immunized with the three immunogens, CD4-BS+/KO- B cells

were isolated 6 weeks later, and their VH/VL genes were sequenced. The evolution of the plasma Ab responses to all three immunogens was also evaluated. The titers and epitope specificities of autologous and heterologous plasma Abs elicited by all three immunogens remained stable over the 6-week observation period (Supplemental Figure 2.4). That is: (A) 426c Core generated autologous, anti-eOD-GT8 and anti-426cOD plasma Abs (the heterologous Ab responses being exclusively directed to the CD4-BS); (b) eOD-GT8 generated autologous but not heterologous Abs; and (c) 426cOD elicited strong autologous and anti-eOD-GT8 Ab responses, but weaker anti-426c Core Ab responses (a fraction of the heterologous Ab responses being exclusively directed to the CD4-BS).

Significantly more AA mutations accumulated in both the VH/VL genes 6 weeks post-immunization, irrespective of the immunogen (Supplemental Figure 2.5 and Supplemental Tables 2.7-2.9). The H35N mutation was present in 90% of VRC01^{glHC} sequences from 426c Core-immunized animals. Additional mutations were also selected in CDRH1, CDRH2 and FW3 of the VH gene (Supplemental Table 2.8). The H35N mutation was also preferentially selected (71%) in the VRC01^{glHC} sequences from 426cOD-immunized animals (Supplemental Table 2.9). In contrast, no clear pattern of AA selection was evident in the VRC01^{glHC} sequences from eOD-GT8 immunized animals (Supplemental Table 2.7).

All VRC01^{glHC}-associated mLCs from the 426c Core-immunized animals were derived from κ8-30*1 and all expressed the five AA CDRL3 QQY**YK** sequence (i.e., the E^{96} mutation was not evident) (Supplemental Table 2.8). This sequence also dominated (64%) the mLCs sequences from the 426cOD-immunized animals (Supplemental Table 2.9). The mLC mutations were primarily confined to the CDRL1s and resulted in the accumulation of negatively charged AAs (Asp or Glu). A more complex pattern of mLCs with 5 AA CDRL3 paired with VRC01^{glHC}

was observed in the eOD-GT8-immunized animals (Supplemental Table 2.7). Between weeks 2 and 6 post-immunization, the relative frequency of κ8-30*01 mLCs decreased by approximately half (from 89% to 47%) while the relative frequencies of non-κ8-30*01 mLCs increased by approximately five-fold (from 11% to 53%). While the κ8-30*01 mLCs isolated from the 426c Core-immunized animals were mutated from germline (Supplemental Tables 2.8), the majority of κ8-30*01 sequences isolated from the eOD-GT8-immunized animals remained unmutated (15/28 sequences had 0 AA mutations) (Supplemental Table 2.7). In contrast, the non-κ8-30 mLCs isolated from eOD-GT8-immunized animals were extensively mutated at week 6 (up to 9 AA mutations).

Of note, all the non-κ8-30*01 mLCs have short CDRL1 domains, as is the case of all known VRC01-class bnAbs (Zhou et al., 2013). As observed at week 2 post-immunization, eOD-GT8 preferentially selected for QQY**YT**, QQY**WT** CDRL3s for all κ8-30*01 mLCs but in the case of κ4-61*01, the QQY**ET** sequence was present in 5/6 mLCs sequenced and paired with VRC01^{glHC}. The 426cOD selection pattern was intermediate to those of 426c Core as most of the κ8-30*01-associated 5 AA CDRL3s expressed the QQY**YK** sequence and the non-κ8-30*01 mLCs were unmutated from germline (Supplemental Table 2.9).

VRC01-like mAbs were generated from paired VH/VL sequences from the eOD-GT8-immunized animals, and their binding to the three immunogens were evaluated (Figure 2.5). We included both κ8-30*01-derived and non-κ8-30*01-derived mAbs, some of which (κ4-61*01) expressed CDRL3s with the QQY**ET** sequence that predominates in the 426c Core-elicited VRC01-like Ab responses (Supplemental Table 2.7). None bound the 426c Core and 426cOD proteins. Thus, the presence of shorter CDRL1s on VRC01-like Abs with κ4-61*01LCs (5 AA

CDRL3) does not appear to improve their binding to the VRC01 epitope on heterologous Envs. We expect, however, that VRC01-like BCRs with short CDRL1s can more easily mature towards broadly neutralizing forms, as short CDRL1s are necessary to accommodate the N276 glycans and elements of the V5 gp120 domains (Zhou et al., 2013).

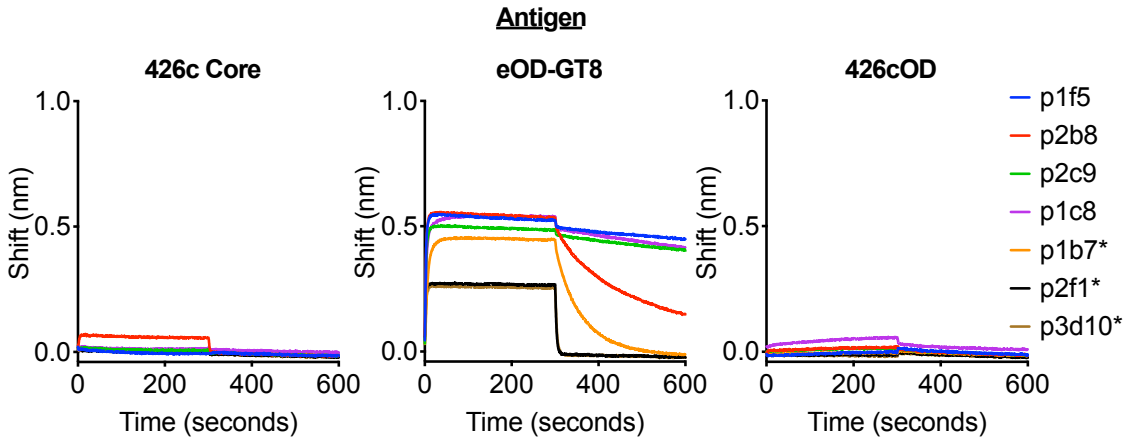

Figure 2.5. Binding properties of mAbs isolated 6 weeks post immunization with eOD-GT8. mAbs isolated 6-weeks post-immunization with eOD-GT8 were evaluated for binding to 426c Core, eOD-GT8 or 426cOD. mAbs utilizing κ4-61*01 are noted with an asterisk.

Interactions of human VRC01-like Abs with 'germline-targeting' immunogens

We generated VRC01-like Abs from previously published VH/VL paired sequences from naïve human B cells sorted with eOD-GT8 (Havenar-Daughton et al., 2018) and examined their binding to the three 'germline-targeting' immunogens (Figure 2.6). The Abs only bound eOD-GT8. These results confirm preferential interaction of eOD-GT8-selected VRC01-like Abs for eOD-GT8 and suggest that the three antigens evaluated here are not recognized by all available variations of human VRC01-like putative Abs precursors.

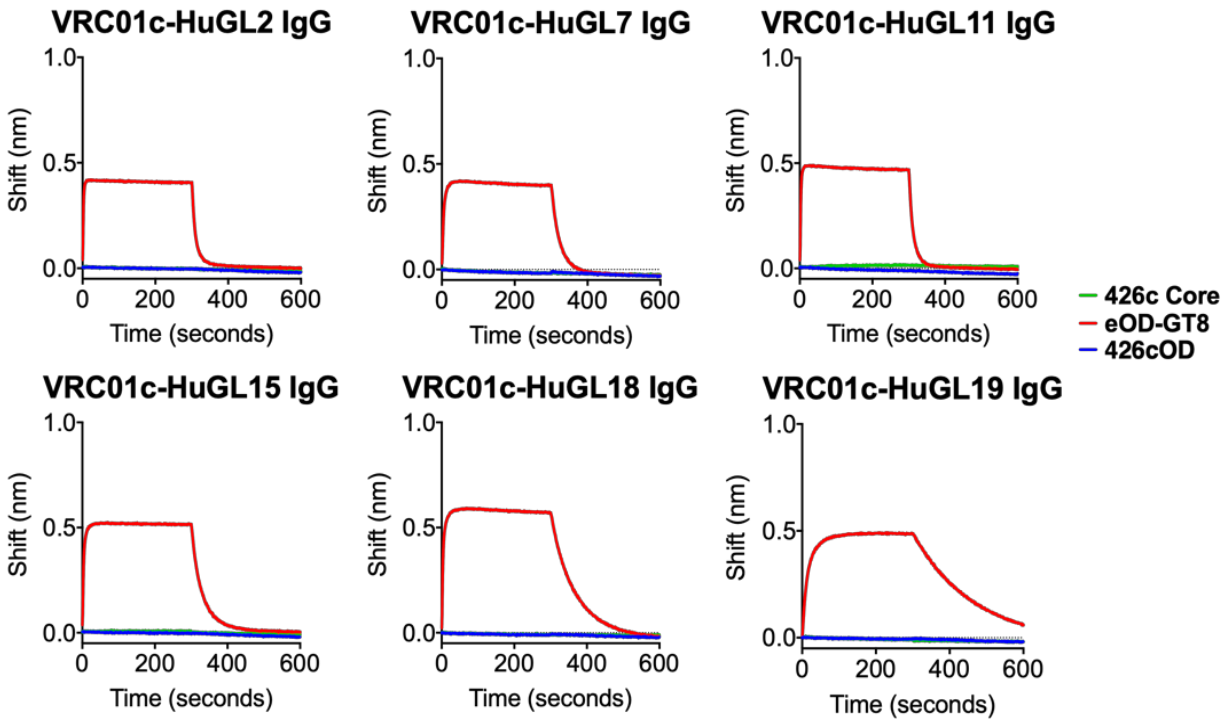

Figure 2.6. Binding properties of human germline VRC01-like Abs isolated with eOD-GT8. Six germline VRC01 Abs derived from naïve human B cells that were sorted by eOD-GT8 were tested for binding against 426c Core, eOD-GT8 or 426cOD. BLI was used to evaluate mAb binding to Env. BLI curves are shown. Data is representative of two replicates.

Discussion

The development of VRC01-class bnAbs by vaccination will require the activation of their unmutated BCR precursors by immunizing with germline-targeting immunogens, and the accumulation of specific VH/VL AA mutations through sequential immunizations with heterologous Envs (Dosenovic et al., 2015). Our study reveals that depending on the background onto which the VRC01 epitope is expressed on the germline-targeting immunogen, B cells with different epitope-specific VH/VL pairs are selected to enter the germinal center reactions. That is, from the available pool of VRC01-like B cells available, each germline-targeting immunogen will select a different subpopulation (containing B cells with different affinities towards that immunogen). As a result, the VRC01-class Ab responses elicited by different germline-targeting immunogens display distinct heterologous Env cross-recognition properties. We have defined a set of mutations responsible for these cross-recognition properties (Figure 2.3C) confirming that our studies unveiled differences in the subpopulations of Abs elicited by different immunogens, without identifying which immunogen drives the most promising B cell subpopulation. We expect therefore that following eOD-GT8 and 426c Core human immunizations, different booster immunogens will be required to further expand the initial waves of VRC01-like B cells stimulated by these two germline-targeting immunogens. Indeed, the VRC01-like Abs elicited in this animal model by 426c Core are boosted by HxB2 WT Core (Parks et al., 2019) while those elicited by eOD-GT8 expand following a boost immunization with BG505 core-GT3 (Briney et al., 2016). Our data, therefore, reveal aspects of immunogen-BCR interactions that may have been underappreciated previously, but which we believe will contribute to the development of more effective prime-boost immunization protocols for the elicitation of bnAbs. Our results highlight potential limitations of eOD-GT8 and 426c Core. eOD-GT8 may not stimulate VRC01

B cells that can bypass the N276 associated glycans, thus necessitating the use of booster immunogens also lacking the N276 glycan site and consequently further increasing the affinities of Abs that cannot overcome this key obstacle, while 426c Core may activate VRC01 Abs with long CDRL1 domains that will be less amenable to maturation towards their broadly neutralizing forms.

The observations we report here are applicable to germline-targeting immunogens against other classes of CD4-BS bnAbs (Bonsignori et al., 2016; Williams et al., 2017) and bnAbs against other Env regions such as the apex domain of the HIV-1 trimer (Andrabi et al., 2015), or the N322 glycan patch (Escolano et al., 2019; Steichen et al., 2019), but also to non-HIV bnAbs such as Influenza and HCV (Chen et al., 2019; Sangesland et al., 2019). We expect that the differences in BCR-selection by germline-targeting immunogens to be even more pronounced in more diverse BCR backgrounds, including humans.

Subsequent to the initial glVRC01 BCR-selection by germline-targeting immunogens, the fate of the corresponding B cells is defined by the relative affinities of the BCR variants, as others have reported in studies conducted with model antigens (Dal Porto et al., 2002; Kouskoff et al., 1998; Silva et al., 2017). The relative numbers of the high affinity, epitope-specific glVRC01^{HC}/κ8-30*01 B cells that are preferentially selected by eOD-GT8 and which predominate the early B cell response, decrease over the 6-week period of observation and their BCRs do not accumulate SHMs. During the same period, the frequencies of lower affinity VRC01-like B cells expressing different LCs (also paired with glVRC01^{HC}) increase and their BCRs accumulate SHMs. In contrast, epitope-specific glVRC01^{HC}/κ8-30*01 B cell variants selected by 426c Core have lower affinity for the VRC01 epitope and predominate both during the early and late B cell response and undergo somatic hypermutation.

Overall, our study indicates that the development of effective germline-targeting immunogens to target specific BCRs, such as those known to give rise to bnAbs, will require a better understanding of how the biophysical properties of the epitope and its surrounding surface on the immunogen influences its interaction with the available BCR variants *in vivo*, as structural information or affinity of the immunogen alone are insufficient to accurately predict which BCRs will initially be selected.

Acknowledgements

This study was supported by NIH/NIAID grants R01 AI104384 and P01 AI138212. We thank the James B. Pendleton Charitable Trust for the support of the Formulatrix robotic instrumentation. X-ray diffraction data were collected at the Berkeley Center for Structural Biology beamline 5.0.1, which is supported in part by the National Institute of General Medical Sciences. The Advanced Light Source is supported by the Director, Office of Science, Office of Basic Energy Sciences, of the United States Department of Energy under contract DE-AC02-05CH11231. P.-S.H. is supported by the U.S. Department of Energy, Office of Science, Office of Advanced Scientific Computing Research, Scientific Discovery through Advanced Computing (SciDAC) program and Stanford's Bio-X Interdisciplinary Initiatives Seed Grants Program.

Declaration of interests

The authors declare no competing financial interests. P.-S.H. is an inventor on the patent for eOD (US Patent 10,421,789). L.S. is an inventor on US Patent US 2018/0117140.

Methods

Resource availability

Lead Contact

Further information and requests for reagents should be directed to and will be fulfilled by Leonidas Stamatatos (lstamata@fredhutch.org).

Materials Availability

All reagents generated in this study can be made available upon request through Materials Transfer Agreements.

Data and Code Availability

The sequences of mAbs reported are deposited on GenBank (MT585207-MT585272). The sequence of 426cOD is reported here and deposited on GenBank (MT671449). Coordinates and structure factors for 426cOD in complex with mature VRC01 Fab have been deposited with the Protein Data Bank under accession code 6VLW. Supplemental information is available.

Experimental Model and Subject Details

Immunizations were performed with the C4b-based nanoparticles (heptameric forms) (Hofmeyer et al., 2013). Immunizations were performed in the glH-VRC01 mouse (Jardine et al., 2015). It is heterozygous for the transgene (glVRC01 HC) and expresses mLCs. Details on the number of animals used are presented in Supplemental Table 2.12. 6-12 week old glH-VRC01 KI mice were immunized intramuscularly with 60 μg or 50 μg of recombinant Env along with 60μg of

polyinosinic:polycytidylic acid (poly (I:C)) or 50 ul GLA-LSQ (IDRI) split between the rear hind legs. Male and female mice were included in this study. Blood was collected via cardiac puncture two- or six-weeks following immunization, at which time spleen and lymph nodes were also harvested. Spleen and lymph nodes were processed into a single cell suspension separately and frozen in FBS + 10% DMSO and stored in liquid nitrogen until further use. Blood, spleens and lymph nodes were also isolated from non-immunized animals. The Fred Hutch Institutional Animal Care and Use Committee approved all mouse studies.

Computational design of the clade C 426c outer domain

RosettaRemodel (Huang et al., 2011) was used to engineer a gp120 outer domain of 426c based on 426c Core (426c TM4Δ1-3)(McGuire et al., 2016). To isolate the outer domain from inner domain, the C terminus of the α5 helix and N terminus of C2 region was closed with RosettaRemodel and a new N and C terminus of the outer domain was introduced before V4. To improve Ab interaction, asparagine(N)-linked glycan groups shielding the CD4-BS, at residues 289_{gp120}, 332_{gp120}, and 391_{gp120}, were mutated to glutamines. A glycan site at position 448_{gp120} was re-introduced to the 426c sequence, as it was previously identified to be kinetically important for proper folding of the engineered outer domain. RosettaRemodel was used to introduce mutations in the residues adjacent CD4-BS. Structural redesign, along with modeled disulfide bonds were used to stabilize the circularly permuted 426c outer domain, called 426c base (Supplemental Methods).

Construction of the clade C 426c outer domain

We ordered 426cOD-base gene segments with flanking segments homologous to pTT3 vector from Integrated DNA Technologies (IDT). We then used In-Fusion HD Cloning Plus system

(Takara Bio USA, Inc.) to clone the gene construct into pTT3 vector with C-terminal 6x His-Avi-Tag.

Construction of yeast library

PCR and sequencing primers were obtained from IDT (Supplemental Table 2.10). The 426c OD-base gene segment was amplified using extension primers to add pETCON yeast homologous recombination segments to each end. The GeneMorph II Random Mutagenesis Kit (Agilent) was used to generate the library which was then run on a 1% agarose gel and the gene was gel extracted and purified (Qiagen QIAquick Gel Extraction Kit). The purified library pool was then amplified with the extension primers to generate 12µg of DNA. Yeast EBY100 cells were transformed with library DNA and linearized pETCON plasmid (McGuire et al., 2016). After transformation (minimum of 1E7 transformants), cells were grown for two days in SDCAA medium at 30 °C. Cells can then be galactose induced with SGCAA media for yeast display experiment or stored in SDCAA with 20% glycerol (w/v) at 1E7 cells per aliquot at -80 °C.

Yeast display

Cell aliquots were thawed on ice and centrifuged at 13,000 RPM for 30s, resuspended at 1E7 cells per ml of C-Trp-Ura medium, and grown at 30°C overnight. Cells were then centrifuged at 13,000 RPM for 1 min and resuspended (1E7 per ml) in SGCAA medium and induced at 30°C for 16-20 hrs. glVRC01 IgG was biotinylated with EZ-Link NHS-PEG$_4$-Biotin and labeling kit (Thermo Fisher Scientific) at a one to one ratio of protein to biotin and tetramerized with streptavidin-phycoerythrin (SA-PE, Invitrogen). Yeast cells expressing Env on their surface (based on glVRC01-SA-PE and anti-c-Myc fluorescein isothiocyanate (FITC, Miltenyi Biotec)

staining) were sorted using a Sony SH800. Sorted cells were grown for two days in C-Trp-Ura medium at 30°C. After 4 rounds of sorting the cells were plated on a C-Trp-Ura agarose plate. DNA from individual colonies was isolated and sequenced (GENEWIZ) to identify potential AA mutations that lead to glVRC01-recognition. Mutations were then introduced into the mammalian pTT3 426c base plasmid by site-directed mutagenesis using Stratagene Quick Change II system (Agilent Technologies, Inc.) and conventional primers ordered from IDT (Supplemental Table 2.11).

Protein expression and purification

All the recombinant Envs were expressed and purified as previously described (McGuire et al., 2016; Parks et al., 2019) Briefly, Envs were produced in 293E or 293F. Cell supernatants were purified by lectin affinity chromatography (*Galanthus nivalis*, Vector Labs), then subjected to Superdex 200 size exclusion chromatography (GE Healthcare).

Monomeric proteins were produced by transfecting 293E cells with Env encoding plasmid. Cells are cultured for 6 days at 37^0C, 5% CO_2, 80% humidity, and shaking at 125 RPM. Cells were centrifuged for 3000 RPM for 30 minutes and the supernatant sterile filtered through at .22 uM filter. Protein was purified by passing the cellular supernatant over a 5ml Fast Flow HisTrap column (Fisher Sci, Cat # 45000326). The eluted protein was purified on SEC as described above.

426c Core and 426cOD CD4-BS KO Env constructs contain the D368R, E370A, and D279A mutations, while the eOD-GT8 KO contains the D368R mutation and the AAs at positions 276-279 have been mutated to “NFTA”.

Crystallization

The VRC01 Fab and 426cOD complex was formed by mixing equal molar parts of VRC01 Fab and 426cOD for 1 hour at room temperature. The complex was concentrated to ~10 mgs/mL for crystallization trials.

Crystallization, data collection and refinement

Crystallization conditions were screened and monitored with an NT8 drop setter and Rock Imager (Formulatrix). Screening was done with Rigaku Wizard Precipitant Synergy block no. 2, Molecular Dimensions Proplex screen HT-96, and Hampton Research Crystal Screen HT using the sitting drop vapor diffusion method. Final crystals were grown in a solution of 18.43% PEG 3350, 11- .01%, Lithium Sulfate, 0.11 M Imidazole pH 6.5. Crystals were cryoprotected in a solution of 30% excess of the crystallization condition and 20% glycerol. Crystals were sent to ALS 5.0.1 and diffraction data was collected to 3.42 Å. Data was processed using HKL2000 (Otwinowski and Minor, 1997). The structure was solved using molecular replacement using PDB ID: 5IFA as a search model in Phaser in Phenix. The structure was further refined with COOT and Phenix. The refinement statistics are summarized in Supplemental Table 2.1 (Adams et al., 2010).

ns EM sample preparation

All nanoparticle constructs used in this study (3 µL) were negatively stained at final concentrations between 10 µg/mL and 20 µg/mL using Gilder Grids overlaid with a thin layer of amorphous carbon and 2% uranyl formate, as previously described (Veesler et al., 2014).

ns EM data collection and processing

Data were collected on an FEI Technai 12 Spirit 120kV electron microscope equipped with a Gatan Ultrascan 4000 CCD camera. A total of 150-200 images were collected per sample by using a random defocus range of 1.5–2.5 µm with a total exposure of 45 e−/A^2. Data were automatically acquired using Leginon (Suloway et al., 2005), and data processing was carried out using Appion (Lander et al., 2009). The parameters of the contrast transfer function (CTF) were estimated using CTFFIND4 (Mindell and Grigorieff, 2003), and particles were picked in a reference-free manner using DoG picker (Voss et al., 2009). Particles were extracted with a binning factor of 2 after correcting for the effect of the CTF by flipping the phases of each micrograph with EMAN 1.9 (Ludtke et al., 1999). Particle stacks were pre-processed in RELION/3.0 with an additional binning factor of 2 applied, resulting in a final pixel size of 6.4 Å. Resulting particles were sorted by reference-free 2D classification over 25 iterations (Kimanius et al., 2016; Scheres, 2012a, 2012b; Zivanov et al., 2018).

BLI

Ab binding to recombinant Env proteins was determined using biolayer interferometry on the Octet Red 96 (ForteBio, Inc, Menlo Park, CA). Briefly, anti-human Fc capture biosensors (ForteBio, Cat#: 18-5063) were activated by immersion into 1x Kinetics Buffer (1x PBS, 0.1% BSA, 0.02% Tween-20, 0.005% NaN3) for 10 minutes. Abs were loaded onto an anti-human Fc capture probe at 20 ug/ml. The probes were then dipped into solutions containing 2 uM recombinant Env. Parameters for all BLI assays were: 30 seconds of baseline measurement, 240 seconds to load the Ab onto the anti-human Fc capture probe, 60 seconds of baseline measurement, 300 seconds of association, 300 seconds of dissociation. All measurements of

Env-Ab binding were corrected by subtracting the background signal obtained from Env traces generated with an irrelevant negative control IgG.

Kinetic analyses were performed by BLI using recombinant Fabs loaded onto FAB2G biosensors (ForteBio, Cat#: 18-5126) (@ 40 ug/ in 1XPBS) and 2-fold dilutions of Env monomers. The assay parameters are the same as for measuring the binding of IgG, but with an extended dissociation phase of 600 seconds. Curve fitting was used to determine relative apparent Ab affinities for envelope was performed using a 1:1 binding model and the data analysis software (ForteBio). Mean k_{on}, k_{off}, and K_D values were determined by averaging all binding curves within a dilution series having R^2 values of greater than 95% confidence level.

Plasma and Ab ELISA (Enzyme linked immunosorbent assay)

Plasma samples were heated inactivated at 56^0 C for 1 hour, centrifuged at 13,000 RPM for 10 min at stored at 4^0 C or -20^0 C. ELISAs were done in a 384 well plate format. 30 ul of protein at 0.1 uM in coating buffer (0.1M sodium bicarbonate, pH: 9.4-9.6) was added to each well and incubated a room temperature overnight. Plates were washed 4x with ELISA wash buffer (1XPBS + .2% Tween-20). 80 ul of blocking buffer (1X PBS + 10% non-fat milk + 0.03% Tween20) was added to the plates and they were incubated at 37^{o}C for 1-2 hours. Plates were then washed 4x with ELISA wash buffer. Plasma was diluted 1:10 in blocking buffer and diluted 1:3 across or down the plate. His tag control started at 1 mg/ml. The plates were incubated for 1 hour at 37^{o}C. The plates were washed 4x with ELISA was buffer. 30 ul of secondary Ab was added to each well. The plates were incubated for an hour at 37^o C. Plates were washed 4x with ELISA wash buffer. Following washing 30 ul of SureBlue Reserve TMB Microwell Peroxidase Substrate: KPL (Cat #: 53-00-02) was added to each well. The plates were incubated for 5

minutes at room temperature. 30 ul of 1N H_2SO_4 was added to each well. Plates were read immediately on the SpectraMax M2 microplate reader (Molecular Devices) at 450 nm. Blank wells were used to subtract the background signal in the analysis.

Single cell sorting

Spleen samples from -80°C were thawed in 37°C water bath until a small ice pellet remained in the sample tube. Then warm (37°C) RPMI was added dropwise to the samples. Cells were then spun down at 300xg for 5 mins and washed with 20ml FACs buffer (1x PBS containing 2% FBS and 1mM EDTA) once and then re-suspended in the remaining drop of FACs buffer after decantation.

Cells were then incubated with 1 pmol PE-DL650 and 3 pmols APC-DL755 (decoys) for 5 mins at room temperature and then 1 pmol PE-antigen tetramer and 1 pmol APC-antigen_KO tetramer for 25 mins on ice in dark. Tetramers were made by combining biotinylated Env with Streptavidin conjugated to either a PE or APC fluorophore (Prozyme, PJFS25 and PJ27S). Cells were then washed with FACs buffer once and then re-suspended in remaining drop of FACs buffer after decantation. 50 ul anti-PE MicroBeads and 50 ul anti-APC MicroBeads (Miltenyi Biotec) were then added to the cells and they were incubated for 15-30 mins on ice. Cells bound with PE and/or APC were then enriched based on MACS cell separation manual.

Antigen-enriched samples were then stained with the following list of Ab-fluorophore conjugates: IgG1 FITC (BD Biosciences Cat#: 553443, 1:100 dilution), IgG2b FITC (BD Biosciences Cat#: 553395, 1:50 dilution), IgG2c FITC (Bio-Rad Cat#: STAR135F, 1:100 dilution), IgG3 FITC (BD Biosciences Cat#: 553403, 1:400 dilution), IgD PerCP-Cy5.5 (Biolegend Cat#: 405710, 1:180 dilution), Fixable viability stain BV510 (Affymetrix Cat#: 65-

0866-14, 1:200 dilution), CD3 BV510 (BD Biosceinces Ct#: 564024, 1:50 dilution), CD4 BV510 (BD Biosciences Cat#: 563106, 1:100 dilution), Gr-1 BV510 (BD Biosciences Cat#: 563040, 1:200 dilution), F4/80 BV510 (BD Biosciences Cat#: 123135, 1:50 dilution), IgM BV605 (Biolegend Cat#: 406523, 1:50 dilution), CD19 BV650 (BD Bioscience Cat#: 563235, 1:100 dilution), and B220 BV786 (BD Bioscience Cat#: 563894, 1:100 dilution). Cells were stained for 30 min on ice in the dark. Cells were then washed 3 times with 2 ml of FACs buffer wash. Samples were then re-suspended in 1-2 ml of FACs buffer.

Naïve, antigen-specific B cells were sorted as CD3-, CD4-, Gr-1-, F4/80-, B220+, CD19+, antigen+/antigen KO-. Class-switched IgG B cells from immunized animals were sorted based on the following markers: CD3-, CD4-, Gr-1-, F4/80-, B220+, CD19+, IgM-, IgD-, IgG1+, IgG2b+, IgG2c+, IgG3+, antigen+/antigen KO-. Individual B cells were sorted using the FACS ARIA II into a 96 well plate containing lysis buffer, as previously reported (Parks et al., 2019). The number of cells sorted from each immunization group is now indicated in Supplemental Table 2.12.

VH/VL amplification and sequencing

The amplification and sequencing of VH and VL genes were performed as previously described (Parks et al., 2019). For LC PCR reactions, 15 ul of cDNA and 15 ul of first round PCR product were used. 7 ul of cDNA or PCR product was used for the HC PCR reactions. Samples were sequenced using Sanger sequencing (Genewiz, Seattle, WA) and sequence analysis was performed as previously described (Parks et al., 2019). AA and nucleotide mutations were identified by aligning the VH/VL gene sequences to the corresponding germline genes (IMGT Repertoire) using the Geneious Software (Version 8.1.9). For VL, mutations were counted

beginning at the CDR1 of the V-gene to the 3' end of FW3. For VH, mutations were counted beginning at the CDR1 of the V-gene to the end of the CDR3. The number of sequences obtained from each immunization group is summarized in Supplemental Table 2.12.

mAb production

Gene-specific PCR was used to amplify the DNA product from the first round PCR using primers designed to anneal to the gene of interest as well as add ligation sites to facilitate insertion of the DNA fragment into the human IgG1 vector [ptt3 k for kappa (Snijder et al., 2018), and PMN 4-341 for gamma (Mouquet et al., 2010)]. Each gene specific PCR reaction contained 0.5 ul each of 10 uM 5' and 3' primer, 22.5 ul Accuprime Pfx Supermix (Cat#: 12344040), and 1.5 ul of 1st or 2nd round PCR product. The gene-specific PCR product was infused into the cut IgG1 vector in a reaction containing 12.5 ng of cut vector, 50 ng of insert, 0.5 ul of 5X Infusion enzyme (InFusion HD Cloning Kit, Cat#: 639649), and nuclease-free water to bring volume to 2.5 ul. The entire reaction was used to transform competent *E. coli* cells and plated on agar plates containing ampicillin. DNA was prepared using QIAprep Spin Miniprep Kit (Qiagen, Cat#: 27106). Equal amounts of heavy and LC DNA and 293F transfection reagent (Millipore Sigma, Cat#: 72181) were used to transfect 293E cells. 5-7 days post transfection cell supernatants were collected, and the Abs were purified using Pierce Protein A agarose beads (ThermoFisher, Cat#: 20334). The Abs were eluted using 0.1 M Citric Acid into a tube containing 1 M Tris. The Abs were buffer exchanged into 1XPBS using an amicon centrifugal filter.

To make Fabs, the IgG was cleaved overnight at 37˚C to generate Fab with Endoproteinase Lys-C (NEB). To remove undigested IgG and IgG Fc fragments, the mixture

was incubated with Protein A Agarose Resin for 1 hour at room temperature. Beads were washed with 1X PBS to remove excess Fab. Fab was further purified on SEC using a HiLoad 16/600 Superdex 200 pg (GE) column.

Quantification and Statistical Analysis

Mean and standard deviations were calculated using R (Version 3.4.1). Statistical analyses were calculated using R (Version 3.4.1) (R Core Team, 2018) and GraphPad Prism. Descriptions of the statistical methods used for each data set are described in the figure legends. The tidyverse packages (Wickham, 2017) were used in R to manipulate data and create graphs in addition to GraphPad Prism. WebLogo was used to generate the logo plots (Crooks et al., 2004).

Supplemental methods

426c outer domain variant design

Comparison of 426cOD and eOD revealed differences in a helix important for CD4 and Ab binding (Supplemental Method Figure 2.1). The highlighted helix is an integral part of the CD4-BS and has a steeper trajectory in 426c than in its eOD counterpart (Supplemental Method Figure 2.1A). The helix is also shifted with respect to the epitope position. In our design approach we lengthened the helix by two residues on its C-terminal end to extend it into the binding region. Analyzing composite structures, examining multiple decoys at the same time, provided additional insight. Across clusters of 426c models, the helix adopted variable conformations, indicating excess flexibility compared to the eOD helix, largely due to the difference in sequence composition. To lock the helix into the conformation compatible with glVRC01 binding, we used RosettaRemodel's *-build_disulf* command. We identified disulfide bonds with the correct geometry by replacing the flexible helix with a rigid-body de novo helix and inserting it into the structure before landing the disulfide.

We also modified the environment directly behind the helix. The space behind the helix in 426c had increased polarity and reduced packing compared to that of eOD (Supplemental Method Figures 2.1B and 2.1C), which includes many nonpolar and bulky residues in the pocket. We therefore replaced the incompatible residues in this region using RosettaRemodel's manual design features.

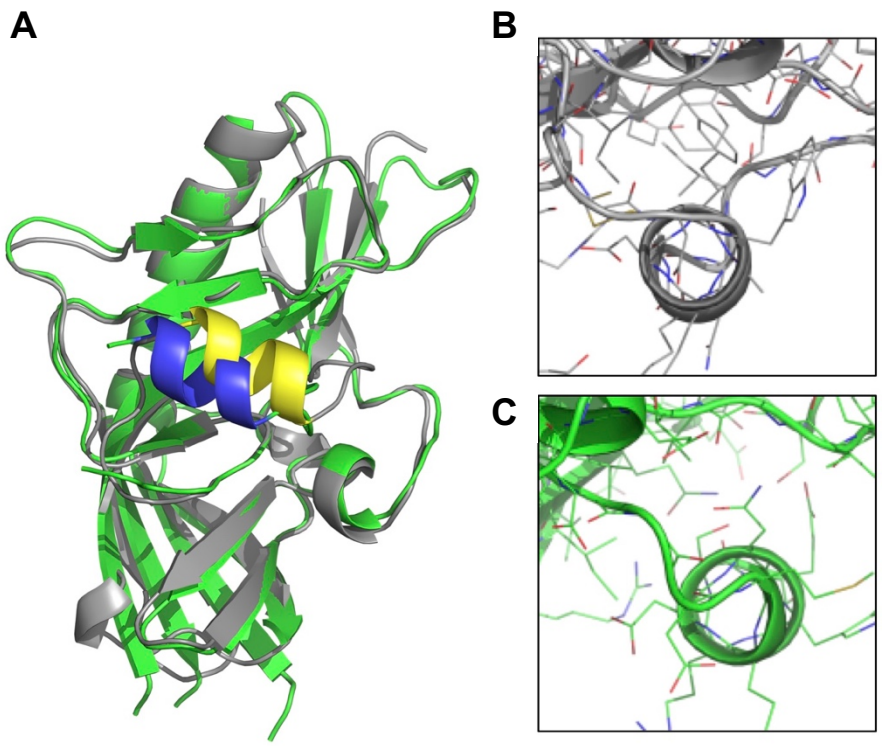

Supplemental Method Figure 2.1. Structural differences between eOD and 426c. **(A)** Superimposed structures of eOD (gray) and 426c (green) are displayed with highlighted helix positioning. The 426c helix (blue) is located farther from the epitope than the eOD helix (yellow). The helix environment (looking down helix) in **(B)** eOD is less polar and more packed than (C) the 426c environment.

We picked S2, which was among the lowest-energy and most-populated clusters of the resulting models for further testing (Supplemental Method Figure 2.2). The sequence of S2 is reported in the appendix, with the mutations from 426c highlighted. S2 was able to bind a subset of mature bnAbs: VRC-PG20, VRC01, and 3BNC60; but not germline ones (Supplemental Method Figure 2.3).

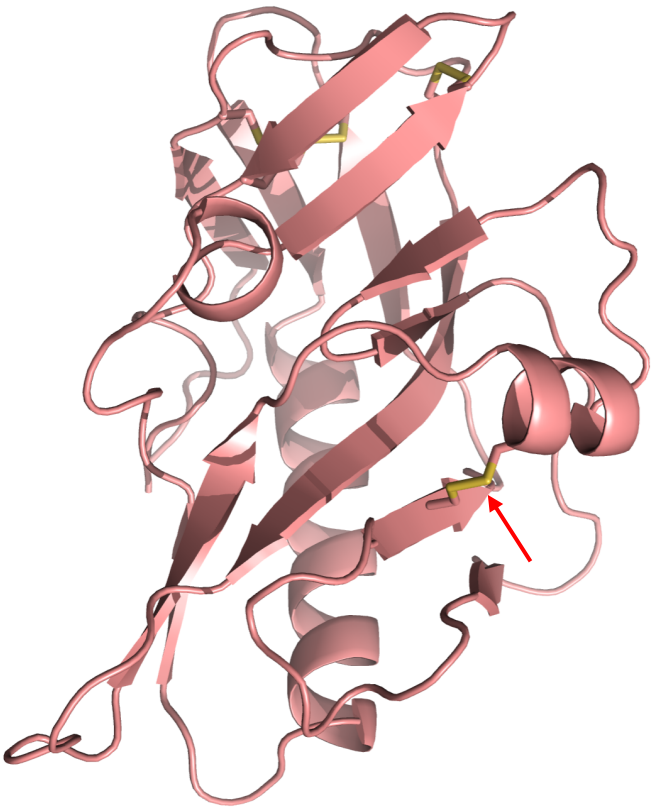

Supplemental Method Figure 2.2. Chosen variants. S2 was chosen among the biggest and lowest-energy clusters. In S2, the helix was extended and a disulfide bond (arrow) was added.

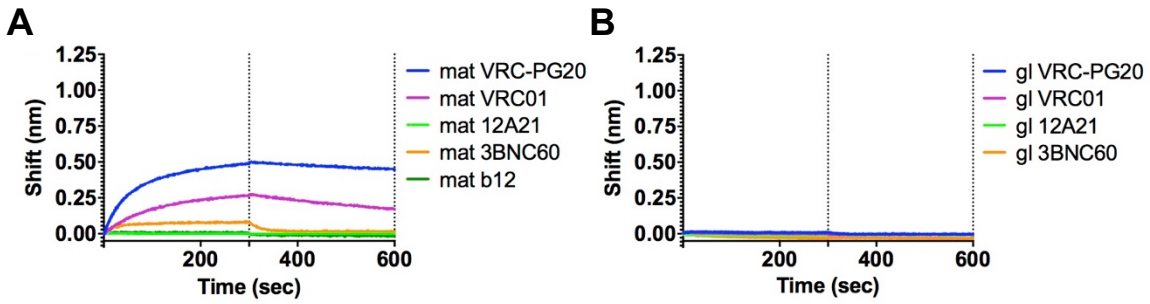

Supplemental Method Figure 2.3. BLI results for S2. BLI was used to measure binding of S2 to VRC01 Abs. (A) Mature Abs were able to bind to S2. **(B)** Germline Abs were not able to bind to S2.

The V5 loop sits directly behind the helix and is important for providing increased support for the helix. For S2, the V5 loop was too far from the helix to engage with it (Supplemental Method Figure 2.4A) and therefore was not adequately supported. To bring the helix and the V5 loop closer together, we extended the helix by one turn, allowing the two structures to better interact (Supplemental Method Figure 2.4A). We then attempted to increase packing and stability by making mutations in the area between the helix and the V5 loop. To do so, we created an extended hydrogen bond network in the space (Supplemental Method Figure 2.4C). With this mutation, S2 gained the ability to bind a germline VRC01 Ab. Interestingly, this binding is dependent upon the residue at position 51 (Supplemental Method Figure 2.4D-2,4E). A possible explanation for this behavior involves stabilization of the V5 loop. In S2, residue 51 is an aspartic acid. It is able to hydrogen bond with residues on the V5 loop to stabilize it. However, when residue 51 is mutated to an isoleucine it cannot make this interaction, the V5 loop is freed from its constraint, and the protein cannot bind to germline Abs (Supplemental Method Figure 2.4D-2.4E). Validation of this hypothesis will require further testing and characterization of these mutants. The high affinity S2-D51, also called 426c base, was further used to develop 426cOD.

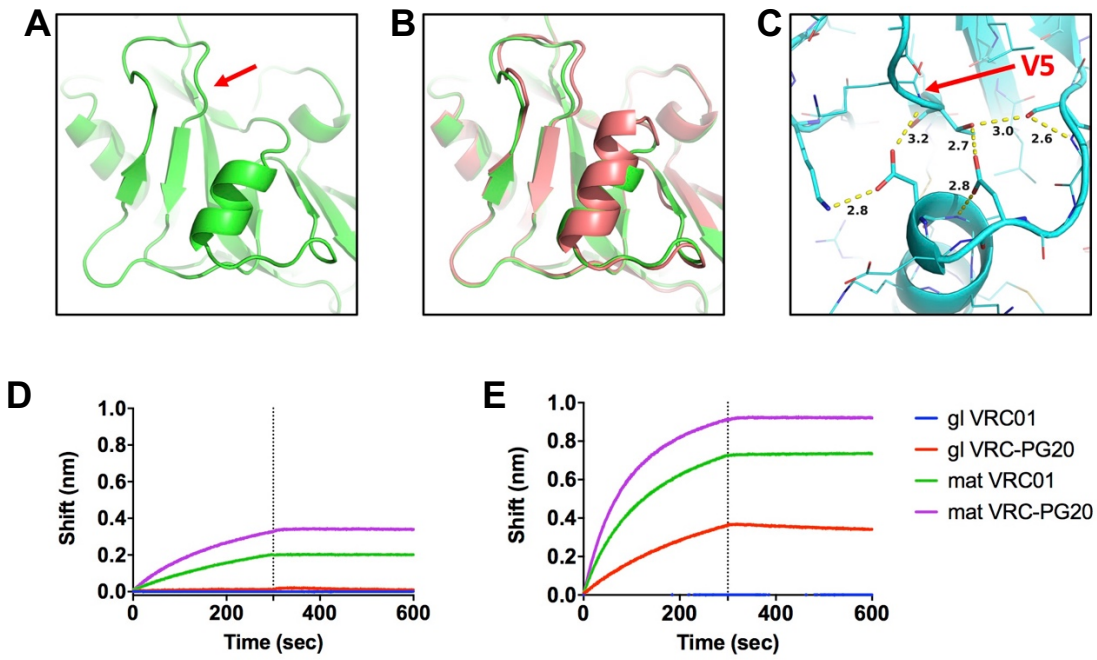

Supplemental Method Figure 2.4. S2 mutations and effects on binding. (A) The V5 loop (arrow) is disengaged from the helix. **(B)** Helix extension (pink) brings helix closer to V5 loop than in original structure (green). **(C)** Hydrogen bond network between helix and V5 loop (arrow) stabilizes helix. **(D)** BLI traces indicate that S2-D51I binds mature Abs. **(E)** S2-D51 binds mature Abs with high affinity and also binds a germline Ab.

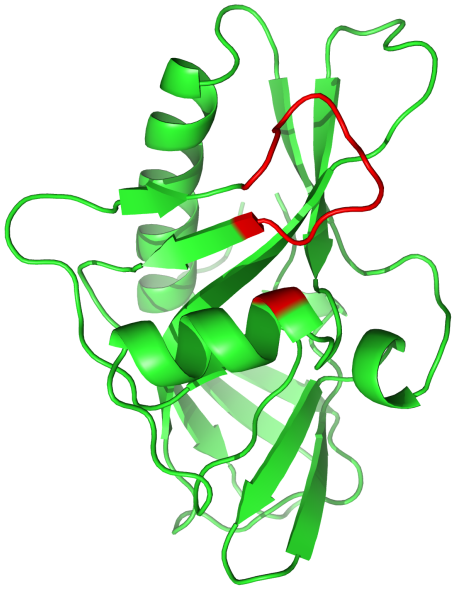

Supplemental Method Figure 2.5. Residue 51 and interaction with V5 loop. Residue 51 (red helix section) interacts with the V5 loop (red loop). Mutating an aspartic acid to an isoleucine at residue 51 (D51I) abrogated germline-binding. This effect is possibly due to reduced ability to hydrogen bond following mutation, resulting in a destabilized V5 loop.

Supplemental figures

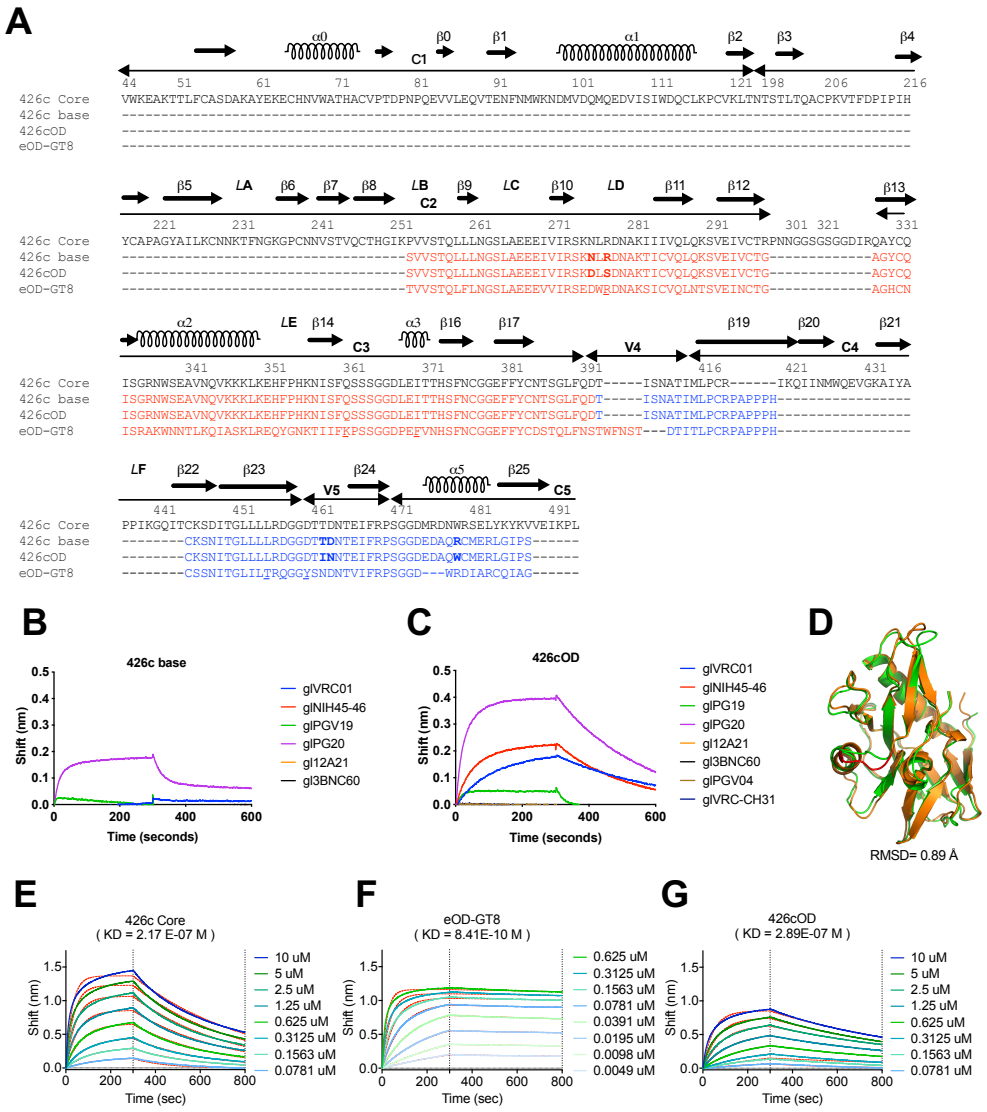

Supplemental Figure 2.1. Characterization of 426cOD. (A) AA alignment of 426c Core, 426c base, 426cOD and eOD-GT8. HxB2 numbering is used. The sequences of 426c base, 426cOD and eOD-GT8 are reverted to align with that of the 426c Core, as their actual sequences from their N to C termini start with sequences highlighted in blue. Residues that differ between 426c base and 426cOD are shown in bold letters. Residues highlighted in magenta in Figure 2.1C are underlined in eOD-GT8 sequence. **(B-C)** BLI binding curves of glVRC01-class Abs to 426c base **(B)** and 426cOD **(C). (D)** 426c base design model (orange) superimposed onto the 426cOD crystal structure (green). The structural difference between the two is highlighted in red. All atom RMSD is 0.89 Å. **(E-G)** Binding kinetics of glVRC01 to the three germline-targeting immunogens.

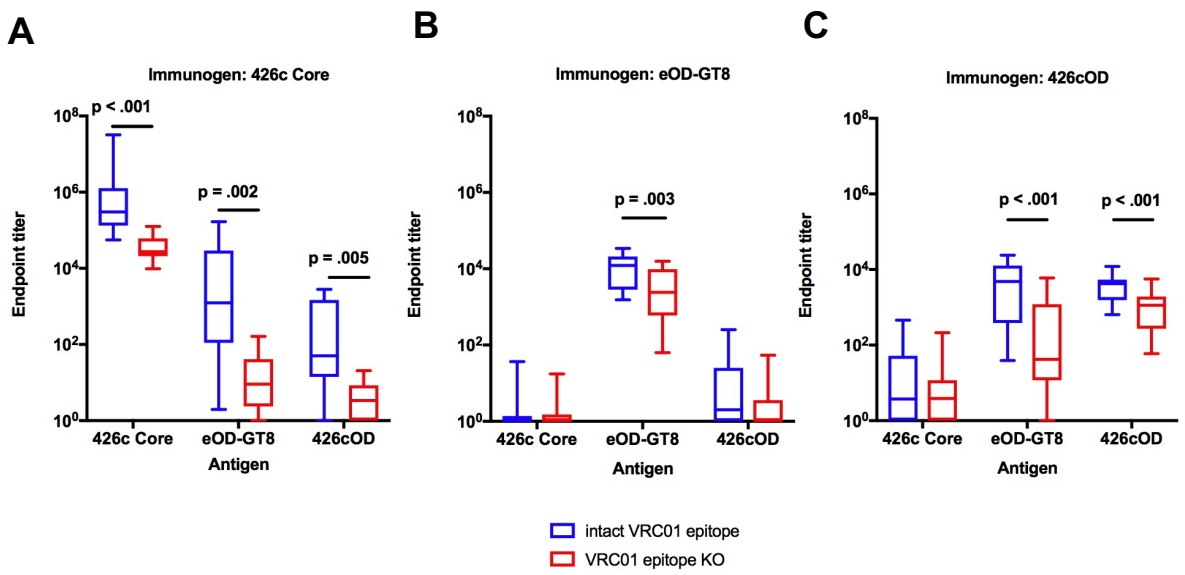

Supplemental Figure 2.2. Plasma endpoint titers 2 weeks post immunization. Plasma Ab endpoint titers 2 weeks post-immunization with 426c Core **(A)**, eOD-GT8 **(B)** or 426cOD **(C)** against the indicated proteins. Data is shown as boxplots. P-values were calculated using paired t-tests.

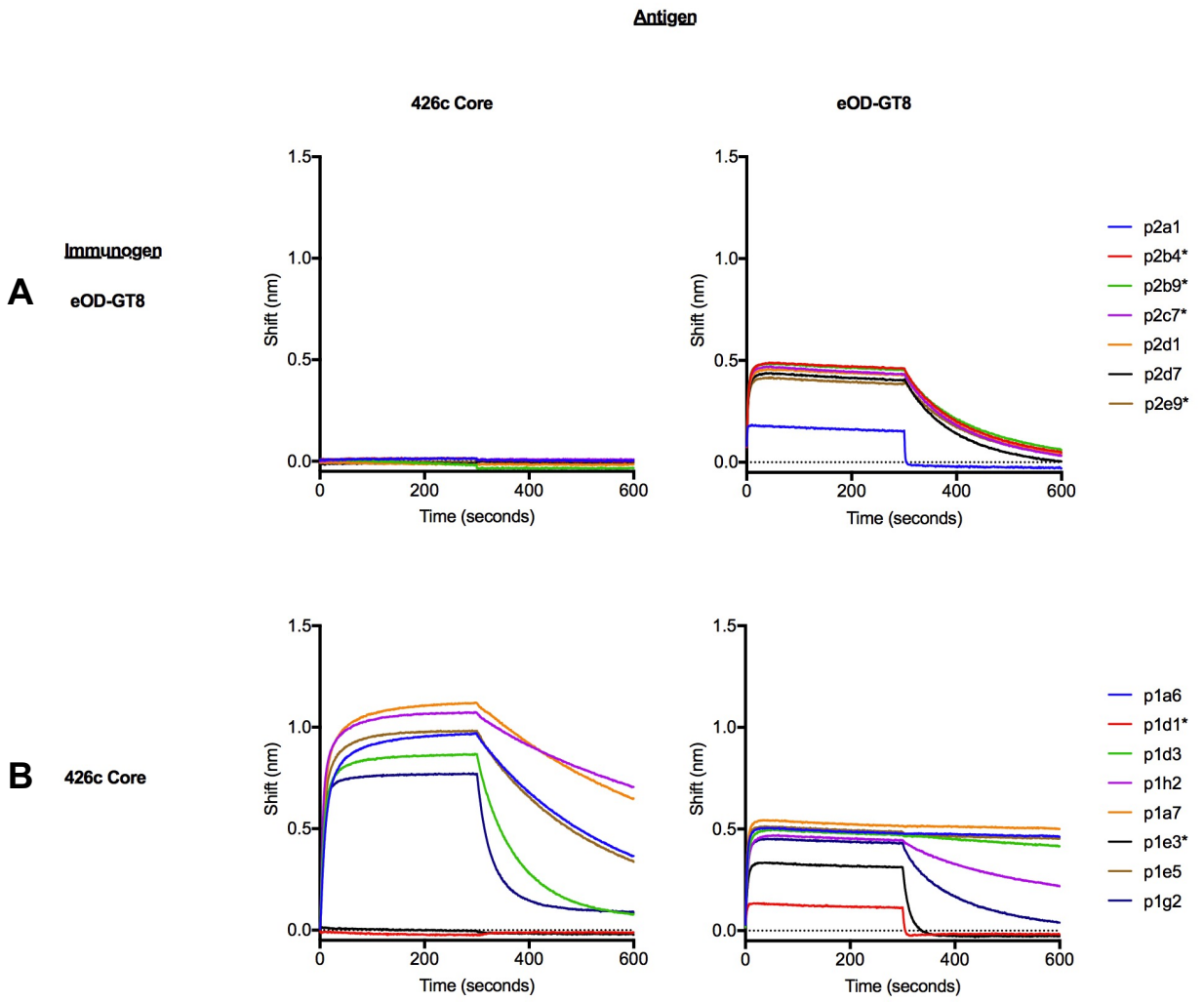

Supplemental Figure 2.3. Vaccine elicited mAbs binding to 426c Core and eOD-GT8. Binding curves of mAbs elicited by eOD-GT8 **(A)** or 426c Core **(B)** against eOD-GT8 or 426c Core. mAbs with no AA mutations as compared to their germline sequences are noted with asterisks.

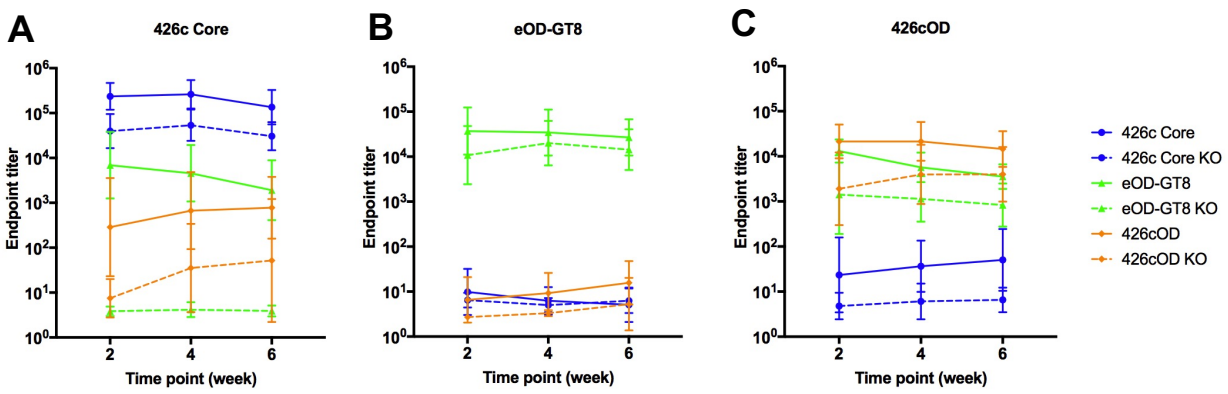

Supplemental Figure 2.4. Vaccine elicited plasma Ab response over time. Group average endpoint titers of plasma Abs against 426c Core, eOD-GT8 and 426cOD at weeks 2, 4, and 6 post-immunization with 426c Core **(A),** eOD-GT8 **(B)**, or 426cOD **(C).** Error bars represent standard deviation.

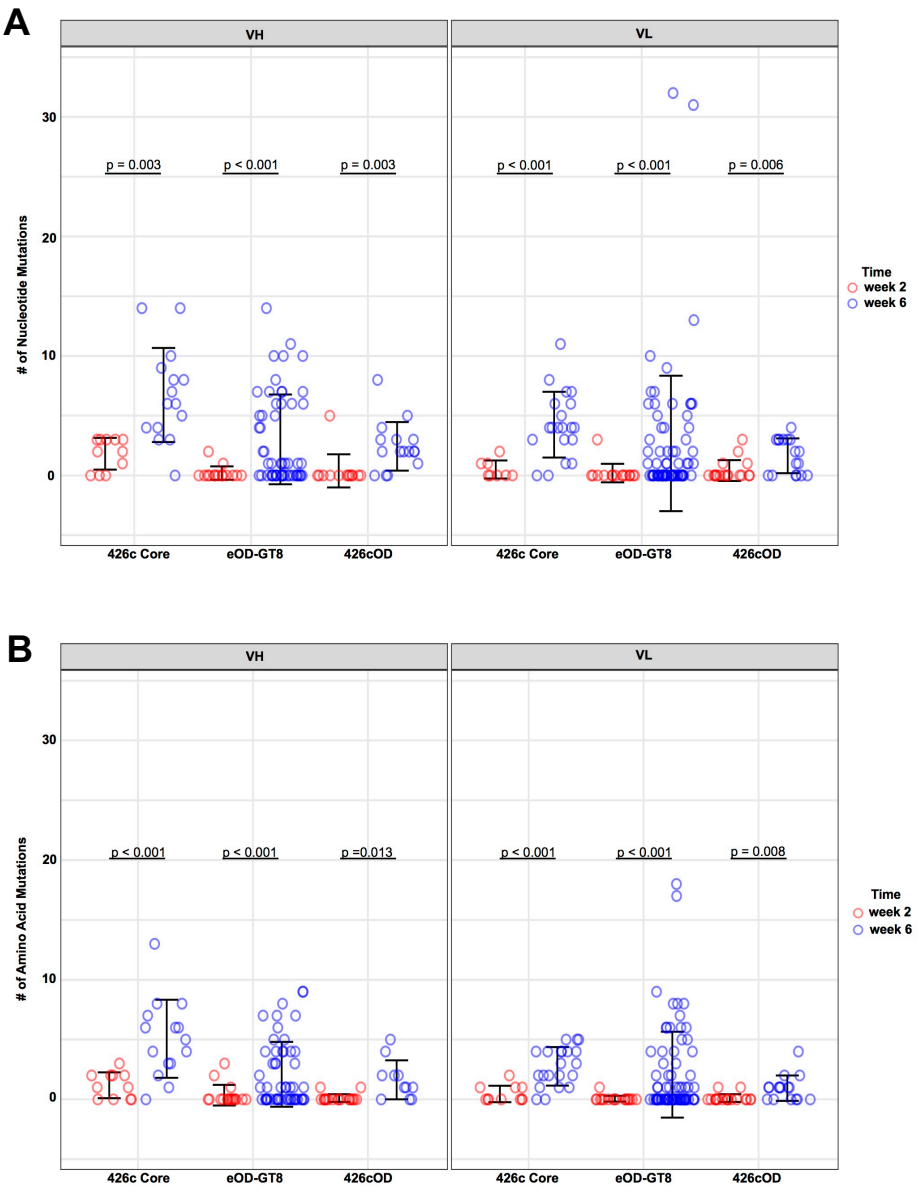

Supplemental Figure 2.5. VH/VL mutations accumulate over time. The number of nucleotide **(A)** and AA mutations **(B)** per each VH and VL domain in sequences isolated at week 2 and 6-post immunization. Significance values were calculated with Welch two-sample T test.

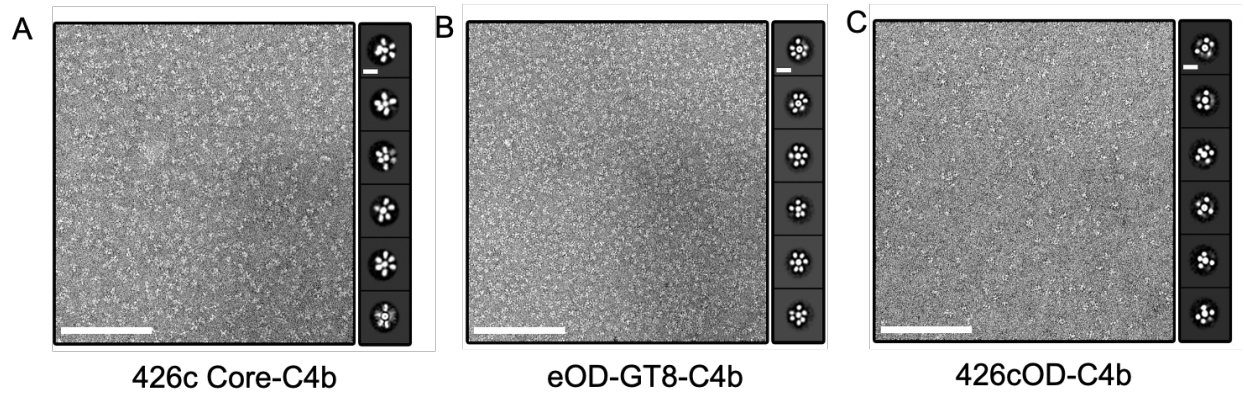

Supplemental Figure 6. Ns EM of germline-targeting C4b-based nanoparticles. Electron micrographs (left) and representative 2D class averages (right) of negatively stained 426c Core-C4b nanoparticles **(A),** eOD-GT8-C4b nanoparticles **(B),** and 426cOD-C4b nanoparticles (C). Scale bars: micrographs (200 nm); 2D class averages (100 Å)

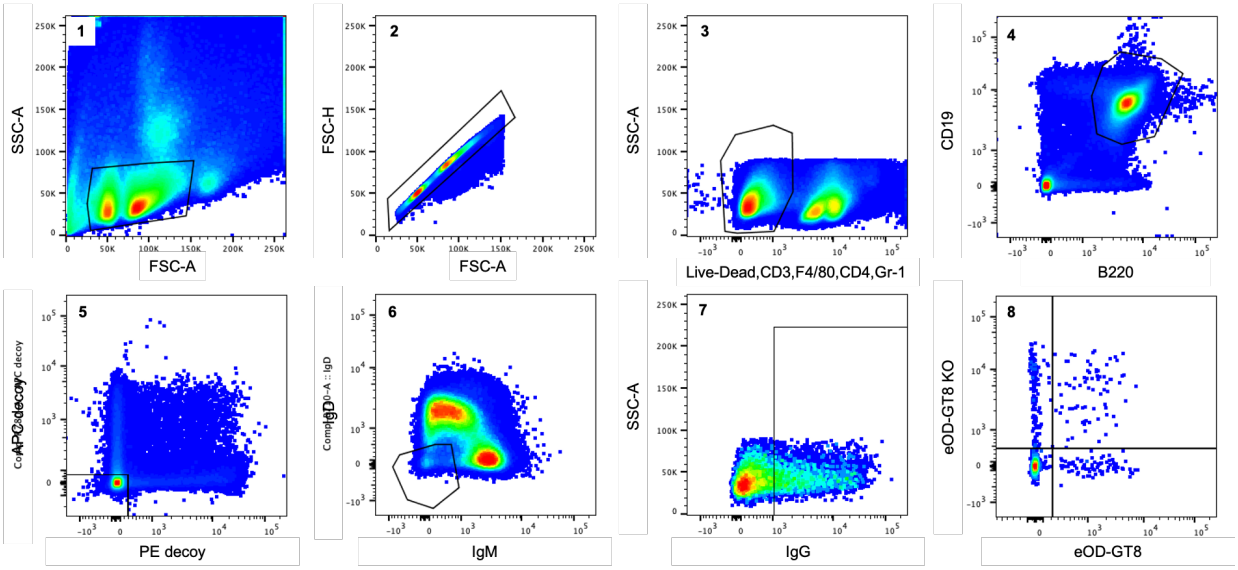

Supplemental Figure 7. Gating strategy to sort antigen-specific B cells post-immunization. Axes are labeled with markers used to select population of interest. The flow plots are labeled 1-8 to indicate order of the gates.

Supplemental tables

Supplemental Table 2.1. Data collection and refinement statistics for 426cOD with VRC01Fab.

	426cOD/VRC01Fab
Data collection	
Space group	P43
Cell dimensions	
a, *b*, *c* (Å)	137.367, 137.367, 66.188
α, β, γ (°)	90, 90, 90
Resolution (Å)	50 – 3.42 (3.48 – 3.42)*
R_{sym} or R_{merge}	1.117 (0.930)*
I/sI	25.57 (1.69)*
Completeness (%)	100 (100)*
Redundancy	6.7 (6.5)*
$CC_{1/2}$	0.992 (0.661)*
Refinement	
Resolution (Å)	48.57 – 3.421 (3.544 – 3.421)*
No. reflections	15984 (854)*
R_{work}/R_{free}	21.04/26.07 (27.32/33.36)
No. atoms	4587
Protein	597
Water	60
Ligand	104
B-factors (Å^2)	59.24
Protein	58.73
Water	26.02
Ligand	100.17
R.m.s deviations	
Bond lengths (Å)	0.004
Bond angles (º)	0.66
Ramachadran Favored %	91.33
Ramachadran Outliers %	0.17
MolProbity all-atoms clashscore	5.65
PDB ID	**6VLW**

* Statistics for the highest-resolution shell are shown in parentheses.

Supplemental Table 2.2. Per-residue BSA and interactions of glVRC01 bound to 426cOD (modeled onto PDB ID 6MFT) and WT 426c Core (PDB ID 6MFT) calculated by PDBePISA (Snijder et al., 2018). Residues with non-zero BSA are shown. Structurally aligned residues in 426cOD and WT 426c Core are shown in the same row. Residues highlighted in bold are part of the gp120 inner domain. Residues highlighted in blue are mutated from WT 426c Core.

	426cOD modeled onto 6MFT			WT 426c Core (PDB ID 6MFT)		
Secondary structure with PDB ID 1GC1 naming	Equivalent 426cOD gp120 residue	Interactions	BSA, Å^2	gp120 residue	Interactions	BSA, Å^2
ΔV1/V2				**G:LYS 97**		**0.3**
Loop D				G:LYS 275		12.5
	A:ASP 86		18.2, HLC	G:ASN 276		21.0, LC
	A:SER 88		32.3, LC	G:SER 278		35.4 LC
	A:ASP 89		52.8, HLC	G:ASP 279		56.8 HLC
	A:ASN 90		63.8, HLC	G:ASN 280	H	68.7, HLC
	A:ALA 91		61.3	G:ALA 281		68.2
	A:LYS 92	H	38.2	G:LYS 282	H	30.8
Loop E	A:LYS 137		12.1, LC	G: LYS 356		15.1, LC
				G:GLN 361		1.0
	A:SER 145		63.3	G: SER 364	H	78.5
β15	A:GLY 146		27.9	G:GLY 365		17.8
	A:GLY 147		24.0	G:GLY 366		23.8
α3	A:ASP 148	HS	45.9	G:ASP 367	HS	52.8
	A:ILE 151		35.0	G:ILE 370		40.0
β20-21				**G:MET 426**		**1.0**
				G:VAL 430		**63.4**
β23	A:LEU 29		34.8	G:LEU 455		34.3
	A:ARG 30	H	13.7, HLC	G:ARG 456	H	8.3, HLC
	A:ASP 31		43.4	G:ASP 457		43.2
	A:GLY 32	H	43.7, HLC	G:GLY 458	H	34.7, HLC
V5 loop	A:GLY 33	H	61.1, HLC	G:CYS 459	H, D	114.3, HLC
	A:ASP 34		62.0, HLC	G:ASN 460	H	103.8, HLC
	A:THR 35		22.0, HLC	G:THR 461		25.1, HLC
	A:ILE 36		40.4	G:THR 462		5.8
				G:ASN 463		2.4
β24	A:THR 39		4.6	G:THR 465		2.5
	A:GLU 40		1.6	G:GLU 466		3.3
	A:ILE 41		21.3	G:ILE 467		18.1
	A:ARG 43		23.3	G;ARG 469		29.9
				G:GLY 472		2.3
				G:GLY 473		5.7
	A:ASP 48		47.1			
	A:GLU 49		78.0			
	Total 426cOD BSA= 971.4 Å²			Total WT 426c Core BSA= 1020.9 Å²		
	818.6 Å² with Heavy chain, 217.2 Å ² with Light chain			710.8 Å² with Heavy chain, 203.5Å² with Light chain		

H Hydrogen-bond, S Salt-bridge, ASA Accessible Surface Area (Å²), BSA Buried Surface Area (Å²), |||| Buried area percentage, one bar per 10%, Bold: gp120 inner domain residues

Supplemental Table 2.3. Per-residue BSA and interactions of glVRC01 bound to 426cOD (modeled onto PDB ID 4JPK) and WT 426c Core (PDB ID 6MFT) calculated by PDBePISA (https://www.ebi.ac.uk/pdbe/pisa/). Residues with non-zero BSA are shown. Structurally aligned residues in 426cOD and WT 426c Core are shown in the same row. Residues highlighted in bold are part of the gp120 inner domain. Residues highlighted in blue are mutated from WT 426c Core.

	426cOD modeled onto 4JPK			WT 426c Core (PDB ID 6MFT)		
Secondary structure with PDB ID 1GC1 naming	Equivalent 426cOD gp120 residue	Interactions	BSA, Å^2	gp120 residue	Interactions	BSA, Å^2
ΔV1/V2				**G:LYS 97**		**0.3**
Loop D	A:LYS 85		5.2	G:LYS 275		12.5
	A:ASP 86	H	24.4, HLC	G:ASN 276		21.0, LC
	A:SER 88		50.2, LC	G:SER 278		35.4 LC
	A:ASP 89	H	52.8, HLC	G:ASP 279		56.8 HLC
	A:ASN 90	H	63.8, HLC	G:ASN 280	H	68.7, HLC
	A:ALA 91		60.7	G:ALA 281		68.2
	A:LYS 92	H	47.7	G:LYS 282	H	30.8
Loop E	A:LYS 137		7.8, LC	G: LYS 356		15.1, LC
				G:GLN 361		1.0
	A:SER 145	H	57.2	G: SER 364	H	78.5
β15	A:GLY 146	H	28.7	G:GLY 365		17.8
	A:GLY 147		28.8	G:GLY 366		23.8
α3	A:ASP 148	HS	47.3	G:ASP 367	HS	52.8
	A:ILE 151		32.1	G:ILE 370		40.0
β20-21				**G:MET 426**		**1.0**
				G:VAL 430		**63.4**
β23	A:LEU 29		34.3	G:LEU 455		34.3
	A:ARG 30	H	12.9, HLC	G:ARG 456	H	8.3, HLC
	A:ASP 31	H	45.3	G:ASP 457		43.2
	A:GLY 32	H	43.7, HLC	G:GLY 458	H	34.7, HLC
V5 loop	A:GLY 33	H	61.1, HLC	G:CYS 459	H, D	114.3, HLC
	A:ASP 34		84.4, HLC	G:ASN 460	H	103.8, HLC
	A:THR 35		20.9, HLC	G:THR 461		25.1, HLC
	A:ILE 36	H	43.9	G:THR 462		5.8
				G:ASN 463		2.4
β24	A:THR 39	H	4.3	G:THR 465		2.5
	A:GLU 40		1.6	G:GLU 466		3.3
	A:ILE 41		19.6	G:ILE 467		18.1
	A:ARG 43		16.1	G;ARG 469		29.9
				G:GLY 472		2.3
				G:GLY 473		5.7
	A:ASP 48	H	41.8			
	A:GLU 49		71.3			
	Total 426cOD BSA= 1007.5 Å²			Total WT 426c Core BSA= 1020.9 Å²		
	850.4 Å² with Heavy chain, 219.1 Å ² with Light chain			758.6 Å² with Heavy chain, 262.3 Å² with Light chain		

H Hydrogen-bond, S Salt-bridge, ASA Accessible Surface Area (Å^2), BSA Buried Surface Area (Å^2), |||| Buried area percentage, one bar per 10%, Bold: gp120 inner domain residues

Supplemental Table 2.4. Per-residue BSA and interactions of glVRC01 bound to 426cOD (modeled) and gl3BNC60 bound to 426c core (PDB ID 5FEC) calculated by PDBePISA (https://www.ebi.ac.uk/pdbe/pisa/). Residues with non-zero BSA are shown. Structurally aligned residues in 426cOD and 426c Core are shown in the same row. Residues highlighted in bold are part of the gp120 inner domain. Residues highlighted in blue are mutated from 426c Core.

	426cOD modeled onto 4JPK			426c Core with gl3BNC60 (PDB ID 5FEC)		
Secondary structure with PDB ID 1GC1 naming	Equivalent 426cOD gp120 residue	Interactions	BSA, Å^2	gp120 residue	Interactions	BSA, Å^2
Loop D	A:LYS 85		5.2	G:LYS 275	HS	11.5
	A:ASP 86	H	24.4, HLC	G:ASN 276	H	26.7, LC
	A:SER 88		50.2, LC	G:ARG 278		36.4, LC
	A:ASP 89	H	52.8, HLC	G:ASP 279	H	49.0, HLC
	A:ASN 90	H	63.8, HLC	G:ASN 280	H	68.8, HLC
	A:ALA 91		60.7	G:ALA 281		67.7
	A:LYS 92	H	47.7	G:LYS 282	HS	27.7
Loop E	A:LYS 137		7.8, LC	G:LYS 356		14.5, LC
				G:GLN 361		2.6
	A:SER 145	H	57.2	G:SER 364	H	74.8
β15	A:GLY 146	H	28.7	G:GLY 365	H	23.9
	A:GLY 147		28.8	G:GLY 366		27.6
α3	A:ASP 148	HS	47.3	G:ASP 367	HS	49.6
	A:ILE 151		32.1	G:ILE 370		36.1
β20-21				**G:VAL 430**		**49.8**
β23	A:LEU 29		34.3	G:LEU 455		**40.7**
	A:ARG 30	H	12.9, HLC	G:ARG 456	H	12.0, HLC
	A:ASP 31	H	45.3	G:ASP 457		43.1
	A:GLY 32	H	43.7, HLC	G:GLY 458	H	48.0, HLC
V5 loop	A:GLY 33	H	61.1, HLC	G:GLY 459	H	69.7, HLC
	A:ASP 34		84.4, HLC	G:ASP 460	HS	53.1, HLC
	A:THR 35		20.9, HLC	G:THR 461	H	20.3, HLC
	A:ILE 36		40.4	G:THR 462		27.2
β24	A:THR 39	H	4.3	G:THR 465	H	7.6
	A:GLU 40		1.6	G:GLU 466		0.9
	A:ILE 41		19.6	G:ILE 467		21.6
	A:ARG 43		16.1	G;ARG 469		28.2
				G:GLY 472		0.5
				G:GLY 473		1.0
	A:ASP 48	H	41.8			
	A:GLU 49		71.3			
	Total 426cOD BSA= 1007.5 Å²			Total 426c Core BSA= 947.4 Å²		
	850.4 Å² with Heavy chain, 219.1 Å ² with Light chain			734.3 Å² with Heavy chain, 280.5 Å² with Light chain		

H Hydrogen-bond, S Salt-bridge, ASA Accessible Surface Area (Å²), BSA Buried Surface Area (Å²), |||| Buried area percentage, one bar per 10%, Bold: gp120 inner domain residues

Supplemental Table 2.5. Per-residue BSA and interactions of glVRC01 bound to 426cOD and to eOD-GT8 (modeled usingPDB ID 4JPK) calculated by PDBePISA (https://www.ebi.ac.uk/pdbe/pisa/). Residues with non-zero BSA are shown. Structurally aligned residues in 426cOD and eOD-GT8 are shown in the same row. Residues colored magenta are the ones that differ in sequence in eOD-GT8 relative to 426cOD.

	426cOD modeled onto 4JPK			eOD-GT8 modeled onto 4JPK		
Secondary structure with PDB ID 1GC1 naming	Equivalent 426cOD gp120 residue	Interactions	BSA, Å^2	Equivalent eOD-GT8 gp120 residue	Interactions	BSA, Å^2
Loop D	A:LYS 85		5.2	C:GLU 78		1.4
	A:ASP 86	H	24.4, HLC	C:ASP 79	H	35.7, HLC
	A:SER 88		50.2, LC	C:ARG 81	H	148.1, LC
	A:ASP 89	H	52.8, HLC	C:ASP 82	H	52.9, HLC
	A:ASN 90	H	63.8, HLC	C:ASN 83	H	69.4, HLC
	A:ALA 91		60.7	C:ALA 84		65.1
	A:LYS 92	H	47.7	C:LYS 85	HS	34.7
Loop E	A:LYS 137		7.8, LC			
	A:SER 145	H	57.2	C:SER 138	H	69.1
β15	A:GLY 146	H	28.7	C:GLY 139		16.7
	A:GLY 147		28.8	C:GLY 140		27.1
α3	A:ASP 148	HS	47.3	C:ASP 141	HS	59.7
	A:ILE 151		32.1	C:PHE 144		22.7
β20-21						
β23	A:LEU 29		34.3	C:THR 25		22.2
	A:ARG 30	H	12.9, HLC	C:ARG 26	H	3.0, HLC
	A:ASP 31	H	45.3	C:GLN 27	H	76.0
	A:GLY 32	H	43.7, HLC	C:GLY 28	H	38.2, HLC
V5 loop	A:GLY 33	H	61.1, HLC	C:GLY 29	H	52.9, HLC
	A:ASP 34		84.4, HLC	C:TYR 30	H	140.7, HLC
	A:THR 35		20.9, HLC			
	A:ILE 36		40.4			
β24	A:THR 39	H	4.3	C:THR 35		7.9
	A:GLU 40		1.6	C:VAL 36		1.3
	A:ILE 41		19.6	C:ILE 37		24.3
	A:ARG 43		16.1	C:ARG 39	H	18.5
				C:GLY 42	H	58.1
				C:GLY 43	H	24.7
	A:ASP 48	H	41.8	C:ASP 44		49.5
	A:GLU 49		71.3	C:TRP 45		6.4
				C:ARG 46		10.4
				C:ASP 47		5.0
	Total 426cOD BSA= 1007.5 Å²			Total eOD-GT8 BSA= 1141.6 Å²		
	850.4 Å² with Heavy chain, 219.1 Å ² with Light chain			712.8 Å² with Heavy chain, 265.9Å² with Light chain		

H Hydrogen-bond, S Salt-bridge, ASA Accessible Surface Area (Å²), BSA Buried Surface Area (Å²), |||| Buried area percentage, one bar per 10%.

Supplemental Table 2.6. BSA of glVRC01 HC and LCs upon binding to 426cOD (2 models), WT 426c Core PDB ID (6MFT), eOD-GT8 (modeled onto 4JPK), 426c Core (5FEC) calculated by PDBePISA (https://www.ebi.ac.uk/pdbe/pisa/).

	glVRC01 Heavy chain BSA (Å²)	glVRC01 Light chain BSA (Å²)	Total BSA (Å²)
426cOD modeled onto 6MFT	818.6	217.2	1035.8
426cOD modeled onto 4JPK	850.4	219.1	1069.5
WT 426c Core (PDB 6MFT)	710.8	203.5	914.3
eOD-GT8 modeled onto 4JPK	712.8	265.9	978.7
426c Core (PDB 5FEC)	734.3	280.5	1014.8

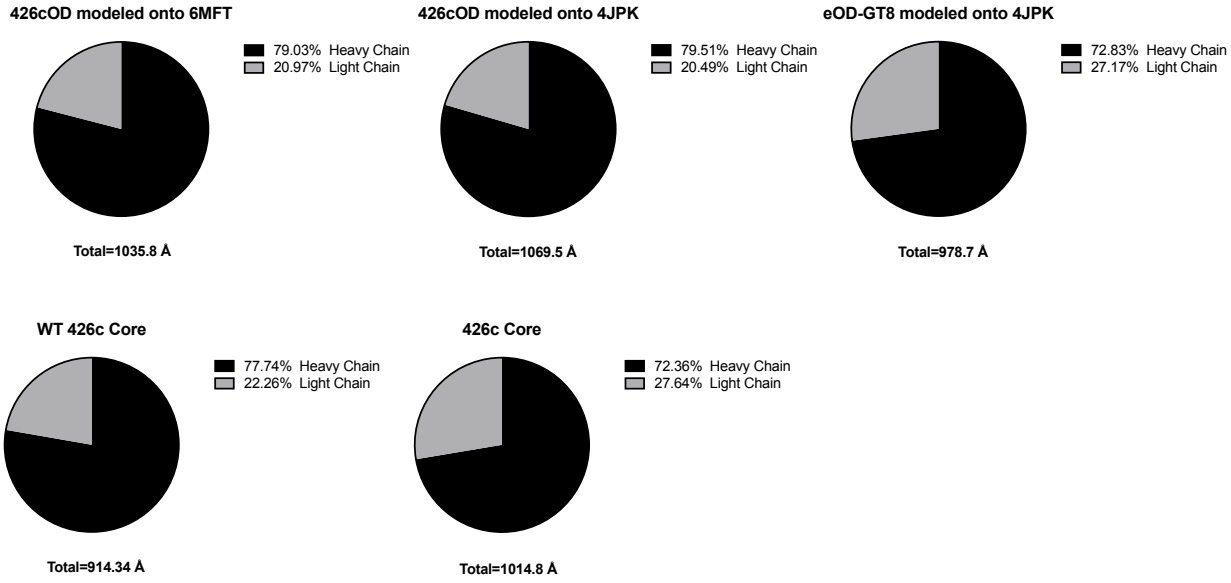

Supplemental Table 2.7. VH/VL sequences isolated following eOD-GT8 immunization.
AA sequences are aligned to the V gene from which they are derived. For sequences where the PCR product did not contain the 5' end, the sequence is shown beginning at CDR1.

VH

immunization group	sort probe	VRC01glHC	QVQLVQSGAEVKKPGASVKVSCKASGYTFTGYYMHWVRQAPGQGLEWMGWINPNSGGTNYAQKFQGRVTMTRDTSISTAYMELSRLRSDDTAVYYCARGKNSDYNWDFQH
week 2	eOD-GT8	p2a1	.....DT..I.....
		p2b4	.....
		p2b9	.....
		p2c7	.....
		p2d1	.....R.....
		p2d7	.....
		p2e9	.....
		p2e3	.....
		p2f2	.....
		p2g6	.....
		p1a6	.....
		p1a8	.....
		p1a9	.....
		p1c1	.....
		p1c2	.....
		p1c4	.....
		p1d8	.....
week 6	eOD-GT8	p1a3	.....
		p1a9	.....
		p1b2	.....G.....G.....C.....LH.
		p1b7	.....L.....L.....T.....R.
		p1c1	.....T.....N.....T.....
		p1c8	.....R.....T.....CT.....
		p1d4	----------.....
		p1d8	.....
		p1e3	.....F.....

		p1e7	..........R.....E.....K..D...I.....
		p1f1	----------.....A.....
		p1f5	..........R.....I.....E.....N.....T.....
		p1g2	----------.....
		p1g5	.....F.....
		p1g7	----------.....
		p1h2	.....T.....D.NL.....D.....V.R.....I.....
		p1h5	.....
		p1h6	----------.....
		p1h8	.....
		p2a10	.....I.....
		p2a11	.....E.....
		p2a7	.....R.....
		p2a8	.....L.....
		p2b1	.....H.....N.....I.....
		p2b11	.....
		p2b4	.....
		p2b8	..........R.....I.....T.....N.....T.....
		p2c1	.....
		p2c10	.....D.....K.....A.....I.....
		p2c9	..........R.....I.....Q.....N.....F.....T.....
		p2d12	.....
		p2d7	.....
		p2e10	.....
		p2e11	.....F..K..H...I.....
		p2e4	.....
		p2e6	----------.....A.N.....G.....ES...I..L..
		p2f1	.....N.....N.....T.E.....I...H.
		p2f4	.....
		p2f6	----------.....H..S.....F..N.....A....M.....D.N.....H.....
		p2g3	.....

		p2h9	.....M.....I.....A.S..M..N.....VN.....T...H.....
		p3e1	.....D..IN.....S.....F......R..Y.....
		p3h10	.....
		p3h9	.....
		p3g9	.....R.....I.....Q.....N.....F.....T.....
		p3e10	----------..T....SD.HL.....I....T.....
		p3d10	.....M.....
		p3d7	.....NF.....R.....
		p1b1	----------.....
		p1b6	----------.....
		p1d5	----------.....
		p1e8	----------.....

VL

immunization group	sort probe	IGKV8-30*01	DIVMSQSPSSLAVSVGEKVTMSCKSSQSLLYSSNQKNYLAWYQQKPGQSPKLLIYWASTRESGVPDRFTGSGSGTDFTLTISSVKAEDLAVYYC	CDRL3 sequence	J gene
week 2	eODGT8	p2b4	.....	QQYWT	1
		p2b9	.....	QQYYT	1
		p2c7	.....	QQYYT	5
		p2d1	.....A.....	QQYWT	2
		p2d7	.....N.....	QQYWT	1
		p2e9	.....	QQYYT	1
		p2e3	.....	QQYFT	4
		p2g6	.....	QQYYT	2
		p1a6	.....	QQYWT	1
		p1a8	.....R.....	QQYYT	5
		p1a9	.....	QQYYT	5
		p1c1	.....	QQYYT	2
		p1c2	.....	QQYYT	1
		p1c4	.....	QQYWT	1
		p1d8	.....	QQYYT	2
week 6	eOD-GT8	p3h9	----------.....	QQYWT	1

		p3f5	----------.....N.....D.....F.	QQYYS	2
		p3d7	----------	QQYYT	2
		p2f7	----------.....N.....D.....F.	QQYYS	2
		p2e6	----------.....ESN	QQYWT	1
		p2e2	----------.....N...H	QQYCE	1
		p2d7	----------	QQYWT	1
		p2d3	----------.....ESN	QQYWT	1
		p2c10	----------..R.....D....D	QQYWT	1
		p2c4	----------	QQYYT	5
		p2c1	----------.....K	QQYYT	1
		p2b4	----------	QQYWT	1
		p2a8	----------	QQYWT	1
		p2a7	----------	QQYYT	5
		p1h8	----------	QQYWT	1
		p1h5	----------	QQYWT	1
		p1h1	----------	QQYWT	1
		p1g7	----------	QQYWT	1
		p1g5	----------.....R	QQYYS	1
		p1e1	----------.....D.....F.	QQYYS	5
		p1d8	----------	QQYYS	2
		p1d4	----------	QQYYT	1
		p1c11	----------.....I...	QQYHT	2
		p1c1	----------.....I...	QQYHT	2
		p1b1	----------	QQYYT	2
		p1a6	----------.....V.....	QHYWT	1
		p1a2	----------	QQYFT	5
		p1f1	----------.....FG.....Q.....	QQYYS	5
		p1a10	----------	QQYYS	2
		p1a11	----------	QQYWT	1
		p1a12	----------	QQYYT	2
		p1b1	----------	QQYWT	1

		p1b4	----------.....	QQYWT	1
		p1b6	----------.....	QQYWT	1
		p1c6	----------.....	QQYYT	2
		p1c9	----------.....	QQYYT	2
		p1d5	----------.....	QQYYT	2
		p1d7	----------.....	QQYWT	1
		p1e5	----------.....N.....	QQYDN	2
		p1e8	----------.....	QQYFT	4
		p1f8	----------.....	QQYFT	4

immunization group	sort probe	IGKV4-72*01	QIVLSQSPAILSASPGEKVTMTCRASSSVSYMHWYQQKPGSSPKPWIYATSNLASGVPARFSGSGSGTSYSLTISRVEAEDAATYYC	CDRL3 sequence	J gene
week 2	eOD-GT8	p2a1	.....	QQWST	1
week 6	eOD-GT8	p1e3	----------.....	QQWST	2
		p2b11	----------.....	QQWST	2 or 4
		p2g3	----------.....S.....	QQWST	5

immunization group	sort probe	IGKV4-86*01	EIVLTQSPAITAASLGQKVTITCSASSSVSYMHWYQQKSGTSPKPWIYEISKLASGVPARFSGSGSGTSYSLTISSMEAEDAAIYYC	CDRL3 sequence	J gene
week 2	eOD-GT8	p2f2	.....	QQWNS	1

immunization group	sort probe	IGKV4-61*01	QIVLTQSPAIMSASPGEKVTISCSASSSVSYMYWYQQKPGSSPKPWIYRTSNLASGVPARFSGSGSGTSYSLTISSMEAEDAATYYC	CDRL3 sequence	J gene
week 6	eOD-GT8	p1c8	.....V.....N.....	QQYET	1
		p1f5	.....	QQYET	1
		p2b8	.....V.....I...	QQYET	1
		p2c9	.....T.....T.....	QHYET	1
		p2e10	----------.....	QQYHS	1
		p3g9	.....T.....T.....	QHYET	1
		p1f7	----------.....	QQYHT	2

immunization group	sort probe	IGKV6-15*01	DIVMTQSQKFMSTSVGDRVSVTCKASQNVGTNVAWYQQKPGQSPKALIYSASYRYSGVPDRFTGSGSGTDFTLTISNVQSEDLAEYFC	CDRL3 sequence	J gene
week 6	eOD-GT8	p1h2	.....R.....SS..V.....S....T...F.....R.....D...	QHYNT	1

		p2e4	----------....	QQYNT	4

immunization group	sort probe	IGKV8-28*01	DIVMTQSPSSLSVSAGEKVTMSCKSSQSLLNSGNQKNYLAWYQQKPGQPPKLLIYGASTRESGVPDRFTGSGSGTDFTLTISSVQAEDLAVYYC	CDRL3 sequence	J gene
week 6	eOD-GT8	p1a3	----------.....V..S.....A.....T.....	QNDLT	5
		p1a9	.....	QNEYT	2

immunization group	sort probe	IGKV12-44*01	DIVMTQSPSSLSASVGETVTITCRASENIYSYLAWYQQKQGKSPQLLVYNAKTLAEGVPSRFSGSGSGTQFSLKINSLQPEDFGSYYC	CDRL3 sequence	J gene
week 6	eOD-GT8	p2a11	----------.....E.....T.....R...	QHHWT	1
		p2d12	----------....	QHHWT	1

immunization group	sort probe	IGKV12-46*01	DIQMTQSPASLSVSVGETVTITCRASENIYSNLAWYQQKQGKSPQLLVYAATNLADGVPSRFSGSGSGTQYSLKINSLQSEDFGSYYC	CDRL3 sequence	J gene
week 6	eOD-GT8	p1b2	.....G.....K.....S.....T...	QHFWT	1
		p1b7	.....N...T.....ID.VE.L.....R.....	QHFFT	2
		p1e7	----------.G.....Y.....K.....S.S.....T...	QHFWT	1
		p1g2	----------....	QHFWT	1
		p2b1	.....I.....D.....T.K...T.....F....S.....N.F.	QYGWF	1
		p2e11	----------.G.....N.....V..K.....S.....T...	QHFWT	1
		p2f1	----------.G...VF.....R.....K.I.....S.....T...	QHFWT	1
		p2f4	----------....	QHFWT	1
		p2f6	----------...K....I....	QHFWT	2
		p3h10	----------.G...FS.....K.....S.....T...	QHFWT	1
		p3d10	----------T.....G.....	QHLLT	5
		p1d9	----------....	QHFWT	1
		p1d11	----------....	QHFWT	1
		p1e1	----------.T....	QHFWA	1
		p1f10	----------....	QHFWA	4

immunization group	sort probe	IGKV18-36*01	TGETTQAPASLSFSLGETATLSCRSSESVGSYLAWYQQKAEQVPRLLIHSASTRAGGVPVRFSGTGSGTDFTLTISSLEPEDAAVYYC	CDRL3 sequence	J gene
week 6	eOD-GT8	p1e10	----------.A.Q..S.N.....PG.A.....YG.....T.I.AK...S....E.....QS..F.....	QQYNA	2
		p1f9	----------.A.Q..S.N.....PG.A.....YG.....T.I.A....S....E.....QS..F.....	QQYNA	2

immunization group	sort probe	IGKV4-57*01	QIVLTQSPAIMSASPGEKVTITCSASSSVSYMHWFQQKPGTSPKLWIYSTSNLASGVPARFSGSGSGTSYSLTISRMEAEDAATYYC	CDRL3 sequence	J gene
week 6	eOD-GT8	p1d2	----------..........	QQRTT	2

Supplemental Table 2.8. VH/VL sequences isolated following 426c Core immunization.
AA sequences are aligned to the V gene from which they are derived. For sequences where the PCR product did not contain the 5' end, the sequence is shown beginning at CDR1.

VH

immunization group	sort probe	VRC01^{glHC}	QVQLVQSGAEVKKPGASVKVSCKASGYTFTGYYMHWVRQAPGQGLEWMGWINPNSGGTNYAQKFQGRVTMTRDTSISTAYMELSRLRSDDTAVYYCARGKNSDYNWDFQH
week 2	eOD-GT8	p1a6	.....N.....H.....
		p1d1	.....
		p1d3	.....N.....
		p1h2	.....N.....N.....
		p1a7	.....N.....K.....
		p1e3	.....
		p1e5	.....D.....K.....D.....
		p1g2	.....H.N.....
		p1e7	.....N.....
		p1e8	.....
		p1g8	.....
week 6	eOD-GT8	p1e9	.....
		p1e8	.....M.....P.....N.....D.....TT.A.....I.....
		p1d9	.....N.....M...N.....
		p1d8	.....N.....N.V...V.....Y
		p1d3	.....D...N.....KR.....M....V.....
		p1c6	.....N.....IN.....V.....
		p1c2	.....S.....I.....N.....R.....
		p1b8	.....N.....
		p1b5	.....RT.....D..LN.....TR.A.....SV.....S.A.....F.....
		p1b3	.....N..N.....R.....Y
		p2a4	.....N.....D.....TT.A.....N.....
	426c Core	p4d6	.....FLN.....F.A.D.....RD.....
		p4b5	.....D...N.....HR.A.....V.....Y.....L.....
		p4a3	.....N.....R.....
		p2c2	----------.....D...N.....R.A.....V.....Y.....

VL

immunization group	sort probe	IGKV8-30*01	DIVMSQSPSSLAVSVGEKVTMSCKSSQSLLYSSNQKNYLAWYQQKPGQSPKLLIYWASTRESGVPDRFTGSGSGTDFTLTISSVKAEDLAVYYC	CDRL3 sequence	J gene
week 2	eOD-GT8	p1a6	.....	QQYEM	1
		p1d3	.....A.....L...	QQYYK	2
		p1h2	.....N.....E.....	QQYYK	2
		p1a7	.....E.....	QQYET	1
		p1e5	.....I.....	QQYET	1
		p1g2	.....E.....	QQYYK	1
		p1e7	...LT.T.....	QQYET	2
		p1g8	.....	QQYYS	2
week 6	eOD-GT8	p1e9	-----.....	QQYYK	2
		p1e8	-----.....E.....R.....	QQYYK	2
		p1d9	-----.....E.....	QQYYK	2
		p1d8	-----.....G...E.....	QQYYK	2
		p1d7	-----.T.....TD.....A.....	QQYYK	2
		p1d3	-----T.....TD.....A.....	QQYYK	2
		p1c6	-----....RI.....E.....H.....	QQYYK	2
		p1c2	-----...E.....R.....	QQYYK	2
		p1b8	-----.....	QQYYK	1
		p1b6	-----....NI..D..EE.....	QQYYK	2
		p1b5	-----...E.....D.....	QQYYK	1
		p1b3	-----.....D..E.....	QQYYK	1
		p2a4	-----.....E.....	QQYYK	1
		p2a5	-----.....D.EE.....A.....G.....	QQYYK	5
	426c Core	p4d6	-----.....NHED.....	QQYYK	5
		p4b5	-----....TF.....E.....	QQYYK	1
		p4a3	-----.....T.....	HQYYK	2
		p2g8	-----..R.....D.E.....D.....	QQYYK	1
		p2f9	-----.....D.E.....D.....	QQYYK	1
		p2c2	-----....NV..N.D.E.....	QQYYK	2

		p2a2	----------...E.....ER.....S.....	QQYYK	2

immunization group	sort probe	IGKV12-46*01	DIQMTQSPASLSVSVGETVTITCRASENIYSNLAWYQQKQGKSPQLLVYAATNLADGVPSRFSGSGSGTQYSLKINSLQSEDFGSYYC	CDRL3 sequence	J gene
week 2	eOD-GT8	p1e3	.....	QHFYT	2

immunization group	sort probe	IGKV4-72*01	QIVLSQSPAILSASPGEKVTMTCRASSSVSYMHWYQQKPGSSPKPWIYATSNLASGVPARFSGSGSGTSYSLTISRVEAEDAATYYC	CDRL3 sequence	J gene
week 2	eOD-GT8	p1d1	.....	QQWST	2

immunization group	sort probe	IGKV4-61*01	QIVLTQSPAIMSASPGEKVTISCSASSSVSYMYWYQQKPGSSPKPWIYRTSNLASGVPARFSGSGSGTSYSLTISSMEAEDAATYYC	CDRL3 sequence	J gene
week 2	eOD-GT8	p1e8	----------.....	QQYHS	2

Supplemental Table 2.9. VH/VL sequences isolated following 426cOD immunization.
AA sequences are aligned to the V gene from which they are derived. For sequences where the PCR product did not contain the 5' end, the sequence is shown beginning at CDR1.

VH

immunization group	sort probe	VRC01^{glHC}	QVQLVQSGAEVKKPGASVKVSCKASGYTFTGYYMHWVRQAPGQGLEWMGWINPNSGGTNYAQKFQGRVTMTRDTSISTAYMELSRLRSDDTAVYYCARGKNSDYNWDFQH
week 2	426cOD	p1e1	.....
		p1b7	.....
		p2g4	.....
	eOD-GT8	p1g7	.....
		p1h2	.......R.....
		p1h7	.....
		p1h11	.....
		p2a6	.....
		p2a12	.....
		p2b12	.....
		p3a8	.....
		p3c2	.....T.....
		p1h1	.....
		p2a9	.....
		p1e4	P.....L.....
		p1d2	.....
		p1e5	.....
		p1f4	.....
week 6	eOD-GT8	p3b7	.....F.....FLN.....N.....
		p3b6	........G.....
		p1a9	.....N..K.....KR.....
		p1a5	.....A.....N.....
		p1b8	----------.....
		p1c4	----------.....

	426cOD	p1c6	.....N.....
		p1c5	.....M.....N.....L.....
		p1b10	.....N.....
		p1b6	.....N.....E.....
		p1a2	----------.....N.....R.....

VL

immunization group	sort probe	IGKV8-30*01	DIVMSQSPSSLAVSVGEKVTMSCKSSQSLLYSSNQKNYLAWYQQKPGQSPKLLIYWASTRESGVPDRFTGSGSGTDFTLTISSVKAEDLAVYYC	CDRL3 sequence	J gene
week 2	426cOD	p1e1	.....	QQYYSF	1
		p1b7	.....	QQYYKF	1
		p2g4	....T.T.....S.....	QQYYKF	2
	eOD-GT8	p1h7	.....	QQYWTF	1
		p1h11	.....	QQYYSY	2
		p2a6	.....	QQYYSY	2
		p2a12	.....	QQYWTF	1
		p1g7	.....	QQYYSF	2
		p1h1	.....K.....	QQYYSF	2
		p1d2	.....	QQYYSF	2
		p1e5	.....	QQYYQF	2
		p1e4	.....	QQYYSF	1
		p1f4	.....	QQYYSF	1
week 6	eOD-GT8	p3b7	----------.....KN.....	QQYYKF	1
		p3b6	----------.....	QQYYSF	1
		p1a9	----------.....N.....	QQYYTF	2
		p1a1	----------.....	QQYYSY	2
		p1a5	----------.....	QQYYKF	1
		p1b8	----------.....	QQYYSY	2
		p1c4	----------.....	QQYYSF	2
	426cOD	p1c6	----------.....N.....	QQYYKF	5
		p1c5	----------.....N.....	QQYYKF	5

		p1c4	----------.....N.....	QQYYKF	5
		p1b10	----------.....	QQYYSF	2
		p1b6	----------.....S.....Q.....	QQYYKF	5
		p1a12	----------.....S...I...N.....F.	QQYYKF	5
		p1a11	----------.....G.....	QQYYKF	1
		p1a3	----------.....N.....	QQYYKF	5
		p1a2	----------.....N.....	QQYYKF	5

immunization group	sort probe	IGKV6-15*01	DIVMTQSQKFMSTSVGDRVSVTCKASQNVGTNVAWYQQKPGQSPKALIYSASYRYSGVPDRFTGSGSGTDFTLTISNVQSEDLAEYFC	CDRL3 sequence	J gene
week 2	eOD-GT8	p1h2	.....	QQYNSF	4
		p3a8	.....	QQYNTF	2

immunization group	sort probe	IGKV4-72*01	QIVLSQSPAILSASPGEKVTMTCRASSSVSYMHWYQQKPGSSPKPWIYATSNLASGVPARFSGSGSGTSYSLTISRVEAEDAATYYC	CDRL3 sequence	J gene
week 2	eOD-GT8	p2b12	.....	QQWSTF	2
		p2a9	.....	QQWSTF	2

immunization group	sort probe	IGKV4-86*01	EIVLTQSPAITAASLGQKVTITCSASSSVSYMHWYQQKSGTSPKPWIYEISKLASGVPARFSGSGSGTSYSLTISSMEAEDAAIYYC	CDRL3 sequence	J gene
week 2	eOD-GT8	p3c2	......T.....	QQWNYF	5

Supplemental Table 2.10. VH/VL sequences of VRC01-class Abs

VH

IGHV1-2*02	QVQLVQSGAEVKKPGASVKVSCKASGYTFTGYYMHWVRQAPGQGLEWMGWINPNSGGTNYAQKFQGRVTMTRDTSISTAYMELSRLRSDDTAVYYC----------
Mature VRC01	........GQM....E.MRI..R....E.IDCTLN.I.L...KRP.....LK.RG.AV...RPL.........VYSD..FL..RS.TV......F.TRGKNCDYNWD-----FEHWGRGTPVIVSS
glVRC01	.....ARGKNCDYNNWD----FQHWGQGTLVTVSS
gl3BNC60	.....ARERSDFWD-------FDLWGRGTLVTVSS
gl12A21	.....ARDGSGDDTSWH----LHPWGQGTLVTVSS
glNIH45-46	.....ARGKYCTARDYYNWD-FQHWGQGTLVTVSS
glPGV04	.....ARQKFYTGGQGW---YFDLWGRGTLVTVSS
glPG19	.....ARMGAAREWD------FQHWGQGTLVTVSS
glPG20	.....ARRMRSQDREWD----FQHWGQGTLVTVSS
glVRC-CH31	.....ARGSKRGRSGWD----FQHWGQGTLVTVSS
VRC01c-HuGL2	.....AKISGSYS--------FDYWGQGTLVTVSS
VRC01c-HuGL7	.....ARSDGYNLGWY-----FDLWGRGTLVTVSS
VRC01c-HuGL11	.....ASKVAAAGTLAK--DAFDIWGQGTMVTVSS
VRC01c-HuGL15	.....ARPTEYSSSWYW----FDPWGQGTLVTVSS
VRC01c-HuGL18	.....ARVRYGSWTGYY----FDYWGQGTLVTVSS
VRC01c-HuGL19	.....ARVPYDFWSGYYVLSHFDYWGQGTLVTVSS

VL

IGKV3-11*01	EIVLTQSPATLSLSPGERATLSCRASQSVSSYLAWYQQKPGQAPRLLIYDASNRATGIPARFSGSGSGTDFTLTISSLEPEDFAVYYC----------
Mature VRC01	........G........T.II...T..YG.--......R.......V..SG.T..A...D.....RW.P.YN....N..SG..G....QQYEFFGQGTKVQVDIK
glVRC01	.....QQYEFFGQGTKLEIK--

IGKV3-15*01	EIVMTQSPATLSVSPGERATLSCRASQSVSSNLAWYQQKPGQAPRLLIYGASTRATGIPARFSGSGSGTEFTLTISSLQSEDFAVYYC----------
VRC01c-HuGL11	.....QQYITFGGGTKVEIK
VRC01c-HuGL19	.....QQYETFGQGTKVEIK

IGKV3-20*01	EIVLTQSPGTLSLSPGERATLSCRASQSVSSSYLAWYQQKPGQAPRLLIYGASSRATGIPDRFSGSGSGTDFTLTISRLEPEDFAVYYC----------
glNIH45-46	.....QQYEFFGQGTKLEIK
glPGV04	.....QQLEFFGQGTRLEIK
VRC01-HuGL18	.....QQYETFGQGTKVEIK

IGKV1-27*01	DIQMTQSPSSLSASVGDRVTITCRASQGISNYLAWYQQKPGKVPKLLIYAASTLQSGVPSRFSGSGSGTDFTLTISSLQPEDVATYYC----------
VRC01-HuGL7	.....QKFETFGQGTKVEIK

IGKV4-1*01	DIVMTQSPDSLAVSLGERATINCKSSQSVLYSSNNKNYLAWYQQKPGQPPKLLIYWASTRESGVPDRFSGSGSGTDFTLTISSLQAEDVAVYYC----------
VRC01c-HuGL2	.....QQYYSFGGGTKVEIK

IGKV1-5*03	DIQMTQSPSTLSASVGDRVTITCRASQSISSWLAWYQQKPGKAPKLLIYKASSLESGVPSRFSGSGSGTEFTLTISSLQPDDFATYYC----------
VRC01c-HuGL15	.....QQYNSFGPGTKVDIK

IGKV1-33*01	DIQMTQSPSSLSASVGDRVTITCQASQDISNYLNWYQQKPGKAPKLLIYDASNLETGVPSRFSGSGSGTDFTFTISSLQPEDIATYYC----------
gl3BNC60	.....QQYEFIGPGTKVDIK
gl12A21	.....AVLEFFGPGTKVDIK
glVRC-CH31	.....QQYETFGQGTKLEIK

IGLV2-14*01	QSALTQPASVSGSPGQSITISCTGTSSDVGGYNYVSWYQQHPGKAPKLMIYEVSNRPSGVSNRFSGSKSGNTASLTISGLQAEDEADYYC----------
glPG19	.....SSYEFFGGGTKVFVLG
glPG20	.....SSYEFFGGGTKVFVLG

Supplemental Table 2.11. Primers for 426cOD-base and 426cOD cloning and mutagenesis.

426cOD primers for pETCON vector cloning	F	AGGCGGAGGGTCGGCTTCGCATATGACCATAAGTAATGCGACTATCATGCTCC
	R	TTTGTTCGGAACCTCCACCCTCGAGGTCTTGAAAGAGTCCTGACGTGTTACAA
426cOD primers for random site mutagenesis	F	AGTGGTGGAGGAGGCTCTGGTGGAGGCGGTAGCGGAGGCGGAGGGTCGGCTTCGCATATG
	R	GATCTCTATTACAAGTCCTCTTCAGAAATAAGCTTTTGTTCGGAACCTCCACCCTCGAG
426cOD-base primers for T462I, D463N mutagenesis	F	CGCGACGGTGGAGATACCATTAATAATACCGAGATTTTC
	R	GAAAATCTCGGTATTATTAATGGTATCTCCACCGTCGCG
426cOD-base primers for R480W mutagenesis	F	AGACGAGGACGCTCAATGGTGTATGGAACGG
	R	CCGTTCCATACACCATTGAGCGTCCTCGTCT
426cOD-base primers for N276D, R278S mutagenesis	F	GAAGAAATTGTAATTCGGAGTAAGGATCTCAGCGATAACGCCAAAACAATTTGCGTG
	R	CACGCAAATTGTTTTGGCGTTATCGCTGAGATCCTTACTCCGAATTACAATTTCTTC
426cOD-base primers for R273W mutagenesis	F	AGCCTTGCTGAGGAAGAAATTGTAATTTGGAGTAAGGATCTC
	R	GAGATCCTTACTCCAAATTACAATTTCTTCCTCAGCAAGGCT
426cOD primers for D368R, E370A mutagenesis	F	CAGTCCTCCAGCGGAGGTCGCCTTGCAATTACAACCCACTCTTT
	R	AAAGAGTGGGTTGTAATTGCAAGGCGACCTCCGCTGGAGGACTG
426cOD primers for D279A mutagenesis	F	CAAATTGTTTTGGCGTTAGCGCTGAGATCCTTACT
	R	AGTAAGGATCTCAGCGCTAACGCCAAAACAATTTG

Supplemental Table 2.12. Summary of the immunization groups and number of B cells sorted from each group.

Immunogen	Group	Adjuvant	Harvest time point	Number of animals	Number of B cells sorted	# of heavy chain sequences	# of light chain sequences
426c Core	a	GLA-LSQ	Week 2	5	166	84	26
	b	poly (I:C)	Week 2	5	56	5	25
	c	GLA-LSQ	Week 6	4	329	56	126
	d	GLA-LSQ	Week 6	4	na	na	na
eOD-GT8	a	poly (I:C)	Week 2	4	79	30	39
	b	GLA-LSQ	Week 2	4	41	18	20
	c	GLA-LSQ	Week 6	4	147	135	75
	d	GLA-LSQ	Week 6	4	64	32	39
426cOD	a	poly (I:C)	Week 2	4	294	59	97
	b	GLA-LSQ	Week 2	4	28	8	13
	c	GLA-LSQ	Week 6	4	111	39	79
	d	GLA-LSQ	Week 6	4	na	na	na

*na indicates not sorted.

Supplemental Table 2.13 AA sequences for OD variants. Mutations from original 426c consensus sequence are highlighted in red for S1 and S2 mutants.

Variant	Sequence
eOD	DTITLPCRPAPPPHCSSNITGLILTRQGGY ANTVIFRPSGGDWRDIARCQIAGTVVSTQLFLNGS LAEEEVVIRSEDWRDNAKSICVQLATSVEIACTGA GHCAISRAKWANTLKQIASKLREQYGAKTIIFKPSS GGDPEFVNHSFNCGGEFFYCASTQLFASTWF
426c core	TISNATIMLPCRPAPPPHCKSDITGLLLLRDGGDTT DNTEIFRPGGGDMRDNWRCQIAGTVVSTQLLLNG SLAEEEIVIRSKNLRDNAKIICVQLNKSVEIVCTGA GYCNISGRNWSEAVNQVKKKLKEHFPHKNISFQSS SGGDLEITTHSFNCGGEFFYCNTSGLFND
S2	TISNATIMLPCRPAPPPHCKS**N**ITGLLLLRDGGDTT DNTEIFRP**S**GGDMR**CAE**R**LG**I**PSS**VVSTQLLLNGS LAEEEIVIRSKNLRDNAKIICVQL**Q**KSVEIVCTGAG YC**Q**ISGRNWSEAVNQVKKKLKEHFPHKNISFQSSS GGDLEITTHSFNCGGEFFYCNTSGLF**Q**D
S2-D51I	TISNATIMLPCRPAPPPHCKS**N**ITGLLLLRDGGDTT DNTEIFRP**S**GGD**EIAQ**RC**MERLG**I**PSS**VVSTQLLL NGSLAEEEIVIRSKNLRDNAK**T**ICVQL**Q**KSVEIVCT GAGYC**Q**ISGRNWSEAVNQVKKKLKEHFPHKNISF QSSSGGDLEITTHSFNCGGEFFYCNTSGLF**Q**D
S2-D51 (426c base)	TISNATIMLPCRPAPPPHCKS**N**ITGLLLLRDGGDTT DNTEIFRP**S**GGD**EDAQ**RC**MERLG**I**PSS**VVSTQLLL NGSLAEEEIVIRSKNLRDNAK**T**ICVQL**Q**KSVEIVCT GAGYC**Q**ISGRNWSEAVNQVKKKLKEHFPHKNISF QSSSGGDLEITTHSFNCGGEFFYCNTSGLF**Q**D

Chapter III: Overcoming steric restrictions of VRC01 HIV-1 neutralizing antibodies through immunization

The following text is from a published article with minor editorial changes:

Parks, K.R., MacCamy, A.J., Trichka, J., Gray, M., Weidle, C., Borst, A.J., Khechaduri, A., Takushi, B., Agrawal, P., Guenaga, J., et al. (2019). Overcoming Steric Restrictions of VRC01 HIV-1 Neutralizing Antibodies through Immunization. Cell Rep *29*, 3060-3072.e7.

Abstract

Broadly HIV-1 neutralizing VRC01-class Abs target the CD4-BS of Env. They are derived from VH1-2*02 Ab HCs paired with rare LCs expressing five AA long CDRL3s. They have been isolated from infected subjects but have not yet been elicited by immunization. Env-derived immunogens capable of binding the germline forms of VRC01 BCRs on naïve B cells have been designed and evaluated in KI mice. However, the elicited Abs cannot bypass glycans present on the conserved position N276 of Env, which restricts access to the CD4-BS. Efforts to guide the appropriate maturation of these Abs by sequential immunization have not yet been successful. Here, we report on a two-step immunization scheme that leads to the maturation of VRC01-like Abs capable of accommodating the N276 glycan and displaying autologous tier 2 neutralizing activities. Our results are relevant to clinical trials aiming to elicit VRC01 Abs.

Introduction

VRC01-class Abs are potent and broad HIV-1 neutralizing Abs that offer protection from experimental animal (S)HIV infection (Balazs et al., 2014; Gautam et al., 2016; Pegu et al., 2014; Shingai et al., 2014), and could be an important component of the protective immune responses elicited by an effective HIV-1 vaccine (Burton and Hangartner, 2016; Kwong and Mascola, 2012). They have been isolated from several HIV-1-infected subjects and share key genetic origins: their HC V genes are derived from the VH1–2*02 allele and are paired with LCs expressing 5 AA long CDRL3, which is rarely found in the human Ab repertoire. The 5 AA CDRL3 contains a hydrophobic residue at position 91 and a Glu96 (Scheid et al., 2011; Wu et al., 2010, 2011; Zhou et al., 2013, 2015). The VRC01-class bnAbs are extensively somatically hypermutated (up to 30% aa difference from germline) and can be up to 50% divergent in AA sequence (Scheid et al., 2011; Wu et al., 2010, 2011; Zhou et al., 2010, 2015). Despite this marked diversity, their CDR domains adopt similar overall structures and recognize the CD4-BS of Env in a manner similar to that of CD4 (Zhou et al., 2010, 2013). Thus, despite their similar genetic origins, during chronic infection with different HIV-1 viruses, VRC01-class Abs mature along different pathways but ultimately adopt similar structures that are associated with their broad neutralizing activity. The “structural convergent evolution” observed during natural HIV-1 infection suggests that more than one evolutionary pathway will be available to develop VRC01-class bnAbs by immunization.

Longitudinal natural viral Env variants associated with the development of bnAbs against the Env apex region (Doria-Rose et al., 2014) and of non-VRC01-class anti-CD4-BS bnAbs have been identified and characterized (Bonsignori et al., 2016; Liao et al.,

2013). Viral Envs associated with the maturation of VRC01-class Ab responses have also been reported in the case of chronic HIV-1 infection (Bonsignori et al., 2018; Lynch et al., 2015a), but such viral Envs were derived from samples collected after the VRC01 B cells lineages had already expanded. More recently however, Umotoy et al. (2019) reported on the longitudinal evolution of virus and VRC01-class B cell lineages in an HIV-1-infected patient from protocol C. So far, however, the natural Env(s) that initiated the production of VRC01-class Abs during HIV-1 infection have yet to be identified. Also, the inferred germline forms of VRC01-class Abs (commonly referred to as glVRC01 Abs), do not display detectable reactivity to diverse recombinant Env-derived soluble proteins (Hoot et al., 2013; Jardine et al., 2013; McGuire et al., 2013). In recent years, we and others reported on the design of "germline VRC01-targeting" recombinant Env-derived proteins capable of binding glVRC01-class Abs (Jardine et al., 2013, 2015; McGuire et al., 2013, 2014, 2016; MedinaRamírez et al., 2017). A key feature of such immunogens is the absence of the conserved NLGS at position 276 within loop D of the gp120 Env subunit, as the N276-associated glycans present a major barrier to glVRC01 Ab binding, through steric obstruction of the germline-encoded CDRL1s (Borst et al., 2018; McGuire et al., 2013; Zhou et al., 2013). Mature VRC01 bnAbs accommodate this glycan by either incorporating glycine residues in their CDRL1 domains or by shortening them during affinity maturation (Zhou et al., 2013).

Although VRC01 germline-targeting immunogens activate B cells engineered to express glVRC01-class BCRs *in vitro* and *in vivo* (Jardine et al., 2013, 2015; McGuire et al., 2013, 2014, 2016; Medina-Ramírez et al., 2017), these cells undergo limited somatic mutation and the secreted Abs fail to bind in the presence of N276-associated glycans on

WT Envs (Dosenovic et al., 2015; Jardine et al., 2015; McGuire et al., 2016). Efforts to guide the maturation of VRC01-like Ab responses elicited by germline-targeting immunogens through subsequent immunizations with heterologous Env derived proteins also lacking the N276 glycans, led to increased somatic mutations, in both the VH and VL Ab genes, but no direct evidence that the elicited Abs could accommodate N276-associated glycans was provided (Briney et al., 2016; Tian et al., 2016).

Here, we report on a two-step immunization scheme that begins with a prime immunization with the VRC01 germline-targeting prime immunogen, 426c Core, that lacks the N276 NLGS, followed by a boost immunization with a heterologous Env-derived immunogen, harboring the 276 NLGS. The outcome of this immunization scheme was the production of VRC01-like Abs capable of accommodating the steric block imposed by the glycans present at N276 on heterologous gp120 Core-derived Envs and neutralizing the autologous, tier 2 426c virus with a modified glycan shield.

Results

The 426c Core germline-targeting immunogen elicits potent plasma Ab responses against the VRC01 epitope in KI mice

We previously reported on the design of a recombinant protein derived from the inner and outer gp120 domains of the clade C Env 426c, lacking the variable domains 1, 2, and 3 as well as three NLGS at positions N276 (loop D), N460, and N463 (V5). That protein (TM4ΔV1–3, herein referred to as "426c Core" for simplicity) binds several of the known glVRC01-class Abs (McGuire et al., 2016). Here, two nanoparticle forms of the 426c Core were employed as immunogens: a 5- to 7-meric form (426c Core C4b) (Hofmeyer et al., 2013; McGuire et al., 2016; Ogun et al., 2008) and a Ferritin-based 24-meric form (426c Core Fer) (Kanekiyo et al., 2013; McGuire et al., 2016). One additional glVRC01- targeting immunogen was investigated for its ability to engage B cells expressing glVRC01 BCRs *in vivo*: the 426c DS-SOSIP D3 (Borst et al., 2018; Joyce et al., 2017). It is derived from the clade C 426c virus (like the 426c Core) and was modified by eliminating the above-mentioned three NLGSs. We also performed an immunization with the non-germline-targeting unmodified 426c WT gp120 as a control.

As animal species, such as mice, rats, rabbits, or non-human primates do not express orthologs of the human VH1–2*02 allele (Jardine et al., 2013; Vigdorovich et al., 2016; West et al., 2012), immunizations were performed in a KI mouse that is heterozygous for the glVRC01 HC, whereas the LCs remain the endogenous mouse LCs (mLCs) (Jardine et al., 2015). Approximately 80% of naive B cells express the glVRC01 HC and 0.1% of mLCs express 5 AA long CDRL3s. Thus, the overall estimated frequency of naive B cells expressing potential glVRC01 BCRs in this mouse model is

approximately 0.08% (compared to approximately 0.01% in humans; Arnaout et al., 2011; DeKosky et al., 2015; Jardine et al., 2015). The elicitation of VRC01-class bnAbs in this model requires overcoming at least two major obstacles: first, the germline-targeting immunogen must select for the B cells expressing extremely rare mLCs with a 5 AA CDRL3 paired with the glVRC01 HC, and second, the immunization regimen must lead to the accumulation of mutations that will allow the maturing B cells to bypass the obstacles presented by the N276 glycans on full-length Envs.

A single immunization with either nanoparticle form of 426c Core with two different adjuvants (poly(I:C) or GLA-LSQ) elicits robust autologous plasma Ab responses (Figure 3.1A), the majority of which target the CD4-BS (Figure 3.1B). Plasma Abs generated in approximately 77% of the 426c Core-immunized animals (66 of 85), also recognized the heterologous VRC01 germline-targeting immunogen eOD-GT8 (Figure 3.1C) in a VRC01 epitope-dependent manner (Supplemental Figures 3.1A and 3.1B). eOD-GT8 is derived from the outer domain of the gp120 subunit of the clade B HxB2 Env (Jardine et al., 2013, 2015). Thus, Abs elicited by the 426c Core that recognize eOD-GT8, but not the eOD-GT8 KO (not recognized by VRC01-class Abs) are most likely VRC01 epitope specific. In contrast, the 426c DS-SOSIP D3 germline-targeting immunogen elicited very weak autologous plasma Ab responses and only one animal elicited Abs against the 426c Core, which were non-CD4-BS directed and did not recognize eOD-GT8 (Supplemental Figure 3.1C). Animals immunized with the non-germline-targeting Env 426c WT gp120 immunogen elicited strong autologous responses, but weak anti-426c Core Ab responses and no eOD-GT8 Ab response (Supplemental Figure 3.1D).

We concluded that the 426c Core immunogen elicits potent anti-CD4-BS Ab responses, which recognize the VRC01 epitope.

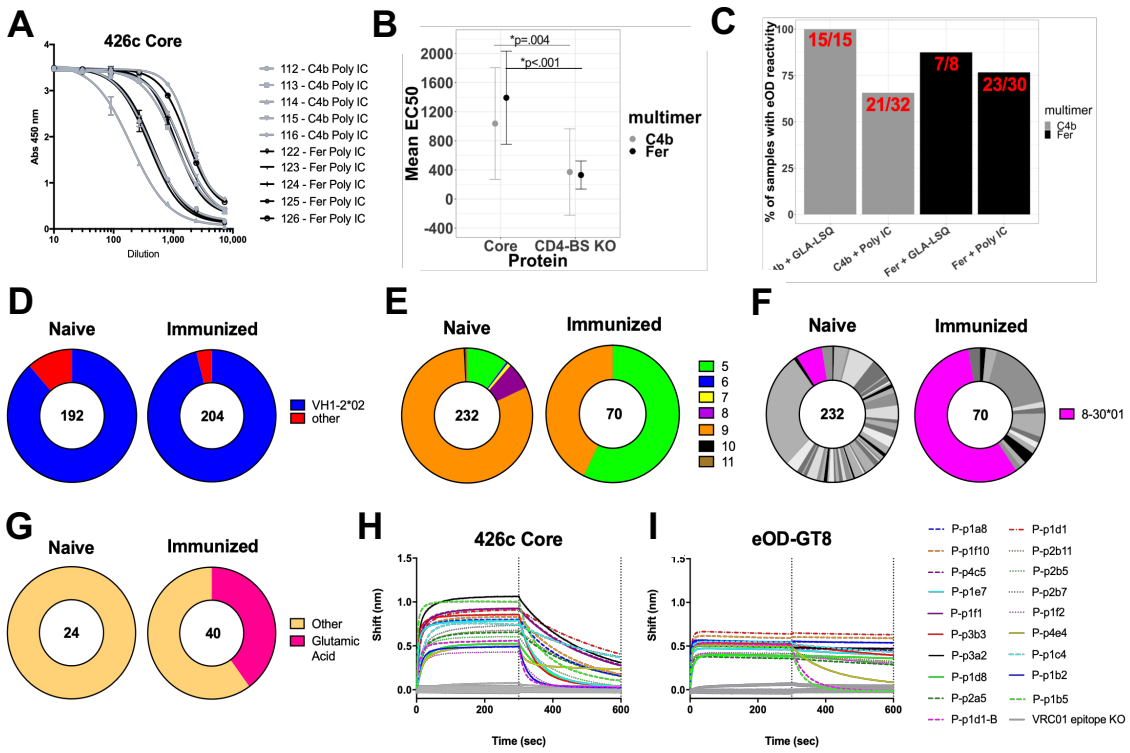

Figure 3.1. 426c Core elicited Ab and B cell response. Plasma from representative animals immunized with 426c Core C4b (gray) or 426c Core Fer (black) were tested for binding against **(A)** 426c Core and its **(B)** CD4-BS KO form. **(B)** Summarizes the data from one experiment with 10 animals in each group. A paired t-test was used to determine statistical significance between the mean EC50 titers against the 426c Core vs those against its CD4-BS KO. **(C)** Summary of the animal frequencies per group of 426c Core immunized animals that developed anti-eOD-GT8 plasma Ab responses (OD 450nm of ≥0.1 at 1:10 dilution; additional information is provided in Supplemental Figure 3.1). The nanoparticle form and the adjuvant used is indicated. The number of animals that developed anti-eOD-GT8 responses out of the total immunized for each group is indicated within each bar. **(A-C)** At least two biological replicates were performed for each immunization group (multimer + adjuvant). **(D-G)** Pie charts indicate HC and LC sequences from individually sorted B cells from immunized (3 independent experiments) and non-immunized animals (one experiment). The number of sequences analyzed is shown in the middle of each pie chart and the percentages of HCs or LCs with the indicated features are shown. **(D)** HC sequences from naïve and immunized animals. **(E)** AA length of the CDRL3 domains in the sequences from the naïve and immunized animals. 5 AA long CDRL3s are shown in green. **(F)** V-gene usage of the LCs from the sequences isolated from naïve and immunized animals. The 8-30*01 V-gene is shown in pink. **(G)** Presence or absence of $Glu96_{LC}$ within the LC sequences with

5 AA long CDRL3 domains. MAbs with VRC01 characteristics were generated from paired VH/VL sequences from class-switched B cells isolated following the prime immunization (indicate by 'P') with the 426c Core **(H).** MAb binding to monomeric 426c Core (colored lines) and to monomeric 426c Core CD4-BS KO (gray lines). **(I)** MAb binding to monomeric eOD-GT8 (colored lines) and to monomeric eOD-GT8 KO (gray lines). Data is representative of 1-2 experiments.

426c Core selects for key mutations in the Ab HC and LCs

To directly demonstrate that the 426c Core expands VRC01-lineage B cells, 2 weeks after immunization, eOD-GT8+/eOD-GT8 KO− specific class-switched B cells from the spleens and lymph nodes of mice displaying plasma Ab cross-reactivity to eOD-GT8 were sorted and their VH/VL genes were sequenced. eOD-GT8+/eOD-GT8 KO− B cells were also sorted from unimmunized animals (a summary of the sequence analysis is presented in Supplemental Figure 3.2). A total of 420 eOD-GT8+/eOD-GT8 KO− class-switched B cells were singly sorted from the immunized animals and their VH and VL genes were amplified using PCR. 204 HC and 70 LCs were successfully sequenced (Supplemental Figures 3.2A and 3.2C).

96% of HCs were VH1–2*02 (Figures 3.1D and Supplemental Figure 3.2B). In the majority (approximately 70%) of VH1–2*02 HCs isolated after the prime immunization, the histidine at position 35 in the CDRH1 domain was replaced by an asparagine (Supplemental Figure 3.4A). The H35N mutation introduces an additional hydrogen bond with N100a in CDRH3 and increases the stability of interaction between CDRH1 and CDRH3 on VRC01-class Abs (Jardine et al., 2015).

Approximately 57% of mLCs contained 5 AA long CDRL3s (Figures 3.1E and Supplemental Figure 3.2E). The majority of the 5 AA long CDRL3s are derived from the mouse 8–30*01 LC V gene, which is represented at approximately 6% in the naive eOD-

GT8+/eOD-GT8 KO− B cell repertoire (Figure 3.1F and Supplemental Figure 3.2D). Other mLCs that utilized a 5 AA CDRL3 are derived from V-genes: 12–46*01, 4–61*01, 4–72*01, and 6–25*01 (representing 2.5% of the LC sequences with 5 AA each). All the identified 5 AA long CDRL3s-containing mLCs were paired with glVRC01 HCs. Immunization with the 426c Core therefore preferentially expanded B cells expressing mLCs with 5 AA long CDRL3s. A large fraction (40%) of the 5 AA long CDRL3s contained a $Glu96_{LC}$ (Figure 3.1G and Supplemental Figure 3.2F), which is a key feature of mature VRC01-class Abs and forms a hydrogen bond with $Gly459_{gp120}$ at the N terminus of the V5 region (West et al., 2012; Zhou et al., 2013). In contrast, 5 AA long CDRL3s with $Glu96_{LC}$ were not detected in the mLC sequenced from naive eOD-GT8+/eOD-GT8 KO− B cells (Figure 3.1G and Supplemental Figure 3.2F).

19 VH/VL pairs with VRC01 characteristics were expressed as IgGs (designated by "P" to indicate they were isolated following the prime immunization). All bound 426c Core and displayed no reactivity with 426c Core CD4-BS KO (Figure 3.1H). All 19 mAbs also bound the eOD-GT8 protein, but not the eOD-GT8 KO (Figure 3.1I). As expected, the binding affinities of these Abs for eOD-GT8 were higher than for 426c Core (Supplemental Figure 3.3).

A 3.6-Å resolution crystal structure of Ab P-p3b3 bound to the 426c Core and a 3.2-Å resolution crystal structure of Ab P-p1f1 bound to eOD-GT8 were solved (Figure 3.2; Supplemental Table 3.1). These Abs bind 426c Core and eOD-GT8 with the same angles of approach that human glVRC01 binds 426c WT Core (all atoms root-mean-square deviation [RMSD] = 0.3 Å for gp120-Fv) (Borst et al., 2018) or eOD-GT6 (all atoms RMSD = 0.8 Å for gp120- Fv) (Jardine et al., 2013) (Figure 3.2A). Critical

contacts, both in the HC (Figure 3.2B) and in the LC (Figure 3.2C), were maintained in these interactions: $Trp50_{HC}$, $Asn58_{HC}$, $Arg71_{HC}$, and $Trp100B_{HC}$ residues were not mutated in the mouse VRC01-like Abs, adopted the same orientations, and participated in the same hydrogen bonding as observed with glVRC01 (Figure 3.2B). Similar to the human glVRC01 Ab, the short 5 AA CDRL3 of the mouse VRC01-like Abs facilitates the interactions with gp120, and $Glu96_{LC}$ maintains the hydrogen bonds with Gly459 and Asn280 of gp120. Only a few residues in the LC seem to contact the gp120, and they are located at the N terminus, CDRL1 and CDRL3 (Figure 3.2C). The mouse VRC01-like Abs have longer CDRL1 than most human VRC01-class Abs (17 versus 11–12 AA long based on the Kabat nomenclature); however, several human VRC01-class Abs, including VRC01c-HuGL2, have been isolated by sorting naive B cells with eOD-GT8 that contain 17 AA long CDRL1 whose sequence is similar to that of the VRC01-like Abs identified here (Figure 3.2C) (Havenar-Daughton et al., 2018; Jardine et al., 2016). Whereas the shorter CDRL1 domain of the human inferred glVRC01 Ab is well ordered in the complex of this Ab with eOD-GT6 (Jardine et al., 2013) or with 426c WT Core (Borst et al., 2018), the CDRL1 of the mouse VRC01-like Abs bound to 426c Core or eOD-GT8 and that of VRC01c-HuGL2 bound to eOD-GT8 (Jardine et al., 2016) were disordered, indicating extensive CDRL1 flexibility. Such flexibility is likely necessary to accommodate glycans present on N276 in the presence of longer CDRL1. We concluded that the 426c Core immunogen elicits Abs with similar genetic and structural features of known human VRC01-class Abs.

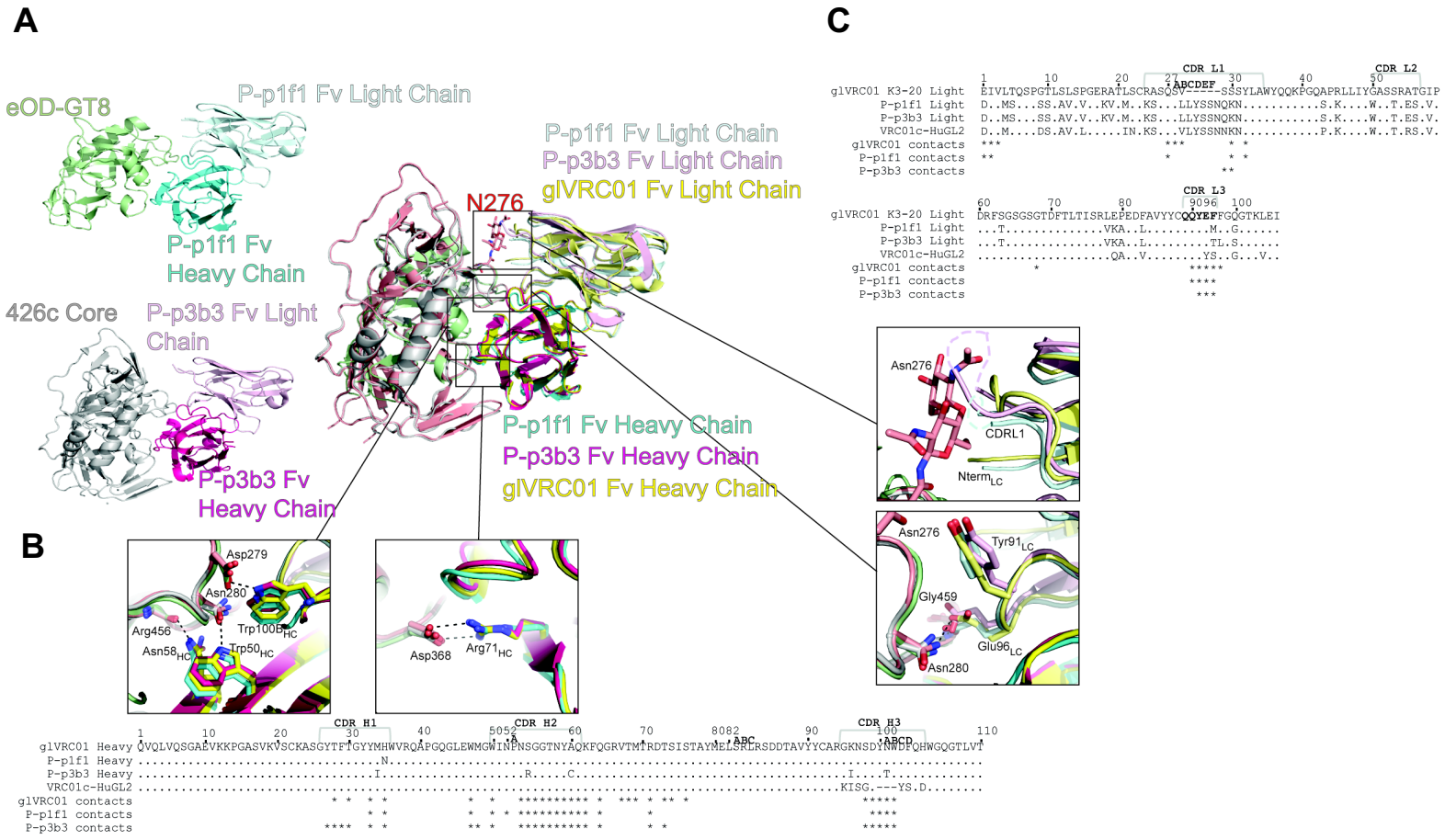

Figure 3.2. Structural information of VRC01-like Abs isolated after immunization with the 426c Core Env. (A) Structures of P-p1f1 (shades of blue) in complex with eOD-GT8 (green) and P-p3b3 (shades of pink) in complex with 426c Core (grey) are shown in

cartoon representation (left). These two structures are superimposed onto the structure of glVRC01 (shades of yellow) bound to 426c WT Core (orange) (PDB ID: 6MFT) (right). The structures are shown in ribbon representation and only the scFv portion of the Fab is shown for clarity. The glycan present at N276 in the structure of 426c WT Core bound to glVRC01 is shown in stick. **(B)** Zoom insets of important contact residues in the HC of glVRC01 and VRC01-like mouse Abs. HC sequence alignments of glVRC01, P-p1f1, P-p3b3 and VRC01c-HuGL2. Residues within 5 Å of each respective antigen are shown with an asterisk under the alignment. **(C)** LC sequence alignments of glVRC01 (k3-20), P-p1f1, P-p3b3 and VRC01c-HuGL2. Residues within 5 Å of each respective antigen are shown with an asterisk under the alignment. Zoom insets of the LC N-terminus, CDRL1 and CDRL3 contacts. The glycan at N276 present in the structure of glVRC01 bound to 426c Core is shown in sticks (PDB ID 6MFT). Disordered CDRL1s are drawn in dotted lines.

Abs elicited by the 426c Core neutralize the 426c virus lacking the N276- associated glycans

Eight of the above 19 mAbs were tested for binding to stabilized soluble trimeric Envs (SOSIP or NFL). None bound the autologous 426c WT DS-SOSIP (Figure 3.3A); however, all bound to the derivative lacking the 276, 460, and 463 NLGS (426c DS-SOSIP D3) (Figure 3.3B), and seven bound the derivative only lacking the 276 NLGS (426c ΔN276 DS-SOSIP) (Figure 3.3C). Those seven mAbs also bound the heterologous 45_01dG5 NFL TD-2CC+(DS +) trimer (Figure 3.3D). 45_01dG5 Env is derived from a virus that circulated in patient 45, from which several VRC01-class Abs have been isolated (including VRC01), and naturally lacks the 276 and 460 NLGS (Lynch et al., 2015). MAb P-p1e7 did not bind to autologous or ΔN276 heterologous stabilized trimeric Envs and is the only Ab of those tested that lacks $Glu96_{LC}$ (Supplemental Figure 3.4).

The neutralizing potency of four mAbs were evaluated against the WT 426c virus or its Δ276 NLGS derivative (Figure 3.3E) produced in either 293T or 293 GnTI−/− cells; viruses produced in 293 GnTI−/− cells can be used to detect the presence of glVRC01 class Ab neutralizing activities (Briney et al., 2016; LaBranche et al., 2018). In agreement with the binding data, the mAbs did not neutralize the WT 426c virus (regardless of whether it was produced in 293T or 293 GnTI−/− cells). However, three of four mAbs neutralized the GnTI −/− produced Δ276 NLGS virus, but not when produced in 293T cells. This could be due to the fact that the shorter glycans produced in the GnTI−/− cell line allow greater access of these still immature VRC01-like mAbs to the CD4-BS (Briney et al., 2016; LaBranche et al., 2018). The fourth, non-neutralizing Ab, P-p1e7, is the one lacking Glu96LC (Supplemental Figure 3.4B).

We concluded that the 426c Core immunogen elicits VRC01-like Abs that can recognize autologous and some heterologous soluble, stabilized Env trimers; avoiding clashes with variable regions 1, 2, and 3; and that the presence of $Glu96_{LC}$ appears to be important for these interactions. However, although these Abs can avoid the glycans present on the V5 Env region, their binding is impaired by the glycan at position N276 in Loop D.

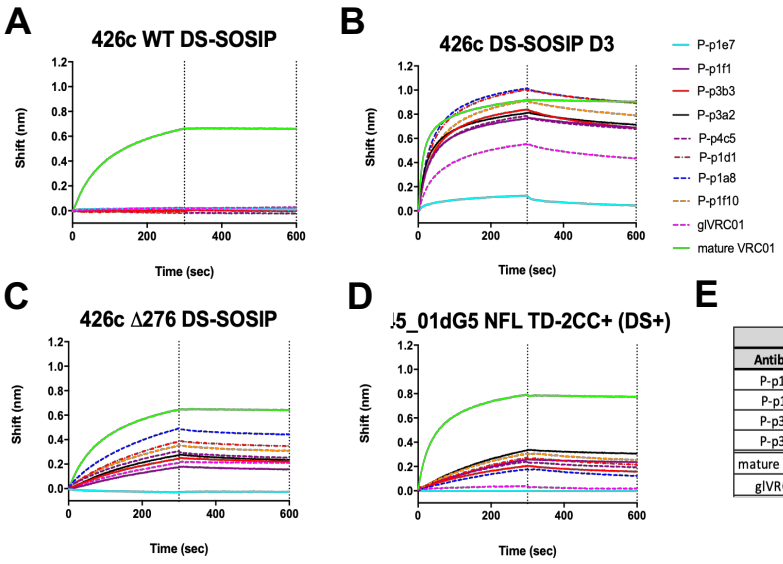

E

	WT 426c		426c △276	
Antibody	293T	GnTI-/-	293T	GnTI-/-
P-p1e7	>50	>50	>50	>50
P-p1f1	>50	>50	>50	**2.98**
P-p3b3	>50	>50	>50	**1.62**
P-p3a2	>50	>50	>50	**3.46**
mature VRC01	**2.19**	**0.11**	**0.10**	**<0.002**
glVRC01	*nt*	>100	*nt*	*nt*

Figure 3.3. Trimeric Env-binding and neutralizing properties of VRC01-like Abs elicited by the 426c Core germline-targeting immunogen. The binding of eight VRC01-like Abs generated following the prime immunization against **(A)** the autologous 426c WT DS-SOSIP; **(B)** its variant that lacks the N276, N460 and N463 NLGS (426c DS-SOSIP D3); **(C)** a variant that only lacks the N276 glycan (426c Δ276 DS-SOSIP); and **(D)** the heterologous 45_01dG5 NFL which also lacks the N276 NLGS, was determined using BLI. **(A-D)** Data is representative of 1-2 experiments. **(E)** EC50 neutralizing titers (μg/ml) of four mAbs tested against the autologous WT 426c virus and its variant lacking the 276 NLGS, grown in either 293T cells or in 293S GnTI-/- cells. Mature VRC01 and glVRC01 mAbs were used as controls during these experiments.

Abs elicited by the 426c Core accommodate the N276 associated glycans on heterologous Env cores

Plasma Abs from 426c Core-immunized animals displayed CD4-BS-dependent recognition of heterologous monomeric WT Core proteins derived from the HxB2 (clade B), 45_01dH1 (clade B), 93TH057 (clade A/E), Q168a2 (clade A), and QH0692 (clade B) Envs (Supplemental Figure 3.5A). These gp120-derived proteins lack the variable domains 1, 2, and 3, but harbor the N-X-T/S sequons at position N276 and in the V5 loop (Supplemental Figure 3.5B). This observation suggested that the VRC01-like Abs elicited by the 426c Core may bind heterologous Env Core proteins even in the presence of the N276-associated glycans.

The binding of the above-mentioned VRC01-like mAbs was examined to both the monomeric and the multimeric (C4b-based) forms of these Cores (Figure 3.4). The mAbs exhibited very weak binding to the monomeric form of HxB2, but not the other WT Cores (Figures 3.4A–3.4E). However, seven of eight mAbs tested bound the multimeric forms of the HxB2 and 45_01dH1 WT Core proteins (P-p1e7 that lacks $Glu96_{LC}$ did not bind) (Figures 3.4F–3.4G), and one mAb (P-p3b3) also bound the multimeric forms of 93TH057 WT Core (Figure 3.4H), Q168a2 WT Core (Figure 3.4I), and QH0692 WT Core (Figure 3.4J). Mature VRC01 strongly recognized both the monomeric and multimerized forms of these Cores, while glVRC01 did not recognize either. Hence, the 426c Core-elicited VRC01 Abs display intermediate binding phenotypes in comparison to those of the germline and mature human VRC01 mAbs.

We conclude that a single immunization with the 426c Core elicits VRC01-like Abs that can bypass the N276 glycans on heterologous Envs as long as the variable domains are absent (i.e., gp120-Core forms).

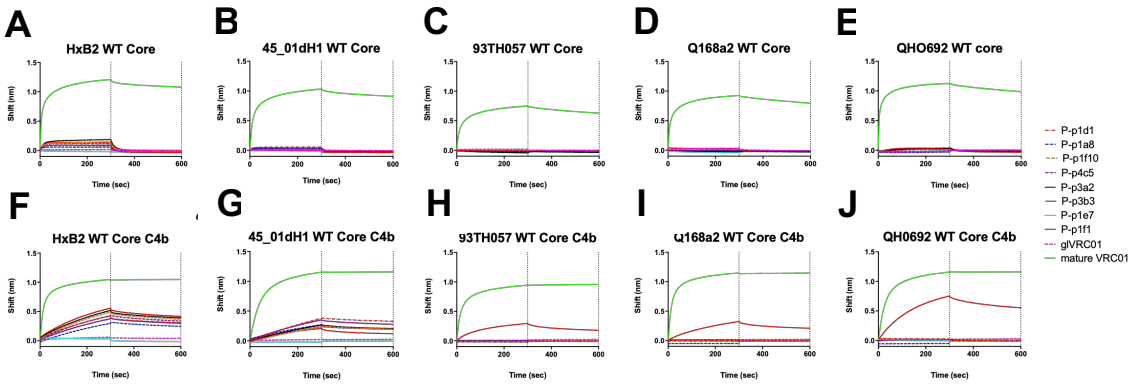

Figure 3.4. VRC01-like Abs elicited by the 426c Core germline-targeting immunogen recognize heterologous wild type Core Env proteins. BLI binding traces of the indicated mAbs to the indicated Env proteins in either monomeric **(A-E)** or nanoparticle (C4b based) **(F-J)** forms (Data is representative of 2 technical replicates). Mature and germline VRC01 mAbs were used as controls.

A heterologous boosting immunization improves the binding affinities of VRC01-like Abs to Env

Based on the above observations, we hypothesized that a boosting immunization with a heterologous Core Env expressing glycans at position N276 may expand the population of B cells that are capable of bypassing the N276-associated glycans. To test this hypothesis, a new group of animals were immunized first with the C4b nanoparticle form of 426c Core and 4 weeks later with the C4b nanoparticle form of the HxB2 WT Core Env. Env-specific B cells were isolated from the spleens and lymph nodes 2 weeks following the boost immunization and analyzed as described above. A total of 160 eOD-GT8+/eOD-GT8 KO− B cells were isolated from these animals. 72 HCs and 79 LCs were successfully amplified and sequenced (Supplemental Figure 3.2). The frequency of somatic mutation in the HC and LCs was higher in the Abs isolated after the boost than after the prime (Figures 3.5A and Supplemental Figure 3.4).

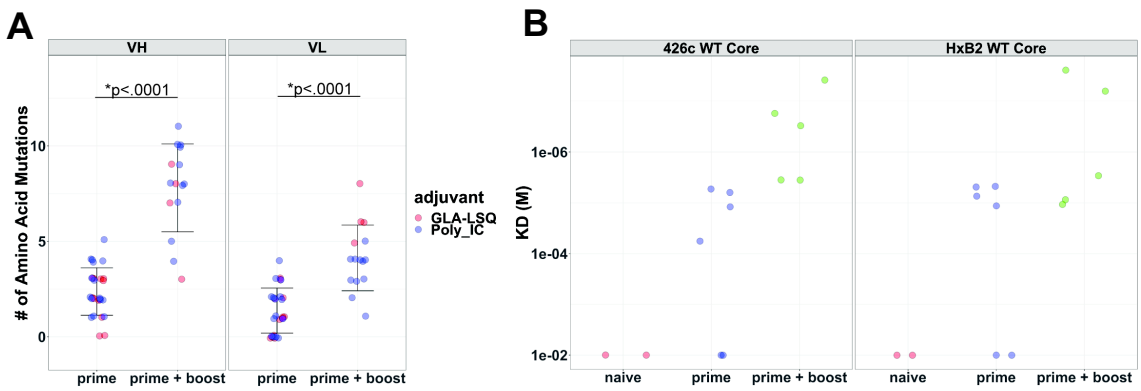

Figure 3.5. VH/VL mutations and binding affinities of VRC01-like Abs isolated throughout the immunization. (A) The number of AA mutations per each VH and VL domains in mAbs generated from sequences isolated following the prime immunization with 426c Core and the boost immunization with HxB2 WT Core are shown (see Supplemental Figure 3.4 for VH and VL sequence alignments). Each dot represents a sequence. A Welch Two Sample t-test (unpaired t-test) was used to determine the statistical significance. Error bars show standard deviation from the mean. **(B)** The binding affinities of Fabs isolated from naïve, non-immunized animals (red), Fabs generated after the prime immunization (blue) and following the boost immunization (green) are shown for the 426c WT Core and the HxB2 WT Core (binding traces and summary affinity information are shown in Supplemental Figure 3.6).

Fifteen Abs (IgG) were generated from paired VH/VL sequences displaying VRC01-class Ab features. These are designated by "B" to indicate they were isolated following the boost immunization. All mAbs recognized the 426c Core immunogen used during the prime in a CD4-BS-dependent manner (Figure 3.6A). They also bound eOD-GT8 in a VRC01 epitope-dependent manner (Figure 3.6B). While the VRC01-like Abs elicited following the prime immunization displayed very weak binding to the monomeric HxB2 WT Core (Figure 3.4A), Abs elicited after the boost, bound more strongly to several monomeric (Figures 3.6C–3.6G) and all multimeric WT Cores tested (Supplemental Figure 3.6). Overall, the VRC01-like Abs isolated after the boost have more mutations in both their HCs and LCs (Figure 3.5A), and higher binding affinities

(Figures 3.5B and Supplemental Figure 3.7) than the Abs isolated after the prime immunization.

One of the 15 mAbs (mAb B-p1b5) displayed binding to the 426c WT DS-SOSIP Env with an intact N276 glycan (Figure 3.6H). The binding was confirmed using ns EM, where 1–3 Fabs can be observed bound per trimer (Figure 3.6I). A 3D ns EM reconstruction of 426c WT DS-SOSIP and B-p1b5 complex was generated in which coordinates of existing 426c DS-SOSIP D3 and glVRC01 (PDB: 6MYY) were fitted (Figure 3.6J) (Borst et al., 2018). Weak binding of a second mAb, B-p2e2, was also observed to the 426c WT DS-SOSIP Env. Importantly, out of the four mAbs tested for neutralization, B-p1b5 neutralized the WT 426c virus (IC50 of 32.05 μg/mL) expressed in GnTI−/− cells (Figure 3.6K). The human germline VRC01 mAb does not neutralize this virus, suggesting that our mouse Ab is one step farther in the evolutionary pathway to VRC01.

B-p1b5 also displays neutralizing activity against the heterologous tier 2 virus CH0505TF when produced in GnTI−/− cells, when the loop D-associated 276 NLGS is absent (Supplemental Table 3.2). The virus lacking 197, 276, 362, and 461/462 was neutralized, but the virus lacking only 197, 276, and 362 was not (Supplemental Table 3.2). The neutralizing activity of B-p1b5 was abrogated by the D279K mutation (Supplemental Table 3.2), as is the case for known human VRC01 Abs suggesting that B-p1b5 recognizes the Env gp120 subunit in a VRC01-like manner (Lynch et al., 2015). Thus, VRC01-like Abs isolated following the heterologous boost immunization have more mutations in their VH/VL domains, bind more efficiently to heterologous WT Core Envs than the Abs isolated following the prime immunization with the 426c Core

germline-targeting immunogen, and some also display autologous neutralization when the virus expresses Env with short glycans and heterologous tier 2 neutralizing activities, when certain NLGS surrounding the CD4-BS are absent. Thus, these Abs have not yet matured sufficiently to become broadly neutralizing.

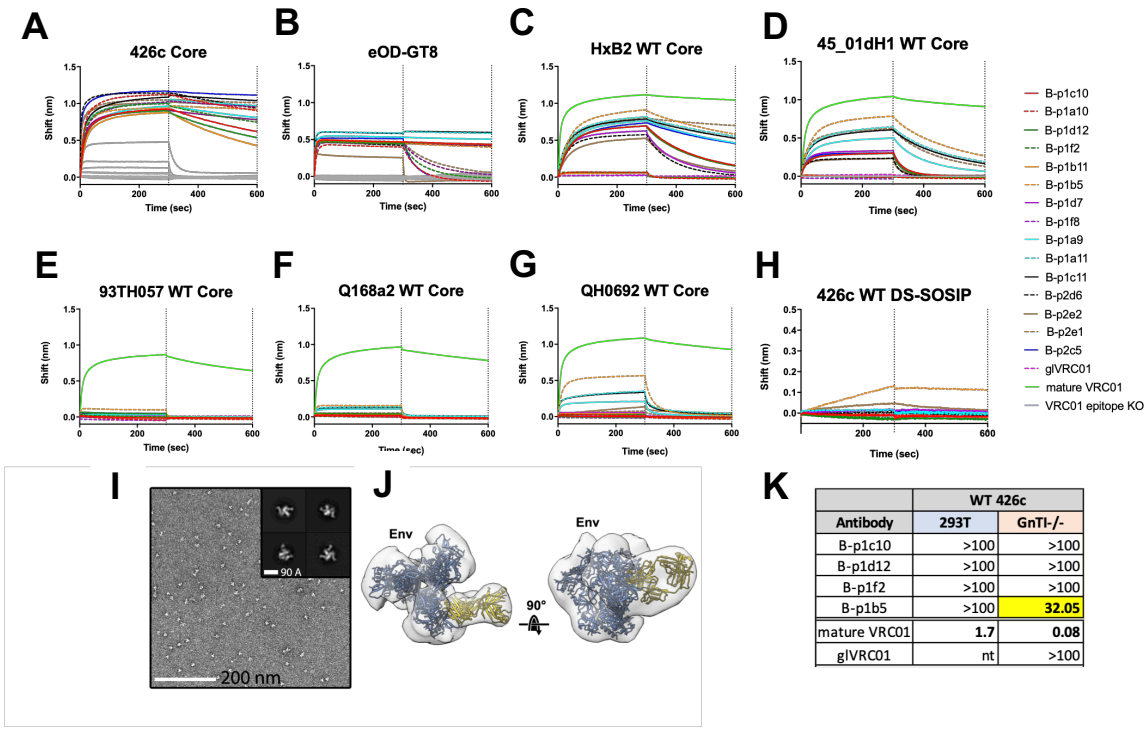

K

	WT 426c	
Antibody	293T	GnTI-/-
B-p1c10	>100	>100
B-p1d12	>100	>100
B-p1f2	>100	>100
B-p1b5	>100	**32.05**
mature VRC01	**1.7**	**0.08**
glVRC01	nt	>100

Figure 3.6. Env-recognition and neutralizing properties of VRC01-like Abs isolated following the boost immunization with the HxB2 WT Core Env. BLI binding traces of the indicated VRC01-like mAbs isolated after the boost immunization (Prefix: B) to the indicated monomeric Env Core proteins **(A, C-H),** monomeric eOD-GT8 **(B)** and the 426c WT SOSIP trimeric Env **(H).** Mature VRC01 (green) and germline VRC01 (dashed pink) were used as controls. **(I)** ns EM analysis of the 426c WT DS-SOSIP/B-p1b5 complex. Raw micrographs (scale bar = 200 nm) and 2D class averages (scale bar = 90 Å) of B-p1b5 bound to 426c WT DS-SOSIP trimers following a mild glutaraldehyde crosslinking (0.25% GTA for 45 seconds followed by quenching with 1M Tris) to increase saturation of the 426c WT DS-SOSIP trimer. **(J)** 3D reconstruction of the negatively stained 426c WT DS-SOSIP/B-p1b5 complex cross-linked with 0.25% GTA. Structures of the 426c DS-SOSIP trimer and germline VRC01 Fab were fit to the density as a reference (grey = negative stain EM density, blue = 426c DS-SOSIP, yellow = Fab) (Borst et al., 2018). **(K)** EC50 neutralizing titers (ug/ml) of indicated mAbs against the WT 426c virus grown in either 293T cells of 293S GnTI -/- cells. Mature and germline VRC01 mAbs were used as controls for the binding and neutralization assays. Neutralization assays against the GnTI-/- produced virus were performed 2-3 times. Neutralization assays against the 293T produced virus is from one experiment.

Vaccine-elicited VRC01-like Abs can avoid clashes with the N276-associated glycan

The results in the previous section suggested, but did not conclusively prove, that the VRC01-like Abs isolated following the prime and boost immunization with 426c Core and HxB2 WT Core could more efficiently circumvent the steric hindrance imposed by the glycan at position N276 than those Abs isolated following the prime immunization with the "germline-targeting" 426c Core immunogen.

To address this point directly, we performed a series of complementary experiments. In one experiment, B-p1b5 was co-expressed in GnTI−/− cells with the 426c WT Core (which expresses the N-X-S/T sequon at position N276) as a disulfide cross-linked complex (Borst et al., 2018). The purified Ab-Env complex was further enzymatically treated with Endo H, and semiquantitative mass spectrometry analysis of the 276 NLGS was performed (Figure 3.7A). Man5 glycans were detected at position N276, confirming that B-p1b5 binds the 426c WT Core in the presence of N276-associated glycans. Despite the additional Endo H treatment following complex formation, no $(GlcNAc)_1$ glycopeptides were detected at the 276 NLGS by liquid chromatography-tandem mass spectrometry (LC-MS/MS). This observation validated that bound B-p1b5 Ab protected the N276 glycan from enzymatic digestion when interacting with its cognate epitope.

Additional experiments were performed to probe these interactions in the absence of disulfide cross-linking. In one such experiment, we used an N276-dependent mAb, 179NC75, to purify the N276-glycosylated HxB2 WT Core Env (Freund et al., 2015)

(Figure 3.7B). Purified monomeric HxB2 WT Core expressed in GnTI−/− cells was incubated with 179NC75 immobilized on magnetic beads and the bound Core molecules were eluted and tested for recognition by mouse VRC01-like Abs N-p4a9 and N-p3g9, isolated from unimmunized animals; P-p3b3, isolated following the prime immunization; and B-p1a11 and B-p1b5, isolated following the boost immunization. As expected, the Abs isolated from unimmunized animals did not display HxB2 WT Core reactivity (Figures 3.7C and 3.7D). P-p3b3 displayed marginal reactivity to HxB2 WT Core molecules expressing N276 glycans ("enriched") (Figure 3.7E), while the two Abs isolated after the boost, bound strongly to the HxB2 WT Core molecules expressing N276 glycans ("enriched") (Figures 3.7F and 3.7G).

In another set of experiments, monomeric 426c WT Core and HxB2 WT Core proteins expressed in GnTI−/− cells were incubated with magnetic beads coated with the above mentioned mouse VRC01-like Abs. Following immunoprecipitation, the flow-through and eluted materials were subjected to gel electrophoresis (Figures 3.7H and 3.7I). As expected, neither 426c WT Core nor HxB2 WT Core proteins were immunoprecipitated by the N-p3g9 and N-p4a9 mAbs. 426c WT Core, but not HxB2 WT Core, was precipitated by P-p3b3. In contrast, both 426c WT Core and HxB2 WT Core were immunoprecipitated by B-p1b5. Semiquantitative mass spectrometry analysis was performed to determine the presence of Man5 glycans at position N276 in the immunoprecipitated material (Figures 3.7J and 3.7K). This analysis confirmed that the mouse VRC01-like Abs isolated following the prime have the potential of recognizing 426c WT Core molecules expressing N276-associated glycans and that the Abs isolated following the boost have the potential of recognizing both the 426c WT Core and HxB2

WT Core in the presence of N276 glycans. We note that these Abs preferentially immunoprecipitated Env molecules lacking the N276- associated glycans, a consequence of not yet being fully matured following the prime-boost immunization scheme.

Collectively, the above experiments confirm that the VRC01-like Abs isolated following the boost immunization can accommodate N276-associated glycans on fully glycosylated heterologous gp120-derived Core proteins, but less so on trimeric Envs present on virions.

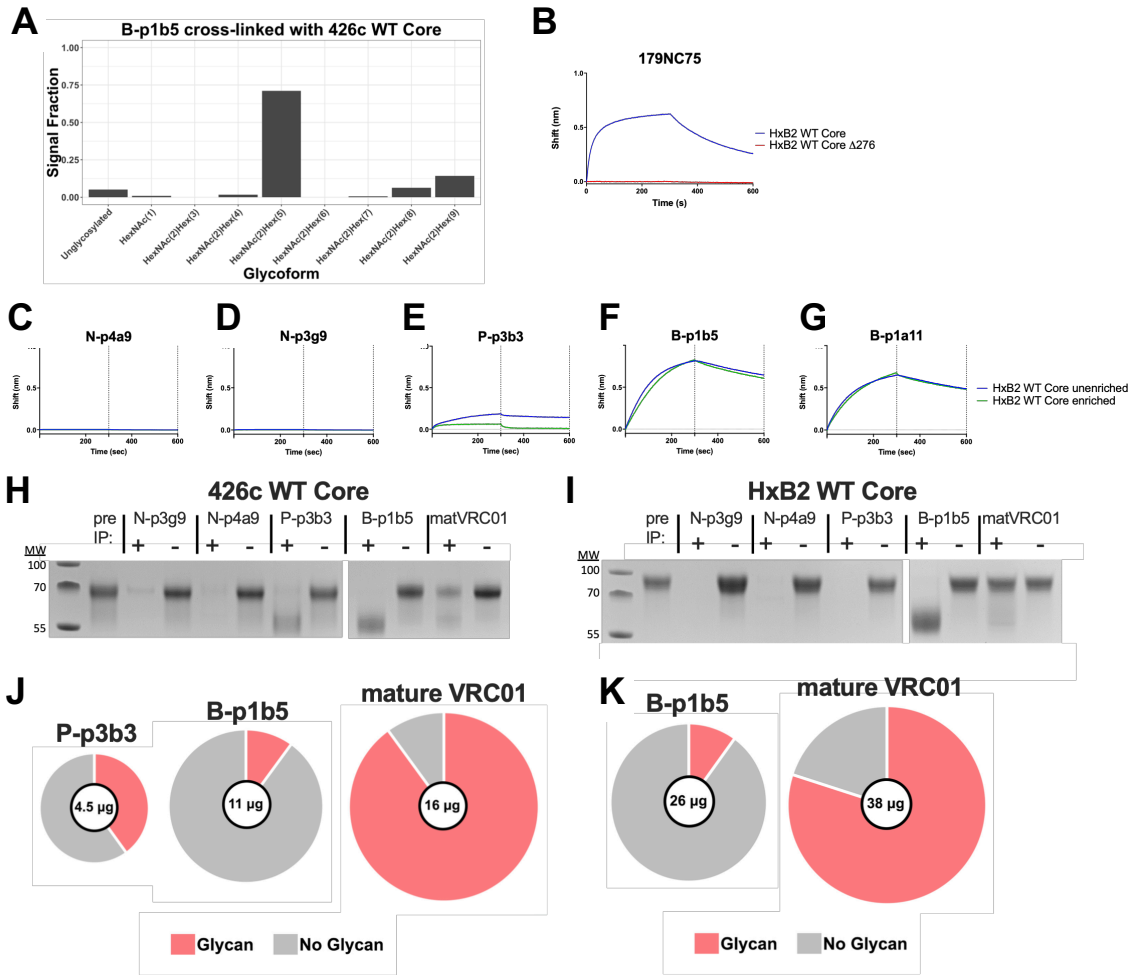

Figure 3.7. Vaccine elicited Abs bind in to Env Core with glycans at N276. (A) The 426c WT Core/B-p1b5 complex was generated in 293 GnTI-/- cells, purified and subjected to semi-quantitative LC-MS/MS analysis. Depicted here are the relative signal intensities of (glyco)peptides comprising the 276 NLGS. The mass spectrometry data represents the average of two technical replicates. **(B)** Binding of mAb 179NC75 to HxB2 WT Core or its derivative lacking the N276 NLGS ("HxB2 WT Core Δ276"). Data is representative of two technical replicates. **(C-G)** Binding of the indicated mAbs to HxB2 WT Core that has been enriched for the glycan at 276 (eluted from a 179NC75 column) or the unenriched fraction. **(H-I)** MAbs generated from unimmunized animals (N-p3g9 and N-p4a9), from animals immunized with the 426c Core (P-p3b3), and from animals immunized with the 426c Core and the HxB2 WT Core (B-p1b5) were immobilized on beads. The beads were incubated with 426c WT Core or HxB2 WT Core proteins expressed in 293 GnTI-/- cells. Following co-immunoprecipitation, 426c WT Core **(H)** and HxB2 WT Core **(I)** were washed and eluted from the beads. **(H,I)**. A fraction of the unbound ("-") and the eluted ("+") material was subjected to SDS-PAGE gel electrophoresis. The gel is representative of two technical replicates. The eluted fractions were further subjected to semi-quantitative LC-MS/MS analysis (two technical replicates) to determine the presence of a glycan at position 276 on 426c WT Core **(J)** and on HxB2 WT Core **(K).** The quantity of material eluted from the beads after co-

immunoprecipitation is shown in the middle of the pie charts, which are scaled relative to the amount of material pulled-down with mature VRC01.

Discussion

A major challenge to the successful maturation of the germline forms of VRC01 Abs toward their broadly neutralizing forms is the steric hindrance imposed by glycan molecules present on the conserved loop D 276 NLGS. As the present germline-targeting Env-based immunogens are designed to specifically lack the 276 NLGS (Jardine et al., 2013, 2015; McGuire et al., 2013, 2014, 2016; Medina-Ramírez et al., 2017), they are expected to preferentially activate BCRs that recognize the VRC01 epitope when N276-associated glycans are absent. Efforts to guide the maturation of such Abs through sequential immunization with Env constructs also lacking 276 NLGS have so far met limited success (Briney et al., 2016; Tian et al., 2016). In the study by Tian et al., six different immunogens (only the fifth and sixth of which expressed N276-associated glycans were sequentially administered in a knockin mouse model that expresses both the human IGHV1–2*02 and the germline human IGKV3–20*01 genes. mAbs isolated at the end of the immunization efficiently neutralized autologous 426c viruses lacking the N276 NLGS, and one Ab weakly neutralized the autologous 426c WT virus, which presumably had glycans occupying N276. The mechanism by which this mAb could bypass the N276-associated glycan was not reported (Tian et al., 2016). The study by Briney et al. was conducted in the same animal model we employed here, which we consider to be more stringent than the one employed by Tian, as only the glVRC01 HC is knocked in. Thus, in this model, the immunogens must first activate the rare B cells that also express a VRC01-like LC; i.e., one with 5 AA CDRL3s. Three different immunogens were administered sequentially, all three lacking N276-associated glycans. The Abs isolated at the end of immunization efficiently neutralized heterologous viruses lacking N276-

asociated glycans, and one Ab neutralized a tier 2 heterologous virus, although it is unclear whether all the virion associated Envs express N276-associated glycans and whether and how this particular Ab bypassed the N276 glycan on this virus but not on the other viruses tested (Briney et al., 2016).

Here, we tested an alternative immunization scheme during which the prime immunization with the 426c Core germline-targeting immunogen is immediately followed by an immunization with a heterologous Core that expresses N276-associated glycans. This scheme was selected because we observed that a fraction of the VRC01-like Abs elicited by the 426c Core immunogen display weak binding to heterologous Cores with N276 glycans. Indeed, the boost immunization improved the ability of the elicited VRC01-like Abs to bypass the N276-associated glycans. Our observations are in agreement with reports by Escolano et al. (2016, 2019), where germline PGT121 BCRs were activated upon immunization with very low-affinity Env-derived immunogen.

The 426c Core immunogen selects for VRC01-like Abs with key features. The H35N mutation in the CDRH1 domain leads to an increased stability between the CDRH1 and CDRH3 domains of the HC, whereas the selection of the $Glu96_{LC}$ allows for the formation of a hydrogen bond with $Gly459_{gp120}$ at the N terminus of the V5 region (West et al., 2012; Zhou et al., 2013). Our data indicate that, within the 5 AA long CDRL3 domains, the presence of $Glu96_{LC}$ appears to be important for the Ab interactions with autologous and heterologous Core proteins. LCs with 5 AA long CDRL3s are identifiable from naive B cells in this mouse model. However, we have not yet identified LCs with 5 AA long CDRL3 containing a $Glu96_{LC}$ in the BCR repertoire analysis of naive B cells from the unimmunized mice. Either these LCs are present at extremely low

frequencies and our germline-targeting immunogen selects for them, or $Glu96_{LC}$ is the result of SHM and subsequent selection in the germinal center following immunization with the 426c Core immunogen.

The majority of mouse VRC01-like Abs elicited by the 426c Core, and which were subsequently boosted by the HxB2 WT Core, express LCs derived from the mouse k8–30*01 VL gene (Figures 3.1C and Supplemental Figure 3.4B), similar to what was previously reported during eOD-GT8-based immunizations in this same mouse model (Briney et al., 2016; Jardine et al., 2015). As a result, their CDRL1 are 17 AA's long (Figures 3.2 and Supplemental Figure 3.4B). Most mature human VRC01 mAbs express shorter CDRL1s (7–11 AA long, per Kabat numbering), which sometimes contain flexible glycine residues (Zhou et al., 2013). These CDRL1 features are believed to be necessary for the Ab LCs to accommodate the N276-associated glycans (Zhou et al., 2013). However, several glVRC01-class Abs isolated from naive B cells using eOD-GT8 as a bait express longer CDRL1s (Havenar-Daughton et al., 2018; Jardine et al., 2016). One of them, VRC01c-HuGL2, recognizes eOD-GT8 in a manner similar to mature VRC01 (Jardine et al., 2016) and has a CDRL1 almost identical in AA sequence as the one present in the mouse VRC01 Abs described here (Figure 3.2).

As compared to the rest of the VL domains, the CDRL1 regions appear to be under intense selective pressure to accumulate negatively charged AA's (Supplemental Figure 3.4B). For instance, in most sequences, $Lys30_{LC}$ is replaced by a glutamic acid and additional negatively charged AA's (Asp or Glu) are also introduced in that same general region of CDRL1. Although we were able to confirm that the mouse VRC01-like Abs elicited by our vaccination strategy recognize the VRC01 epitope in the presence of

N276-associated glycans, the disordered CDRL1 structures limit our understanding on how the introduction of negatively charged aa's allow these LCs to accommodate these glycans. Affinity maturation of the Abs outside of the CDRL1 region may have compensated for the entropic cost of binding in the presence of the N276-associated glycan as has been observed in the VRC08 Ab lineage, which has a long rigid CDRL1 (Bonsignori et al., 2018). VRC01-like Abs that do not express k8–30*01-derived VL domains were also isolated after the prime immunization (Supplemental Figure 3.4B). These express shorter CDRL1 domains (10–11 AA's), but in contrast to the k8–30*01-expressing Abs, they were not mutated from germline, nor did they contain Glu96. So far, the neutralizing activities of mAbs isolated following the prime-boost immunization are evident against the 426c-derived virus lacking the 276 NLGS and against the heterologous CH0505TF-derived virus that not only lacks the N276 NLGS but also V5-associated NLGS (positions 461/462) (Supplemental Table 3.2). The observation that the D279K mutation abolished the neutralizing activity of mouse VRC01-like Abs indicates that this activity is indeed targeting the VRC01 epitope. In that case, the absence of V5-associated NLGS appears to be required for neutralization. In all cases, the potency of neutralization was higher when the target virus was expressed in 293 GnTI−/− cells, an indication that the mouse VRC01-like Abs have not yet accumulated the necessary mutations to accommodate complex glycans surrounding the CD4-BS. Presently, it is unknown whether further maturation of the mouse VRC01-like Abs toward their broad neutralizing activities will be delayed by the presence of long CDRL1 domains.

Although approximately 0.08% of B cells express glVRC01-like BCRs in the mouse model employed here (as compared to approximately 0.01% in humans),

approximately 80% of the B cells express the already rearranged VDJ germline HC VRC01 chain (Jardine et al., 2015). It will therefore be important to evaluate the prime-boost immunization protocol discussed here, at more physiological frequencies of target B cells. Such experiments would most likely require adoptive transfer of target B cells into a WT animal, as recently reported (Abbott et al., 2018; Dosenovic et al., 2018).

The data presented here inform how VRC01-class Ab responses may be generated during natural HIV-1 infection. It suggests that although viral Env species that initiated the expansion of precursor VRC01-class BCRs in the context of infection may either lack N276-associated glycans or have short N276-associated glycans, the subsequent viral Envs that guide the maturation of these Abs to bypass the N276-associated glycans most likely express glycans at N276. Indeed, sequence analysis of viral Envs in patient 45 (Lynch et al., 2015), from which VRC01 was isolated from (Wu et al., 2010), indicate the early presence of viral variants lacking N276-associated glycans, which were gradually replaced by viral Env variants expressing N276-associated glycans. Also, the recent report by Umotoy et al. (2019) suggests that in the context of HIV-1 infection the development of VRC01 bnAbs may benefit from an early B cell response to Envs with N276-associated glycans. In this last study, VRC01-class lineages with preferred reactivity in the presence of N276-associated glycans were also identified.

Our study informs on how to guide the maturation of glVRC01-class Abs during immunization, so that the immunogens employed during the boost select for Abs with mutations that allow them to accommodate the N276-associated glycan. As such, our results are relevant to current and upcoming clinical trials that evaluate the ability of germline-targeting immunogens to elicit cross-reactive VRC01-class Ab responses.

Acknowledgements

Claire Levy and Pavitra Roychoudhury for help with somatic hypermutation analysis.

This study was supported by NIH grants: R01 AI104384, P01 AI138212 and U19 AI109632 to LS; NIH contract: HHSN272201800004C to DCM; and R01GM120553 to DV as well as by a Pew Biomedical Scholars Award and an Investigators in the Pathogenesis of Infectious Disease Award from the Burroughs Wellcome Fund to DV. This work was also supported by the Arnold and Mabel Beckman cryoEM center at the University of Washington and the Proteomics Resource UWPR95794. We thank the J. B. Pendleton Charitable Trust for its generous support of Formulatrix robotic instruments. X-ray diffraction data was collected at the Berkeley Center for Structural Biology beamline 5.0.2, which is supported in part by the National Institute of General Medical Sciences. The Advanced Light Source is supported by the Director, Office of Science, Office of Basic Energy Sciences, of the United States Department of Energy under contract number DE-AC02-05CH11231.

Declaration of interests

The authors declare no competing interests. Patent US 2018/0117140 "ENGINEERED AND MULTIMERIZED HUMAN IMMUNODEFICIENCY VIRUS ENVELOPE GLYCOPROTEINS AND USES THEREOF" is awarded to A. McGuire and L. Stamatatos.

Methods

Lead contact and materials availability

Further information and requests for reagents should be directed to and will be fulfilled by Leonidas Stamatatos (lstamata@fredhutch.org). All reagents generated in this study can be made available upon request through Materials Transfer Agreements.

Experimental model and subject details

Immunizations were performed in the glH-VRC01 mouse (Jardine et al., 2015). It is heterozygous for the transgene (glVRC01 HC with the CDRH3 found in the mutated Ab) and only expresses mouse LCs. The Fred Hutch Institutional Animal Care and Use Committee approved all mouse studies. Mice were 6–12 weeks old at the beginning of the studies. Both male and female mice were included in these studies. Mice were immunized intramuscularly with a dose of 60 ug of protein and 60 ug of poly(I:C) (InvivoGen, Cat# tlrl-pic-5) split between the rear hind legs or with 50 ug of protein and 50 ul of GLA-LSQ (IDRI). Blood was collected retro-orbitally during immunization and via a cardiac puncture 2 weeks following the last immunization, at which time spleen and LNs were also harvested. Spleen and LNs were processed into a single cell suspension separately, frozen in FBS + 10% DMSO and stored in liquid nitrogen until further use. Blood, spleens and LNs were also isolated from non-immunized animals.

Protein expression and purification

Recombinant Env proteins expressed in nanoparticle (Ferritin or C4b-based) and NFL forms were expressed and purified as previously described (Guenaga et al., 2015;

McGuire et al., 2016). Briefly, Envs were produced in 293E or 293F. Cell supernatants were purified by lectin affinity chromatography (Galanthus nivalis, Vector Labs), then subjected to Superdex 200 size exclusion chromatography (GE Healthcare). Ferritin nanoparticles underwent two rounds of size exclusion chromatography, first on a Superose 6 10/300GL column and then on a HiLoad 16/600 Superdex 200pg column. Soluble trimeric SOSIP-based Envs were expressed and purified as previously described (Borst et al., 2018). In short, Env-expressing and furin-expressing plasmids were cotransfected (at 5:1 DNA ratio) into 293E cells. The Envs were purified from the cell supernatants using a Ni-affinity column followed by a Streptactin affinity column. Proteins were then subjected to enzymatic cleavage to remove the his-tag. Monomeric proteins were produced by transfecting 293E or GnTI−/− cells with Env encoding plasmid. Cells are cultured for 6 days at 37°C, 5% CO2, 80% humidity, and shaking at 125 RPM. Cells were centrifuged for 3000 RPM for 30 minutes and the supernatant sterile filtered through at 0.22 uM filter. Protein was purified by passing the cellular supernatant over a 5ml Fast Flow HisTrap column (Fisher Sci, Cat # 45000326). The eluted protein was purified on SEC as described above.

Core CD4-BS KO Env constructs contain the D368R and E370A mutations, while the eODGT8 KO contains the D368R mutation and the AAs at positions 276–279 have been mutated to “NFTA.”

Flow cytometry

Spleen and lymph node samples were thawed in a 37°C water bath until a smallice pellet remained in the tube and warm RPMI was then added dropwise. B cells wereisolated

using a mouse B cell isolation kit (EasySep, Cat#: 19854). If the antigen-specific cells were infrequent, an antigen enrichment protocol was used during which tetramers and decoys were first added to the cells and then anti-PE microbeads (Miltenyi Biotech Cat#: 130–048-801) and anti-APC microbeads (Miltenyi Biotech Cat#: 130–090-855) were added. Stained cells were then flowed over LS Columns (Miltenyi Biotec Cat#: 130–042-401) to separate the antigen-specific cells from the non-antigen specific. The B cells were then stained with a combination of the following Abs: IgG1 FITC (BD Biosciences Cat#: 553443), IgG2b FITC (BD Biosciences Cat#: 553395), IgG2c FITC (Bio-Rad Cat#: STAR135F), IgG3 FITC (BD Biosciences Cat#: 553403), IgD PerCP-Cy5.5 (Biolegend Cat#: 405710), GL7 eFluor 450 (Thermo Fisher Scientific Cat#: 48–5902-80), eBioscience Fixable Viability Dye eFluor 506 (Thermo Fisher Scientific Cat#: 65–0866-14), CD3 BV510 (BD Biosciences Cat#: 563024), CD4 BV510 (BD Biosciences Cat#: 563106), Ly-6G/Ly-6C BV510 (BD Biosciences Cat#: 563040), F4/80 BV510 (BD Biosciences Cat#: 123135), IgM BV605 (Biolegend Cat#: 406523), B220 BV786 (BD Biosciences Cat#: 563894), CD38 AF700 (Thermo Fisher Scientific Cat#: 56–0381-82), CD19 BUV395 (BD Biosciences Cat#: 563557) or CD19 BV650 (BD Biosciences Cat#: 563235).The cells were stained with either 426c DMRS Core/426c DMRS DREA (D368R and E279A) Core or eOD-GT8/eODGT8 KO tetramers to select for Env specific and CD4-BS specific B cells. Tetramers were made by combining biotinylated Env with Streptavidin conjugated to either a PE or APC fluorophore (Prozyme, PJFS25 and PJ27S). From the groups of immunized mice, only samples from animals which showed eOD-GT8 plasma cross-reactivity were used for sorting.

Single B cell sorting

Naive, antigen-specific B cells were sorted as CD3−, CD4−,Gr-1−, F4/80−, B220+, CD19+, antigen+/antigen KO−. Class-switched IgG B cells from immunized animals were sorted based on the following markers: CD3−, CD4−, Gr-1−, F4/80−, B220+, CD19+, IgG1+, IgG2b+, IgG2c+, IgG3+, antigen+/antigen KO-. Individual B cells were sorted using the FACS ARIA II into a 96 well plate containing 20 ul of lysis buffer (20 U of RNase out (Thermo Fisher Scientific, Cat#: 10777019), 5 ul 5X Superscript IV RT buffer, 1.25 ul of 0.1M DTT, 0.625 ul of 10% Igepal, 13 ul nuclease free H20) in each well. Plates with the sorted cells were stored at −80°C until further processing.

PCR amplification and sequencing of VH and VL genes

RNA was reverse transcribed to cDNA. For the reverse transcription reaction, 0.1 ul of Random Primers (3ug/ul, ThermoFisher Scientific Cat#: 48190011), 2 ul 10mM GeneAmp dNTP Blend (ThermoFisher Scientific, Cat#: N8080261), 1 ul SuperScript IV RT (200 U, ThermoFisher Scientific Cat#: 18090200), and 2.9 ul of nuclease free H20 was added to the wells containing lysed cells. The reaction was run on a thermocycler for 10 minutes at 42°C, 10 minutes at 25°C, 60 minutes at 50°C, and 5 min at 94°C. Following reverse transcription, the cDNA was diluted 1:2. Two rounds of PCR were employed to amplify both VH and VL genes. Each PCR reaction contains: 7 ul of cDNA, 2.4 units of HotStar Taq Plus (QIAGEN, Cat#: 203607), 240 nM of 5′ and 3′ primer, 350 uM GeneAmp dNTP Blend (ThermoFisher Scientific, Cat#: N8080261), 4 ul of 10X buffer, and 27.8 ul nuclease free H20. All primers and cycling conditions can be found in Tables S3 and S4. After the second round of PCR, samples were subjected to

electrophoresis on a 1.5% agarose gel containing 0.1% Gel Red Nucleic Acid Stain (Biotium, Cat#: 41002). cDNA was purified using the enzyme ExoSap-IT (Affymetrix, Cat#: 78201). The purification reaction contained 5 ul of second round PCR product and 2 ul of ExoSap-IT. This reaction was run on a thermocycler for 15 min at 37°C followed by 15 min at 80°C. Following enzymatic purification, 5 ul of 5 uM second round 5′ primer was added to the sample and 3 ul of nuclease free water. Samples underwent sanger sequencing to identify the DNA sequence (Genewiz, Seattle, WA). Upon receiving the sequence, IMGT/V-QUEST was used to assign V, D, and J gene identity to the sequences and CDRL3 length (Brochet et al., 2008; Giudicelli et al., 2011). Sequences were included in the analysis (Supplemental Figure 3.2) if they had an identifiable CDR3 region. AA mutations were identified by aligning the VH/VL gene sequences to the corresponding germline genes (IMGT Repertoire) using the Geneious Software (Version 8.1.9). For VL, mutations were counted beginning at the 5′ end of the V-gene to the 3′ end of the FW3. For VH, mutations were counted beginning at the 5′ end of the V-gene to the end of the KI gene. See Figure S3.4 for sequence alignments. To quantify the number of AA mutations, the sequence alignments were exported from Geneious and imported into R (Version 3.4.1) for analysis (R Core Team, 2018). This analysis uses the packages Biostrings (Pages et al., 2018), seqinr (Charif and Lobry, 2007), and tidyverse (Wickham, 2017). The sequences and code for this analysis can be found here: https://github.com/krparks/glVRC01_sequential_immunization.

VH and VL cloning and Ab expression

Gene-specific PCR was used to amplify the DNA product from the first round PCR using primers designed to anneal to the gene of interest as well as add ligation sites to facilitate insertion of the DNA fragment into the human IgG1 vector [ptt3 k for kappa (Snijder et al., 2018), and PMN 4–341 for gamma (Mouquet et al., 2010)]. Each gene specific PCR reaction contained 0.5 ul each of 10 uM 5′ and 3′ primer, 22.5 ul Accuprime Pfx Supermix (Cat#: 12344040), and 1.5 ul of 1st or 2nd round PCR product. The gene-specific PCR product was infused into the cut IgG1 vector in a reaction containing 12.5 ng of cut vector, 50 ng of insert, 0.5 ul of 5X Infusion enzyme (InFusion HD Cloning Kit, Cat#: 639649), and nuclease-free water to bring volume to 2.5 ul. The entire reaction was used to transform competent E. coli cells and plated on agar plates containing ampicillin. In some cases, gBlocks were synthesized to make the VH or VL containing plasmid (GenScript). 60 ng of glBlock was added to 15 ng of cut vector and 0.5 ul of 5× In-Fusion enzyme (Takara, Cat#: 1805251A). This reaction was run on the thermocycler for 15 min at 50°C. The entire reaction was used to transform competent E. coli cells (New England Biolabs, Cat#: C2987HI) and plated on agar plates containing ampicillin. Once a colony containing the insert sequence was identified, it was grown in LB broth containing ampicillin. DNA was prepared using QIAprep Spin Miniprep Kit (QIAGEN, Cat#: 27106). Equal amounts of heavy and LC DNA and 293F transfection reagent (Millipore Sigma, Cat#: 72181) were used to transfect 293E cells. 5–7 days post transfection cell supernatants were collected, and the Abs were purified using Pierce Protein A agarose beads (Thermo Fisher Scientific, Cat#: 20334). The Abs were eluted using 0.1 M Citric Acid into a tube containing 1 M Tris. The Abs were buffer exchanged into 1XPBS using an amicon centrifugal filter.

To make Fabs, the IgG was cleaved overnight at 37°C to generate antigen binding fragment (Fab) with Endoproteinase Lys-C (NEB). To remove undigested IgG and IgG Fc fragments, the mixture was incubated with Protein A Agarose Resin for 1 hour at room temperature. Beads were washed with 1X PBS to remove excess Fab. Fab was further purified on SEC using a HiLoad 16/600 Superdex 200 pg (GE) column.

Protein Production for structural studies

P-p1f1Fab and eOD-GT8 (PDB ID: 6P8N)

eOD-GT8 was expressed in HEK293S GnTI−/− cells. Cells were cultured in suspension and transfected using 500 μg eOD-GT8 plasmid with 293 Free Transfection Reagent (Novagen) in 1 L. After 6 days, cells were centrifuged at 4,500 rpm for 20 min and supernatant was filter-sterilized. A His-tag was utilized for purification by adding His60 Ni-Superflow Resin (Takara, Cat #:636660) in the supernatant at 4°C overnight. Ni Resin was washed with a solution of 150mM NaCl, 20 mM Tris pH 8.0, 20 mM Imidazole pH 7.0 and eluted with a solution of 300 mM NaCl, 50 mM Tris pH 8.0, 250 mM Imidazole pH 7.0. Protein was further purified using SEC as previously described.

Complexes of eOD-GT8 and P-p1f1Fab were made by mixing equal molar ratio of both proteins for 1 hour at room temperature. Complexes were then mixed with Endo H (NEB, Cat#: P0702S) for 1hour at 37°C. SEC was used to remove any uncomplexed protein and Endo H. Complexes were concentrated to ~10 mg/mL for crystallization trials.

P-p3b3Fab and 426c Core (PDB ID: 6P8M)

P-p3b3Fab crosslinked to 426c Core was expressed in HEK293S GnTI−/− cells. Cells were cultured in suspension and transfected with equal parts of 426c Core G459C, P-p3b3Fab-A60C HC, and P-p3b3 LC plasmids (500 μg total/L) as previously described (Borst et al., 2018). Complexes were purified with a His tag on the Fab HC C terminus followed by SEC to remove nonspecific proteins and excess unliganded Fab. An SDS gel was run on the complex to confirm the disulfide bond formation between the P-p3b3Fab and the 426c Core.

Complexes were treated with EndoH (New England Biolabs, Cat#: P0702S) for 1hr at 37°C and run on SEC to remove Endo H. Complexes were concentrated to ~10 mg/mL for crystallization trials.

Crystallization

Crystallization conditions were screened and monitored with an NT8 drop setter and Rock Imager (Formulatrix). Screening was done with Rigaku Wizard Precipitant Synergy block no. 2 (MD15-PS-B), Molecular Dimensions Proplex screen HT-96 (MD1–38), and Hampton Research Crystal Screen HT (HR2–130) using the sitting drop vapor diffusion method. P-p1f1fab + eOD-GT8 crystals were further optimized with hanging drop trays using vapor diffusion method. Final crystals for P-p1f1Fab + eODGT8 were grown in 22.5% PEG 3350, 13.5% Isopropanol, 0.18M Ammonium Citrate pH 4.0. Final crystals for P-p3b3Fab + 426c Core were grown in 0.67% PEG 4000, 0.67M Ammonium Citrate pH 5.5. P-p1f1Fab + eOD-GT8 crystal were cryo protected in a solution of 20% molar excess of the crystallization condition and 20% Ethylene Glycol. P-p3b3Fab + 426c Core were cryoprotected in the original crystallization condition. P-p3b3Fab + 426c Core and

P-p1f1Fab + eOD-GT8 were sent to ALS 5.0.2 and diffraction data was collected to 3.59 Å and 3.2 Å respectively. Data were processed using HKL2000 (Otwinowski and Minor, 1997).

Structure solution and refinement

The structure of P-p1f1Fab + eOD-GT8 was solved by molecular replacement using PDB ID: 4JPK as a search model in Phaser in Phenix. The structure of P-p3b3Fab + 426c Core was solved by molecular replacement using PDB ID: 6MFT as a search. The structures were further refined with COOT (Emsley and Cowtan, 2004) and Phenix (Adams et al., 2004). The refinement statistics are summarized in Supplemental Table 3.1.

ns EM

The 426c WT DS-SOSIP/B-p1b5 complex was formed by co-incubating B-p1b5 Fab to 426c WT DS-SOSIP trimer at a 2:1 B-p1b5:gp120 monomer ratio (alternatively referred to as 6:1 B-p1b5 trimer ratio) ratio for 10 minutes at 4°C. Samples treated with glutaraldehyde were cross-linked in 0.25% GTA for 45 s followed by quenching with 1M Tris, followed by purification of bound complexes via a Superdex 200 10/300 GL Increase column. 426c WT DS-SOSIP/B-p1b5 Fab complexes examined in this study (3 μL) were negatively stained at a final concentration of 0.010 mg/mL using Gilder Grids overlaid with a thin layer of carbon and 2% uranyl formate (Electron Microscopy Sciences, Cat#: 22451) as previously described (Veesler et al., 2014). Data were collected on an FEI Technai 12 Spirit 120kV electron microscope equipped with a Gatan Ultrascan 4000 CCD camera. A total of ~300 images were collected per sample by using a random

defocus range of 1.1–2.0 μm with a total exposure of 45 e−/A2. Data were automatically acquired using Leginon (Suloway et al., 2005) and data processing was carried out using Appion (Lander et al., 2009). The parameters of the contrast transfer function (CTF) were estimated using CTFFIND4 (Mindell and Grigorieff, 2003), and particles were picked in a reference-free manner using DoG picker (Voss et al., 2009). Particles were extracted with a binning factor of 2 after correcting for the effect of the CTF by flipping the phases of each micrograph with EMAN 1.9 (Ludtke et al., 1999). The GTA cross-linked 426c WT DS-SOSIP B-p1b5 Fab stack was pre-processed in RELION/2.1 (Kimanius et al., 2016; Scheres, 2012a, 2012b) with an additional binning factor of 2 applied, resulting in a final pixel size of 6.4 Å. Resulting particles were sorted by reference-free 2D classification over 25 iterations. The best particles were chosen for 3D classification into 2 classes using C1 symmetry in RELION/2.1 (Kimanius et al., 2016). The best class of particles were refined using Relion/3.0 (Zivanov et al., 2018).

BLI

Ab binding to recombinant Env proteins was determined using BLI on the Octet Red 96 (ForteBio, Inc, Menlo Park, CA), as previously described (Yacoob et al., 2016). Briefly, anti-human Fc capture biosensors (ForteBio, Cat#: 18–5063) were activated by immersion into 1× Kinetics Buffer (1× PBS, 0.1% BSA, 0.02% Tween-20, 0.005% NaN3) for 10 minutes. Abs were loaded onto an anti-human Fc capture probe at 20 ug/ml. The probes were then dipped into solutions containing recombinant Env: 2 uM for monomeric gp120-derived Envs or 1 uM for C4b and trimeric Env (SOSIP or NFL designs). Parameters for all BLI assays were: 30 s of baseline measurement, 240 s to load

the Ab onto the anti-human Fc capture probe, 60 s of baseline measurement, 300 s of association, 300 s of dissociation. All measurements of Env-Ab binding were corrected by subtracting the background signal obtained from Env traces generated with an irrelevant negative control IgG.

Kinetic analyses were performed by BLI as described above using recombinant Fabs loaded onto FAB2G biosensors (ForteBio, Cat#: 18–5126) (@ 40 ug/ in 1XPBS) and 2-fold dilutions of envelope monomers (ranging from 50 uM - 391 nM), and by extending the dissociation phase of binding to 600 s. Curve fitting was used to determine relative apparent Ab affinities for envelope using a 1:1 binding model and the data analysis software (ForteBio). Mean k_{on}, k_{off}, and KD values were determined by averaging all binding curves within a dilution series having R2 values of greater than 95% confidence level.

ELISAs

Plasma samples were heated inactivated at 56°C for 1 hour, centrifuged at 13,000 for 10 min and stored at 4°C or −20°C. ELISAs were done in either a half-area 96 well or 384 well plate format. For a 384 well plate ELISA, 30 ul of protein at 0.1 uM in coating buffer (0.1M sodium bicarbonate, pH: 9.4–9.6) was added to each well and incubated a room temperature overnight. Plates were washed 4× with ELISA wash buffer (1XPBS + 0.2% Tween-20). 80 ul of blocking buffer (1X PBS + 10% non-fat milk + 0.03% Tween20) was added to the plates and they were incubated at 37°C for 1–2 hours. Plates were then washed 4× with ELISA wash buffer. Plasma was diluted 1:10 in blocking buffer and diluted 1:3 across or down the plate. His tag control started at 1 μg/ml. The

plates were incubated for 1 hour at 37°C. The plates were washed 4× with ELISA was buffer. 30 ul of secondary Ab was added to each well. The plates were incubated for an hour at 37°C. Plates were washed 4× with ELISA wash buffer. Following washing 30 ul of SureBlue Reserve TMB Microwell Peroxidase Substrate: KPL (Cat #: 53–00-02) was added to each well. The plates were incubated for 5 minutes at room temperature. 30 ul of 1N H_2SO_4 was added to each well. Plates were read immediately on the SpectraMax M2 microplate reader (Molecular Devices) at 450 nm. Blank wells were used to subtract the background signal in the analysis. 96 well plate ELISAs followed a similar protocol but used 50 ul of volume for the coating of protein, dilution volumes, secondary Ab volume, and development steps. 120 ul of blocking buffer was used to block the plates.

Neutralization assays

Neutralizing Ab activity was measured in 96-well culture plates by using Tat-regulated luciferase (Luc) reporter gene expression to quantify reductions in virus infection in TZM-bl cells. TZM-bl cells were obtained from the NIH AIDS Research and Reference Reagent Program, as contributed by John Kappes and Xiaoyun Wu. Assays were performed with HIV-1 Env-pseudotyped viruses as described previously (Montefiori, 2009). For the assays, mAbs were used at 100 ug/ml or the highest concentration possible. Samples were then diluted over seven 3-fold dilutions and preincubated with virus (~150,000 relative light unit equivalents) for 1 hr at 37°C before addition of cells. Following an additional 48 hr incubation, cells were lysed and Luc activity determined using a microtiter plate luminometer and BriteLite Plus Reagent (PerkinElmer, Cat#: 6066766). Neutralization titers are the Ab concentration at which relative luminescence

units (RLU) were reduced by 50% compared to RLU in virus control wells after subtraction of background RLU in cell control wells.

Immunoprecipitation

Purified recombinant IgGs were covalently coupled to MyOne Tosylactivated Dynabeads (Thermo Fisher Scientific, Cat#: 65501). Coupling and Env immunoprecipitation were carried out according to the manufacturer's protocol. Briefly, 5 mg of Env produced in HEK293S GnTI−/− were incubated with 200 μg of IgG-beads for 30 min. The IgG-Env protein complexes were then precipitated using magnetic separation and washed 3–4× before performing acidic elution and pH neutralization of the bound material. Env-samples of the original input of 426c WT Core or HxB2 WT Core, and bead-bound/eluted and unbound fractions were subjected to SDS gel electrophoresis under reducing conditions. A sample of the bound fractions were subjected to LC-MS/MS analysis or used for BLI.

Mass spectrometry

For analysis of the NLGS profile of the crosslinked 426c WT Core-P1B5 complex, 250 pmol of sample was denatured, reduced, and alkylated by dilution to 5 μM in 50 μL of buffer containing 100 mM Tris (pH 8.5), 10 mM Tris (2-carboxyethylphosphine (TCEP), 40 mM iodoacetamide or 40 mM iodoacetic acid, and 2% (wt/vol) sodium deoxycholate. Samples were first heated to 95°C for 5 min and then incubated for an additional 25 min at room temperature in the dark. The samples were digested with trypsin (Thermo Fisher Scientific, Cat#: 90057), by diluting 20 μL of sample to a total volume of 100 μL of

buffer containing 50 mM ammonium bicarbonate (pH 8.5). Trypsin was added in a ratio of 1:50 (w/w) before incubation at 37°C overnight. Subsequently, 2 µL of formic acid was added to precipitate the sodium deoxycholate from the solution. Following centrifugation at 17,000 × g for 25 min, 85 µL of the supernatant was collected and centrifuged again at 17,000 × g for 5 min to ensure removal of any residual precipitated deoxycholate. 80 µL of this supernatant was collected. For each sample, 8 µL was injected on a Thermo Scientific Orbitrap Fusion Tribrid mass spectrometer. A 35 cm analytical column and a 3 cm trap column filled with ReproSil-Pur C18AQ 5 µM (Dr. Maisch) beads were used. Nanospray LC-MS/MS was used to separate peptides over a 90 min gradient from 5% to 30% acetonitrile with 0.1% formic acid. A positive spray voltage of 2100 was used with an ion transfer tube temperature of 350°C. An electron-transfer/higher energy collision dissociation ion-fragmentation scheme was used with calibrated charge-dependent entity-type definition parameters and supplemental higher energy collision dissociation energy of 0.15 (Frese et al., 2013). A resolution setting of 120,000 with an AGC target of 2×10^5 was used for MS1, and a resolution setting of 30,000 with an AGC target of 1×10^5 was used for MS2. Data were searched with the Protein Metrics Byonic software, using a small custom database of recombinant protein sequences including the proteases used to prepare the glycopeptides (Bern et al., 2012). Reverse decoy sequences were also included in the search. Specificity of the search was set to C-terminal cleavage at R/K (trypsin), allowing up to three missed cleavages, with EthcD fragmentation (b/y- and c/ztype ions). We used a precursor mass and product mass tolerance of 12 ppm and 24 ppm, respectively. Carbamidomethylation of cysteines was set as fixed modification, carbamidomethylation of lysines was set as a variable

modification, methionine oxidation as variable modification, and a concatenated N-linked glycan database (derived from the four software-included databases) was used to identify glycopeptides. All analyzed glycopeptide hits were manually inspected to ensure their quality and accuracy. Semi quantitative LC-MS/MS of P-p3b3, B-p1b5 and VRC01-immunoprecipitation experiments were performed using Skyline (MacLean et al., 2010) with peak integration and LC-MS/MS searches imported from Byonic, as previously described (Borst et al., 2018). Missed cleavages and post-translational modifications listed above for qualitative LC-MS/MS searches were included in the quantification of glycopeptides. All MS1 peak areas used for integration were manually inspected. Each fraction was performed as part of two technical replicates and was subsequently averaged. Calculations and plots for glycoform enrichment graphs were generated by subtracting the relative signal values of the input Core fraction from the unbound or bound Core fractions.

Quantification and statistical analysis

Mean and standard deviations were calculated using R (Version 3.4.1). Statistical analyses were calculated using R (Version 3.4.1) (R Core Team, 2018) and GraphPad Prism. Descriptions of the statistical methods used for each dataset are described in the figure legends. The tidyverse packages (Wickham, 2017) were used in R to manipulate data and create graphs in addition to GraphPad Prism.

Data and code availability

The sequences of mAbs reported here have been deposited on GenBank and in the GitHub respository: https://github.com/krparks/glVRC01_sequential_immunization. The accession numbers of the mAb sequences are GenBank: MN087228 - MN087315 (Supplemental Table 3.5). Multimeric and monomeric heterologous Env sequences have been deposited on GenBank, accession numbers GenBank: MN179660-MN179671 (Supplemental Table 3.5). Coordinates and structure factors have been deposited on the Protein Data Bank under PDB: 6P8N and PDB: 6P8M. Raw and analyzed Mass Spectrometry data have been deposited on PRIDE. The accession number for the mass spectrometry data is PRIDE: PXD015168.

Supplemental figures

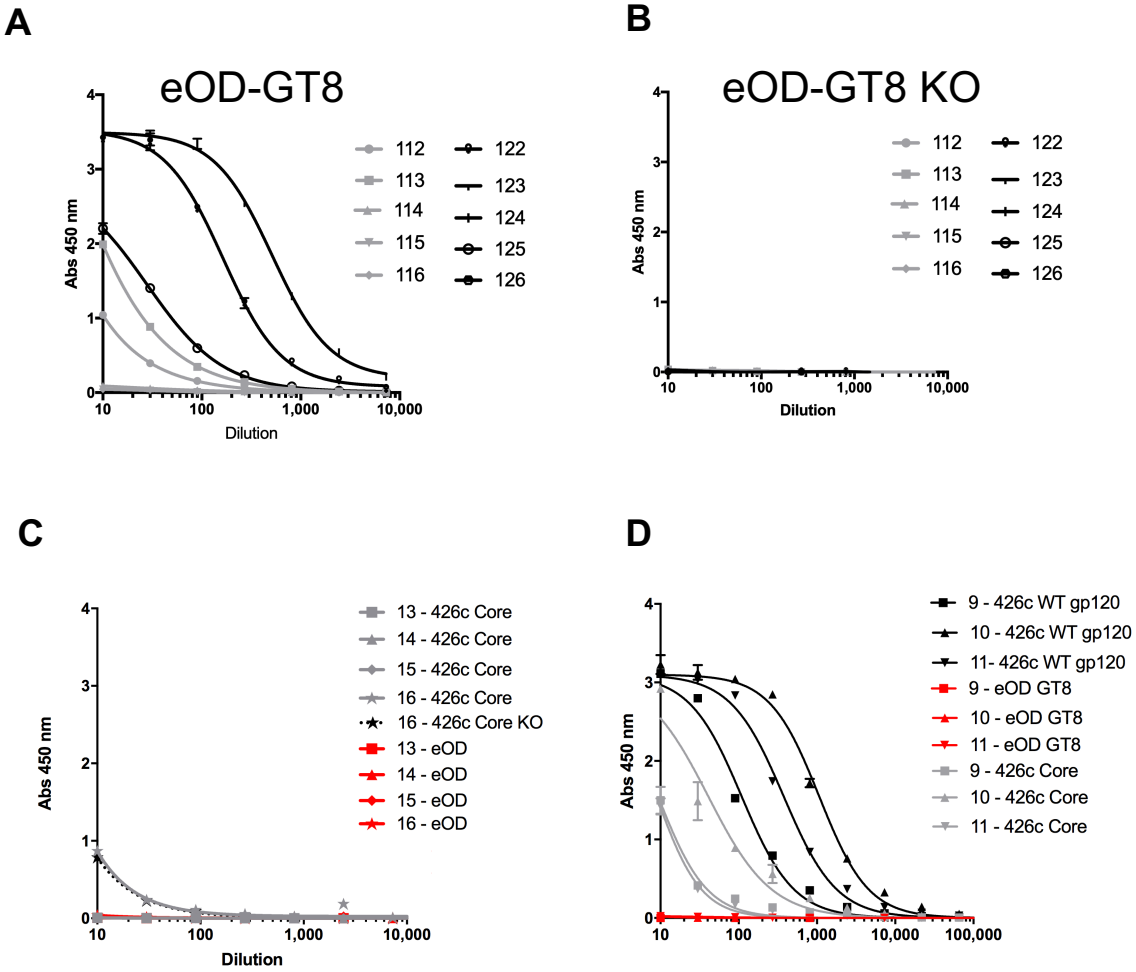

Supplemental Figure 3.1. Plasma Ab responses elicited by the 426c Core, 426c WT gp120 and 426c DS-SOSIP immunogens. Binding curves of plasma Abs to eOD-GT8 **(A)** and eOD-GT8 KO **(B)** from the same animals shown in Figure 1A, immunized with 426c Core Fer (black)- or C4b (gray)-based nanoparticle forms. ELISA curves shown here are representative of at least two biological replicates per group. **(C)** Plasma Abs from four animals (13-16) immunized with the 426c DS-SOSIP D3 were tested for binding to the 426c Core (gray), 426c Core KO (black), or eOD-GT8 (red). ELISA curves are representative of 1-2 technical replicates. **(D)** Plasma Abs from three animals (9-11) immunized with 426c WT gp120 (C4b nanoparticle form) were tested for binding to 426c WT gp120 (black), eOD-GT8 (red) and 426c Core (gray). ELISA curves are representative of 1-2 technical replicates.

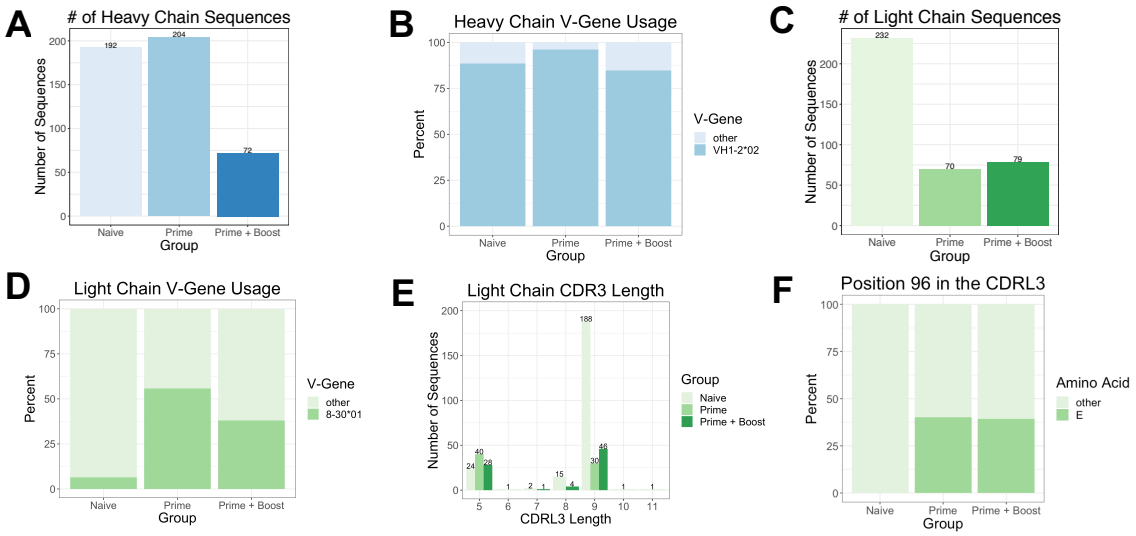

Supplemental Figure 3.2. Characteristics of the HC and LC sequences from unimmunized and immunized animals. B cells were isolated from unimmunized (naïve B cells) and from immunized animals (following the prime and following the boost immunization) as discussed in detail in the Methods section. In the case of the unimmunized animals, spleens and LNs from 3 different animals were pooled and the B cells were then single-cell sorted. In the case of immunized animals, class-switched B cells were single cell sorted. The data following the prime are from three independent sorts and the data following the boost (prime+boost) are from two independent experiments. Data from animals immunized with C4b- or Ferritin-based nanoparticles and Poly (I:C) or GLA-LSQ are combined. **(A)** The total number of HC sequences and the **(B)** V-gene usage of the HC sequences. **(C)** The total number of LC sequences and the **(D)** LC V-usage. **(E)** Number of CDRL3 domains with the indicated lengths. **(F)** Frequency of five AA long CDRL3 domains with and without a Glu at position 96.

A

426c Core	Average Kinetic Values						
	KD (M)	KD Error	kon(1/Ms)	kon Error	kdis(1/s)	kdis Error	Full R^2
P-p3b3	1.13E-07	4.62E-09	7.29E+04	2.56E+03	4.83E-03	5.23E-05	0.9611
P-p1f1	8.69E-08	1.40E-09	4.59E+04	8.29E+02	2.03E-03	1.13E-05	0.9824
P-p3a2	7.39E-08	1.39E-09	5.95E+04	1.19E+03	2.23E-03	1.41E-05	0.9775
P-p1d1	5.58E-08	7.08E-10	4.14E+04	4.59E+02	1.40E-03	6.35E-06	0.9869

B

eOD-GT8	Average Kinetic Values						
	KD (M)	KD Error	kon(1/Ms)	kon Error	kdis(1/s)	kdis Error	Full R^2
P-p3b3	2.78E-09	3.39E-11	2.68E+05	5.07E+03	3.44E-04	2.35E-06	0.9849
P-p1f1	5.02E-10	1.80E-11	2.59E+05	6.82E+03	9.90E-05	1.55E-06	0.9807
P-p3a2	4.01E-10	1.48E-11	2.60E+05	2.84E+03	9.75E-05	1.20E-06	0.9853
P-p1d1	3.22E-10	1.55E-11	3.28E+05	7.24E+03	8.79E-05	8.97E-07	0.9815

C

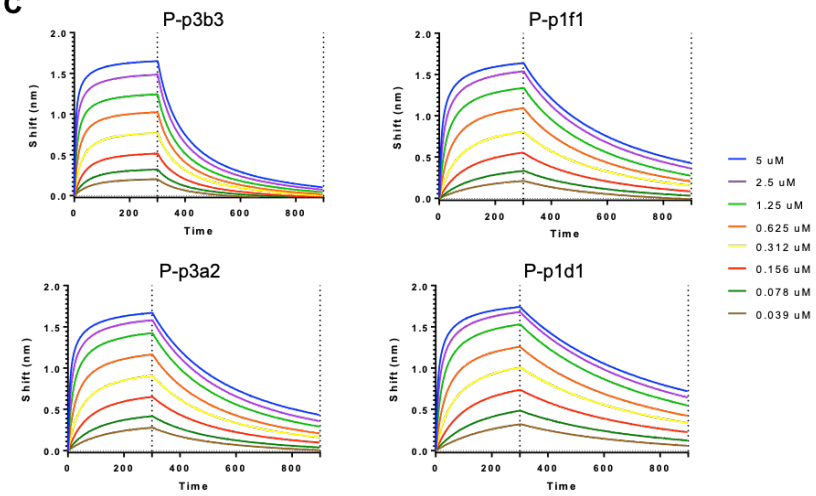

D

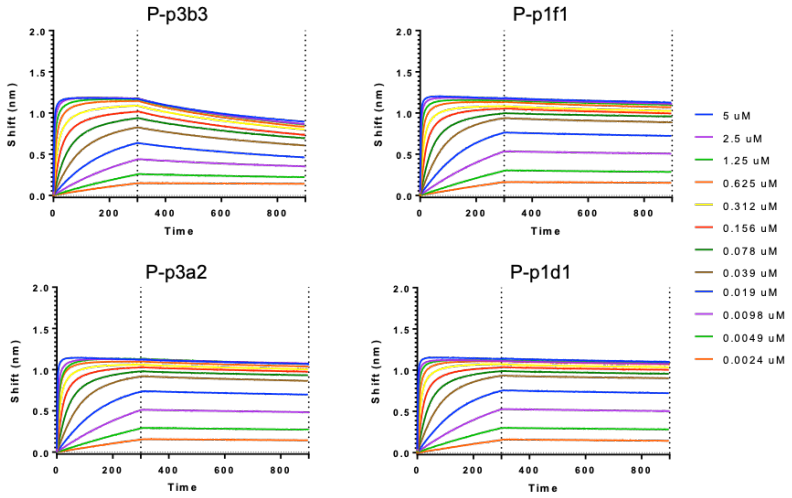

Supplemental Figure 3.3. Binding kinetics of Ab Fabs isolated from mice immunized with 426c Core. BLI was used to determine affinity of Fabs for Env. Here we report kinetic values determined for each Fab for **(A)** 426c Core, **(B)** eOD-GT8, and the BLI traces used to determine these values **(C, D).**

A

B

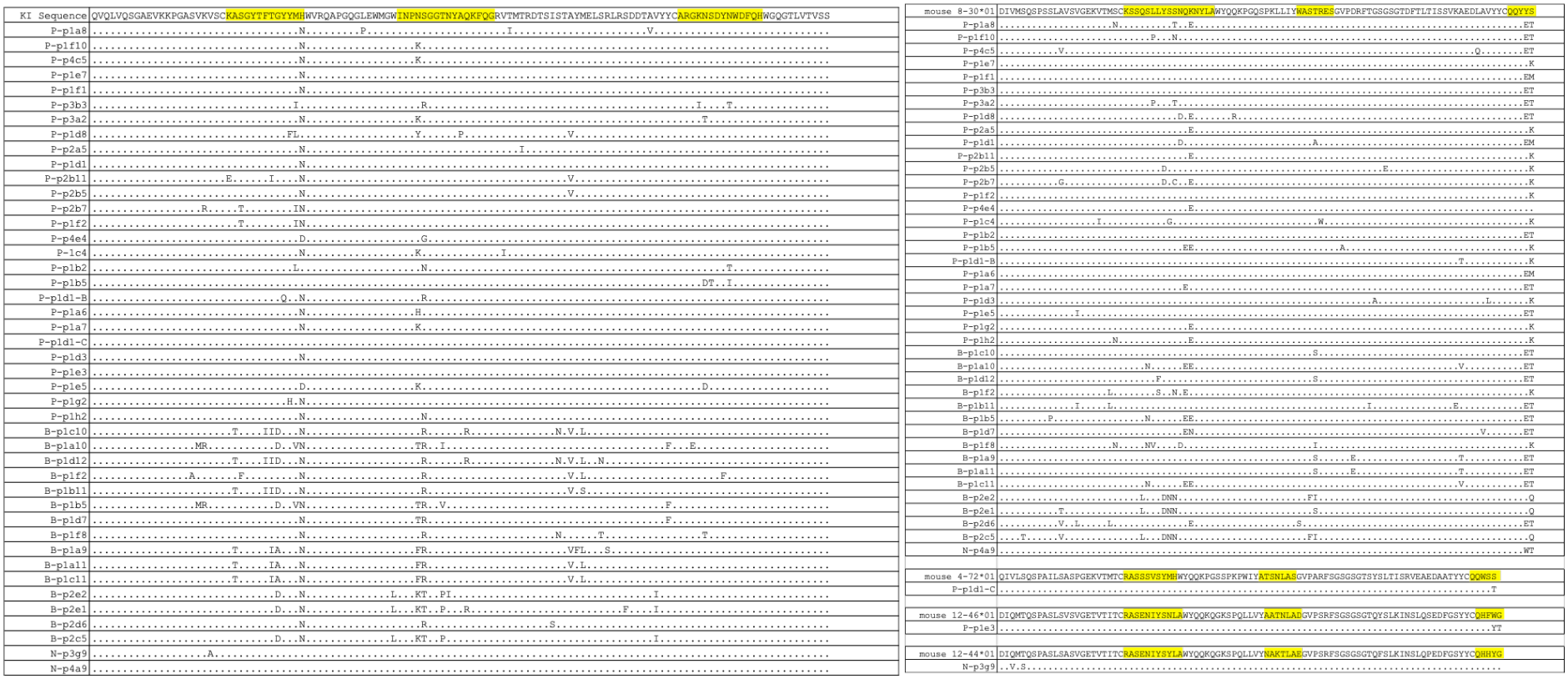

Supplemental Figure 3.4. AA sequence of the isolated Abs. (A) AA alignment of the VH1-2*02 domains. The sequence of the knocked-in human glVRC01 gene is indicated at the top. **(B)** AA alignment of the mouse VL domains. The prefix 'P' indicates Abs isolated following the prime immunization, the prefix 'B' indicates Abs isolated following the boost immunization, and the prefix 'N' indicates Abs isolated from naïve animals. The sequences of the mouse genes from which the VL sequences were derived from are indicated. CDRs are highlighted in yellow in the reference sequences.

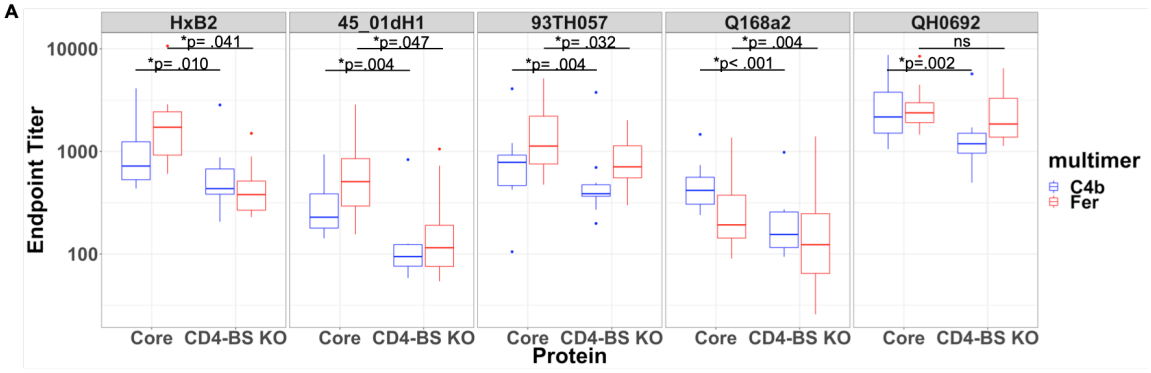

B

```
                 272        282   458              473
Hxb2 Core        IRSVNFTDNAK      GGNSNN--ESEIFRPGGG
45_01dH1 Core    IRSENLTDNAK      GGNITNETTTETFRPGGG
93TH057 Core     IRSENLTNNAK      GGANN--TSTETFRPGGG
Q168a2 Core      IRSENFTNNAK      GGNNNS--TNETFRPGGG
QH0692 Core      IRSENFTNNAK      GGVN-G--TRETFRPGGG
```

Supplemental Figure 3.5. Plasma Abs elicited by the 426c Core recognize heterologous wild type gp120 Core proteins. (A) Plasma from animals (n = 10 in each group) immunized with the 426c Core were tested for binding by ELISA against five heterologous WT gp120 Core proteins and their CD4-BS KO derivatives. Data is shown as a box plot. Statistical values compare the plasma Ab endpoint titer of the indicated Core proteins to their CD4-BS KO derivatives. Statistical significance was calculated using a paired t-test. One independent experiment was performed for each group. **(B) AA** alignment of the loop D and V5 loop sequences from these five Core proteins. The position of potential NLGS in these two envelope regions are in red text.

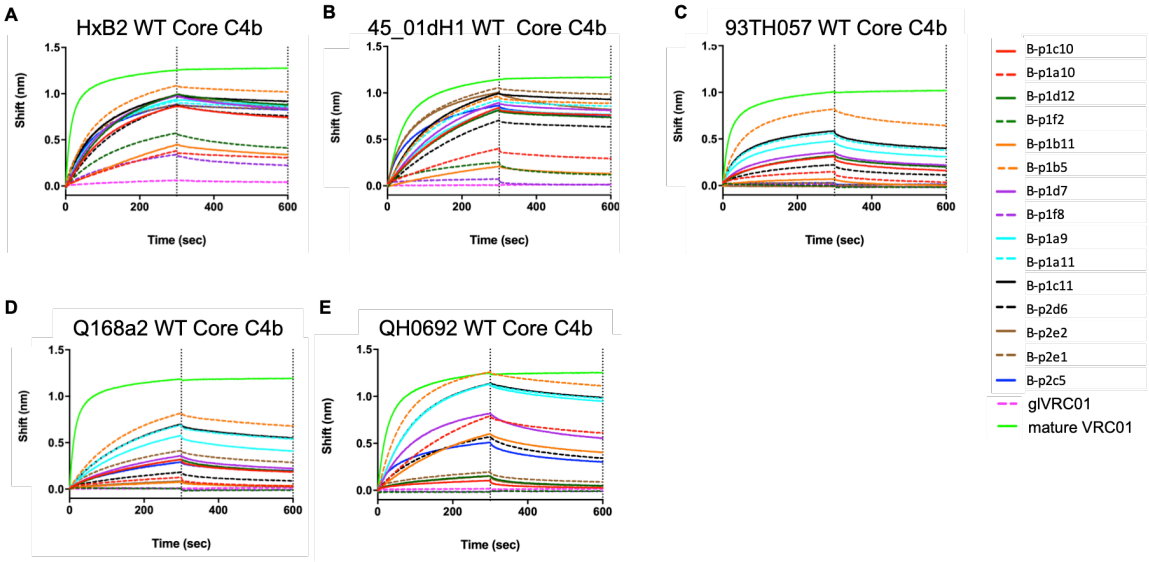

Supplemental Figure 3.6. Binding of mAbs isolated following the boost immunization to multimeric WT Core Env. BLI binding traces of the indicated mAbs isolated after the boost immunization to multimeric WT Core Env proteins **(A-E).** Data is representative of 1-2 technical replicates.

A

426c WT Core	Average Kinetic Values						
	KD (M)	KD Error	kon(1/Ms)	kon Error	kdis(1/s)	kdis Error	Full R^2
gl VRC01	1.67E-05	3.74E-07	3.45E+02	8.65E+00	5.33E-03	2.41E-05	0.9933
N-p3g9	N.B.						
N-p4a9	N.B.						
P-p1e7	N.B.						
P-p2b7	N.B.						
P-p1f1	5.66E-05	9.76E-05	2.00E+02	4.31E+01	6.09E-03	8.94E-05	0.9537
P-p3a2	1.20E-05	1.03E-06	5.72E+02	5.48E+01	6.44E-03	9.20E-05	0.9608
P-p1d1	6.25E-06	1.16E-06	8.17E+02	4.28E+01	3.69E-03	2.73E-05	0.9757
P-p3b3	5.32E-06	3.25E-07	1.67E+03	6.08E+01	1.24E-02	1.13E-04	0.9981
B-p1f8	3.57E-06	8.15E-08	2.11E+03	5.11E+01	5.46E-03	3.30E-05	0.9886
B-p1f2	3.53E-06	8.10E-08	2.39E+03	5.89E+01	6.02E-03	3.76E-05	0.9901
B-p1a10	3.04E-07	5.64E-09	4.36E+03	5.19E+01	1.21E-03	5.29E-06	0.9879
B-p1a11	1.74E-07	2.42E-09	6.43E+03	7.26E+01	1.06E-03	6.39E-06	0.9790
B-p1b5	3.86E-08	1.39E-09	9.79E+03	1.30E+02	2.64E-04	7.64E-06	0.9713

B

HxB2 WT Core	Average Kinetic Values						
	KD (M)	KD Error	kon(1/Ms)	kon Error	kdis(1/s)	kdis Error	Full R^2
gl VRC01	2.82E-05	8.01E-08	3.69E+03	1.22E+02	1.28E-01	3.62E-03	0.9677
N-p3g9	N.B.						
N-p4a9	N.B.						
P-p1e7	N.B.						
P-p2b7	N.B.						
P-p1f1	1.15E-05	1.10E-06	2.09E+03	2.01E+02	2.24E-02	1.01E-03	0.9577
P-p3a2	4.75E-06	1.89E-07	3.58E+03	2.11E+02	1.37E-02	2.26E-04	0.9801
P-p1d1	7.42E-06	4.23E-07	2.75E+03	1.89E+02	1.72E-02	3.73E-04	0.9736
P-p3b3	4.90E-06	2.61E-07	4.71E+03	3.56E+02	1.75E-02	3.85E-04	0.9735
B-p1f8	1.08E-05	1.34E-06	3.31E+03	2.55E+02	3.99E-02	1.28E-03	0.9725
B-p1f2	8.72E-06	7.74E-07	4.21E+03	4.08E+02	3.22E-02	1.07E-03	0.9683
B-p1a10	2.91E-06	9.59E-08	7.16E+03	2.82E+02	8.39E-03	9.05E-05	0.9764
B-p1a11	2.46E-08	5.92E-10	9.64E+03	5.98E+01	1.90E-04	3.86E-06	0.9857
B-p1b5	6.38E-08	1.37E-09	5.94E+03	4.52E+01	2.98E-04	4.44E-06	0.9966

C

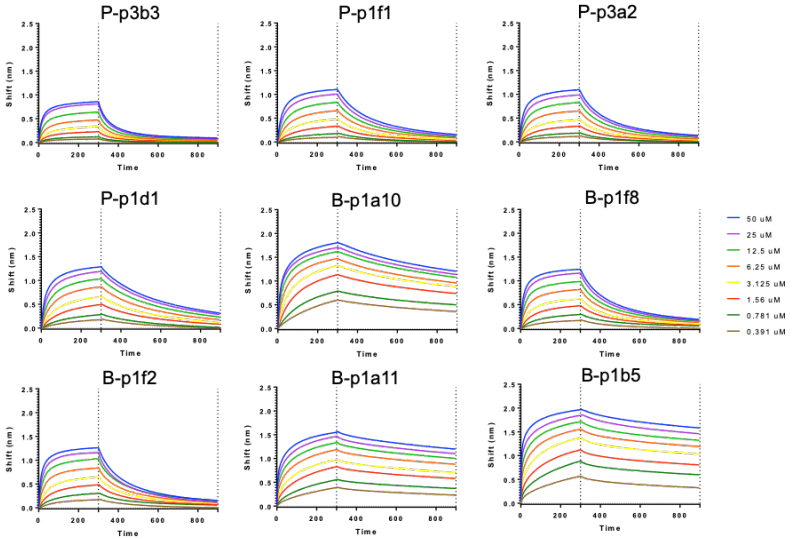

D

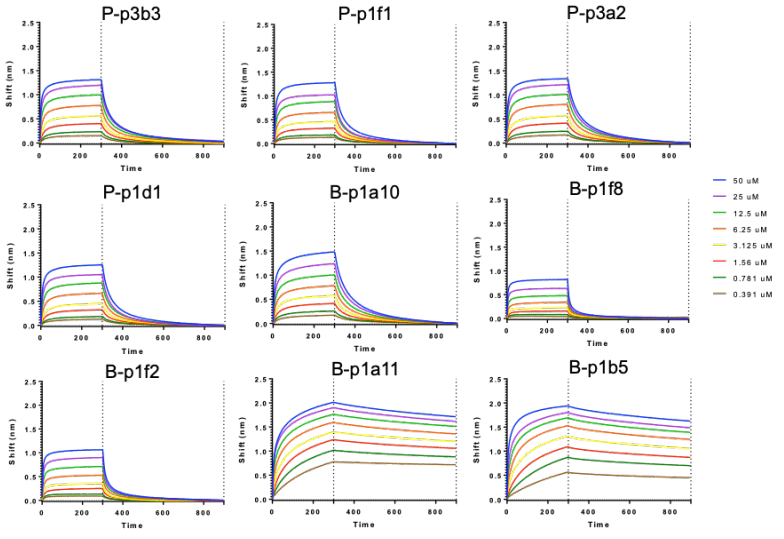

Supplemental Figure 3.7. Binding kinetics of Ab Fabs isolated from naïve and immunized mice. BLI was used to determine affinity of Fabs for Env. Here we report kinetic values determined for each Fab for **(A)** 426c WT Core, (B) HxB2 WT Core, and the BLI traces used to determine these values **(C, D).** N.B. indicates no binding.

Supplemental tables

Supplemental Table 3.1. Data collection and refinement statistics for crystal structures.

	P-p1f1 with eOD-GT8	P-p3b3 with 426c core
Data collection		
Space group	$P22_12_1$	C222
Cell dimensions		
***a*, *b*, *c* (Å)**	60.88, 92.41, 223.50	146.80, 176.76, 108.57
α, β, γ (°)	90, 90, 90	90, 90, 90
Resolution (Å)	50.00-3.20 (3.26-3.20)*	50.00–3.59 (3.65-3.59)*
R_{sym} or R_{merge}	0.227 (1.089)*	0.105 (0.573)*
I/sI	7.9 (1.6)*	7.8 (1.08)*
Completeness (%)	98.7 (99.7)*	82.5 (75.8)*
Redundancy	6.2 (5.8)*	2.8 (2.4)*
$CC_{1/2}$	0.970 (0.659)*	0.990 (0.801)*
Refinement		
Resolution (Å)	41.16-3.20 (3.31-3.20)*	50.00-3.59 (3.72-3.59)*
No. unique reflections	20643 (1702)*	11541 (469)*
R_{work}/R_{free}	22.6/28.7 (29.8/37.3)*	23.3/26.9 (27.4/24.2)*
No. atoms	8755	5868
Protein	8677	5638
Water	49	12
Ligand	29	218
B-factors (Å²)	65	95
Protein	65	94
Water	31	42
Ligand	104	122
R.m.s deviations		
Bond lengths (Å)	0.005	0.009
Bond angles (º)	1.02	1.09
Ramachadran Favored %	92.35	93.79
Ramachadran Outliers %	0.00	0.13
MolProbity all-atoms clashscore	5.88	5.38
PDB ID	6P8N	6P8M

*Statistics for the highest-resolution shell are shown in parentheses.

Supplemental Table 3.2. Neutralization of mAbs isolated following immunization

		Prime Antibodies				Boost Antibodies				controls	
Virus	Cell Type	P-p1f1	P-p1e7	P-p3a2	P-p3b3	B-p1c10	B-p1d12	B-p1f2	B-p1b5	Mature VRC01	glVRC01
WT 426c	293T	>50	>50	>50	>50	>100	>100	>100	>100	1.7	na
	GnTI-/-	>50	>50	>50	>50	>100	>100	>100	32.05	0.08	>100
426c Δ276, 460, 463	293T	>50	>50	>50	28.09	16.80	18.34	0.17	0.04	<0.01	na
	GnTI-/-	1.36	0.36	1.84	0.45	0.04	0.04	0.01	0.01	0.01	0.642
426c Δ276, 460, 463 D279K	GnTI-/-	na	na	na	na	>50	>50	>50	>50	>25	na
426c Δ276	293T	>50	>50	>50	>50	>50	>50	>50	0.64	0.20	na
	GnTI-/-	2.98	>50	3.46	1.62	0.89	1.25	>50	<0.02	<0.01	na
426c Δ276 D279K	GnTI-/-	na	na	na	na	>50	>50	>50	>50	>25	na
426c Δ460, 463	293T	>50	>50	>50	>50	na	na	na	na	0.29	na
	GnTI-/-	>50	>50	>50	>50	na	na	na	na	0.03	na
CH0505TF	293T	na	na	na	na	>100	>100	>100	>100	0.12	na
	GnTI-/-	na	na	na	na	>100	>100	>100	>100	<0.02	na
CH0505TF	293T	na	na	na	na	>100	>100	>100	>100	<0.02	na

Δ197, 276, 362, 461/462	GnTI-/-	na	na	na	na	>100	>100	>100	8.93	<0.02	na
CH0505TF Δ197, 362, 461/462	293T	na	na	na	na	>100	>100	>100	>100	<0.02	na
	GnTI-/-	na	na	na	na	>100	>100	>100	>100	<0.02	na
CH0505TF Δ276, 362, 461/462	293T	na	na	na	na	>100	>100	>100	>100	<0.02	na
	GnTI-/-	na	na	na	na	>100	>100	>100	2.21	<0.02	na
CH0505TF Δ197, 276, 362	293T	na	na	na	na	>100	>100	>100	>100	1.61	na
	GnTI-/-	na	na	na	na	>100	>100	>100	>100	<0.02	na
HxB2	293T	na	na	na	>75	na	na	na	>75	.081	na

[a]na, not tested

Supplemental Table 3.3. Primers used to amplify HCs and LCs of murine antigen-specific specific B cells.

Name	Sequence	Forward/Reverse	First/Second	Heavy/Light	Source
5′ L-Vκ_3	TGCTGCTGCTCTGGGTTCCAG	Forward	First	Light	(Tiller et al., 2009)
5′ L-Vκ_4	ATTWTCAGCTTCCTGCTAATC	Forward	First	Light	
5′ L-Vκ_5	TTTTGCTTTTCTGGATTYCAG	Forward	First	Light	
5′ L-Vκ_6	TCGTGTTKCTSTGGTTGTCTG	Forward	First	Light	
5′ L-Vκ_6,8,9	ATGGAATCACAGRCYCWGGT	Forward	First	Light	
5′ L-Vκ_14	TCTTGTTGCTCTGGTTYCCAG	Forward	First	Light	
5′ L-Vκ_19	CAGTTCCTGGGGCTCTTGTTGTTC	Forward	First	Light	
5′ L-Vκ_20	CTCACTAGCTCTTCTCCTC	Forward	First	Light	
3’ mCk	GATGGTGGGAAGATGGATACAGTT	Reverse	First	Light	
3’ BsiWI P-mJK01	GCCACCGTACGTTTGATTTCCAGCTTGGTG	Reverse	Second	Light	
3’ BsiWI P-mJK02	GCCACCGTACGTTTTATTTCCAGCTTGGTC	Reverse	Second	Light	
3’ BsiWI P-mJK03	GCCACCGTACGTTTTATTTCCAACTTTGTC	Reverse	Second	Light	
3’ BsiWI P-mJK04	GCCACCGTACGTTTCAGCTCCAGCTTGGTC	Reverse	Second	Light	
5′ mVkappa	GAYATTGTGMTSACMCARWCTMCA	Forward	Second	Light	
5’ Mouse leader	CTCTTCCTCCTGTCAGTAACTGAAGGTGTCC	Forward	First	Heavy	N/A
3′ KI Rev	TGAGGAGACGGTGACCAGGGTGCC	Reverse	First/Second	Heavy	N/A
5’ glVRC01	CAGGTGCAGCTGGTGCAGTCTGG	Forward	Second	Heavy	(Jardine et al., 2015)

Supplemental Table 3.4. Cycling conditions used for PCR.

Temperature (C)	**Time**	
94	5 min	
94	30 sec	Repeat 50X
X (IgH 1st round: 56, IgH 2nd round: 60, IgK 1st round: 50, IgK 2nd round: 45)	30 sec	
72	55 sec	
72	10 min	
4	Infinity	

Supplemental Table 3.5 GenBank accession numbers.

Sequence	GenBank Accession Number
N-p4a9 light chain	MN087228
N-p3g9 light chain	MN087229
P-p1h2 light chain	MN087230
P-p1g2 light chain	MN087231
P-p1e5 light chain	MN087232
P-p1e3 light chain	MN087233
P-p1d3 light chain	MN087234
P-p1d1-C light chain	MN087235
P-p1a7 light chain	MN087236
P-p1a6 light chain	MN087237
B-p2e1 light chain	MN087238
B-p2e2 light chain	MN087239
B-p2d6 light chain	MN087240
B-p2c5 light chain	MN087241
B-p1f8 light chain	MN087242
B-p1f2 light chain	MN087243
B-p1d12 light chain	MN087244
B-p1d7 light chain	MN087245
B-p1c11 light chain	MN087246
B-p1c10 light chain	MN087247
B-p1b11 light chain	MN087248
B-p1b5 light chain	MN087249
B-p1a10 light chain	MN087250
B-p1a9 light chain	MN087251
B-p1a11 light chain	MN087252
P-p1d1-B light chain	MN087253
P-p1c4 light chain	MN087254
P-p1b5 light chain	MN087255
P-p1b2 light chain	MN087256
P-p2b11 light chain	MN087257
P-p2b7 light chain	MN087258
P-p2b5 light chain	MN087259
P-p2a5 light chain	MN087260
P-p1f2 light chain	MN087261
P-p1d8 light chain	MN087262
P-p4c5 light chain	MN087263
P-p4e4 light chain	MN087264

P-p3b3 light chain	MN087265
P-p3a2 light chain	MN087266
P-p1f10 light chain	MN087267
P-p1f1 light chain	MN087268
P-p1e7 light chain	MN087269
P-p1d1 light chain	MN087270
P-p1a8 light chain	MN087271
N-p4a9 heavy chain	MN087272
N-p3g9 heavy chain	MN087273
P-p1h2 heavy chain	MN087274
P-p1g2 heavy chain	MN087275
P-p1e5 heavy chain	MN087276
P-p1e3 heavy chain	MN087277
P-p1d3 heavy chain	MN087278
P-p1d1-C heavy chain	MN087279
P-p1a7 heavy chain	MN087280
P-p1a6 heavy chain	MN087281
B-p2e2 heavy chain	MN087282
B-p2e1 heavy chain	MN087283
B-p2d6 heavy chain	MN087284
B-p2c5 heavy chain	MN087285
B-p1f8 heavy chain	MN087286
B-p1f2 heavy chain	MN087287
B-p1d12 heavy chain	MN087288
B-p1d7 heavy chain	MN087289
B-p1c11 heavy chain	MN087290
B-p1c10 heavy chain	MN087291
B-p1b11 heavy chain	MN087292
B-p1b5 heavy chain	MN087293
B-p1a11 heavy chain	MN087294
B-p1a10 heavy chain	MN087295
B-p1a9 heavy chain	MN087296
P-p1d1-B heavy chain	MN087297
P-p1c4 heavy chain	MN087298
P-p1b5 heavy chain	MN087299
P-p1b2 heavy chain	MN087300
P-p2b11 heavy chain	MN087301
P-p2b7 heavy chain	MN087302
P-p2b5 heavy chain	MN087303

P-p2a5 heavy chain	MN087304
P-p1f2 heavy chain	MN087305
P-p1d8 heavy chain	MN087306
P-p4c5 heavy chain	MN087307
P-p4e4 heavy chain	MN087308
P-p3b3 heavy chain	MN087309
P-p3a2 heavy chain	MN087310
P-p1f10 heavy chain	MN087311
P-p1f1 heavy chain	MN087312
P-p1e7 heavy chain	MN087313
P-p1d1 heavy chain	MN087314
P-p1a8 heavy chain	MN087315
QH0692 WT Core C4b	MN179660
Q168a2 WT Core C4b	MN179661
45_01dH1 WT Core C4b	MN179662
93TH057 WT Core C4b	MN179663
426c WT Core	MN179664
HxB2 WT Core	MN179665
QH0692 WT Core	MN179666
Q168a2 WT Core	MN179667
45_01dH1 WT Core	MN179668
93TH057 WT Core	MN179669
HxB2 WT Core C4b	MN179670
HxB2 WT Core C4b 2W1S	MN179671

Chapter IV. Anti-idiotypic antibodies elicit anti-HIV-1–specific B cell responses

The following text summarizes the results published in the article:

Dosenovic, P., Kara, E.E., Pettersson, A.-K., McGuire, A.T., Gray, M., Hartweger, H., Thientosapol, E.S., Stamatatos, L., and Nussenzweig, M.C. (2018). Anti–HIV-1 B cell responses are dependent on B cell precursor frequency and antigen-binding affinity. PNAS *115*, 4743–4748.

I participated in this study by isolating and preparing the B cells from human PBMCs for 10x sequencing on the chromium platform (Figure 4.5).

Introduction

While, the previous chapters have discussed the use of Env-derived immunogens to engage the germline forms of bnAbs against HIV-1 as the first step in a series of prime-boost immunizations, an alternative approach we explored was based on the use of aiAbs as priming immunogens. AiAbs are mAbs selected to recognize signature features of the variable region of a particular Ab, or a class of Abs or BCRs. aiAbs can be used as immunogens against classes of bnAbs for which no Env-based germline-targeting immunogen exists. This is for example the case of aiAbs developed against the germline form of bnAb b12, a CD4-BS directed Ab. It has now been shown that these aiAb can activate glb12 expressing B cells *in vivo* (Bancroft et al., 2019).

aiAbs could also be used as alternatives to germline-targeting Env-based immunogens. As we discuss in the previous Chapters, and as many others also reported, B cells of numerous specificities will be activated by an Env immunogen, including a germline-targeting immunogen, due to the numerous epitopes presented on such an immunogen (Briney et al., 2016; Dosenovic et al., 2015; Escolano et al., 2016, 2019; Jardine et al., 2015; McGuire et al., 2016; Parks et al., 2019; Tian et al., 2016). The use of an aiAb in the place of an Env immunogen as the first immunization in a prime-boost regimen will limit the potential of off target Env B cell responses being boosted with subsequent immunizations, as those epitopes are not presented by the aiAb in the first immunization.

In this Chapter, I report on the development of the aiAb, iv8, as a VRC01-class germline-targeting immunogen. We show the potential of iv8 to function as a VRC01-class germline-targeting immunogen using an adoptive-transfer model and tracked the

expansion and proliferation of VRC01-class B cells in response to immunization with iv8. We find that iv8 can expand and cause proliferation of glVRC01-class B cells *in vivo* and serological analysis showed that iv8 minimized the non-VRC01 epitope specific response in comparison to an Env based immunogen.

Results

Iv8 is an aiAb that was developed by immunizing a WT mouse three times with glVRC01. Following the final immunization, the B cells were immortalized using hybridoma technology and screened for binding to glVRC01-class Abs (Methods). The result of this screen is the aiAb iv8. Iv8 binds the germline forms of VRC01, NIH45-46, 3BNC60, 12A21, and VRC-CH31. Iv8 does not bind mature VRC01-class Abs or other non-VRC01-class anti-HIV-1 bnAbs. It could bind a synthetic intermediate that is the mature 3BNC60 HC and gl3BNC60 LC. It also bound a chimeric Ab consisting of the gl8ANC131 HC (VH1-46) paired with the glVRC01 LC. A second aiAb, iv1, was developed but binds fewer inferred germline VRC01-class Abs (Figure 4.1A). The binding data suggest that iv8 depends on the glVRC01 LC for binding.

This mechanism of binding was confirmed using crystallography. Iv8 single-chain variable fragment (scFv) was crystalized in combination with the glVRC01 scFv at 2.4 Å (Figure 4.1B). The crystal structure demonstrated that the primary interactions between iv8 and glVRC01 are through glVRC01's LC (80% of the buried surface area) and the remainder are through the glVRC01 CDRH3 and the Trp47, Trp50, and Asn58 which make critical contacts with Env (Figure 4.1C).

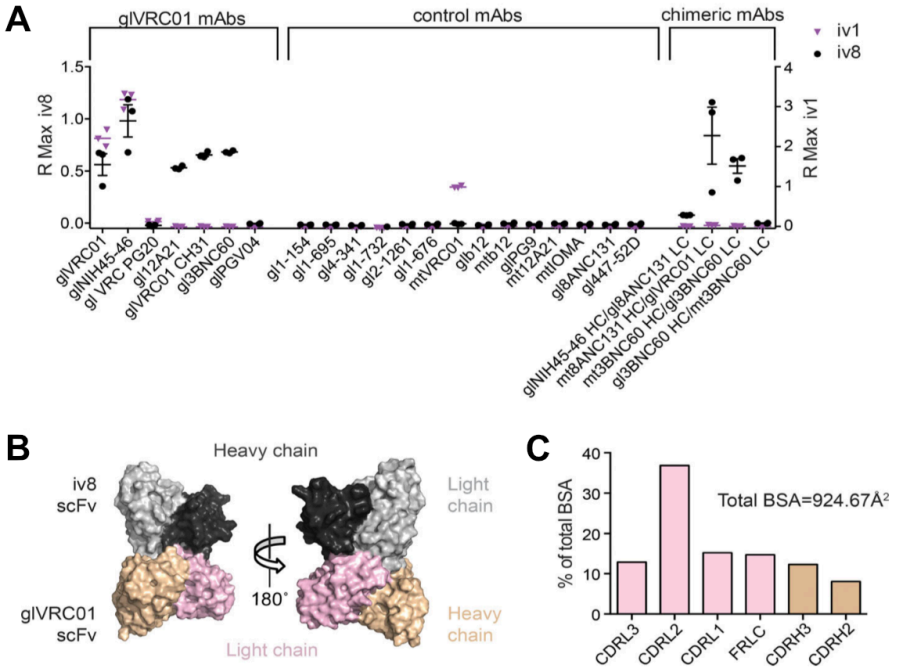

Figure 4.1 iv8 binding to inferred germline VRC01-class Abs. (A) iv8 (black circles) and iv1 (purple triangles) binding to germline (gl), mature (mt) or chimeric mAb. Data points depict the maximum binding response (R Max) of the mAb following a 500 second association step. Each point represents the R Max of an independent replicate (n = 3). Lines indicate arithmetic means; error bars indicate standard error of the mean (SEM); HC and LC indicate HC and LC, respectively. **(B)** Structure of iv8 scFv bound to germline VRC01 scFv. The iv8 HC and LCs are shown in dark and light gray, respectively. Germline VRC01 HC and LCs are shown in beige and pink, respectively. **(C)** Distribution of BSA on glVRC01 upon iv8 binding. BSA on the LC regions is shown in pink; BSA on the HC regions is shown in beige.

To test the ability of iv8 to expand a glVRC01-class B cells in a polyclonal immune system, SI-3BNC60 cells (>2x10^6), which express the mature 3BNC60 HC and the gl3BNC60 LC (Table 1.3), were adoptively transferred into a WT mouse. Prior to transferring, the cells were labeled using cell trace violet (CTV) to track the cells and measure cellular proliferation (Dosenovic et al., 2018). The recipient WT mouse was immunized with iv8 or a control aiAb ib5 in Ribi adjuvant (Bancroft et al., 2019). On day 5 following immunization, iv8 was able to induce cellular proliferation. In contrast the control Ab, ib5, did not. The proliferation induced by iv8 was enhanced by its

multimerization and use of an adjuvant (Figure 4.2). Therefore iv8 can activate VRC01-class B cells *in vivo* in the context of a polyclonal immune system.

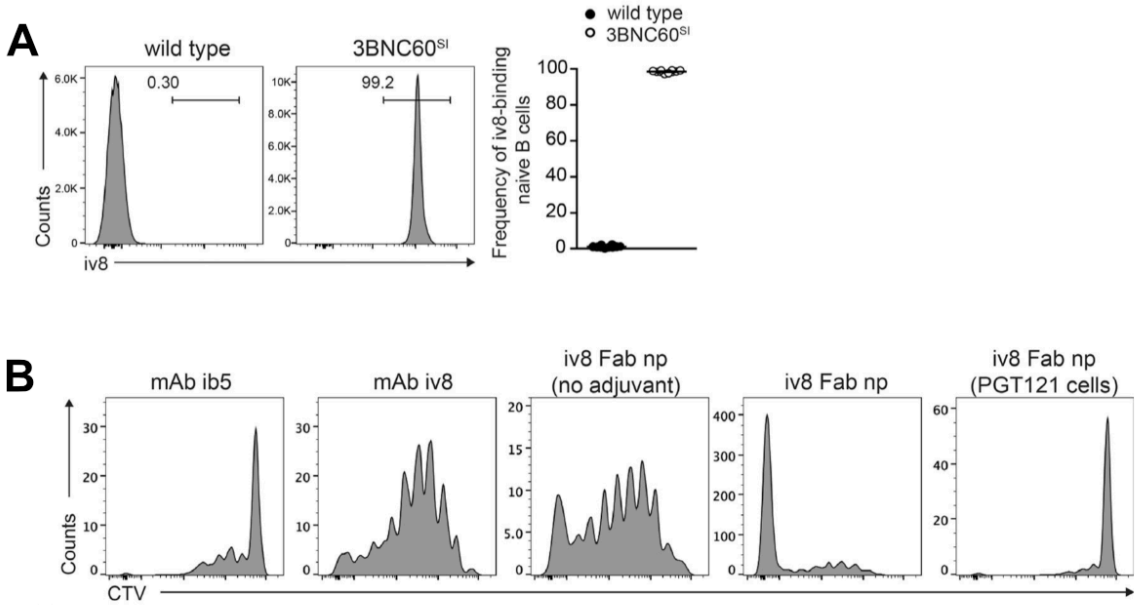

Figure 4.2 Expansion of VRC01-class B cells in vivo. (A) Representative flow cytometry plots of iv8-binding naive B cells from one WT mouse and one SI-3BNC60 (indicated as 3BNC60^{SI}) mouse of 10 analyzed (left panels). Arithmetic mean frequency of iv8-binding naive B cells from 10 mice per group. Error bars indicate SEM (right). One representative experiment of three is shown. **(B)** Representative flow cytometry plots showing proliferation of adoptively transferred SI-3BNC60 cells as indicated by CTV dilution at 5 days after injection of (from left to right) control mAb (ib5, binds glb12 but not gl3BNC60) with Ribi, mAb iv8 with Ribi, iv8 Fab nanoparticles (indicated as np) without Ribi, iv8 Fab nanoparticles (indicated as np) with Ribi, and CTV-labeled control PGT121 KI B cells in response to iv8 Fab nanoparticles (indicated as np) with Ribi. One representative animal of four per group is shown from one experiment of three.

The plasma Abs from mice immunized with iv8 were isolated and tested for binding to eOD-GT8 and eOD-GT8 KO. We found that iv8 immunized mice elicited an eOD-GT8 Ab response and that this response largely targeted the VRC01-epitope on eOD-GT8 as there was minimal binding to the eOD-GT8 KO. This is in contrast to an immunization with a 426c Env based immunogen (426c Δ276) that elicited a greater

response to the eOD-GT8 KO (Figure 4.3). Therefore, iv8 elicits a VRC01-epitope specific response with minimal off target Env responses.

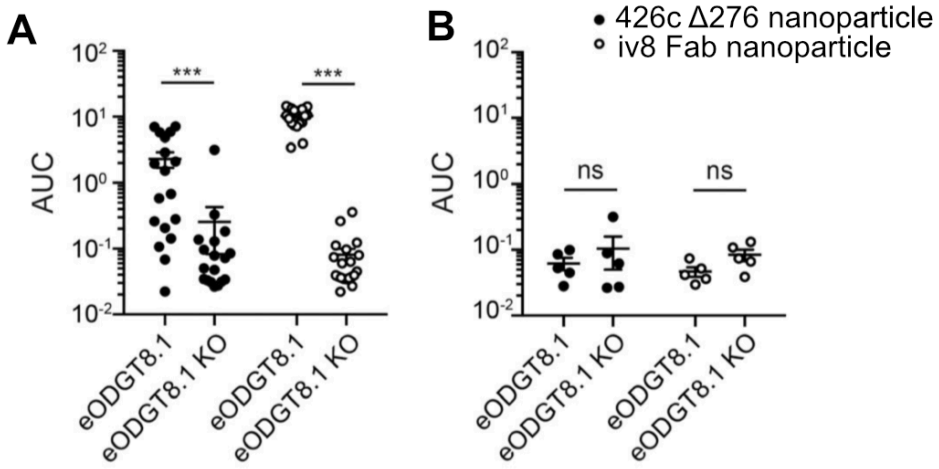

Figure 4.3 Serum Ab titers. Serum Ab titers against eOD-GT8 and eOD-GT8-KO in WT mice 14 days after injection with the 426c Δ276 nanoparticle or iv8 Fab nanoparticles in the presence **(A)** or absence **(B)** of adoptively transferred SI-3BNC60 cells. Merged data from three independent experiments is shown with five to nine mice per group (A: n = 18 426c Δ276 nanoparticle injected, n = 20 iv8 Fab nanoparticle injected; B: n = 5 426c Δ276 nanoparticle injected, n = 5 iv8 Fab nanoparticle injected). Lines indicate arithmetic means. Error bars indicate SEM.

To determine if iv8 can select for VRC01-class B cells *in vivo*, we employed the glH-3BNC60 mouse model that expresses the glH-3BNC60 HC and pairs with the endogenous mLCs (Table 1.3, (Dosenovic et al., 2015)). IgG1+, germinal center (CD95+,CD38-) B cells were sorted from mice immunized with iv8 or iv1 nanoparticles. Iv1 is a control aiAb that binds to glVRC01 and glNIH45-46, but not gl3BNC60. There was a preference for the use of short CDRL3s in the LC sequences from iv8 immunized mice in comparison to iv1 immunized mice (Figure 4.1A-C). 5 mAbs were made from LC sequences isolated from iv8 immunized mice with a 6 AA long CDRL3. 4/5 of these bound to iv8. However, none of these bound to 426c.TM4ΔV1-3, which is similar to 426c Core in that it lacks glycans surrounding the CD4-BS and variable loops, but it is

the gp140 subunit of the trimeric Env. They also did not bind to eOD-GT8 (Figure 4.4D, eOD-GT8 data not shown).

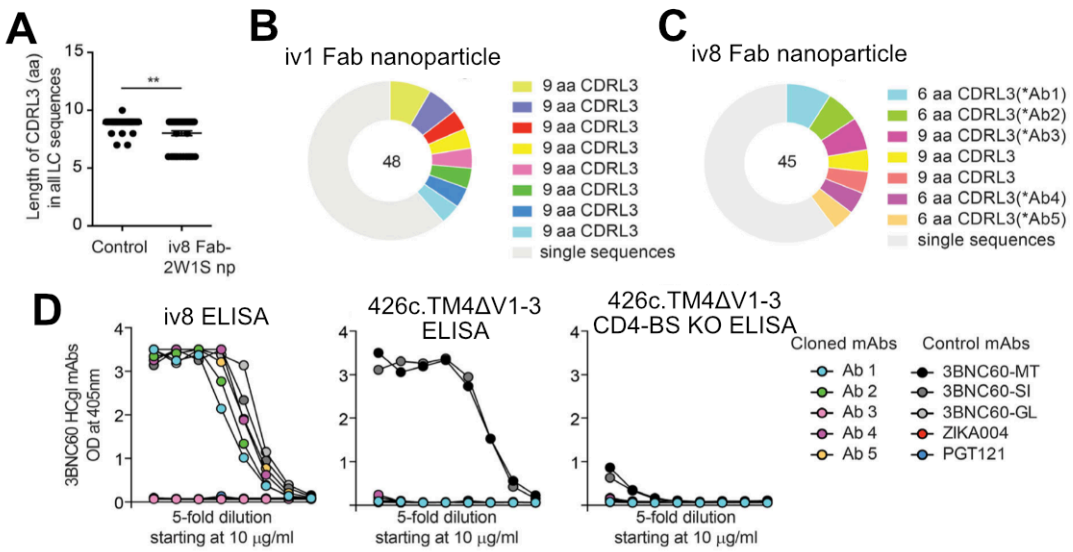

Figure 4.4 Selection for VRC01-class light chain characteristics by iv8 in HC glH-3BNC60 mouse. (A) CDRL3 lengths in AAs of BCRs from single-cell sorted IgG1+ GC B cells (B220+CD95+CD38−IgG1+) from two control-injected (iv1 Fab nanoparticles, which bind glVRC01 and glNIH45-46 but not gl3BNC60) and two iv8 Fab nanoparticle injected glH-3BNC60 mice obtained 14 days after injection. Lines indicate arithmetic means; error bars indicate SEM. Pie charts indicate B cell clones from sequences obtained from **(B)** iv1 immunized mice and **(C)** iv8 immunized mice. Each color represents a clone. Light gray indicates single sequences obtained from nonclonal B cells. Numbers in the middle of the pie chart indicate the total number of sequences analyzed. **(D)** Representative mAbs corresponding to the BCR sequences determined in C (Ab1–Ab5) were tested in ELISA against iv8 (left), 426c.TM4ΔV1-3 (middle), or 426c.TM4ΔV1-3 CD4-BS KO (right). Graphs are representative of two independent experiments.

To determine if iv8 can select for B cells with VRC01-class characteristics in humans, B cells were sorted from naïve humans using fluorescently labeled iv8. The iv8 specific B cells were sorted and the VH/VL genes were sequenced. 80% of the B cells sorted with iv8 express the IGKV3-11 used by VRC01-class Abs. Of those LCs utilizing the IGKV3-11 gene, ~2.8% of them express a 5 AA CDRL3. This is an increase compared to the unsorted cells, which express a 5 AA CDRL3 in less than 1% of the B cells (Figure 4.5). However, iv8 did not select for B cells expressing for the VH1-2*02 allele used by VRC01-class Abs, which is not unexpected, given the fact that iv8 binds predominately through the glVRC01 LC (Figure 4.1B-C).

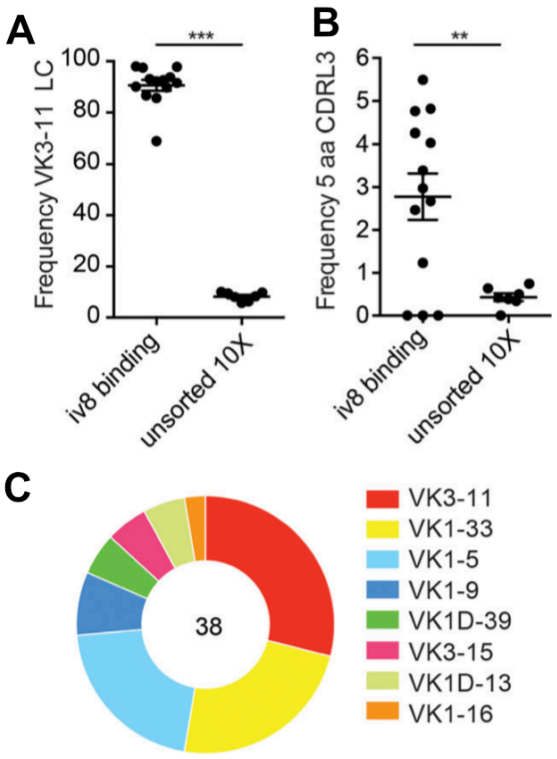

Figure 4.5 iv8 binding to human B cells. Human B cells were purified by cell sorting with fluorescently labeled iv8, and the kappa transcripts were recovered by RT-PCR and sequenced or subjected to paired BCR sequencing using the chromium platform from 10X Genomics. As a control, naive human B cells were enriched using magnetic beads, and paired BCR sequencing was performed using the chromium platform. **(A)** Frequency

of kappa transcripts derived from VK3-11 in iv8^{+} or unsorted B cells. Each dot represents one iv8^{+} sort (n = 13) or paired chromium-sequencing run of magnetic bead–enriched (total naive) B cells (n = 7). **(B)** Frequency of sequenced kappa transcripts with a 5 AA CDLR3 in iv8^{+} or total B cells. Each dot represents one iv8^{+} sort (n = 13) or chromium-sequencing run of magnetic bead–enriched (total naive) B cells (n = 7). Lines in A and B indicate arithmetic means, and error bars indicate SEM. **(C)** Kappa gene usage for of iv8^{+} B cells with 5 AA CDRL3s identified in B. Number in the middle of the pie chart indicates the total number of kappa sequences analyzed. Statistics were calculated using two-tailed unpaired Student's t tests in A and B. **, $P \leq 0.01$; ***, $P \leq 0.001$.

Discussion

In conclusion, this work has identified a novel VRC01-class germline-targeting immunogen, iv8, and demonstrated its ability to function *in vivo*. We show that in comparison to a 426c based Env immunogen, an immunization with iv8 decreases the amount of off target or non CD4-BS targeted response on Env. Therefore, B cells activated by iv8, which do not target the VRC01-epitope, should not be activated by a boosting immunization with Env. However, as the previous chapters have discussed and others have shown: a single immunization with a germline-targeting immunization is not sufficient to elicit neutralizing Abs (Briney et al., 2016; Dosenovic et al., 2015; Escolano et al., 2016, 2019; Jardine et al., 2015; McGuire et al., 2016; Parks et al., 2019; Tian et al., 2016). Future studies should implement boosting immunogens that aim to continue the maturation of the VRC01-class B cells activated by iv8 and drive them to their mature, neutralizing forms. This will likely be an Env based immunogen so as to guide the B cells to recognize the HIV-1 Env.

Here, we show the implementation of an aiAb as an immunogen for an HIV-1 vaccine, but we believe this strategy could be used to develop immunogens for any disease in which the signature of the neutralizing Abs are known. For example, it is known that neutralizing flu Abs use the VH1-69 gene (Corti et al., 2010b; Ekiert et al., 2011; Sui et al., 2009) and those to Zika utilize the VH3-23 gene paired with the VK1-5 gene (Robbiani et al., 2017). Furthermore, this method of immunogen design requires no prerequisite knowledge of the Ab's interaction with the antigen, and therefore requires no specific immunogen design and in turn facilitates rapid immunogen design.

In summary, we showed that an aiAb can activate specific BCRs in a polyclonal system. Here, we have developed a germline-targeting immunogen for HIV-1, but this immunogen design platform can be applied to diverse pathogens.

Methods

Hybridoma generation

We injected mice three times with germline VRC01 (VH1-2*02 HC/VK3-11 LC). 3 days after the final injection spleens were harvested and used to generate hybridomas at the Fred Hutchinson Ab Technology Center. Hybridoma supernatants were initially screened against glVRC01 to identify antigen-specific hybridomas. Supernatants from positive wells were then screened against a small panel of mAbs that included glVRC01 as well as other germline non-VRC01-class Abs that served as isotype controls by ELISA. Wells containing hybridomas that displayed positive binding for glVRC01, but negative binding to isotype controls, were sub-cloned by limiting dilution and screened for binding to a larger panel of Abs using BLI on the Octet Red96 (ForteBio). Anti-mouse IgG Fc capture sensors (ForteBio) were immersed in hybridoma supernatant for 200 s. After loading, the baseline signal was then recorded for 60 s in kinetics buffer (KB; 1× PBS, 0.01% BSA, 0.02%Tween 20, and 0.005% NaN pH 7.4). The sensors were then immersed in KB containing 20 μg/ml of purified human Ab for a 500 s association step. The maximum response was determined by averaging the nm shift over the last 5 s of the association step after subtracting the background signal from each analyte-containing well using empty anti-mouse IgG Fc capture sensors at each time point. The binding screen included germline and mature VRC01-class mAbs, non-VRC01-class mAbs, and chimeric mAbs comprised of either a VRC01-class IgH paired with a non-VRC01-class IgL, or a non-VRC01-class IgH paired with a VRC01-class IgL. Most hybridomas including iv1 bound glVRC01 or glNIH45-46 which differ only in the CDRH3 region, but showed no cross reactivity to other Abs in the panel.

Plasmids

The VH and VL sequences of the iv8 and iv1 hybridomas (GenBank accession nos. MK611925–MK611928) were recovered using the mouse iG primer set (Millipore) using the protocol outlined in (Siegal, 2009) and Sanger sequenced (Genewiz). The VH/VL sequences were codon-optimized and cloned into full-length pTT3 derived IgG1 and IgL kappa expression vectors containing human constant regions using Gibson assembly (Snijder et al., 2018). The iv8 and iv1 VH regions were also cloned in frame with the human IgG-C1 domain fused to the modified multimerization domain of the C4b binding protein from Gallus gallus (Ogun et al., 2008) followed by a cathepsin cleavage site (Schneider et al., 2000) and the 2W1S peptide (Rees et al., 1999). Another variant of iv8-C4b was made without the C-terminal cathepsin-2W1S fusion. pTT3-426c-Δ276-gp140-KO was generated by introducing the D368R and E370A mutations (McGuire et al., 2014) into pTT3- 426c-Δ276 gp140 (McGuire et al., 2013) plasmid using site directed mutagenesis according to the manufacturer's recommendations (Agilent Quickchange XLII). pTT3-426c-Δ276-C4b-2W1S was created by cloning cDNA corresponding to AAs 1–479 of the 426c Δ276 from pTT3-426c-Δ276 gp140 in-frame with the C4b multimerization domain and 2W1S peptide described above. The coding sequence of eOD-GT8 (Jardine et al., 2015) preceded by a leader peptide (MDAMKRGLCCVLLLCGAVFVSPSAS) was synthesized by IDT DNA technologies and cloned into pTT3 followed by a gly-ser linker and a his-avi tag (McGuire et al., 2014) to create pTT3 eOD-GT8- his-avi. pTT3 eOD-GT8-KO was generated by introducing the D276N, W277F, R278T, D279A, and D368R mutations into pTT3- eOD-GT8-his-avi by site directed mutagenesis.

Ab purification

Plasmids encoding mAb HC and LCs were transfected into 293F cells at a density of 10^6 cells ml^{-1} in Freestyle 293 media using the 293Free transfection reagent according to the manufacturer's instructions or PEI. Expression was performed for 6 days, after which cells and cellular debris were removed by centrifugation at 4,000 ×g followed by filtration through a 0.22-μm filter. Clarified cell supernatant containing recombinant Abs was passed over Protein A or G Agarose, followed by extensive washing with PBS, and then eluted with 1 ml of Pierce IgG Elution Buffer, pH 2.0, into 0.1 ml of Tris HCl, pH 8.0. Purified Abs were then dialyzed overnight into PBS, and stored at −20°C before use.

Binding screen with recombinant aiAbs

To verify the specificity of recombinant iv8 and iv1, they were biotinylated at a theoretical 1:1 mAb to biotin ratio using the EZ-Link NHS-PEG4-Biotin kit (Thermo Fisher Scientific) and then subjected to the BLI screen described in the "hybridoma generation" section with the following change to the first capture step: iv8 or iv1 was immobilized on a streptavidin biosensor (ForteBio) by immersing the biosensor into a 10 μg/ml solution of biotinylated mAb.

scFv expression and complex formation

scFv constructs were cloned into the pTT3 plasmid vector. ScFvs contain only the variable Ab domains of VH/VL connected by an AA linker GGGGSGGGGSGGGGS from the C-terminus of the LC to the N-terminus of the HC. Iv8 scFv and glVRC01 scFv were expressed using HEK293ENBA cells (Tom et al., 2008). Cells were cultured in

suspension and transfected with 500 μg/liter plasmid DNA using 293 Free Transfection Reagent (Novagen). After 6 days, cells were centrifuged at 4,500 rpm for 20 min. Supernatant was filter sterilized and incubated with His60 Ni-Superflow Resin (Novagen) overnight at 4°C, capturing scFv's with a 6 his-tag on the C-terminus of the proteins. The Ni resin was separated from the supernatant and washed with a solution of 150 mM NaCl, 20 mM Tris (pH 8.0), 20 mM imidazole (pH 7.0) and eluted with a solution of 300 mM NaCl, 50 mM Tris pH 8.0, 250 mM imidazole (pH 7.0). To separate the scFv monomers from diabodies and triabodies and to further purify the proteins, the sample was run on size-exclusion chromatography using a HiLoad 16/600 Superdex 200 pg (GE) column. Complexes of iv8 scFv and glVRC01 scFv were formed by mixing proteins at a 1:1 molar ratio. ScFv complexes were removed from monomeric scFv using size-exclusion chromatography. Complexes were concentrated to ~10 mg/ml for crystallization trials.

Crystallization

Crystallization conditions for iv8scFv and glVRC01scFv complexes were screened and monitored with a Formulatrix NT8 drop setting and Rock Imager. Screening was done with Hampton Research Crystal Screen HT, Molecular Dimensions Proplex screen HT-96, and Rigaku Wizard Precipitant Synergy block no. 2 using the vapor diffusion method. Final crystals were grown in a solution of 0.13 M NaCl, 0.13 M Tris (pH 8.0), 10.4% PEG 20,000. Crystals were cryoprotected in solutions containing 30% molar excess of their original reagents and 20% ethylene glycol. Crystals diffracted to 2.42 A˚. Data were

collected at Advanced Light Source 5.0.2 and processed using HKL2000 (Otwinowski and Minor, 1997).

Structure solution and refinement

The structure of iv8scFv-glVRC01scFv was solved by molecular replacement with Phaser in the CCP4 suite (Collaborative Computation Project, Number 4, 1994) using the glVRC01 Fv portion of PDB ID: 6MFT (Borst et al., 2018) as the search model for both iv8 and glVRC01. Model building and refinement were performed using COOT (Emsley and Cowtan, 2004) and Phenix (Adams et al., 2010).

Multimeric iv8 Fab purification

Plasmids encoding iv8-IgH (Fab)-C4b or iv8 IgH (Fab)-C4b- 2W1S were cotransfected with plasmids of iv8-Igk (1:1) into Expi-293 cells (Invitrogen) according to the manufacturers' instructions. The supernatants were collected after 5 days of culture, filtered through 0.45 μm filter units (Millipore), and diluted 1:1 in IgG binding buffer (Thermo Fisher Scientific). Multimeric iv8 Fab complexes were purified by Protein G Agarose beads (Thermo Fisher Scientific), concentrated in centrifugal filter (30-kD cutout; Amicon), buffer exchanged with TBS pH 5.5, and further purified using size exclusion chromatography (Superdex200, GE Healthcare). The multimeric state of iv8 Fab-C4b were verified by nonreducing SDS-PAGE and the binding activity was verified by BLI.

Recombinant protein expression

pTT3-426c-Δ276-C4b-2W1S, pTT3-426c-Δ276-gp140, pTT3-426c-Δ276-gp140-KO, pTT3-eOD-GT8-his-avi, and pTT3-eOD-GT8-KO-his-avi expression plasmids were transfected into 293 F cells at a density of 10^6 cells ml^{-1} in Freestyle 293 media (Life Technologies) using the 293Free transfection reagent (EMD Millipore). Expression was performed in Freestyle 293 media for 6 days with gentle shaking at 37°C in the presence of 5% CO2 after which cells and cellular debris were removed by centrifugation at 10,000 ×g followed by filtration through a 0.2 μM filter. Clarified cell supernatant containing 426c-Δ276-C4b-2W1S, 426c-Δ276-gp140, and pTT3-426c-Δ276-gp140-KO was passed over Agarose-bound Galanthus Nivalis Lectin (GNL) resin (Vector Laboratories), preequilibrated with 20 mM Tris, 100 mM NaCl, 1 mM EDTA (pH 7.4; GNL binding buffer), followed by extensive washing with GNL binding buffer. Bound protein was eluted with GNL binding buffer containing 1 M methyl mannopyranoside. Clarified cell supernatant containing eOD-GT8-his-avi and eOD-GT8-KO-his-avi, was passed over nickel ni-trilotriacetic acid (Ni-NTA) resin preequilibrated with Ni-NTA binding buffer (0.3 M NaCl, 20 mM Tris, 10 mM imidazole [pH 8.0]), followed by extensive washing with Ni-NTA binding buffer, and then eluted with 250 mM imidazole, 0.3 M NaCl, 20 mM Tris (pH 8.0; Ni-NTA elution buffer). All affinity purified proteins were further purified using a 16/60 S200 size exclusion column (GE Healthcare) preequilibrated in PBS. Fractions containing purified proteins were pooled, aliquoted, frozen in liquid nitrogen, and stored at −20°C.

Mice

glH-3BNC60 KI mice (CD45.2+) carry the pre-rearranged V(D)J genes encoding the predicted germline IgH respectively, of human bnAb 3BNC60. SI-3BNC60 KI mice (CD45.2+) carry the prerearranged V(D)J genes encoding the mature IgH and predicted germline IgL of human bnAb 3BNC60 (Dosenovic et al., 2015; McGuire et al., 2016). Mice used in experiments were homozygous for KI alleles. B6.SJL (CD45.1+) mice were obtained from the Jackson Laboratory. All experiments were conducted at The Rockefeller University according to approved Institutional Animal Care and Use Committee protocols.

Animal experiments

40 μ g 2W1S peptide was immunized intraperitoneally in CFA adjuvant (Sigma) according to manufacturers' instructions 2–4 weeks before adoptive transfer or antigen injection. CD43-depleted SI-3BNC60 B cells (MACS Miltenyi Biotec) were transferred intravenously into B6.SJL recipient mice. 10–30 μg of indicated protein (mAb iv8, iv8 Fab-2W1S, and Env 426c-Δ276-2W1S nanoparticles or control Abs) were injected intraperitoneally or subcutaneously in Sigma Adjuvant System (Sigma-Aldrich; Ribi) according to manufacturers' instructions.

Murine lymphocyte preparation and adoptive transfer

Lymphocytes were harvested by forcing lymph nodes and/or spleen through 70 μm filters (BD) into RPMI 1640 media (Gibco) containing 6% fetal bovine serum (FBS) and 10 mM HEPES, followed by lysis of erythrocytes using 1X ACK Lysis Buffer (Gibco). B

cells were enriched by negative selection using anti-CD43 MicroBeads (Militenyi Biotec) with magnetized LS columns according to manufacturers' instructions. In some experiments, enriched B cells were labeled with CTV (Thermo Fisher Scientific) according to manufacturers' instructions. Upon analysis of SI-3BNC60 plasmablast and early memory B cell differentiation, >2 × 10^6 CTV-labeled SI-3BNC60 B cells were transferred i.v. Approximately 100,000 B cells are then present in the mouse according to calculations in (Dosenovic et al., 2018) where ~5% of the transferred B cells were shown to survive. The high number of B cells is needed to be accurately detected at early times after injection. In experiments where adoptively transferred SI-3BNC60 cells or serum responses were analyzed at later time points (>10 day), 500,000 enriched naive SI-3BNC60 B cells were transferred intravenously, resulting in 25,000 naive SI-3BNC60 B cells/mouse.

Flow cytometry and single cell sorting of murine cells

For murine B cell sorting, single cell suspensions of lymphocytes were maintained at 4°C in FACS buffer (PBS containing 2% FBS and 1 mM EDTA). Fc receptors were blocked using rat anti-mouse CD16/32 (clone 2.4G2; BD). Cells were stained with fluorophore-conjugated Abs to: B220, IgM, CD38, CD45.1, CD45.2 (eBioscience), IgD, CD138 (BioLegend) GL7, CD95, CD4, CD8, NK1.1, Gr1, or F4/80 (BD). Dump staining including CD4, CD8, NK1.1, Gr1, and F4/80 were included in all flow cytometry stainings. Dead cells were excluded from analyses using Zombie NIR Fixable Viability Kit (BioLegend). Adoptive-transfer samples were acquired on a BD Fortessa or BD Symphony and analyzed using FlowJo software (TreeStar). In single cell sorting

experiments, IgG1+ GC B cells were single cells sorted based on CD4−, CD8−, Gr-1−, F4/ 80−, NK1.1−, B220+, CD95+, CD38−, IgG1+ expression. Cells were single cell–sorted into 96-well plates using a FACSAria III sorter (Becton Dickinson). The cells were lysed with 4 µl lysis buffer containing RNasin (Promega) in 40 U/µl (0.3 µl), 10× Dulbecco's PBS (DPBS; 0.2 µl), dithiothreitol (Invitrogen) 100 mM (0.4 µl), and nuclease-free water (3.1 µl). The sorted plates were stored at −80°C until further processing (Tiller et al., 2009). LC sequences were retrieved using primers described in (Dosenovic et al., 2015). A clone was defined as nucleotide sequences with the same V and J LC germline gene and similar CDRL3 nucleotide sequences (similarity of CDRL3 was defined using hamming distance threshold of 0.15). Samples were acquired on a BD FACSAria.

ELISA

Corning 3690 half-well 96-well plates were coated overnight at 4°C with 50 µl/well of 2 µg/ml eOD-GT8, eOD-GT8-KO, 426cTM4ΔV1-3, 426cTM4ΔV1-3-KO, or murine iv8 Fab in PBS. Plates were washed six times in PBS 0.05% Tween 20 (wash buffer). Plates were blocked with 100 µl/well PBS 5% milk (blocking buffer) for 2 h at room temperature (RT). Sera or mAbs were prepared at 1:30 dilution or a concentration of 10 µg/ml in fresh blocking buffer, respectively, and further diluted in threefold or fivefold serial dilutions, respectively. A total volume of 50 µl was added to the plates and incubated for 2 h at RT. Binding was revealed by either anti-mouse IgG-HRP (Jackson ImmunoResearch) or anti-human IgG-HRP (Jackson ImmunoResearch) diluted 1:5,000 in wash buffer. Plates were incubated for 1 h at RT. Plates were washed six times in wash

buffer. HRP activity was determined using ABTS (2,29-azinobis [3-ethylbenzothiazoline-6-sulfonic acid]-diammonium salt) substrate solution (Life Technologies), adding 50 µl/well. Plates were read at 405 nm on a FLUOstar Omega microplate reader (BMG Labtech). Data were analyzed with Microsoft Excel and GraphPad Prism 6.0.

Preparation of zenon mAb labeling decoys

Zenon APC-DL755 was generated by conjugating the Zenon APC Human IgG labeling reagent, from the Zenon Allophycocyanin Human IgG Labeling Kit (Z25451) to DyLight 755 NHS Ester (62279; Thermo Fisher Scientific) according to manufacturers' instructions. Zenon PE-DL650, was generated by conjugating the Zenon PE Human IgG labeling reagent from the Zenon R-Phycoerythrin Human IgG Labeling Kit (Z25455) with DyLight 650 NHS Ester (62266; Thermo Fisher Scientific) according to the manufacturers' instructions. To create decoy reagents, Zenon APC-DL755 and Zenon PE-DL650 were incubated with Zenon blocking reagent at a 1:1 ratio.

Fluorescent iv8 probes

To generate iv8-APC, 1 µg of iv8 was incubated with 5 µl Zenon APC Human IgG labeling reagent, and incubated at RT for 10 min, then incubated with 5 µl of Zenon blocking reagent and stored at RT until use. To generate iv8-PE, 1 µg of iv8 was incubated with 5 µl Zenon PE Human IgG labeling reagent, and incubated at RT for 10 min, then incubated with 5 µl of Zenon blocking reagent and stored at RT until use.

Human subjects

Peripheral blood mononuclear cells (PBMCs) and serum were collected from HIV-uninfected adults recruited at the Seattle HIV Vaccine Trials Unit (Seattle, Washington) as part of the study "Establishing Immunologic Assays for Determining HIV-1 Prevention and Control," also referred to as Seattle Assay Control. All participants signed informed consent, and the following institutional human subjects review committee approved the protocol before study initiation: Fred Hutchinson Cancer Research Center institutional review board (Seattle, Washington). PBMC samples from donors were blindly selected at random with no considerations made for age or sex.

Human B cell sorting

Cryopreserved PBMC were thawed and resuspended in 200 µl of EasySep buffer (1× PBS, 2% heat inactivated fetal bovine serum, 1 µM EDTA). B cells were isolated using the StemCell Human B Cell Enrichment Kit (19054; StemCell Technologies) according to the manufacturers' instructions. Enriched B cells were resuspended in 200 µl EasySep buffer and incubated with 10 µl rat serum, 10 µl mouse serum, 10 µl mouse–anti-human CD32 (551900; BD), 10 µl mouse–anti-human CD23 (555707; BD), and 10 µl mouse–anti-human CD16 (550383; BD). Cells were then washed with EasySep buffer and resuspended in 200 µl EasySep buffer and incubated with 5 µl of Zenon APC-DL755 and 5 µl of Zenon PE-DL650 and incubated on ice for 10 min. Next, B cells were stained with iv8 conjugated to either Zenon-PE or Zenon-APC and CD19-BV711 (302246; BioLegend) at 1:200 dilution, CD27-PECy7 (25-0271-82; eBioscience) at a 1:600 dilution, CD14- FITC (557153; BD) at 1:60 dilution, CD3-FITC (556611; BD) at a 1:60

dilution, CD20-AF700 (302322; BioLegend) at a 1:300 di- lution, IgD-PerCP-Cy5.5 (46-9868-42; eBioscience) at a 1:120 dilution, IgM-BV605 (314524; BioLegend) at a 1:120 dilution, and Fixable Viability Dye eFluor 506 (65-0866-14; eBioscience) at a 1:300 dilution. Cells were then washed with 5 ml of EasySep buffer and suspended in 0.5 ml of EasySep buffer. Cells were analyzed by flow cytometry using a BD FACS Aria II. Naive iv8+ B cells were defined as live (eFluor 506−), CD14−, CD3−, CD19+, CD20+, IgM+, IgD+, CD27−, APC-DL755−, PE-DL650−, PE+, APC+. Naive iv8+ B cells were single-cell sorted into 96-well plates. cDNA was generated using iScript (Bio-Rad) and the VH and VK sequences were recovered using gene specific primers and cycling conditions previously described (Tiller et al., 2009). Alternatively, naive iv8+ B cells were bulk-sorted and sequenced using the human B Cell V(D)J Enrichment Kit on the Chromium platform (10X Genomics). As a control, naive unsorted B cells were isolated using the EasySep Human B cell isolation kit (Stemcell Technologies). BCR sequences were obtained using the using the human B Cell V(D)J Enrichment Kit on the Chromium platform (10X Genomics). Because iv8 strongly selects for kappa LCs, lambda LC transcripts were excluded from analysis of the 10X sequencing data.

Statistical analysis

Data were analyzed with Prism 6 (GraphPad) for normal distribution using the D'Agostino-Pearson normality test. Data points that displayed normal Gaussian distribution were further analyzed for significant differences with Prism 6 (GraphPad) using two-tailed unpaired Student's t tests. Data points that did not display a normal

Gaussian distribution were analyzed for statistical differences using the Mann-Whitney U test. Data were considered significant at *, $P \leq 0.05$; **, $P \leq 0.01$, ***, $P \leq 0.001$.

Chapter V. Discussion

Summary of results

While, there is no precedent for eliciting bnAbs through vaccination, as no vaccine evaluated thus far has elicited bnAbs; bnAbs do show the ability to protect in animal models (Baba et al., 2000; Gautam et al., 2016; Hessell et al., 2009, 2010; Julg et al., 2017; Klein et al., 2012b; Mascola et al., 1999, 2000; Nishimura et al., 2002; Parren et al., 2001; Parsons et al., 2019; Pegu et al., 2014; Shibata et al., 1999; Wu et al., 2018). Therefore, a goal of an effective HIV-1 vaccine is to generate bnAbs. The goal of this thesis has primarily been to elicit VRC01-class Abs through immunization. It has now been well established that the germline form of VRC01-class Abs do not bind to recombinant Env (Hoot et al., 2013; McGuire et al., 2013, 2014b; Xiao et al., 2009). Therefore, specifically designed immunogens have been developed to engage the germline form. In the studies reported here, we evaluate germline-targeting immunogens *in vivo* and use a prime-boost immunization to guide their maturation towards the neutralizing form.

In Chapter II, we identify a novel germline-targeting immunogen 426cOD and compare its ability to activate a glVRC01 expressing B cell *in vivo* with two established germline-targeting immunogens: 426c Core and eOD-GT8 (Jardine et al., 2015). While, all three can engage the same glVRC01 BCR, they differ genetically, structurally, in affinitiy and in the electrostatic potential of the VRC01 epitope. 426c Core and 426cOD are derived from the 426c Env, where as eOD-GT8 is derived from the HxB2 Env. Structurally, 426cOD and eOD-GT8 represent just the outer domain of the gp120 subunit of Env, where as 426c Core is composed of both the inner and outer domains of the gp120 subunit. eOD-GT8 also has a much higher affinity for the glVRC01 Ab than the

426c Env based immunogens. Lastly, the VRC01 epitope on the 3 immunogens differs in the electrostatic potential, with the 426c-based immunogens having a negative charge and eOD-GT8 a positive charge (Figure 2.1).

Previous studies have shown many factors that are important for the activation and maturation of B cells, including affinity for the antigen, precursor frequency, and multimerization (Abbott et al., 2018; Dosenovic et al., 2018; Schwickert et al., 2011). In the case of VRC01-class germline-targeting immunization efforts, B cells expressing a single VRC01-class VH/VL pair combination are transferred to WT mice, which are then immunized with different forms of a germline-targeting immunogen. One such study, reported by Abbott et al., utilizes an adoptive transfer experiment, transferring B cells from the glH/L-VRC01 mouse model (Table 1.3) to a WT mouse. The recipient mouse is then immunized with eOD-GT-based immunogens. These immunogens have a range of affinities for the glVRC01 precursor. Here, they show that affinity, glVRC01 precursor frequency and multimerization of antigen impacts participation in the germinal center.

In the studies presented in Chapter II, we have identified the biophysical and biochemical properties of the epitope, along with the overall presentation of the epitope within the context of each immunogen, to be important factors in the initial selection of B cells to participate in the response to immunization. We show that, because of these factors, each germline-targeting immunogen will select only a subset of available glVRC01-class B cells and that within each selected pool, B cells with a range of affinities will be present. We believe that after the initial BCR selection, affinity and other determining factors will influence the fate of the B cells. For example, a high affinity antigen is known to stimulate a B cell to differentiate into a plasma cell (Phan et

al., 2006; Taylor et al., 2015). The reason why we made these observations is because we used the glH-VRC01 mouse model, which in contrast to the one used in Abbott et al., expresses a wide range of VRC01-like BCRs because of the diversity in the LC.

A consequence of the previously discussed differential BCR selection between 426c Core and eOD-GT8 is that the selected B cells display different Env-recognition properties. We show that these differences in cross-reactivity are due to different amino acids selections in CDRL3 and CDRH1 by the two immunogens. Presently, it is unknown whether the above observations will also be made in the context of human immunization. We propose that eOD-GT8 will elicit VRC01-like BCRs with limited cross-reactivity to heterologous Envs expressing N276 glycans while 426c Core will select for VRC01-like BCRs with long CDRL1 domains.

While others and we have shown that the germline-targeting immunogens can activate a glVRC01 precursor *in vivo*, they do not produce neutralizing Abs. In the case of VRC01-class Abs the major challenge to the maturation of VRC01-class Abs are the glycans surrounding the CD4-BS, in particular the glycan at position 276. In Chapter III, we developed a prime-boost immunization protocol that leads to the expansion of VRC01-like B cells that are capable of bypassing the N276 glycans and begin to show WT neutralizing activity. In this protocol, the 426c Core nanoparticle is used as the prime immunogen and the HxB2 WT Core nanoparticle immunogen is used as a boost. The reasons for selecting HXB2 WT Core as the boost immunogen are discussed in detail in Chapter III. We report that following the boosting immunization the elicited VRC01-like Abs could bind Env trimers with a glycan at position 276 and neutralize the autologous WT virus. Furthermore, we definitively proved that these Abs could bind Env in the

presence of the 276 glycan using a combination of techniques including mass spectrometry and isolation of the glycosylated Env species to be used in binding assays.

Others who have tried to elicit VRC01-class Abs through immunization either do not use an immunogen with a glycan at position 276 or introduce it very late in the immunization scheme (Briney et al., 2016; Tian et al., 2016). As a consequence, we believe that this approach will preferentially expand B cells not capable of recognizing Env and viruses with a glycan at position 276. While both studies report the identification of Abs capable of neutralizing a virus that encodes the glycosylation sequon at position 276; they did not determine if a glycan was present on that virus or demonstrate the mechanism through which the Abs could accommodate this glycan (Briney et al., 2016; Tian et al., 2016). Therefore, we believe that it is important to introduce the glycan at position 276 early in the immunization scheme so that the B cell may mature to accommodate the glycan at position 276. We were able to do this in the studies reported in Chapter III, as the priming immunogen 426c Core, activated B cells capable of recognizing Env expressing a glycan at position 276. Therefore, there was a population of B cells that could be boosted by such an immunogen.

In addition to analyzing the B cell response to 3 Env based immunogens, work in this thesis also evaluated the use of an aiAb, iv8, as a VRC01-class germline-targeting immunogen (Chapter IV). As shown, in Chapter II and III and as reported by others, germline-targeting immunogens will elicit a large non-CD4-BS targeted Ab response, because of the many epitopes they present (Briney et al., 2016; Dosenovic et al., 2015; Duan et al., 2018; Jardine et al., 2015; McGuire et al., 2016; Parks et al., 2019; Tian et al., 2016). This will be a challenge for prime-boost studies utilizing Env based

immunogens as with each immunization non-CD4-BS directed and non-neutralizing Abs can be boosted by the conserved epitopes among the immunogens. In these studies, we showed that iv8 activated and expanded glVRC01-class B cells *in vivo* in the adoptive transfer model. Additionally, iv8 had reduced off target Abs present in the plasma compared to a 426c Env based immunogen. When evaluated in the glH-3BNC60 mouse model, mice immunized with iv8 showed an enrichment for short CDRL3s, a characteristic present in mature VRC01 Abs. Iv8 was also able to identify B cells from naïve humans, which utilize the IGKV3-11 LC expressing a 5 AA CDRL3, which is found in mature VRC01-class bnAbs. However, these B cells did not pair with a VH1-2*02 HC. We have shown that Iv8 binds primarily through the glVRC01 IGKV3-11 LC and can therefore bind Abs expressing non-VH1-2*02 HCs (Figure 4.1). As a result human B cells utilizing the IGKV3-11 with a 5 AA CDRL3, but not a VH1-2*02 HC were isolated.

Like the other germline-targeting immunogens evaluated here, the B cells activated by iv8 will require boosting immunogens to continue the B cells maturation to the neutralizing form. The Abs generated from HC and LC paired sequences isolated post-immunization with iv8 did not show reactivity with 426c.TM4ΔV1-3. Mature VRC01-class Abs have 5 AA CDRL3s which orientate the $Glu96_{LC}$ to make key contacts with the HIV-1 Env in loop D and the V5 loop. Iv8 expanded B cells with a 6 AA long CDRL3s and could therefore potentially alter the position of this residue and not allow for these interactions (Diskin et al., 2011; West et al., 2012; Zhou et al., 2013). Alternatively, the mouse V gene utilized (k10-96*01, and k14-111*01) by these Abs may not confer binding to 426c.TM4ΔV1-3, as we find some Abs isolated following

immunization with eOD-GT8 despite expressing a 5 AA CDRL3 and VH1-2*02 allele in the HC do not bind 426c Core. As a result of the lack of reactivity, 426c.TM4ΔV1-3 may not boost the glVRC01-class B cells activated by iv8 and future work must be done to identify a boosting immunogen to iv8.

Iv8, along with ib5, an aiAb designed to activate glb12 expressing B cells, represent a novel type of germline-targeting immunogen (Bancroft et al., 2019). While, we apply the use of an aiAb to HIV-1 vaccine design, aiAb immunogen design could be applied to diverse pathogens.

Limitations and future directions

While these studies add to the fundamental understanding of B cell activation and identify and evaluate novel HIV-1 immunogens, there are limitations of these studies, which should be addressed. I will discuss some of these limitations and future experiments, which may provide clarity. In our evaluation of the VRC01-class germline-targeting immunogens 426c Core and eOD-GT8, we identify subpopulations of glVRC01-class B cells that will become activated during immunization. However, from the studies presented here, we cannot say which of these populations will be more amenable to maturing towards the VRC01-class neutralizing form. Furthermore, due to these differences in BCR selection, it is likely that the two immunogens will require different boosting immunogens. We do find that the 426c Core elicited Abs can bind and be boosted by heterologous Core Env with a glycan at position 276, where as those elicited by eOD-GT8 cannot. eOD-GT8 elicited Abs can be boosted by BG505 core-GT3, but this protein does not express a glycan at position 276. Therefore, it will be a challenge to mature eOD-GT8 elicited Abs to accommodate the glycan at position 276.

Furthermore, while we have shown maturation of VRC01-like B cells so that they may accommodate the N276 glycan, the Abs isolated in these studies do not neutralize heterologous virus with a glycan at position 276. Future studies should be aimed at identifying additional boosting immunizations, which will increase the neutralization potency and breadth of the Abs reported here. One study has shown that immunizing a transgenic mouse expressing thr mature 3BNC60 HC with a trimeric Env immunogen will produce neutralizing Abs (Dosenovic et al., 2015). Therefore, once far enough along the maturation pathway, a trimeric Env immunogen will likely be needed to cause the B

cells to secrete VRC01-class neutralizing Abs. In the case of our studies, it would be interesting to follow the HxB2 WT Core boosting immunization with a trimeric Env expressed in GnTI-/- cells and then follow with another trimeric Env immunization, but this time expressed in 293 cells. This will hopefully cause the B cells to be able to accommodate the N276 glycan by gradually introducing larger sugar molecules on the trimeric Env.

The use of aiAb as a germline-targeting immunogen represents a novel approach to elicit VRC01-class Ab. It was successful at activating B cells from a transgenic mouse expressing both the mature 3BNC60 HC and the germline 3BNC60 LC (SI-3BNC60 mouse, Figure 4.2, Table 1.3, (Dosenovic et al., 2018)). However, when used to immunize the glH-3BNC60 mouse, which have the gl3BNC60 HC only knocked-in, there was an enrichment for short CDRL3, but these were 6 AAs, where as the CDRL3 in mature VRC01-class Abs is 5 AAs long (Figure 4.4). When applied as a sort probe to human PBMCs, iv8 was successful in isolating B cells with a IGKV3-11 light chain with 5 AA long CDRL3s, but these did not pair with a VH1-2*02 HC (Figure 4.5). Therefore, aiAbs that can select for B cells expressing paired VRC01 HC and LC sequences should be generated. Abs expressing the glVRC01 HC only, LC only and both could be incorporated into the hybridoma screening process. Cells secreting Abs that bind only to an Ab expressing the glVRC01 HC and LC should be selected for further development as an aiAb immunogen.

While, these studies evaluate the germline-targeting immunization strategy in transgenic mouse models, the extent to which this strategy will succeed in humans is unknown. The glVRC01 precursor is expressed at a higher frequency in the mouse

models implemented here than in humans. It has been shown that the precursor frequency of the VRC01-class B cell influences its participation in the response to vaccination (Abbott et al., 2018). Therefore, the results presented here may not be representative of what will happen in a more polyclonal immune system, such as humans. I expect there will be greater non-CD4-BS target response in humans which may make it challenging for the VRC01-class B cells to compete for antigen and T cell help, both of which will be important for the activation and maturation of a VRC01-class B cell.

Furthermore, here we show the evolution of only one class of bnAb; however, a protective HIV-1 vaccine may require the elicitation of more than one class of bnAb. This may be necessary due to the diverse viral variants of HIV-1 present in circulation or due to the fact that some people may not express the VH1-2*02 allele used in VRC01-class antibodies (Yacoob et al., 2016) and therefore will require an alternative bnAb to be elicited in a protective vaccine. In either case, a cocktail of germline-targeting immunogens designed to elicit multiple classes of bnAbs could be administered, or germline-targeting immunogens capable of activating more than one class of bnAb, such as BG505 SOSIP.v4.1-GT1.1, should be developed (Medina-Ramírez et al., 2017). The idea of eliciting multiple classes of bnAbs through vaccination is supported by the fact that combination bnAb therapy in HIV-1 infected individuals undergoing ART interruption suppresses viremia for longer than in individuals given monotherapy (Bar et al., 2016; Caskey et al., 2015, 2017; Lynch et al., 2015b; Scheid et al., 2016).

Furthermore, the high level of SHM found in mature VRC01-class bnAbs poses a challenge to a HIV-1 vaccine aiming to elicit bnAbs. The SHM found in bnAbs occurs in HIV-1 infected individuals over the course of many years. Vaccinating humans over the

course of many years is not feasible. Therefore, this level of SHM will be challenging to recapitulate through immunization. For a B cell to undergo SHM, it must go into the germinal center where changes are introduced into the BCR. In the germinal center, a B cell acquires AA mutations that can give it higher affinity for antigen and the ability to recognize diverse antigens. We have shown this is possible through immunization in Chapter II and III, as immunization led B cells to acquire mutations that gave them the ability to bind Env with higher affinity and heterologous Env proteins. Further boosting immunizations must cause a B cell to undergo further SHM in a germinal center. Whether or not the level of SHM found in VRC01-class Abs is possible to elicit via vaccination is unknown. However, there is some indication that we can guide the appropriate affinity maturing mutations, as immunizing with the same immunogen repeatedly does not increase the number of mutations, but immunizing with a heterologous immunogen does (Escolano et al., 2016). Testing different adjuvants and multimerization platforms could be used to modulate the duration of the germinal center to increase the opportunity for B cells to participate (Abbott et al., 2018; Lofano et al., 2015). Additionally, there is evidence that bnAbs can develop faster in infants than adult humans (Simonich et al., 2016). Therefore, we may need to consider immunizing humans early in life.

An additional challenge to the success of the germline-targeting strategy in humans will be whether or not bnAbs can be elicited at a sufficient titer and in the right location to provide protection. Animal model challenge studies have shown that low titers of bnAbs delivered intravenously can make it to the site of HIV-1 challenge and provide protection against repeat challenge (Hessell et al., 2009). However, it is not yet known

what titers of bnAbs will need to be present in circulation in humans to provide protection against HIV-1. The mature VRC01 mAb will soon be evaluated via passive infusion in humans in the AMP study. If VRC01 can mediate protection, this study should help us identify the concentration of Ab necessary to provide protection.

Conclusion

The germline-targeting strategy is now being evaluated in human clinical trial. eOD-GT8 has begun a human phase I clinical trial and 426c Core will begin phase I clinical trial in early 2021. Therefore, these results presented here have immediate relevance to human health. The results here inform HIV-1 vaccine design, but can also be applied more broadly to vaccine design as we have identified factors in B cell selection and activation as well as demonstrated the application of a novel immunogen design platform, both of which can be applied to diseases beyond HIV-1.

Acknowledgments

The completion of this thesis would not have been possible without the help of so many people. Thank you to my parents and family for always supporting and loving me. To my friends: thank you for always listening, caring and reminding me to have fun.

Thank you to all of the students in pathobiology graduate program for your support and encouragement throughout my time in the program. Thank you Ernie Lefler the pathobiology program manager. Futhermore, I want to give a huge thanks to the program director, Lee Ann Campbell. Thank you for being available to talk at a moments notice. I'd also like to thank those who served on my thesis committee: Julie McElrath, Jesse Bloom, Rhea Coler, and Justin Taylor.

I would also like to thank all of our collaborators who helped make this work possible: the Veesler lab at the University of Washington, Michael Seaman at Harvard Medical School, Celia LeBranche and David Montefiori at the NIH Vaccine Research Center, Anika Naidu and Po-Ssu Huang from Stanford, and Javier Guenaga and Richard Wyatt from IAVI Neutralizing Antibody Center.

At the Fred Hutch, I would like to thank everyone in the Vaccine and Infectious Disease Division. I have made so many friends while working here and am grateful for all of you. I would also like to thank Comparative Medicine for all of your help managing and caring for the mouse colony. Thank you to the HVTN for all your support using the flow cytometers and cell sorters. I would also like to thank the members of the Office of Scientific Career Development, Karen Peterson and Amber Ismael, for all of your guidance and advice throughout my PhD.

I would like to thank all the current and past members of the Stamatatos lab. Anna MacCamy and Josephine Trichka especially for helping me get my work off the ground and for being fantastic colleagues. I would like to thank Andy McGuire for all of your advice and encouragement. Thank you to Ericka Sjogren and Andrew Stuart for all of your logistical support. I would also like to thank Yu-Ru Lin, who worked with me on the work presented in the Chapter II. Finally, I would like to thank my mentor Dr. Leo Stamatatos. Thank you for being critical of my work, your guidance to make it better and all of your support throughout my time in your lab. Your curiosity and passion for science are an inspiration to me. Thanks for taking a chance on me.

References

Abbott, R.K., Lee, J.H., Menis, S., Skog, P., Rossi, M., Ota, T., Kulp, D.W., Bhullar, D., Kalyuzhniy, O., Havenar-Daughton, C., et al. (2018). Precursor Frequency and Affinity Determine B Cell Competitive Fitness in Germinal Centers, Tested with Germline-Targeting HIV Vaccine Immunogens. Immunity *48*, 133-146.e6.

Adams, P.D., Gopal, K., Grosse-Kunstleve, R.W., Hung, L.-W., Ioerger, T.R., McCoy, A.J., Moriarty, N.W., Pai, R.K., Read, R.J., Romo, T.D., et al. (2004). Recent developments in the PHENIX software for automated crystallographic structure determination. J Synchrotron Radiat *11*, 53–55.

Adams, P.D., Afonine, P.V., Bunkóczi, G., Chen, V.B., Davis, I.W., Echols, N., Headd, J.J., Hung, L.-W., Kapral, G.J., Grosse-Kunstleve, R.W., et al. (2010). PHENIX: a comprehensive Python-based system for macromolecular structure solution. Acta Crystallogr D Biol Crystallogr *66*, 213–221.

Arnaout, R., Lee, W., Cahill, P., Honan, T., Sparrow, T., Weiand, M., Nusbaum, C., Rajewsky, K., and Koralov, S.B. (2011). High-resolution description of antibody heavy-chain repertoires in humans. PLoS ONE *6*, e22365.

Arrildt, K.T., Joseph, S.B., and Swanstrom, R. (2012). The HIV-1 Env Protein: A Coat of Many Colors. Curr HIV/AIDS Rep *9*, 52–63.

Baba, T.W., Liska, V., Hofmann-Lehmann, R., Vlasak, J., Xu, W., Ayehunie, S., Cavacini, L.A., Posner, M.R., Katinger, H., Stiegler, G., et al. (2000). Human neutralizing monoclonal antibodies of the IgG1 subtype protect against mucosal simian–human immunodeficiency virus infection. Nat Med *6*, 200–206.

Balazs, A.B., Ouyang, Y., Hong, C.M., Chen, J., Nguyen, S.M., Rao, D.S., An, D.S., and Baltimore, D. (2014). Vectored immunoprophylaxis protects humanized mice from mucosal HIV transmission. Nat. Med. *20*, 296–300.

Bancroft, T., DeBuysscher, B.L., Weidle, C., Schwartz, A., Wall, A., Gray, M.D., Feng, J., Steach, H.R., Fitzpatrick, K.S., Gewe, M.M., et al. (2019). Detection and activation of HIV broadly neutralizing antibody precursor B cells using anti-idiotypes. J Exp Med *216*, 2331–2347.

Bar, K.J., Sneller, M.C., Harrison, L.J., Justement, J.S., Overton, E.T., Petrone, M.E., Salantes, D.B., Seamon, C.A., Scheinfeld, B., Kwan, R.W., et al. (2016). Effect of HIV Antibody VRC01 on Viral Rebound after Treatment Interruption.

Barbas, C., Collet, T., Amberg, W., Roben, P., Binley, J., Hoekstra, D., Cababa, D., Jones, T., Williamson, R., and Pilkington (1993). Molecular Profile of an Antibody Response to HIV-1 as Probed by Combinatorial Libraries.

Bar-On, Y., Gruell, H., Schoofs, T., Pai, J.A., Nogueira, L., Butler, A.L., Millard, K., Lehmann, C., Suárez, I., Oliveira, T.Y., et al. (2018). Safety and anti-viral activity of combination HIV-1 broadly neutralizing antibodies in viremic individuals. Nat Med *24*, 1701–1707.

Barré-Sinoussi, F., Chermann, J., Rey, F., Nugeyre, M., Chamaret, S., Gruest, S., Dauguet, C., Axler-Blin, C., Vézinet-Brun, F., Rouzioux, C., et al. (1983). Isolation of a T-lymphotropic Retrovirus From a Patient at Risk for Acquired Immune Deficiency Syndrome (AIDS).

Bern, M., Kil, Y.J., and Becker, C. (2012). Byonic: advanced peptide and protein identification software. Curr Protoc Bioinformatics *Chapter 13*, Unit13.20.

Bonsignori, M., Hwang, K.-K., Chen, X., Tsao, C.-Y., Morris, L., Gray, E., Marshall, D.J., Crump, J.A., Kapiga, S.H., Sam, N.E., et al. (2011). Analysis of a Clonal Lineage of HIV-1 Envelope V2/V3 Conformational Epitope-Specific Broadly Neutralizing Antibodies and Their Inferred Unmutated Common Ancestors ▽. J Virol *85*, 9998–10009.

Bonsignori, M., Wiehe, K., Grimm, S.K., Lynch, R., Yang, G., Kozink, D.M., Perrin, F., Cooper, A.J., Hwang, K.-K., Chen, X., et al. (2014). An autoreactive antibody from an SLE/HIV-1 individual broadly neutralizes HIV-1. J Clin Invest *124*, 1835–1843.

Bonsignori, M., Kreider, E.F., Fera, D., Meyerhoff, R.R., Bradley, T., Wiehe, K., Alam, S.M., Aussedat, B., Walkowicz, W.E., Hwang, K.-K., et al. (2017). Staged induction of HIV-1 glycan–dependent broadly neutralizing antibodies. Sci Transl Med *9*.

Bonsignori, M., Scott, E., Wiehe, K., Easterhoff, D., Alam, S.M., Hwang, K.-K., Cooper, M., Xia, S.-M., Zhang, R., Montefiori, D.C., et al. (2018). Inference of the HIV-1 VRC01 Antibody Lineage Unmutated Common Ancestor Reveals Alternative Pathways to Overcome a Key Glycan Barrier. Immunity *49*, 1162-1174.e8.

Borrow, P., Lewicki, H., Hahn, B.H., Shaw, G.M., and Oldstone, M.B. (1994). Virus-specific CD8+ cytotoxic T-lymphocyte activity associated with control of viremia in primary human immunodeficiency virus type 1 infection. J Virol *68*, 6103–6110.

Borst, A.J., Weidle, C.E., Gray, M.D., Frenz, B., Snijder, J., Joyce, M.G., Georgiev, I.S., Stewart-Jones, G.B., Kwong, P.D., McGuire, A.T., et al. (2018). Germline VRC01 antibody recognition of a modified clade C HIV-1 envelope trimer and a glycosylated HIV-1 gp120 core. Elife *7*, e37688.

Briney, B., Sok, D., Jardine, J.G., Kulp, D.W., Skog, P., Menis, S., Jacak, R., Kalyuzhniy, O., de Val, N., Sesterhenn, F., et al. (2016). Tailored Immunogens Direct Affinity Maturation toward HIV Neutralizing Antibodies. Cell *166*, 1459-1470.e11.

Brochet, X., Lefranc, M.-P., and Giudicelli, V. (2008). IMGT/V-QUEST: the highly customized and integrated system for IG and TR standardized V-J and V-D-J sequence analysis. Nucleic Acids Res. *36*, W503-508.

Buchacher, A., Predl, R., Strutzenberger, K., Steinfellner, W., Trkola, A., Purtscher, M., Gruber, G., Tauer, C., Steindl, F., Jungbauer, A., et al. (1994). Generation of Human Monoclonal Antibodies against HIV-1 Proteins; Electrofusion and Epstein-Barr Virus Transformation for Peripheral Blood Lymphocyte Immortalization. AIDS Research and Human Retroviruses *10*, 359–369.

Burton, D.R., and Hangartner, L. (2016). Broadly Neutralizing Antibodies to HIV and Their Role in Vaccine Design. Annual Review of Immunology *34*, 635–659.

Caskey, M., Klein, F., Lorenzi, J.C.C., Seaman, M.S., West, A.P., Buckley, N., Kremer, G., Nogueira, L., Braunschweig, M., Scheid, J.F., et al. (2015). 3BNC117 a Broadly Neutralizing Antibody Suppresses Viremia in HIV-1-Infected Humans. Nature *522*, 487–491.

Caskey, M., Schoofs, T., Gruell, H., Settler, A., Karagounis, T., Kreider, E.F., Murrell, B., Pfeifer, N., Nogueira, L., Oliveira, T.Y., et al. (2017). Antibody 10-1074 suppresses viremia in HIV-1-infected individuals. Nat Med *23*, 185–191.

Charif, and Lobry (2007). Seqin{R} 1.0-2: a contributed package to the {R} project for statistical computing devoted to biological sequences retrieval and analysis. In Structural Approaches to Sequence Evolution: Molecules, Networks, Populations, (Springer Verlag), pp. 207–232.

Chen, F., Tzarum, N., Wilson, I.A., and Law, M. (2019). VH1-69 antiviral broadly neutralizing antibodies: genetics, structures, and relevance to rational vaccine design. Curr Opin Virol *34*, 149–159.

Cohen, K., Altfeld, M., Alter, G., and Stamatatos, L. (2014). Early Preservation of CXCR5+ PD-1+ Helper T Cells and B Cell Activation Predict the Breadth of Neutralizing Antibody Responses in Chronic HIV-1 Infection. J Virol *88*, 13310–13321.

Collaborative Computation Project, Number 4 (1994). The CCP4 Suite: Programs for Protein Crystallography (Acta Crystallogr D Biol Crystallogr).

Corti, D., Langedijk, J.P.M., Hinz, A., Seaman, M.S., Vanzetta, F., Fernandez-Rodriguez, B.M., Silacci, C., Pinna, D., Jarrossay, D., Balla-Jhagjhoorsingh, S., et al. (2010a). Analysis of Memory B Cell Responses and Isolation of Novel Monoclonal Antibodies with Neutralizing Breadth from HIV-1-Infected Individuals. PLoS One *5*.

Corti, D., Suguitan, A.L., Pinna, D., Silacci, C., Fernandez-Rodriguez, B.M., Vanzetta, F., Santos, C., Luke, C.J., Torres-Velez, F.J., Temperton, N.J., et al. (2010b). Heterosubtypic neutralizing antibodies are produced by individuals immunized with a seasonal influenza vaccine. J Clin Invest *120*, 1663–1673.

Crooks, G.E., Hong, G., Chandonia, J.-M., and Brenner, S.E. (2004). WebLogo: A Sequence Logo Generator. Genome Research *14*, 1188–1190.

Crowe, S., Mills, J., and McGrath, M. (1987). Quantitative Immunocytofluorographic Analysis of CD4 Surface Antigen Expression and HIV Infection of Human Peripheral Blood Monocyte/Macrophages.

Dal Porto, J.M., Haberman, A.M., Kelsoe, G., and Shlomchik, M.J. (2002). Very Low Affinity B Cells Form Germinal Centers, Become Memory B Cells, and Participate in Secondary Immune Responses When Higher Affinity Competition Is Reduced. J Exp Med *195*, 1215–1221.

Decroly, E., Vandenbranden, M., Ruysschaert, J.M., Cogniaux, J., Jacob, G.S., Howard, S.C., Marshall, G., Kompelli, A., Basak, A., and Jean, F. (1994). The convertases furin and PC1 can both cleave the human immunodeficiency virus (HIV)-1 envelope glycoprotein gp160 into gp120 (HIV-1 SU) and gp41 (HIV-I TM). J. Biol. Chem. *269*, 12240–12247.

Deeks, S.G., Overbaugh, J., Phillips, A., and Buchbinder, S. (2015). HIV infection. Nat Rev Dis Primers *1*, 1–22.

DeKosky, B.J., Kojima, T., Rodin, A., Charab, W., Ippolito, G.C., Ellington, A.D., and Georgiou, G. (2015). In-depth determination and analysis of the human paired heavy- and light-chain antibody repertoire. Nat. Med. *21*, 86–91.

Deng, H., Liu, R., Ellmeier, W., Choe, S., Unutmaz, D., Burkhart, M., Marzio, P.D., Marmon, S., Sutton, R.E., Hill, C.M., et al. (1996). Identification of a major co-receptor for primary isolates of HIV-1. Nature *381*, 661–666.

Diskin, R., Scheid, J.F., Marcovecchio, P.M., West, A.P., Klein, F., Gao, H., Gnanapragasam, P.N.P., Abadir, A., Seaman, M.S., Nussenzweig, M.C., et al. (2011). Increasing the Potency and Breadth of an HIV Antibody by using Structure-Based Rational Design. Science *334*, 1289–1293.

Doria-Rose, N.A., Klein, R.M., Daniels, M.G., O'Dell, S., Nason, M., Lapedes, A., Bhattacharya, T., Migueles, S.A., Wyatt, R.T., Korber, B.T., et al. (2010). Breadth of Human Immunodeficiency Virus-Specific Neutralizing Activity in Sera: Clustering Analysis and Association with Clinical Variables. J. Virol. *84*, 1631–1636.

Doria-Rose, N.A., Schramm, C.A., Gorman, J., Moore, P.L., Bhiman, J.N., DeKosky, B.J., Ernandes, M.J., Georgiev, I.S., Kim, H.J., Pancera, M., et al. (2014). Developmental pathway for potent V1V2-directed HIV-neutralizing antibodies. Nature *509*, 55–62.

Doria-Rose, N.A., Bhiman, J.N., Roark, R.S., Schramm, C.A., Gorman, J., Chuang, G.-Y., Pancera, M., Cale, E.M., Ernandes, M.J., Louder, M.K., et al. (2015). New Member of the V1V2-Directed CAP256-VRC26 Lineage That Shows Increased Breadth and Exceptional Potency. J Virol *90*, 76–91.

Dosenovic, P., von Boehmer, L., Escolano, A., Jardine, J., Freund, N.T., Gitlin, A.D., McGuire, A.T., Kulp, D.W., Oliveira, T., Scharf, L., et al. (2015). Immunization for HIV-1 Broadly Neutralizing Antibodies in Human Ig Knockin Mice. Cell *161*, 1505–1515.

Dosenovic, P., Kara, E.E., Pettersson, A.-K., McGuire, A.T., Gray, M., Hartweger, H., Thientosapol, E.S., Stamatatos, L., and Nussenzweig, M.C. (2018). Anti–HIV-1 B cell responses are dependent on B cell precursor frequency and antigen-binding affinity. PNAS *115*, 4743–4748.

Dragic, T., Litwin, V., Allaway, G.P., Martin, S.R., Huang, Y., Nagashima, K.A., Cayanan, C., Maddon, P.J., Koup, R.A., Moore, J.P., et al. (1996). HIV-1 entry into CD4+ cells is mediated by the chemokine receptor CC-CKR-5. Nature *381*, 667–673.

Duan, H., Chen, X., Boyington, J.C., Cheng, C., Zhang, Y., Jafari, A.J., Stephens, T., Tsybovsky, Y., Kalyuzhniy, O., Zhao, P., et al. (2018). Glycan-Masking Focuses Immune Responses to the HIV-1 CD4-Binding Site and Enhances Elicitation of VRC01-Class Precursor Antibodies. Immunity *49*, 301-311.e5.

Ekiert, D.C., Friesen, R.H.E., Bhabha, G., Kwaks, T., Jongeneelen, M., Yu, W., Ophorst, C., Cox, F., Korse, H.J.W.M., Brandenburg, B., et al. (2011). A Highly Conserved Neutralizing Epitope on Group 2 Influenza A Viruses. Science *333*, 843–850.

Emsley, P., and Cowtan, K. (2004). Coot: model-building tools for molecular graphics. Acta Crystallogr. D Biol. Crystallogr. *60*, 2126–2132.

Escolano, A., Steichen, J.M., Dosenovic, P., Kulp, D.W., Golijanin, J., Sok, D., Freund, N.T., Gitlin, A.D., Oliveira, T., Araki, T., et al. (2016). Sequential Immunization Elicits Broadly Neutralizing Anti-HIV-1 Antibodies in Ig Knockin Mice. Cell *166*, 1445-1458.e12.

Escolano, A., Gristick, H.B., Abernathy, M.E., Merkenschlager, J., Gautam, R., Oliveira, T.Y., Pai, J., West, A.P., Barnes, C.O., Cohen, A.A., et al. (2019). Immunization expands B cells specific to HIV-1 V3 glycan in mice and macaques. Nature *570*, 468–473.

Falkowska, E., Le, K.M., Ramos, A., Doores, K.J., Lee, J.H., Blattner, C., Ramirez, A., Derking, R., van Gils, M.J., Liang, C.-H., et al. (2014). Broadly neutralizing HIV antibodies define a glycan-dependent epitope on the pre-fusion conformation of the gp41 protein on cleaved Envelope trimers. Immunity *40*, 657–668.

Feng, Y., Broder, C.C., Kennedy, P.E., and Berger, E.A. (1996). HIV-1 Entry Cofactor: Functional cDNA Cloning of a Seven-Transmembrane, G Protein-Coupled Receptor. Science *272*, 872–877.

Flynn, N., Forthal, D., Harro, C., Judson, F., Mayer, F., and Para (2005). Placebo-controlled Phase 3 Trial of a Recombinant Glycoprotein 120 Vaccine to Prevent HIV-1 Infection.

Frese, C.K., Zhou, H., Taus, T., Altelaar, A.F.M., Mechtler, K., Heck, A.J.R., and Mohammed, S. (2013). Unambiguous phosphosite localization using electron-transfer/higher-energy collision dissociation (EThcD). J. Proteome Res. *12*, 1520–1525.

Freund, N.T., Horwitz, J.A., Nogueira, L., Sievers, S.A., Scharf, L., Scheid, J.F., Gazumyan, A., Liu, C., Velinzon, K., Goldenthal, A., et al. (2015). A New Glycan-Dependent CD4-Binding Site Neutralizing Antibody Exerts Pressure on HIV-1 In Vivo. PLoS Pathog. *11*, e1005238.

Frost, S.D.W., Wrin, T., Smith, D.M., Pond, S.L.K., Liu, Y., Paxinos, E., Chappey, C., Galovich, J., Beauchaine, J., Petropoulos, C.J., et al. (2005). Neutralizing antibody responses drive the evolution of human immunodeficiency virus type 1 envelope during recent HIV infection. Proc Natl Acad Sci U S A *102*, 18514–18519.

Gallo, R.C., Sarin, P.S., Gelmann, E.P., Robert-Guroff, M., Richardson, E., Kalyanaraman, V.S., Mann, D., Sidhu, G.D., Stahl, R.E., Zolla-Pazner, S., et al. (1983). Isolation of human T-cell leukemia virus in acquired immune deficiency syndrome (AIDS). Science *220*, 865–867.

Gautam, R., Nishimura, Y., Pegu, A., Nason, M.C., Klein, F., Gazumyan, A., Golijanin, J., Buckler-White, A., Sadjadpour, R., Wang, K., et al. (2016). A single injection of anti-HIV-1 antibodies protects against repeated SHIV challenges. Nature *533*, 105–109.

Georgiev, I.S., Doria-Rose, N.A., Zhou, T., Kwon, Y.D., Staupe, R.P., Moquin, S., Chuang, G.-Y., Louder, M.K., Schmidt, S.D., Altae-Tran, H.R., et al. (2013). Delineating Antibody Recognition in Polyclonal Sera from Patterns of HIV-1 Isolate Neutralization. Science *340*, 751–756.

van Gils, M.J., van den Kerkhof, T.L.G.M., Ozorowski, G., Cottrell, C.A., Sok, D., Pauthner, M., Pallesen, J., de Val, N., Yasmeen, A., de Taeye, S.W., et al. (2016). An HIV-1 antibody from an elite neutralizer implicates the fusion peptide as a site of vulnerability. Nat Microbiol *2*, 16199.

Giudicelli, V., Brochet, X., and Lefranc, M.-P. (2011). IMGT/V-QUEST: IMGT Standardized Analysis of the Immunoglobulin (IG) and T Cell Receptor (TR) Nucleotide Sequences. Cold Spring Harbor Protocols *2011*, pdb.prot5633-pdb.prot5633.

Goodman, D.S., Teplitz, E.D., Wishner, A., Klein, R.S., Burk, P.G., and Hershenbaum, E. (1987). Prevalence of cutaneous disease in patients with acquired immunodeficiency syndrome (AIDS) or AIDS-related complex. Journal of the American Academy of Dermatology *17*, 210–220.

Gottlieb, M., Schroff, R., Schanker, H., Weisman, J., Fan, P., Wolf, R., and Saxon, A. (1981). Pneumocystis Carinii Pneumonia and Mucosal Candidiasis in Previously Healthy Homosexual Men: Evidence of a New Acquired Cellular Immunodeficiency.

Graham, B.S., Koup, R.A., Roederer, M., Bailer, R.T., Enama, M.E., Moodie, Z., Martin, J.E., McCluskey, M.M., Chakrabarti, B.K., Lamoreaux, L., et al. (2006). Phase 1 Safety and Immunogenicity Evaluation of a Multiclade HIV-1 DNA Candidate Vaccine. J Infect Dis *194*, 1650–1660.

Gray, E.S., Madiga, M.C., Hermanus, T., Moore, P.L., Wibmer, C.K., Tumba, N.L., Werner, L., Mlisana, K., Sibeko, S., Williamson, C., et al. (2011). The Neutralization Breadth of HIV-1 Develops Incrementally over Four Years and Is Associated with CD4+ T Cell Decline and High Viral Load during Acute Infection ▽. J Virol *85*, 4828–4840.

Gristick, H.B., von Boehmer, L., West, A.P., Schamber, M., Gazumyan, A., Golijanin, J., Seaman, M.S., Fätkenheuer, G., Klein, F., Nussenzweig, M.C., et al. (2016). Natively glycosylated HIV-1 Env structure reveals new mode for antibody recognition of the CD4-binding site. Nat Struct Mol Biol *23*, 906–915.

Havenar-Daughton, C., Sarkar, A., Kulp, D.W., Toy, L., Hu, X., Deresa, I., Kalyuzhniy, O., Kaushik, K., Upadhyay, A.A., Menis, S., et al. (2018). The human naive B cell repertoire contains distinct subclasses for a germline-targeting HIV-1 vaccine immunogen. Sci Transl Med *10*, eaat0381.

Haynes, B.F., Gilbert, P.B., McElrath, M.J., Zolla-Pazner, S., Tomaras, G.D., Alam, S.M., Evans, D.T., Montefiori, D.C., Karnasuta, C., Sutthent, R., et al. (2012). Immune-Correlates Analysis of an HIV-1 Vaccine Efficacy Trial. N Engl J Med *366*, 1275–1286.

He, J., Chen, Y., Farzan, M., Choe, H., Ohagen, A., Gartner, S., Busciglio, J., Yang, X., Hofmann, W., Newman, W., et al. (1997). CCR3 and CCR5 are co-receptors for HIV-1 infection of microglia. Nature *385*, 645–649.

Hessell, A.J., Poignard, P., Hunter, M., Hangartner, L., Tehrani, D.M., Bleeker, W.K., Parren, P.W.H.I., Marx, P.A., and Burton, D.R. (2009). Effective, low-titer antibody protection against low-dose repeated mucosal SHIV challenge in macaques. Nat. Med. *15*, 951–954.

Hessell, A.J., Rakasz, E.G., Tehrani, D.M., Huber, M., Weisgrau, K.L., Landucci, G., Forthal, D.N., Koff, W.C., Poignard, P., Watkins, D.I., et al. (2010). Broadly neutralizing monoclonal antibodies 2F5 and 4E10 directed against the human immunodeficiency virus type 1 gp41 membrane-proximal external region protect against mucosal challenge by simian-human immunodeficiency virus SHIVBa-L. J. Virol. *84*, 1302–1313.

Hofmeyer, T., Schmelz, S., Degiacomi, M.T., Dal Peraro, M., Daneschdar, M., Scrima, A., van den Heuvel, J., Heinz, D.W., and Kolmar, H. (2013). Arranged sevenfold: structural insights into the C-terminal oligomerization domain of human C4b-binding protein. J. Mol. Biol. *425*, 1302–1317.

Hoot, S., McGuire, A.T., Cohen, K.W., Strong, R.K., Hangartner, L., Klein, F., Diskin, R., Scheid, J.F., Sather, D.N., Burton, D.R., et al. (2013). Recombinant HIV envelope proteins fail to engage germline versions of anti-CD4bs bNAbs. PLoS Pathog. *9*, e1003106.

Hraber, P., Seaman, M.S., Bailer, R.T., Mascola, J.R., Montefiori, D.C., and Korber, B.T. (2014). Prevalence of broadly neutralizing antibody responses during chronic HIV-1 infection. AIDS *28*, 163–169.

Huang, J., Ofek, G., Laub, L., Louder, M.K., Doria-Rose, N.A., Longo, N.S., Imamichi, H., Bailer, R.T., Chakrabarti, B., Sharma, S.K., et al. (2012). Broad and potent neutralization of HIV-1 by a gp41-specific human antibody. Nature *491*, 406–412.

Huang, J., Kang, B.H., Pancera, M., Lee, J.H., Tong, T., Feng, Y., Georgiev, I.S., Chuang, G.-Y., Druz, A., Doria-Rose, N.A., et al. (2014). Broad and potent HIV-1 neutralization by a human antibody that binds the gp41-120 interface. Nature *515*, 138–142.

Huang, J., Kang, B.H., Ishida, E., Zhou, T., Griesman, T., Sheng, Z., Wu, F., Doria-Rose, N.A., Zhang, B., McKee, K., et al. (2016). Identification of a CD4-Binding-Site Antibody to HIV that Evolved Near-Pan Neutralization Breadth. Immunity *45*, 1108–1121.

Huang, P.-S., Ban, Y.-E.A., Richter, F., Andre, I., Vernon, R., Schief, W.R., and Baker, D. (2011). RosettaRemodel: A Generalized Framework for Flexible Backbone Protein Design. PLOS ONE *6*, e24109.

Hübner, A., Kruhoffer, M., Grosse, F., and Krauss, G. (1992). Fidelity of Human Immunodeficiency Virus Type I Reverse Transcriptase in Copying Natural RNA.

Jardine, J., Julien, J.-P., Menis, S., Ota, T., Kalyuzhniy, O., McGuire, A., Sok, D., Huang, P.-S., MacPherson, S., Jones, M., et al. (2013). Rational HIV immunogen design to target specific germline B cell receptors. Science *340*, 711–716.

Jardine, J.G., Ota, T., Sok, D., Pauthner, M., Kulp, D.W., Kalyuzhniy, O., Skog, P.D., Thinnes, T.C., Bhullar, D., Briney, B., et al. (2015). Priming a broadly neutralizing antibody response to HIV-1 using a germline-targeting immunogen. Science *349*, 156–161.

Jardine, J.G., Kulp, D.W., Havenar-Daughton, C., Sarkar, A., Briney, B., Sok, D., Sesterhenn, F., Ereño-Orbea, J., Kalyuzhniy, O., Deresa, I., et al. (2016). HIV-1 broadly neutralizing antibody precursor B cells revealed by germline-targeting immunogen. Science *351*, 1458–1463.

Ji, Y., and Lu, H. (2017). Malignancies in HIV-Infected and AIDS Patients. In Infectious Agents Associated Cancers: Epidemiology and Molecular Biology, Q. Cai, Z. Yuan, and K. Lan, eds. (Singapore: Springer Singapore), pp. 167–179.

Joyce, M.G., Georgiev, I.S., Yang, Y., Druz, A., Geng, H., Chuang, G.-Y., Kwon, Y.D., Pancera, M., Rawi, R., Sastry, M., et al. (2017). Soluble Prefusion Closed DS-SOSIP.664-Env Trimers of Diverse HIV-1 Strains. Cell Rep *21*, 2992–3002.

Julg, B., Tartaglia, L.J., Keele, B.F., Wagh, K., Pegu, A., Sok, D., Abbink, P., Schmidt, S.D., Wang, K., Chen, X., et al. (2017). Broadly neutralizing antibodies targeting the HIV-1 envelope V2 apex confer robust protection against a clade C SHIV challenge. Sci Transl Med *9*.

Kimanius, D., Forsberg, B.O., Scheres, S.H., and Lindahl, E. (2016). Accelerated cryo-EM structure determination with parallelisation using GPUs in RELION-2. Elife *5*, e18722.

Klatzmann, D., Champagne, E., Chamaret, S., Gruest, J., Guetard, D., Hercend, T., Gluckman, J.-C., and Montagnier, L. (1984). T-lymphocyte T4 molecule behaves as the receptor for human retrovirus LAV. Nature *312*, 767–768.

Klein, F., Gaebler, C., Mouquet, H., Sather, D.N., Lehmann, C., Scheid, J.F., Kraft, Z., Liu, Y., Pietzsch, J., Hurley, A., et al. (2012a). Broad neutralization by a combination of antibodies recognizing the CD4 binding site and a new conformational epitope on the HIV-1 envelope protein. J Exp Med *209*, 1469–1479.

Klein, F., Halper-Stromberg, A., Horwitz, J.A., Gruell, H., Scheid, J.F., Bournazos, S., Mouquet, H., Spatz, L.A., Diskin, R., Abadir, A., et al. (2012b). HIV therapy by a combination of broadly neutralizing antibodies in humanized mice. Nature *492*, 118–122.

Kong, L., Ju, B., Chen, Y., He, L., Ren, L., Liu, J., Hong, K., Su, B., Wang, Z., Ozorowski, G., et al. (2016a). Key gp120 glycans pose roadblocks to the rapid development of VRC01-class antibodies within an HIV-1-infected Chinese donor. Immunity *44*, 939–950.

Kong, R., Xu, K., Zhou, T., Acharya, P., Lemmin, T., Liu, K., Ozorowski, G., Soto, C., Taft, J.D., Bailer, R.T., et al. (2016b). Fusion peptide of HIV-1 as a site of vulnerability to neutralizing antibody. Science *352*, 828–833.

Koup, R.A., Safrit, J.T., Cao, Y., Andrews, C.A., McLeod, G., Borkowsky, W., Farthing, C., and Ho, D.D. (1994). Temporal association of cellular immune responses with the initial control of viremia in primary human immunodeficiency virus type 1 syndrome. J Virol *68*, 4650–4655.

Kouskoff, V., Famiglietti, S., Lacaud, G., Lang, P., Rider, J.E., Kay, B.K., Cambier, J.C., and Nemazee, D. (1998). Antigens Varying in Affinity for the B Cell Receptor Induce Differential B Lymphocyte Responses. J Exp Med *188*, 1453–1464.

Kwong, P.D., and Mascola, J.R. (2012). Human Antibodies that Neutralize HIV-1: Identification, Structures, and B Cell Ontogenies. Immunity *37*, 412–425.

Kwong, P.D., and Mascola, J.R. (2018). HIV-1 Vaccines Based on Antibody Identification, B Cell Ontogeny, and Epitope Structure. Immunity *48*, 855–871.

LaBranche, C.C., McGuire, A.T., Gray, M.D., Behrens, S., Kwong, P.D., Chen, X., Zhou, T., Sattentau, Q.J., Peacock, J., Eaton, A., et al. (2018). HIV-1 envelope glycan modifications that permit neutralization by germline-reverted VRC01-class broadly neutralizing antibodies. PLoS Pathog. *14*, e1007431.

Landais, E., Huang, X., Havenar-Daughton, C., Murrell, B., Price, M.A., Wickramasinghe, L., Ramos, A., Bian, C.B., Simek, M., Allen, S., et al. (2016). Broadly Neutralizing Antibody Responses in a Large Longitudinal Sub-Saharan HIV Primary Infection Cohort. PLoS Pathog. *12*, e1005369.

Lander, G.C., Stagg, S.M., Voss, N.R., Cheng, A., Fellmann, D., Pulokas, J., Yoshioka, C., Irving, C., Mulder, A., Lau, P.-W., et al. (2009). Appion: an integrated, database-driven pipeline to facilitate EM image processing. J. Struct. Biol. *166*, 95–102.

Lau, K.A., and Wong, J.J.L. (2013). Current Trends of HIV Recombination Worldwide. Infect Dis Rep *5*.

Lee, E.-C., Liang, Q., Ali, H., Bayliss, L., Beasley, A., Bloomfield-Gerdes, T., Bonoli, L., Brown, R., Campbell, J., Carpenter, A., et al. (2014). Complete humanization of the mouse immunoglobulin loci enables efficient therapeutic antibody discovery. Nat Biotechnol *32*, 356–363.

Liao, H.-X., Lynch, R., Zhou, T., Gao, F., Alam, S.M., Boyd, S.D., Fire, A.Z., Roskin, K.M., Schramm, C.A., Zhang, Z., et al. (2013). Co-evolution of a broadly neutralizing HIV-1 antibody and founder virus. Nature *496*, 469–476.

Locci, M., Havenar-Daughton, C., Landais, E., Wu, J., Kroenke, M.A., Arlehamn, C.L., Su, L.F., Cubas, R., Davis, M.M., Sette, A., et al. (2013). Human Circulating PD-1+CXCR3−CXCR5+ Memory Tfh Cells Are Highly Functional and Correlate with Broadly Neutralizing HIV Antibody Responses. Immunity *39*, 758–769.

Lofano, G., Mancini, F., Salvatore, G., Cantisani, R., Monaci, E., Carrisi, C., Tavarini, S., Sammicheli, C., Paccani, S.R., Soldaini, E., et al. (2015). Oil-in-Water Emulsion MF59 Increases Germinal Center B Cell Differentiation and Persistence in Response to Vaccination. The Journal of Immunology *195*, 1617–1627.

Ludtke, S.J., Baldwin, P.R., and Chiu, W. (1999). EMAN: semiautomated software for high-resolution single-particle reconstructions. J. Struct. Biol. *128*, 82–97.

Lynch, R.M., Wong, P., Tran, L., O'Dell, S., Nason, M.C., Li, Y., Wu, X., and Mascola, J.R. (2015a). HIV-1 fitness cost associated with escape from the VRC01 class of CD4 binding site neutralizing antibodies. J. Virol. *89*, 4201–4213.

Lynch, R.M., Boritz, E., Coates, E.E., DeZure, A., Madden, P., Costner, P., Enama, M.E., Plummer, S., Holman, L., Hendel, C.S., et al. (2015b). Virologic effects of broadly neutralizing antibody VRC01 administration during chronic HIV-1 infection. Science Translational Medicine *7*, 319ra206-319ra206.

MacLean, B., Tomazela, D.M., Shulman, N., Chambers, M., Finney, G.L., Frewen, B., Kern, R., Tabb, D.L., Liebler, D.C., and MacCoss, M.J. (2010). Skyline: an open source document editor for creating and analyzing targeted proteomics experiments. Bioinformatics *26*, 966–968.

Mascola, J.R., Lewis, M.G., Stiegler, G., Harris, D., VanCott, T.C., Hayes, D., Louder, M.K., Brown, C.R., Sapan, C.V., Frankel, S.S., et al. (1999). Protection of Macaques against Pathogenic Simian/Human Immunodeficiency Virus 89.6PD by Passive Transfer of Neutralizing Antibodies. J Virol *73*, 4009–4018.

Mascola, J.R., Stiegler, G., VanCott, T.C., Katinger, H., Carpenter, C.B., Hanson, C.E., Beary, H., Hayes, D., Frankel, S.S., Birx, D.L., et al. (2000). Protection of macaques against vaginal transmission of a pathogenic HIV-1/SIV chimeric virus by passive infusion of neutralizing antibodies. Nat Med *6*, 207–210.

McElrath, M.J., De Rosa, S.C., Moodie, Z., Dubey, S., Kierstead, L., Janes, H., Defawe, O.D., Carter, D.K., Hural, J., Akondy, R., et al. (2008). HIV-1 vaccine-induced immunity in the test-of-concept Step Study: a case–cohort analysis. The Lancet *372*, 1894–1905.

McGuire, A.T., Hoot, S., Dreyer, A.M., Lippy, A., Stuart, A., Cohen, K.W., Jardine, J., Menis, S., Scheid, J.F., West, A.P., et al. (2013). Engineering HIV envelope protein to activate germline B cell receptors of broadly neutralizing anti-CD4 binding site antibodies. J. Exp. Med. *210*, 655–663.

McGuire, A.T., Dreyer, A.M., Carbonetti, S., Lippy, A., Glenn, J., Scheid, J.F., Mouquet, H., and Stamatatos, L. (2014a). HIV antibodies. Antigen modification regulates competition of broad and narrow neutralizing HIV antibodies. Science *346*, 1380–1383.

McGuire, A.T., Glenn, J.A., Lippy, A., and Stamatatos, L. (2014b). Diverse Recombinant HIV-1 Envs Fail To Activate B Cells Expressing the Germline B Cell Receptors of the Broadly Neutralizing Anti-HIV-1 Antibodies PG9 and 447-52D. J Virol *88*, 2645–2657.

McGuire, A.T., Gray, M.D., Dosenovic, P., Gitlin, A.D., Freund, N.T., Petersen, J., Correnti, C., Johnsen, W., Kegel, R., Stuart, A.B., et al. (2016). Specifically modified Env immunogens activate B-cell precursors of broadly neutralizing HIV-1 antibodies in transgenic mice. Nat Commun *7*, 10618.

Medina-Ramírez, M., Garces, F., Escolano, A., Skog, P., de Taeye, S.W., Del Moral-Sanchez, I., McGuire, A.T., Yasmeen, A., Behrens, A.-J., Ozorowski, G., et al. (2017).

Design and crystal structure of a native-like HIV-1 envelope trimer that engages multiple broadly neutralizing antibody precursors in vivo. J. Exp. Med. *214*, 2573–2590.

Mendoza, P., Gruell, H., Nogueira, L., Pai, J.A., Butler, A.L., Millard, K., Lehmann, C., Suárez, I., Oliveira, T.Y., Lorenzi, J.C.C., et al. (2018). Combination therapy with anti-HIV-1 antibodies maintains viral suppression. Nature *561*, 479–484.

Mindell, J.A., and Grigorieff, N. (2003). Accurate determination of local defocus and specimen tilt in electron microscopy. J. Struct. Biol. *142*, 334–347.

Moir, S., Chun, T., and Fauci, A.S. (2011). Pathogenic Mechanisms of HIV Disease.

Moore, P.L., Crooks, E.T., Porter, L., Zhu, P., Cayanan, C.S., Grise, H., Corcoran, P., Zwick, M.B., Franti, M., Morris, L., et al. (2006). Nature of Nonfunctional Envelope Proteins on the Surface of Human Immunodeficiency Virus Type 1. J Virol *80*, 2515–2528.

Morris, L., Chen, X., Alam, M., Tomaras, G., Zhang, R., Marshall, D.J., Chen, B., Parks, R., Foulger, A., Jaeger, F., et al. (2011). Isolation of a Human Anti-HIV gp41 Membrane Proximal Region Neutralizing Antibody by Antigen-Specific Single B Cell Sorting. PLoS One *6*.

Mouquet, H., Scheid, J.F., Zoller, M.J., Krogsgaard, M., Ott, R.G., Shukair, S., Artyomov, M.N., Pietzsch, J., Connors, M., Pereyra, F., et al. (2010). Polyreactivity increases the apparent affinity of anti-HIV antibodies by heteroligation. Nature *467*, 591–595.

Mouquet, H., Scharf, L., Euler, Z., Liu, Y., Eden, C., Scheid, J.F., Halper-Stromberg, A., Gnanapragasam, P.N.P., Spencer, D.I.R., Seaman, M.S., et al. (2012). Complex-type N-glycan recognition by potent broadly neutralizing HIV antibodies. Proc Natl Acad Sci U S A *109*, E3268–E3277.

Murphy, A.J., Macdonald, L.E., Stevens, S., Karow, M., Dore, A.T., Pobursky, K., Huang, T.T., Poueymirou, W.T., Esau, L., Meola, M., et al. (2014). Mice With Megabase Humanization of Their Immunoglobulin Genes Generate Antibodies as Efficiently as Normal Mice.

Nishimura, Y., Igarashi, T., Haigwood, N., Sadjadpour, R., Plishka, R.J., Buckler-White, A., Shibata, R., and Martin, M.A. (2002). Determination of a Statistically Valid Neutralization Titer in Plasma That Confers Protection against Simian-Human Immunodeficiency Virus Challenge following Passive Transfer of High-Titered Neutralizing Antibodies. J Virol *76*, 2123–2130.

Ogun, S.A., Dumon-Seignovert, L., Marchand, J.-B., Holder, A.A., and Hill, F. (2008). The oligomerization domain of C4-binding protein (C4bp) acts as an adjuvant, and the fusion protein comprised of the 19-kilodalton merozoite surface protein 1 fused

with the murine C4bp domain protects mice against malaria. Infect. Immun. *76*, 3817–3823.

Otwinowski, Z., and Minor, W. (1997). Processing of X-ray diffraction data collected in oscillation mode. Meth. Enzymol. *276*, 307–326.

Pages, H., Aboyoun, P., Gentleman, R., and DebRoy, S. (2018). Biostrings: Efficient manipulation of biological strings.

Palmer, C., Balfe, P., Fox, D., May, J.C., Frederiksson, R., Fenyö, E.-M., and Mckeating, J.A. (1996). Functional Characterization of the V1V2 Region of Human Immunodeficiency Virus Type I. Virology *220*, 436–449.

Parks, K.R., MacCamy, A.J., Trichka, J., Gray, M., Weidle, C., Borst, A.J., Khechaduri, A., Takushi, B., Agrawal, P., Guenaga, J., et al. (2019). Overcoming Steric Restrictions of VRC01 HIV-1 Neutralizing Antibodies through Immunization. Cell Rep *29*, 3060-3072.e7.

Parren, P.W.H.I., Marx, P.A., Hessell, A.J., Luckay, A., Harouse, J., Cheng-Mayer, C., Moore, J.P., and Burton, D.R. (2001). Antibody Protects Macaques against Vaginal Challenge with a Pathogenic R5 Simian/Human Immunodeficiency Virus at Serum Levels Giving Complete Neutralization In Vitro. J Virol *75*, 8340–8347.

Parsons, M.S., Lee, W.S., Kristensen, A.B., Amarasena, T., Khoury, G., Wheatley, A.K., Reynaldi, A., Wines, B.D., Hogarth, P.M., Davenport, M.P., et al. (2019). Fc-dependent functions are redundant to efficacy of anti-HIV antibody PGT121 in macaques. J Clin Invest *129*, 182–191.

Pau, A.K., and George, J.M. (2014). Antiretroviral Therapy: Current Drugs. Infect Dis Clin North Am *28*, 371–402.

Pegu, A., Yang, Z., Boyington, J.C., Wu, L., Ko, S.-Y., Schmidt, S.D., McKee, K., Kong, W.-P., Shi, W., Chen, X., et al. (2014). Neutralizing antibodies to HIV-1 envelope protect more effectively in vivo than those to the CD4 receptor. Sci Transl Med *6*, 243ra88.

Pejchal, R., Doores, K.J., Walker, L.M., Khayat, R., Huang, P.-S., Wang, S.-K., Stanfield, R.L., Julien, J.-P., Ramos, A., Crispin, M., et al. (2011). A Potent and Broad Neutralizing Antibody Recognizes and Penetrates the HIV Glycan Shield. Science *334*, 1097–1103.

Phan, T.G., Paus, D., Chan, T.D., Turner, M.L., Nutt, S.L., Basten, A., and Brink, R. (2006). High affinity germinal center B cells are actively selected into the plasma cell compartment. J Exp Med *203*, 2419–2424.

Pitisuttithum, P., Gilbert, P., Gurwith, M., Heyward, W., Martin, M., van Griensven, F., Hu, D., and Tappero, J.W. (2006). Randomized, Double-Blind, Placebo-Controlled Efficacy Trial of a Bivalent Recombinant Glycoprotein 120 HIV-1 Vaccine among Injection Drug Users in Bangkok, Thailand. J Infect Dis *194*, 1661–1671.

Plotkin, S.A., and Plotkin, S.L. (2011). The development of vaccines: how the past led to the future. Nat Rev Microbiol *9*, 889–893.

R Core Team (2018). R: The R Project for Statistical Computing.

Rees, W., Bender, J., Teague, T.K., Kedl, R.M., Crawford, F., Marrack, P., and Kappler, J. (1999). An inverse relationship between T cell receptor affinity and antigen dose during CD4+ T cell responses in vivo and in vitro. Proc Natl Acad Sci U S A *96*, 9781–9786.

Rerks-Ngarm, S., Pitisuttithum, P., Nitayaphan, S., Kaewkungwal, J., Chiu, J., Paris, R., Premsri, N., Namwat, C., de Souza, M., Adams, E., et al. (2009). Vaccination with ALVAC and AIDSVAX to Prevent HIV-1 Infection in Thailand. New England Journal of Medicine *361*, 2209–2220.

Robbiani, D.F., Bozzacco, L., Keeffe, J.R., Khouri, R., Olsen, P.C., Gazumyan, A., Schaefer-Babajew, D., Avila-Rios, S., Nogueira, L., Patel, R., et al. (2017). Recurrent Potent Human Neutralizing Antibodies to Zika Virus in Brazil and Mexico. Cell *169*, 597-609.e11.

Rong, R., Li, B., Lynch, R.M., Haaland, R.E., Murphy, M.K., Mulenga, J., Allen, S.A., Pinter, A., Shaw, G.M., Hunter, E., et al. (2009). Escape from Autologous Neutralizing Antibodies in Acute/Early Subtype C HIV-1 Infection Requires Multiple Pathways. PLoS Pathog *5*.

Rusert, P., Kouyos, R.D., Kadelka, C., Ebner, H., Schanz, M., Huber, M., Braun, D.L., Hozé, N., Scherrer, A., Magnus, C., et al. (2016). Determinants of HIV-1 broadly neutralizing antibody induction. Nat Med *22*, 1260–1267.

Sajadi, M.M., Dashti, A., Tehrani, Z.R., Tolbert, W.D., Seaman, M.S., Ouyang, X., Gohain, N., Pazgier, M., Kim, D., Cavet, G., et al. (2018). Identification of near pan-neutralizing antibodies against HIV-1 by deconvolution of plasma humoral responses. Cell *173*, 1783-1795.e14.

Sangesland, M., Ronsard, L., Kazer, S.W., Bals, J., Boyoglu-Barnum, S., Yousif, A.S., Barnes, R., Feldman, J., Quirindongo-Crespo, M., McTamney, P.M., et al. (2019). Germline-Encoded Affinity for Cognate Antigen Enables Vaccine Amplification of a Human Broadly Neutralizing Response against Influenza Virus. Immunity *51*, 735-749.e8.

Sather, D.N., Armann, J., Ching, L.K., Mavrantoni, A., Sellhorn, G., Caldwell, Z., Yu, X., Wood, B., Self, S., Kalams, S., et al. (2009). Factors Associated with the Development of Cross-Reactive Neutralizing Antibodies during Human Immunodeficiency Virus Type 1 Infection. J Virol *83*, 757–769.

Scharf, L., West, A.P., Sievers, S.A., Chen, C., Jiang, S., Gao, H., Gray, M.D., McGuire, A.T., Scheid, J.F., Nussenzweig, M.C., et al. (2016). Structural basis for germline antibody recognition of HIV-1 immunogens. ELife *5*.

Scheid, J.F., Mouquet, H., Feldhahn, N., Seaman, M.S., Velinzon, K., Pietzsch, J., Ott, R.G., Anthony, R.M., Zebroski, H., Hurley, A., et al. (2009). Broad diversity of neutralizing antibodies isolated from memory B cells in HIV-infected individuals. Nature *458*, 636–640.

Scheid, J.F., Mouquet, H., Ueberheide, B., Diskin, R., Klein, F., Oliveira, T.Y.K., Pietzsch, J., Fenyo, D., Abadir, A., Velinzon, K., et al. (2011). Sequence and Structural Convergence of Broad and Potent HIV Antibodies That Mimic CD4 Binding. Science *333*, 1633–1637.

Scheid, J.F., Horwitz, J.A., Bar-On, Y., Kreider, E.F., Lu, C.-L., Lorenzi, J.C.C., Feldmann, A., Braunschweig, M., Nogueira, L., Oliveira, T., et al. (2016). HIV-1 antibody 3BNC117 suppresses viral rebound in humans during treatment interruption. Nature *535*, 556–560.

Scheres, S.H.W. (2012a). A Bayesian View on Cryo-EM Structure Determination. J Mol Biol *415*, 406–418.

Scheres, S.H.W. (2012b). RELION: Implementation of a Bayesian approach to cryo-EM structure determination. J Struct Biol *180*, 519–530.

Schneider, S.C., Ohmen, J., Fosdick, L., Gladstone, B., Guo, J., Ametani, A., Sercarz, E.E., and Deng, H. (2000). Cutting Edge: Introduction of an Endopeptidase Cleavage Motif into a Determinant Flanking Region of Hen Egg Lysozyme Results in Enhanced T Cell Determinant Display. The Journal of Immunology *165*, 20–23.

Schroeder, H.W., and Cavacini, L. (2010). Structure and Function of Immunoglobulins. J Allergy Clin Immunol *125*, S41–S52.

Schwickert, T.A., Victora, G.D., Fooksman, D.R., Kamphorst, A.O., Mugnier, M.R., Gitlin, A.D., Dustin, M.L., and Nussenzweig, M.C. (2011). A dynamic T cell–limited checkpoint regulates affinity-dependent B cell entry into the germinal center. J Exp Med *208*, 1243–1252.

Sharp, P.M., and Hahn, B.H. (2011). Origins of HIV and the AIDS Pandemic. Cold Spring Harb Perspect Med *1*.

Shibata, R., Igarashi, T., Haigwood, N., Buckler–White, A., Ogert, R., Ross, W., Willey, R., Cho, M.W., and Martin, M.A. (1999). Neutralizing antibody directed against the HIV–1 envelope glycoprotein can completely block HIV–1/SIV chimeric virus infections of macaque monkeys. Nat Med *5*, 204–210.

Shingai, M., Donau, O.K., Plishka, R.J., Buckler-White, A., Mascola, J.R., Nabel, G.J., Nason, M.C., Montefiori, D., Moldt, B., Poignard, P., et al. (2014). Passive transfer of modest titers of potent and broadly neutralizing anti-HIV monoclonal antibodies block SHIV infection in macaques. J. Exp. Med. *211*, 2061–2074.

Siegal, R.W. (2009). Antibody Affinity Optimization Using Yeast Cell Surface Display (Methods Mol Biol).

Silva, M., Nguyen, T.H., Philbrook, P., Chu, M., Sears, O., Hatfield, S., Abbott, R.K., Kelsoe, G., and Sitkovsky, M.V. (2017). Targeted Elimination of Immunodominant B Cells Drives the Germinal Center Reaction toward Subdominant Epitopes. Cell Rep *21*, 3672–3680.

Simek, M.D., Rida, W., Priddy, F.H., Pung, P., Carrow, E., Laufer, D.S., Lehrman, J.K., Boaz, M., Tarragona-Fiol, T., Miiro, G., et al. (2009). Human Immunodeficiency Virus Type 1 Elite Neutralizers: Individuals with Broad and Potent Neutralizing Activity Identified by Using a High-Throughput Neutralization Assay together with an Analytical Selection Algorithm. J Virol *83*, 7337–7348.

Simonich, C.A., Williams, K.L., Verkerke, H.P., Williams, J.A., Nduati, R., Lee, K.K., and Overbaugh, J. (2016). HIV-1 Neutralizing Antibodies with Limited Hypermutation from an Infant. Cell *166*, 77–87.

Snijder, J., Ortego, M.S., Weidle, C., Stuart, A.B., Gray, M.D., McElrath, M.J., Pancera, M., Veesler, D., and McGuire, A.T. (2018). An Antibody Targeting the Fusion Machinery Neutralizes Dual-Tropic Infection and Defines a Site of Vulnerability on Epstein-Barr Virus. Immunity *48*, 799-811.e9.

Sok, D., van Gils, M.J., Pauthner, M., Julien, J.-P., Saye-Francisco, K.L., Hsueh, J., Briney, B., Lee, J.H., Le, K.M., Lee, P.S., et al. (2014). Recombinant HIV envelope trimer selects for quaternary-dependent antibodies targeting the trimer apex. Proc Natl Acad Sci U S A *111*, 17624–17629.

Sok, D., Briney, B., Jardine, J.G., Kulp, D.W., Menis, S., Pauthner, M., Wood, A., Lee, E.-C., Le, K.M., Jones, M., et al. (2016). Priming HIV-1 broadly neutralizing antibody precursors in human Ig loci transgenic mice. Science *353*, 1557–1560.

Stanfield, R.L., and Wilson, I.A. (2014). Antibody Structure. Microbiology Spectrum *2*.

Steichen, J.M., Kulp, D.W., Tokatlian, T., Escolano, A., Dosenovic, P., Stanfield, R.L., McCoy, L.E., Ozorowski, G., Hu, X., Kalyuzhniy, O., et al. (2016). HIV Vaccine Design to Target Germline Precursors of Glycan-Dependent Broadly Neutralizing Antibodies. Immunity *45*, 483–496.

Steichen, J.M., Lin, Y.-C., Havenar-Daughton, C., Pecetta, S., Ozorowski, G., Willis, J.R., Toy, L., Sok, D., Liguori, A., Kratochvil, S., et al. (2019). A generalized HIV vaccine design strategy for priming of broadly neutralizing antibody responses. Science *366*.

Sui, J., Hwang, W.C., Perez, S., Wei, G., Aird, D., Chen, L., Santelli, E., Stec, B., Cadwell, G., Ali, M., et al. (2009). Structural and functional bases for broad-spectrum neutralization of avian and human influenza A viruses. Nat Struct Mol Biol *16*, 265–273.

Suloway, C., Pulokas, J., Fellmann, D., Cheng, A., Guerra, F., Quispe, J., Stagg, S., Potter, C.S., and Carragher, B. (2005). Automated molecular microscopy: the new Leginon system. J. Struct. Biol. *151*, 41–60.

Taylor, J.J., Pape, K.A., Steach, H.R., and Jenkins, M.K. (2015). Apoptosis and antigen affinity limits effector cell differentiation of a single naïve B cell. Science *347*, 784–787.

Tian, M., Cheng, C., Chen, X., Duan, H., Cheng, H.-L., Dao, M., Sheng, Z., Kimble, M., Wang, L., Lin, S., et al. (2016). Induction of HIV Neutralizing Antibody Lineages in Mice with Diverse Precursor Repertoires. Cell *166*, 1471-1484.e18.

Tiller, T., Busse, C.E., and Wardemann, H. (2009). Cloning and expression of murine Ig genes from single B cells. Journal of Immunological Methods *350*, 183–193.

Tom, R., Bisson, L., and Durocher, Y. (2008). Culture of HEK293-EBNA1 Cells for Production of Recombinant Proteins. Cold Spring Harb Protoc *2008*, pdb.prot4976.

Tomaras, G.D., Yates, N.L., Liu, P., Qin, L., Fouda, G.G., Chavez, L.L., Decamp, A.C., Parks, R.J., Ashley, V.C., Lucas, J.T., et al. (2008). Initial B-Cell Responses to Transmitted Human Immunodeficiency Virus Type 1: Virion-Binding Immunoglobulin M (IgM) and IgG Antibodies Followed by Plasma Anti-gp41 Antibodies with Ineffective Control of Initial Viremia. J Virol *82*, 12449–12463.

Umotoy, J., Bagaya, B.S., Joyce, C., Schiffner, T., Menis, S., Saye-Francisco, K.L., Biddle, T., Mohan, S., Vollbrecht, T., Kalyuzhniy, O., et al. (2019). Rapid and Focused Maturation of a VRC01-Class HIV Broadly Neutralizing Antibody Lineage Involves Both Binding and Accommodation of the N276-Glycan. Immunity *51*, 141-154.e6.

Veesler, D., Cupelli, K., Burger, M., Gräber, P., Stehle, T., and Johnson, J.E. (2014). Single-particle EM reveals plasticity of interactions between the adenovirus penton base and integrin αVβ3. Proc. Natl. Acad. Sci. U.S.A. *111*, 8815–8819.

Verkoczy, L. (2017). Humanized immunoglobulin mice: models for HIV vaccine testing and studying the broadly neutralizing antibody problem. Adv Immunol *134*, 235–352.

Voss, N.R., Yoshioka, C.K., Radermacher, M., Potter, C.S., and Carragher, B. (2009). DoG Picker and TiltPicker: software tools to facilitate particle selection in single particle electron microscopy. J. Struct. Biol. *166*, 205–213.

Walker, L.M., Phogat, S.K., Chan-Hui, P.-Y., Wagner, D., Phung, P., Goss, J.L., Wrin, T., Simek, M.D., Fling, S., Mitcham, J.L., et al. (2009). Broad and Potent Neutralizing Antibodies from an African Donor Reveal a New HIV-1 Vaccine Target. Science *326*, 285–289.

Walker, L.M., Huber, M., Doores, K.J., Falkowska, E., Pejchal, R., Julien, J.-P., Wang, S.-K., Ramos, A., Chan-Hui, P.-Y., Moyle, M., et al. (2011). Broad neutralization coverage of HIV by multiple highly potent antibodies. Nature *477*, 466–470.

West, A.P., Diskin, R., Nussenzweig, M.C., and Bjorkman, P.J. (2012). Structural basis for germ-line gene usage of a potent class of antibodies targeting the CD4-binding site of HIV-1 gp120. Proc. Natl. Acad. Sci. U.S.A. *109*, E2083-2090.

Wibmer, C.K., Gorman, J., Anthony, C.S., Mkhize, N.N., Druz, A., York, T., Schmidt, S.D., Labuschagne, P., Louder, M.K., Bailer, R.T., et al. (2016). Structure of an N276-Dependent HIV-1 Neutralizing Antibody Targeting a Rare V5 Glycan Hole Adjacent to the CD4 Binding Site. J Virol *90*, 10220–10235.

Wickham, H. (2017). tidyverse: Easily Install and Load the "Tidyverse."

Williams, L.D., Ofek, G., Schätzle, S., McDaniel, J.R., Lu, X., Nicely, N.I., Wu, L., Lougheed, C.S., Bradley, T., Louder, M.K., et al. (2017). Potent and broad HIV-neutralizing antibodies in memory B cells and plasma. Sci Immunol *2*.

Wu, X., Yang, Z.-Y., Li, Y., Hogerkorp, C.-M., Schief, W.R., Seaman, M.S., Zhou, T., Schmidt, S.D., Wu, L., Xu, L., et al. (2010). Rational design of envelope identifies broadly neutralizing human monoclonal antibodies to HIV-1. Science *329*, 856–861.

Wu, X., Zhou, T., Zhu, J., Zhang, B., Georgiev, I., Wang, C., Chen, X., Longo, N.S., Louder, M., McKee, K., et al. (2011). Focused evolution of HIV-1 neutralizing antibodies revealed by structures and deep sequencing. Science *333*, 1593–1602.

Wu, X., Guo, J., Niu, M., An, M., Liu, L., Wang, H., Jin, X., Zhang, Q., Lam, K.S., Wu, T., et al. (2018). Tandem bispecific neutralizing antibody eliminates HIV-1 infection in humanized mice. J Clin Invest *128*, 2239–2251.

Xiao, X., Chen, W., Feng, Y., Zhu, Z., Prabakaran, P., Wang, Y., Zhang, M.-Y., Longo, N.S., and Dimitrov, D.S. (2009). Germline-like predecessors of broadly neutralizing antibodies lack measurable binding to HIV-1 envelope glycoproteins: Implications for evasion of immune responses and design of vaccine immunogens. Biochem Biophys Res Commun *390*, 404–409.

Yacoob, C., Pancera, M., Vigdorovich, V., Oliver, B.G., Glenn, J.A., Feng, J., Sather, D.N., McGuire, A.T., and Stamatatos, L. (2016). Differences in Allelic Frequency and CDRH3 Region Limit the Engagement of HIV Env Immunogens by Putative VRC01 Neutralizing Antibody Precursors. Cell Rep *17*, 1560–1570.

Yang Shih, T.-A., Meffre, E., Roederer, M., and Nussenzweig, M.C. (2002). Role of BCR affinity in T cell–dependent antibody responses in vivo. Nature Immunology *3*, 570–575.

Zhou, T., Georgiev, I., Wu, X., Yang, Z.-Y., Dai, K., Finzi, A., Kwon, Y.D., Scheid, J.F., Shi, W., Xu, L., et al. (2010). Structural basis for broad and potent neutralization of HIV-1 by antibody VRC01. Science *329*, 811–817.

Zhou, T., Zhu, J., Wu, X., Moquin, S., Zhang, B., Acharya, P., Georgiev, I.S., Altae-Tran, H.R., Chuang, G.-Y., Joyce, M.G., et al. (2013). Multidonor analysis reveals structural elements, genetic determinants, and maturation pathway for HIV-1 neutralization by VRC01-class antibodies. Immunity *39*, 245–258.

Zhou, T., Lynch, R.M., Chen, L., Acharya, P., Wu, X., Doria-Rose, N.A., Joyce, M.G., Lingwood, D., Soto, C., Bailer, R.T., et al. (2015). Structural Repertoire of HIV-1-Neutralizing Antibodies Targeting the CD4 Supersite in 14 Donors. Cell *161*, 1280–1292.

Zhou, T., Zheng, A., Baxa, U., Chuang, G.-Y., Georgiev, I.S., Kong, R., O'Dell, S., Shahzad-ul-Hussan, S., Shen, C.-H., Tsybovsky, Y., et al. (2018). A Neutralizing Antibody Recognizing Primarily N-linked Glycan Targets the Silent Face of the HIV Envelope. Immunity *48*, 500-513.e6.

Zhu, P., Chertova, E., Bess, J., Lifson, J.D., Arthur, L.O., Liu, J., Taylor, K.A., and Roux, K.H. (2003). Electron tomography analysis of envelope glycoprotein trimers on HIV and simian immunodeficiency virus virions. Proc Natl Acad Sci U S A *100*, 15812–15817.

Zhu, Z., Qin, H.R., Chen, W., Zhao, Q., Shen, X., Schutte, R., Wang, Y., Ofek, G., Streaker, E., Prabakaran, P., et al. (2011). Cross-Reactive HIV-1-Neutralizing Human Monoclonal Antibodies Identified from a Patient with 2F5-Like Antibodies ▽. J Virol *85*, 11401–11408.

Zivanov, J., Nakane, T., Forsberg, B.O., Kimanius, D., Hagen, W.J., Lindahl, E., and Scheres, S.H. (2018). New tools for automated high-resolution cryo-EM structure determination in RELION-3. Elife *7*, e42166.

Zwick, M.B., Labrijn, A.F., Wang, M., Spenlehauer, C., Saphire, E.O., Binley, J.M., Moore, J.P., Stiegler, G., Katinger, H., Burton, D.R., et al. (2001). Broadly Neutralizing Antibodies Targeted to the Membrane-Proximal External Region of Human Immunodeficiency Virus Type 1 Glycoprotein gp41. Journal of Virology *75*, 10892–10905.

(2017). Basic Statistics | HIV Basics | HIV/AIDS | CDC.